



PHD

**Assessing diesel fuel stability: a predictive approach**

McCollom, Matthew

*Award date:*  
1992

*Awarding institution:*  
University of Bath

[Link to publication](#)

**Alternative formats**

If you require this document in an alternative format, please contact:  
[openaccess@bath.ac.uk](mailto:openaccess@bath.ac.uk)

Copyright of this thesis rests with the author. Access is subject to the above licence, if given. If no licence is specified above, original content in this thesis is licensed under the terms of the Creative Commons Attribution-NonCommercial 4.0 International (CC BY-NC-ND 4.0) Licence (<https://creativecommons.org/licenses/by-nc-nd/4.0/>). Any third-party copyright material present remains the property of its respective owner(s) and is licensed under its existing terms.

**Take down policy**

If you consider content within Bath's Research Portal to be in breach of UK law, please contact: [openaccess@bath.ac.uk](mailto:openaccess@bath.ac.uk) with the details. Your claim will be investigated and, where appropriate, the item will be removed from public view as soon as possible.

# Assessing Diesel Fuel Stability: A Predictive Approach

by Matthew McCollom

A Thesis submitted in partial fulfillment of the requirements for  
the degree of Doctor of Philosophy at the University of Bath.

University of Bath

April 1992

Attention is drawn to the fact that copyright of this thesis rests with its author. This copy of the thesis has been supplied on condition that anyone who consults it is understood to recognise that its copyright rests with its author and that no quotation from the thesis and no information derived from it may be published without prior written consent of the author.

This thesis may be made available for consultation within the University library and may be photocopied or lent to other libraries for the purpose of consultation.

*M. McCollom*

UMI Number: U044120

All rights reserved

INFORMATION TO ALL USERS

The quality of this reproduction is dependent upon the quality of the copy submitted.

In the unlikely event that the author did not send a complete manuscript and there are missing pages, these will be noted. Also, if material had to be removed, a note will indicate the deletion.



UMI U044120

Published by ProQuest LLC 2014. Copyright in the Dissertation held by the Author.  
Microform Edition © ProQuest LLC.

All rights reserved. This work is protected against  
unauthorized copying under Title 17, United States Code.



ProQuest LLC  
789 East Eisenhower Parkway  
P.O. Box 1346  
Ann Arbor, MI 48106-1346

12140092

UNIVERSITY OF BATH LIBRARY		
21	27 NOV 1992	
PHD		



### Abstract

The work in this thesis is concerned with the area of diesel fuel degradation. Particular emphasis has been placed upon certain compounds found in fuels and known to cause instability. Chapter one contains a brief review of existing tests for the assessment of fuel stability. The various effects of fuel instability are also reported along with a review of investigations into the causes of fuel instability and techniques to investigate this.

Chapter two details the investigations performed in the thesis and covers a kinetic study of some of the compounds which have been shown to cause instability. Computer modelling of the degradation process is also included with the long term intention of developing a method of predicting fuel stability from a simple fuel analysis. The effects of various compounds and fuel treatments are also investigated. These treatments include doping with free radical initiators, the use of heat, ultraviolet irradiation and ultrasonic irradiation. The compounds selected for the work are 2,5 and 1,2,5 methyl substituted pyrroles as these compounds have been shown to have a very deleterious effect on the storage stability characteristics of diesel fuels. Due to the complexity of diesel fuel and the difficulty in obtaining reproducible analysis of the fuel by chromatographic methods, the kinetic study was performed in a model fuel system.

Chapter three presents the results and their discussion. The stability of the chosen fuel was established. The fuel was found to be susceptible to these dopants and rate constants and activation energies for consumption in a model system were measured. These compared favourably with literature results on similar systems and allowed kinetic modelling which provided a good prediction of the rates of degradation processes. The use of high intensity ultrasound as a degradation technique was investigated. Sonication was found to have a significant effect on hydrocarbon distribution and also to produce sediments which were qualitatively similar to those from other degradation processes. The results compared well with those obtained from thermal experiments and showed that the method has promise as an alternative to other fuel stability assessment procedures.

The appendix contains plots of raw data from the model fuel systems and first order plots of this data, which were used to determine rate constants for the measurement of activation energies.

### Acknowledgements

First and foremost I would like to thank Dr. Gareth J. Price for his advice and guidance throughout the course of this thesis.

I would also like to offer my thanks to Mr. Alan Carver for elemental analyses and Mr. Kevin Smith for gas chromatography-mass spectroscopy done on my behalf.

Thanks are also due to the other members of the School of Chemistry whose presence has made my three years most enjoyable and successful.

SERC and ESSO plc are also gratefully acknowledged for funding the C.A.S.E. award.

Finally, most grateful thanks must go to Dr. Caroline B.M. Nation for help and support during the assembly of this thesis.

Memorandum

The work described in this thesis was carried out by the author between October 1987 and September 1990 within the Department of Chemistry, City University London and the School of Chemistry, University of Bath, under the supervision of Dr. G.J. Price.

Unless otherwise indicated, the work is original and has not been submitted for any other degree.

	<u>CONTENTS</u>	<u>Page Number</u>
1	<u>Introduction</u>	1
1.1	An Introduction to Diesel Fuel	2
1.1.1	The Cetane Number	3
1.1.2	Other Fuel Characteristics	4
1.2	Fuel Stability	5
1.2.1	The Meaning of Fuel Stability	5
1.2.2	The Effects of Fuel Instability	5
1.2.3	Characterisation and Prediction of Fuel Stability	5
1.3	A Review of Storage Tests	9
1.3.1	Post Storage Test Analysis	12
1.3.2	Instrumental Chemical Analysis	15
1.3.3	Reduction of Fuel Instability	19
1.4	Factors Affecting Diesel Fuel Stability	20
1.4.1	Effect of Hydrocarbon Composition	21
1.4.2	Effect of Sulphur Compounds	21
1.4.3	Effect of Oxygen Compounds	23
1.4.4	Effect of Nitrogen Compounds	25
1.4.5	Effect of Metals	31
1.4.6	Effect of Storage Environment	32
1.4.7	Effect of Temperature and Pressure	33
1.5	Chemical Reaction Mechanisms	34
1.6	The Nature of Ultrasound	39
1.7	Kinetics and Computers	42
1.7.1	Determination of Reaction Order, Rate Constants, Activation Energies and Pre-exponentials	43
1.7.2	Modelling of Reactant Concentration.	45

	<u>Contents</u>	<u>Page Number</u>
1.8	Aims and Objectives	46
2	<u>Experimental</u>	47
2.1	General Practical Details	48
	2.1.1 Chemicals	48
	2.1.2 Filtration	48
2.2	Experiments on Diesel Fuel: Stability Testing	50
	2.2.1 Long Term Thermal Degradation of Diesel	50
	2.2.2 Thermal Degradation with Free Radical Initiators	50
	2.2.3 Ultra-violet Degradation with Free Radical Initiators	50
2.3	Thermal Degradation Experiments on Pyrrole Doped Diesel and Model Fuels	52
	2.3.1 2,5-Dimethylpyrrole in Diesel	52
	2.3.2 The Model Systems	53
2.4	Ultrasonic Experiments	54
	2.4.1 General Experimental Details for Ultrasonic Experiments	54
	2.4.2 Low Energy Sonication and Storage of Diesel Fuel	62
	2.4.3 Ultra-violet and Low Energy Ultrasonic Degradation: A Comparison	62
	2.4.4 Low Energy Sonication of 2,5-Dimethylpyrrole Doped Model Fuel	63
	2.4.5 High Energy Sonication of n-Dodecane (a Simple Model Fuel)	63
	2.4.6 High Energy Sonication of Diesel for Sedimentation Kinetics	63

<u>Contents</u>	<u>Page Number</u>
2.4.7 High Energy Sonication of Diesel, The Effect on Alkane Distribution	64
2.5 Analytical Techniques	65
2.5.1 Elemental Analysis	65
2.5.2 Chromatography	65
2.5.3 Gas Chromatography	65
2.5.4 Gas Chromatography/ Mass Spectrometry	70
2.5.5 Capillary Chromatography	71
2.5.6 Gel Permeation Chromatography	72
3 <u>Results and Discussion</u>	74
3.1 Introduction	75
3.2 Experiments on Diesel	75
3.2.1 Long Term Storage of Undoped Diesel	76
3.2.2 Thermal Degradation of Free Radical Initiator Doped Diesel	76
3.2.3 Ultraviolet Degradation of Doped Diesel Fuel	77
3.2.4 Thermal Degradation of 2,5-Dimethylpyrrole Doped Diesel	79
3.3 Experiments on Model Systems	83
3.3.1 Thermal Degradation of 2,5-Dimethylpyrrole in Dodecane and Toluene	83
3.3.2 Thermal Degradation of 2,5-Dimethylpyrrole and of 1,2,5-Trimethylpyrrole in Dodecane	85
3.3.3 C:H:N Analysis of the Sediments from the Model Systems	103

	<u>Contents</u>	<u>Page Number</u>
3.4	Computing Results	105
3.4.1	Modelled Concentration Curves for 2,5-Dimethylpyrrole and for 1,2,5-Dimethylpyrrole	105
3.4.2	The Combined Dopant System	119
3.4.3	Concluding Comments on Modelling	120
3.5	Results from Low Energy Ultrasound Experiments	122
3.5.1	Low Energy Ultrasonic Degradation of Diesel Fuel	122
3.5.2	Low Energy Ultrasonic Degradation Initiation and Storage of Diesel	122
3.5.3	Ultra-violet and Ultrasonic Degradation: A Comparison	123
3.5.4	Ultrasonic Degradation of 2,5-Dimethylpyrrole Doped Model Fuel	125
3.6	Results from High Energy Ultrasound Experiments	131
3.6.1	Ultrasonic Degradation of Dodecane (a Model Fuel)	131
3.6.2	High Energy Sonication of Diesel Fuel	137
3.6.3	High Energy Long Term Sonication of Diesel	144
4	<u>Conclusion</u>	153
5	<u>References</u>	156
6	<u>Appendix</u>	

## Introduction



## INTRODUCTION

The introduction to this thesis contains an overview of some of the research in the area of fuel stability. This includes a description of some of the factors which influence the stability of diesel fuels and the mechanisms whereby this occurs. The assessment of fuel stability is of great importance and therefore various methods for assessing this have been developed and are reviewed in this chapter. The emphasis of the work carried out in this thesis has been the development of a new method of stability assessment, together with a predictive technique. The application of ultrasound and computer modelling to these two areas respectively is novel to the field of fuel stability studies and an introduction to these two topics is also presented in this chapter.

### 1.1 AN INTRODUCTION TO DIESEL FUEL

The modern, highly developed diesel engine is characterised by its reliability, durability, high performance, low fuel consumption, low noise and ability to meet emission standards. It is anticipated<sup>1</sup> that these characteristics will lead to a future increase in the demand for the diesel engine and thus, also for the fuel. The characteristics of the diesel engine are only attainable by using good quality diesel fuels. This increased demand will force suppliers to utilise alternative fuel sources and the further development of the diesel engine could be impaired by using fuel of an inferior quality. Consequently, recent attention has focussed on assessing the quality of fuels from these sources. One such area of interest has been that of storage stability, since unstable fuels may suffer a reduction in quality with time. The work presented in this thesis centres around predicting and assessing fuel stability.

Diesel fuels are hydrocarbon products which boil between approximately 150 °C and 400 °C and have a carbon content in the range  $C_{14}$  to  $C_{21}$ <sup>2</sup>. They are used in diesel engines which are high compression self ignition engines, and which vary extensively in their fuel requirements. For example, high speed diesels (in engines

working at 2000 r.p.m.) may use fuels with initial boiling points as low as 140 °C, while slow speed marine diesels operate on heavy residual fuel oils which require pre-heating before use to reduce viscosity to an acceptable level. Diesel fuels are characterised by a combination of properties, which include the cetane number, specific gravity, viscosity, carbon residue values and sulphur and ash.

#### 1.1.1 The Cetane Number

Cetane numbers are used to indicate the quality of a fuel oil for compression ignition engines. Cetane is the old nomenclature for hexadecane ( $n\text{-C}_{16}\text{H}_{34}$ ) and the cetane number is named after this. Hexadecane is considered to be perhaps the best high speed diesel fuel known and for the purposes of determining cetane number is given a rating of 100. Aromatic hydrocarbons are poor diesel fuels, and the aromatic hydrocarbon methyl-naphthalene is given a rating of 0. The cetane number of a diesel fuel is defined as the percentage by volume of cetane in a cetane/methyl-naphthalene mixture that has the same performance in a standard compression ignition engine as that of the fuel. High speed diesels should have a cetane number of not less than 50, whereas for slow speed diesels the cetane number is not important, but should preferably be greater than 15. A number of standard reference fuel oils are available with a range of cetane numbers for use in any compression ignition engine. Two test methods are generally used, these are the ignition delay test and the throttling test.

The ignition delay test is carried out at constant engine speed and load and compares the delay time of the oil under test with those of standard reference fuels having delay times shorter and longer than that of the test fuel. The cetane number is obtained by interpolation. The delay time is the period of time between start of ignition and first combustion.

The throttling test involves running the engine at the lowest load which gives steady conditions. A surge chamber and throttle device is attached to the engine intake port. This device reduces the surge chamber pressure and increases the delay

time until a misfire occurs, which is indicated by a puff of white smoke. The air pressure at this point is related to the delay time and is a function of the cetane number. By referring this misfire pressure to misfire pressures of fuels of higher and lower quality, the cetane number can be calculated.

### 1.1.2 Other Fuel Characteristics

Since automotive fuels are sold on a volume basis, an increase in density increases the amount of heat purchased per unit volume. The extent to which this increase in specific gravity is permissible depends upon the cetane number of the fuel, since an increase in specific gravity also means an decrease in n-alkane content.

The viscosity determines the flow of fluid through the fuel injector mechanism. So the higher the viscosity the more difficult it becomes to deliver fuel to the cylinders. However, an increase in viscosity reduces leakage past the fuel pump plunger, increasing the maximum power obtainable from a given engine.

High carbon residues, sulphur and ash are together responsible for fouling engine parts and for excessive wear, particularly in the case of slow speed diesels. Higher speed diesels contain lower proportions of sulphur and virtually no ash. In all cases if the cetane number of the fuel is too low to give smooth running, engine fouling increases.

## 1.2 FUEL STABILITY

### 1.2.1 The Meaning of Fuel Stability

Originally diesel fuels were straight run products obtained directly from the crude distilling unit of the refinery. Today, where the demand for quality gasolines and distillate fuels is high and various refinery cracking processes are available, diesel fuels also may contain varying amounts of selected cracked distillates such as light cycle oils. The basic requirements of a diesel fuel are that it must ignite spontaneously, burn satisfactorily, have suitable low temperature properties and possess storage and thermal stability.

The term fuel stability implies the general resistance of a fuel to change<sup>3</sup>. It can refer to storage stability under ambient conditions, that is the ability of a fuel to remain in storage over extended periods of time without appreciably affecting its performance in a deleterious manner. Another term frequently used is 'thermal stability' which may be defined as the ability of a fuel to withstand relatively high temperature for short periods of time, without appreciable deterioration. Such change or degradation in fuels manifests itself in a variety of ways including colour change, development of gums either soluble or insoluble, development of particulate matter followed by sedimentation or deposition, development of coke and fouling materials, change in physical properties, change in chemical properties or fuel composition, change in combustion properties and change in compatibility or favourable miscibility with other fuels.

### 1.2.2 The Effects of Fuel Instability

During the lifetime of fuel, from production in the refinery, to consumption in the engine, the problem of instability always exists. Instability of liquid fuels is of increasing importance. Every machine in industry and every engine in the transportation system requires stable fuel in order to maintain full time operation and efficient service performance. Thus, the problem of instability in fuels is becoming of

increasing concern and as the anticipated worldwide demand for middle distillates is expected to increase, this concern would seem justified. In order to satisfy demand, refiners have cut deeper into less traditional blend components to replace the dwindling supply of straight run components, this is also exacerbated by the development of alternative fuel sources such as synfuels from shale, coal and tar sands extracts. These factors have led to a sharp loss of distillate stability.

As has been stated, instability in fuels is exhibited by a variety of detectable changes. Colour change occurs as a darkening or deepening in colour, which is relatively unimportant in fuel quality, except as a general indication of fuel instability. However, the customer preference is always for lightly coloured fuel products.

Soluble gum development does not cause any particular difficulty in fuel utilisation, although very high amounts may lead to screen or filter clogging. The soluble gum content is a measure of the existent state of the fuel and may also be a guide to the future storage behaviour of the fuel<sup>4,5</sup>. Insoluble gum must be filtered from the fuel before it passes to the combustion chamber, as with any insoluble material. Excessive amounts of insoluble gum cause various problems which include clogging of screens and filters, reduction or alteration of fuel flow through engine nozzles or injectors and sticking of injectors.

Development of particulate matter followed by sediment deposition may result in fuel filter plugging. In addition, these deposits can serve as binding agents for water, dirt, rust and other corrosive products found in the fuel distribution systems. Sediments form an environment suitable for the growth of microorganisms, leading to microbial contamination, fuel degradation and corrosion.

The presence of coke and fouling materials in the fuel has been found to cause engine operating difficulties. These materials can form varnishes on heat exchanger surfaces, which reduce heat transfer efficiency. Engine noise, excessive smoke, loss of power, poor fuel economy, degraded emissions and poor drivability have also been

cited as problems arising from the presence of coke<sup>6</sup>.

Change in physical properties such as viscosity, colour, density or pour point tend to reduce oil quality and lead to the product being off specification. However, the effects of these physical changes are generally slight and are of little consequence to fuel systems or stability problems. If the chemical properties or fuel composition change during storage, increased instability problems generally occur. These can manifest themselves as any of the changes which indicate fuel instability.

Changes in combustion properties may impair engine performance and combustion or burning efficiency. Autoxidation can change the heat of combustion and ignition properties of the fuel. The reduction of the heat of combustion will reduce combustion and effect engine performance. Ignition qualities or cetane numbers of diesel fuels may be improved by formation of peroxide during storage<sup>4</sup>. However, this effect depends on the amount of material oxidised in terms of the whole fuel and may be minimal in a real system.

Incompatibility is the tendency of a fuel to produce deposits on dilution or blending with another fuel. This problem, which is more noticeable in residual fuel oils, leads to difficulty in handling due to its formation of solids or sludge, which may solidify in tanks, foul heaters, plug strainers and cause pumps to fail and to plug lines.

### 1.2.3 Characterisation and Prediction of Fuel Stability

A reliable laboratory technique for the characterisation and prediction of the stability of liquid fuels has long been sought after both by industry and the military. Several researchers have conducted long term storage tests to establish the reliability and accuracy of a particular accelerated test, or to define whether instability was in fact a problem. Many researchers have carried out a considerable amount of work on fuel stability characterisation and test studies. At present however, there is no adequate test procedure or technique that has found universal acceptance for the prediction of instability of fuels from various sources and under varying storage

conditions. To be acceptable, a method developed for the study of instability should give a reliable predictive answer in a reasonable length of time without resort to unrealistic accelerating techniques<sup>7</sup>.

There are two categories for testing the storage stability of liquid fuels: the long term storage stability test and the accelerated storage stability test. The long term test predicts how fuel will behave under a range of storage conditions. It is not a reasonable specification test because, to be useful, such a test must give a reliable answer in a short period of time. The second test is an accelerated stability test method, which has commonly been approached by attempting to accelerate artificially the chemical processes involved. These include temperature elevation in the presence of air or oxygen under increased pressure, and the use of catalysts or steam. As well as the conditions imposed upon fuels for accelerated stability tests, there are other factors which may also have a bearing on the results. One such factor is the material from which storage vessels are made.

These experiments must be coupled with techniques to show appropriate changes in the fuel. Colour changes can be detected by a colour comparator utilising the ASTM (American Standards for Testing and Materials) colour test. Light transmission or scattering using standard lamps or lasers has also been used. Measurement of sediment formation may be carried out by gravimetric or volumetric analysis, visual inspection, measurement of the filtration rate, or determination of the filterability ratio. Instrumental chemical analysis can be carried out by mass spectrometry, infrared spectrometry, chromatography, atomic absorption, inductively coupled plasma emission spectroscopy, nuclear magnetic resonance, electron spin resonance spectroscopy and electron microscopy.

Other tests check the listed fuel specification relevant to fuel stability. For example ASTM colour (ASTM D 1500), viscosity (ASTM D 445/1P71), and accelerated stability test (ASTM D 2274) are relevant to diesel fuel stability<sup>8-10</sup>.

### 1.3 A REVIEW OF STORAGE TESTS

A large number of tests have been used, or are still in use for evaluating diesel fuel stability. Several tests have been modified in order to attain better and more accurate results. Fuels aged by using these methods are evaluated for insoluble gum, soluble gum, colour, filtration performance and light absorbance together with composition or structural analysis.

Early storage tests carried out on diesel fuel were performed in suitable bulk containers for fixed times to simulate realistically those storage environments then in use. These methods were soon found to be impractical, uneconomic and unrealistic, as researchers showed that storage in 100 barrel test tanks gave approximately the same results as bulk storage in 80000-120000 barrel tanks<sup>3,11</sup>. It was subsequently shown by Garner and White<sup>12</sup> from their studies of correlation of long term storage and accelerated stability tests, that bottles after 3 years of storage gave results very similar to those obtained on storage of large volumes. Thus, the use of bottles for long term storage experiments at ambient temperatures was shown to be a reasonable substitution for bulk storage containers as used commercially.

Ritchie<sup>5</sup> conducted an early and informative test. Ritchie's experiments involved the correlation of long term ambient storage with three accelerated storage tests to assess the utility of the accelerated tests as predictive methods. Six types of diesel fuel marine were selected to encompass a wide range of stability characteristics (straight run, hydrofined, catalytically cracked, caustic washed and blends of one fuel with another). Samples of the six fuels were stored at ambient temperature for up to six years. The three laboratory predictive test methods considered were, a 4 week ageing period at 120 °F (50 °C), a 16 hour ageing period at 210 °F (100 °C) and a steam jet evaporation procedure at 450 °F (232 °C) (ASTM D 381). The results showed that the 4 week and 16 hour ageing tests techniques gave reasonably satisfactory correlation for predicting the amount of sediment which will form in a 12-18 month storage period.



A test which is widely recognised for its good correlation with actual fuel performance is the 43.3 °C (100 °F) oven storage test. Bottle storage at 43.3 °C for 13 weeks is reported to be approximately equivalent to either drum or bottle storage at ambient 18-24 °C temperatures for 1 year<sup>13-16</sup>. This test has been accepted by ASTM (method D 4625-86)<sup>17</sup>. This test is suitable for research purposes because the low temperature used is only a small increase over ambient conditions and therefore the relative importance of the various reactions which create insolubles is not appreciably changed. However, due to the relatively long storage period required this test has restricted commercial use.

A more expeditious test which has shown good reproducibility and correlates with the 43.3 °C test is a version of the Du Pont F31 test<sup>15</sup>. This test involves ageing a sample at 80 °C for 7 days and subsequent determination of deposit levels<sup>18,19</sup>. Stavinoha et al.<sup>19</sup> found that this 80 °C test has the best correlation with the 43.3 °C storage test data for total gum and total insolubles. Hardy et al.<sup>18</sup> found that the prediction from the 43.3 °C test was always matched by the same prediction from the 80 °C test. For USA diesel fuel, an acceptable gum limit of less than 2.0 mg/100 ml has been suggested for both the 80 °C (175 °F) 7 day and 43.3 °C (110 °F) 13 weeks tests. A limit of 2.0 mg/100 ml in the 43.3 °C is equivalent to 1.2 mg/100 ml in the 80 °C test<sup>15</sup>.

A test which has been used for many years to monitor stability properties of diesel fuels is the Du Pont F21 accelerated stability test which is conducted at 149 °C (300 °F). The basic procedure includes heating a small (50 ml) fuel sample to 149 °C (300 °F) for 90 minutes or more, cooling to room temperature, filtering and estimating the insoluble residue formed by comparison with visual or instrumental evaluation using a standard filter pad. This test differs from others in two respects. A high ageing temperature is used to permit short test times and insoluble formation is estimated rather than gravimetrically determined. The test is easy to carry out but its reproducibility has not been statistically evaluated<sup>20</sup> and depends on the skill of the

operator, cleanliness of glassware and other possible variables. Other tests use similar procedures, these include the Nalco 300 °F test, the EMD diesel fuel stability test and the Union Pacific Diesel Blotter Test.

A long term storage test which may be used for research purposes was developed by Bhan et al.<sup>21</sup> in which fuel samples are aged at 65 °C and the final colour and total sediment formed are determined. Weighed nylon membrane filters of 1.2 µm pore size are placed at the bottom of tared storage vials for sediment collection. A 10 ml sample of the test fuel is poured into each vial and then stored in the dark in an oven at 65±0.5 °C for periods of 3, 6, 8, 12 and 16 weeks. Three sediment values are determined, these are precipitated, suspended and adherent sediments. The sum of these three weights is taken as the total sediment weight.

Two storage tests developed by industry are the British Petroleum (BP) method or DEF 2000 method 17 and the ESSO method or DEF 2000 method 16. The former is a 4 week storage test at 48.9 °C (120 °F). Fuel samples are aged for 4 weeks in an oven at 48.9 °C and then filtered through a number 3 sintered crucible. The latter test requires that the fuel sample be aged for 16 hours at 98.9 °C (210 °F) and the resultant sediment be filtered through a glass fibre filter pad. In both tests the weight of filtered sediment plus any remaining in the bottle is reported as milligrams of total sediment per hundred millilitres (mg/100 ml) of fuel<sup>5</sup>.

A test which is commonly used in industry and gives good results is the ASTM D 2274 accelerated stability test. Oxygen sparging and elevated temperature are used to artificially age fuel samples<sup>22</sup>. This test simulates storage stability of up to 3 years at ambient temperature. Although the method is relatively rapid the results may not be accurate because it uses high stress temperature. This test has been found to be unreliable, particularly for fuels containing cracked stock. Stavinoha and Westbrook<sup>13</sup> reported that the test has good repeatability but is not reproducible. Poor reproducibility among other laboratories has also been reported<sup>23,24</sup>. Active efforts are underway to replace this test<sup>25</sup>.

This has been a brief introduction to the field of fuel storage tests. A more detailed review is not appropriate or necessary to this thesis.

### 1.3.1 Post Storage Test Analysis

There are many different ways of assessing the degree of degradation resulting from storage tests. Several of the most commonly used methods are described in the following section, with the emphasis being placed on those most relevant to this thesis.

#### **Gravimetric and Volumetric Analysis**

Gravimetric analysis is the most commonly used method for the analysis of degradation products. The amount of soluble and/or insoluble gum produced on ageing is weighed after filtering, washing with specified solvents and then drying in a fixed type of apparatus. Gravimetric analysis for assessment of fuel stability is commonly used because it is easy to carry out, simple, sensitive and accurate for large amounts of sample.

Volumetric analysis may also be used for the estimation of degradation products. Cooney et al.<sup>26</sup> have used iodometric titration (ASTM D 1583-60) for analysis of filtrate hydroperoxide levels after stressing samples of diesel marine fuel and concluded that 2,5-dimethylpyrrole doped diesel marine fuel samples exhibited very low peroxide content after stress.

#### **ASTM Colour**

Colour of diesel fuel is commonly measured by the ASTM colour test (ASTM D 1500) in which a diesel fuel sample is placed in a test tube and compared with distilled water in another tube. The determination is made by the use of coloured glass disks ranging in value from 0.5 to 8 in which glass disks match the colour of the sample in transmitted light<sup>27</sup>. Species in the fuel which absorb light in the visible

region will colour the fuel and the intensity of this colouration will be dependent upon their concentration. Generally, the heavier the product or the higher the product concentration, the darker will be the colour.

### **Light Scattering**

A number of researchers<sup>7,28-36</sup> have used light scattering techniques extensively to examine the growth of small particles which are precursors to deposit formation. This technique is based on the principle that, as a fuel ages, particles grow in size and scatter light. Light scattering techniques have been used by Johnson et al.<sup>7</sup> and Chiantella and Johnson<sup>37</sup> and these techniques were found to give a good estimate of long term stability of liquid fuels.

Compared with other methods, light scattering requires smaller quantities of sample (5-10 ml), shorter times, lower stress temperature and no external heating and also gives greater sensitivity for initial deposit formation. Light scattering results have been found to correlate with accepted measures of stability.

Almost all applications of light scattering techniques have been applied to studies in jet fuel (JP-5), from shale, coal derived oil and petroleum. Definitive work remains to be done in the area of diesel fuel stability to help elucidate the mechanism of diesel fuel instability and to develop the most practical and reliable test techniques.

### **Light Transmission**

Light transmission is another method for the early detection of insoluble gum. This technique measures colour development or darkening of the ageing fuel using a Lumetron Colorimeter, the results being reported as percent transmission. A decrease in light transmission with time indicates darkening of the fuel and gum development. Johnson et al.<sup>38</sup> concluded that light transmission studies gave the same result as light scattering methods. Stavinoha et al.<sup>19</sup> reported however, that light transmission does not correlate with deposit formation.

### **Oxygen Absorption**

Oxygen absorption is a useful method for monitoring instability. It is generally accepted in the chemistry of fuel stability that the rate of gum formation in unstable fuel is a function of the amount of oxygen available in the sample.

Several researchers<sup>35,36,39,40</sup> have reported studies of oxygen absorption by fuels under various conditions. It has been found<sup>39</sup> that 2,5-dimethylpyrrole promoted extensive oxygen absorption in studies of light fuels. Furthermore, it was shown that oxygen absorption by 2,5-dimethylpyrrole is much higher than by N-methylpyrrole. Cooney and Wechter<sup>40</sup> found that the depletion of soluble 2,5-dimethylpyrrole in the fuel was correlated with oxygen uptake in doped fuel samples at temperatures of 65 and 80 °C. They also concluded that autoxidation of 2,5-dimethylpyrrole in the fuel was a first order reaction with an approximate activation energy of 46.2-50.4 kJ mol<sup>-1</sup>.

Hardy et al.<sup>36</sup> have developed a new method for assessing distillate fuel stability during ambient storage by oxygen overpressure. In this method, oxygen is forced into the fuel at pressures and temperatures of up to 750 kPa (100 psi) and 80 °C respectively, and for up to 96 hours duration. This method is reported to be predictive for 3 years at ambient conditions.

### **Filtration Rate and Filterability Ratio**

The filtration rate measures the time required to filter a fixed volume of a fuel sample using a specified type of apparatus. A ratio of filtration time for the test fuel against the time to filter the same volume of fuel sample after it has been prefiltered through an equivalent membrane is called the filterability ratio or filterability index<sup>41</sup>. A variant of this method is the ratio of the time for a fixed filtration volume at the beginning of the filtration to the time for the same volume at the end of the filtration<sup>42</sup>. These tests are used by several workers to detect diesel fuel stability and cleanliness from degradation product or other solid contaminants<sup>43</sup>. With these tests it is possible to predict if a fuel will cause filter plugging problems when used.

### **Field Test Method**

The need of establishing a test method for the accurate assessment of diesel fuel instability is a problem. In the case of a field test some type of portable equipment would be practicable.

A method for measuring the filter choking propensity of diesel fuels has been published by Onion and Bartlett<sup>44</sup>. The device used is small, light, easily cleaned, completely self contained and easy to operate and could be used in the field. Westbrook et al.<sup>45</sup> have developed a portable field fuel quality monitor which tests for colour and particulates and allows an estimate of stability to be made. This kit has been shown to be a practicable tool, enabling the operator to conduct on site tests, monitoring the stability and cleanliness of diesel fuel in storage. A method called the dieso filtration test has been developed by Hiley<sup>46</sup> and has good repeatability and an acceptable reproducibility. The equipment is portable and can be effectively used on site.

#### **1.3.2 Instrumental Chemical Analysis**

Instrumental chemical analysis has been utilised by a large number of researchers for a variety of purposes. These include examination of sediments formed during fuel degradation, analysis of sediment precursors, prediction of fuel stability and monitoring of various fuel components during degradation. A wide variety of analytical techniques have been used by workers in this area<sup>21,31,32,47,54</sup>. These techniques include various types of gas chromatography-mass spectrometry, mass spectrometry, infrared spectroscopy, nuclear magnetic resonance spectroscopy and thin layer chromatography. In general, instrumental chemical analysis techniques require smaller quantities of sample and are capable of greater sensitivity and accuracy than those methods employing standard wet chemistry. However, the cost is usually higher and a professional operator may be required.

Pedley et al.<sup>50</sup> have used infrared spectroscopy, gas chromatography-mass

spectrometry (GC-MS), mass spectrometry (pyrolysis, electron impact and fast atom bombardment ionisation), and thin layer chromatography to analyse sediment precursors formed during the ambient storage of petroleum diesel fuel. They concluded that these characterisation techniques can be used to analyse model sediments and to compare them with naturally occurring fuel sediments. It was shown that the sediment produced during storage of an unstable diesel fuel could be separated by TLC into five fractions, all of which contained alkylindoles. However, the nitrogen contents of these fractions were found to be too low for them to consist entirely of indoles. Analysis of these sediments has shown two classes of compounds<sup>47</sup>. The basic structure of these compounds is an indole ring system (indolylphenalenes and bis(indolyl)phenalenes). These compounds, which are soluble in diesel fuels, react with acids to form insoluble sediment. Pedley et al.<sup>51</sup> went further in this investigation and synthesised these sediment precursors in order to test their action in model fuel systems. They obtained strong evidence to support the role of indolylphenalenes in sediment formation in diesel fuels although this is obviously not the only mechanism for sediment formation.

Electron Spin Resonance (ESR) has been used by Anderson et al.<sup>55</sup> as a possible predictor for long term stability of diesel fuel. Free radicals and molecules containing unpaired electrons can be detected and quantified by ESR measurements<sup>55,56</sup>. The fuel found to have the highest free radical concentration also shows the highest degree of instability, but no exact relationship was found between the free radical concentration and the stability for all fuels<sup>56</sup>.

Some workers have found applications for less familiar techniques, these include X-ray diffraction and X-ray photoelectron spectroscopy (XPS)<sup>30,52,57</sup>. Whilst these techniques have been used to analyse soluble fuel sediments some have also been used to examine insoluble sediments.

Direct fluid injection mass spectrometry (DFI-MS) has been used by Smith et al.<sup>58</sup> to study the characterisation of the polar components of diesel marine fuels.

They used two fractionating schemes involving alumina and silica column chromatography for initial separation into four fractions. Chemical ionisation with ammonia was used to provide selective detection of the more polar diesel fuel components. The results showed that DFI-MS allows a rapid evaluation of the molecular weight distribution of the polar components in the fuels. The most polar components which are not normally responsive to conventional extraction and analysis methods are included in this determination. The polar components of diesel fuel are suspected of having a role in the formation of insoluble gum during ageing and general problems relating to fuel instability. Mayo and Lan<sup>54</sup> have used field ionisation mass spectrometry (FI-MS) to analyse oxidised and unoxidised fuel. They were able to obtain molecular weight profiles of the fuel samples and of the less volatile components of the oxidised fuel.

High Pressure Liquid Chromatography (HPLC) has been used by Brinkman and Bowden<sup>59</sup> for the measurement of molecular weight distribution in gums. They observed that most of the compounds in the gums appeared to be in the region of a molecular weight of 500. They also used gas chromatographic procedures to measure dissolved oxygen, a method which was found to be sensitive to as low as 2 ppm by weight (argon, if present, is included in the oxygen value).

Finseth<sup>60</sup> claimed that IR spectroscopy is the most widely used analytical technique for the detection of oxidation products in complex oil matrices. It is useful for identification of both hydroxyl and carbonyl functionality, but it is not well suited for the analysis of ether groups. An infrared spectroscopic study of some petroleum diesel fuels by Power<sup>61</sup> concluded that gums derived from accelerated storage are not the same as those which form during ambient storage. From this finding it follows that the results obtained during accelerated oxidation stability tests may be unreliable. He examined soluble and insoluble gums derived from petroleum diesel fuels by infrared spectroscopy. The ambient ageing samples were stored in darkness for 1 year in borosilicate glass bottles at 20-30 °C. The accelerated ageing tests were



ASTM D 2274 and a modification of ASTM D873. The infrared spectra showed that the accelerated oxidation of petroleum diesel fuel yielded soluble gums which contain higher proportions of  $C=O$ ,  $ArC=C(-O)$  and  $C-O$  species than those formed during ambient storage. Power and Hazlett<sup>62</sup> were able to show that the sediment produced by the addition of a phenolic extract of a light cycle oil to a straight run distillate was the result of oxidative coupling.

Power and Davidson<sup>63</sup> from their studies of infrared spectroscopy of carbonyl species in oxidised diesel distillates, also concluded that a lack of correlation exists between the degree of oxidation in fuels aged for short terms at elevated temperatures in the presence of added oxygen, and under conditions of bulk storage (long term, ambient temperature, limited  $O_2$  supply). It follows that accelerated oxidation stability tests do not necessarily give a prediction of the long term storage stability characteristics of a fuel. This means that accelerated stability test methods have questionable significance in prediction of subsequent deposit for long term storage conditions.

There is a need to develop new and better test techniques for the evaluation of storage stability of diesel fuels in day to day quality control for specification testing, surveillance, research and procurement activities. Although many laboratories and researchers have in the past carried out a considerable amount of work on fuel stability studies, at present there is no adequate test method that has been found satisfactory for diesel fuels from a range of sources and under a range of storage conditions. To be acceptable a test technique should give reliable predictive answers in a reasonable length of time and be inexpensive, quick, simple to run, with a short ageing period and yield reliable answers.

### 1.3.3 Reduction of Fuel Instability

Another important area of research has been the improvement of fuel stability and to prevent the processes which cause fuel degradation.

Hydrotreatment is the catalytic hydrogenation of fuel components. Palmer and Copson<sup>64</sup> have found that hydrotreatment was superior to using available chemical stabilising additives and produced lower deposit yields and less colour development. Furthermore, the highly deleterious compound classes pyrrole/indole and thiophenols are relatively easy to remove by hydrotreating.

Washing with sodium hydroxide (40 % wt/wt) may also be used to improve diesel fuel stability. The results obtained by this process may be influenced by the strength of caustic used. Powers and Wotring<sup>65</sup> observed that a stable fuel was obtained when the fuel so treated contained less than or equal to 10 ppm thiophenol. Caustic treatment was found to remove most of the thiophenol and phenol and the majority of thiols present in the fuel. However, this treatment was found to have no effect on pyrrolic nitrogen and therefore additional treatment may be necessary to produce a completely stable fuel. The deleterious effects of nitrogen containing compounds has been well established and is covered in section 1.4.4. Powers and Wotring<sup>65</sup> however, claimed that caustic treatment alone improved thermal stability and colour while Clinkenbeard<sup>66</sup> showed that caustic treatment decreased the amount of carbon residue formed in the oil and improved the colour.

Hiley and Pedley<sup>67</sup> found that the caustic improvement of diesel fuel stability is reversible by the addition of 10 ppm naphthalenesulphonic acid. A linear relationship was found to prevail between sediment level and acid concentration. They concluded that the formation of strong acid is a limiting factor in the extent of sediment formation during diesel fuel storage.

#### 1.4 FACTORS AFFECTING DIESEL FUEL STABILITY

The area of fuel stability has been extensively investigated since the 1920's<sup>68</sup> and several reviews of the field have been produced. A number of these reviews<sup>3-5,19,69-73</sup> show that the stability of fuels depends on such factors as the fuel hydrocarbon composition, source of crude oil, boiling range, type and severity of the refining process and storage conditions.

It has been found that stability decreases as one moves from light to heavy crudes. This trend also applies to the transition from petroleum oils to coal derived liquids, tar sand crudes and to shale oils<sup>74</sup>. In general, light boiling fractions are more stable than heavier boiling fractions.

The type and severity of refining processes also affects the stability. Studies have shown that cracked distillates tend to deteriorate more rapidly than straight run distillates during storage<sup>7</sup>. Thermal or catalytically cracked fractions are more susceptible to sediment formation and to colour change than straight run fractions<sup>70</sup> and severe cracking processes can lead to increased problems with stability. Generally, a greater degree of cracking leads to poorer quality distillates or residual fractions.

It is evident from the literature that the whole picture of fuel stability is very complex. There may be no single explanation for all of the phenomena associated with fuel deterioration. However, fuel instability has been attributed to oxidation and autoxidation reactions, chemical reactions involving polymerisation of unsaturated hydrocarbons and reactive compounds of sulphur, nitrogen and oxygen. These reactions can be accelerated by the catalytic effect of trace amounts of dissolved metals<sup>7,16,65,70,75,76</sup>. Each fuel has its own mechanism which is different from other fuel types.

One of the effects of the chemical reactions that occur during storage is to produce soluble and insoluble materials of higher molecular weight and boiling point than the original fuel. These materials have a carbon to hydrogen ratio of about unity

and an oxygen content varying between 7 and 25%. The nitrogen and sulphur contents vary but are usually at higher levels than those present in the original fuel<sup>4</sup>.

Some of the important factors leading to fuel instability are summarised in the following sections.

#### 1.4.1 Effect of Hydrocarbon Composition

The correlation of instability with hydrocarbon composition has been an actively studied area for some time. Various investigations<sup>4,69,77,78</sup> have reported that stability decreases as the proportion of unsaturated hydrocarbon components in the fuel increases: the order of this being alkanes, naphthenes, aromatics, alkenes and dienes. The most unstable hydrocarbon constituents in diesel fuels have been shown to be dienes, including aliphatic dienes and aromatic alkenes. These are then followed by mono-olefins and then alkanes (and unsubstituted alkanes) with tertiary hydrogens such as in cumene and 2,4-dimethylalkanes.

Pure alkyl naphthalenes and other polyaromatic hydrocarbons are also an important source of gum and some of the least stable fuels have the highest proportions of these hydrocarbons. From work on shale oil however, it has been shown that there is considerable variation in the reactivities of alkene types, for example, terminal alkenes are not as reactive as their internal isomers. The differences in reactivity are consistent with the relative rates of alkene free-radical oxidation. In addition the cis-1,2-disubstituted alkenes are more reactive than the trans species.

#### 1.4.2 Effect of Sulphur Compounds

It has been found by several researchers<sup>78-81</sup> that a high concentration of some heteroatomic compounds in synfuels may lead to considerable instability if these compounds are found in any deposit formed. Some of the most important heteroatomic compounds studied are those containing sulphur, oxygen and nitrogen.

The storage stability of catalytically cracked distillate has been shown to increase when aromatic thiols, naphthols or pyrrole type compounds are removed.

The sulphur compounds found to cause instability cover a wide range of types. These range from simple free sulphur and sulphides to thiols and more complex sulphur bearing organic compounds. The addition of free sulphur, disulphides and polysulphides to fuels has been found to cause an increase in sediment deposition. However, thiophenes and alkyl sulphides were shown to have little effect upon gum formation. Thiols at low levels, especially for long storage periods in the presence of light, act as gum accelerators. However, primary thiols were found to stabilise the fuel slightly, while tert-butyl thiol caused no change in the amount of deposit. The addition of thiophenol to a mixture of catalytically cracked and straight run fuels has been shown to produce large increases in the amount of soluble gum in the fuel and little change in the rate of formation of insoluble deposits<sup>81</sup>. In contrast, some workers have reported thiophenol to be very active in stimulating sediment formation<sup>70,82</sup>. Thiophenol can also cause problems by reaction with brass in fuel systems to form mercaptide gels. Frankenfeld and Taylor<sup>53</sup> have reported that thiols at high concentration levels (3000 ppm S) for short storage periods, inhibit sediment formation when present with 2,5-dimethylpyrrole as an antioxidant.

Most workers<sup>66,82-84</sup> agree that thiophenol is the most damaging of the sulphur compounds. Thiophene, however, has been shown to be equally harmful<sup>4</sup>. Loeffler and Li<sup>57</sup> consider that the decreasing order of reactivity is thiophenols, tetrahydrothiophene and thiophene, followed possibly by polysulphides and alkyl thiols.

Offenhauer et al.<sup>85</sup> have reported that aromatic thiols and organic sulphonic acids in a catalytically cracked fuel contribute to sediment formation. *p*-Thiocresol and *p*-toluenesulphonic acids may produce measurable sediments when tested by themselves on long term storage but are inactive for short term storage periods. However, aliphatic thiols and diaryl disulphides do not cause instability; the thiols

participate in gum formation primarily through first being oxidised to sulphonic acid. These findings are in agreement with those of Malhotra and St. John<sup>86</sup>. Hazlett et al.<sup>87</sup>, Hazlett and Kelso<sup>82</sup> and Hiley and Pedley<sup>67</sup> reported that organic sulphonic acids added to distillate fuel blends containing catalytically cracked stock increase deposit formation, sometimes very dramatically. Some of the mechanisms involved in these processes are discussed in section 1.5.

#### 1.4.3 Effect of Oxygen Compounds

Compounds containing oxygen have also been examined and have been found to have a deleterious effect on fuel stability. Taylor and Wallace<sup>88</sup> found that, of the oxygen compounds studied, peroxides as a class were detrimental to stability. Some acids, esters and ketones were moderately harmful while ethers had no significant effect on deposit formation. In general, cycloalkyl compounds were less harmful than their aliphatic or aromatic counterparts.

Taylor and Frankenfeld<sup>89</sup> concluded from their studies of deposit formation from deoxygenated hydrocarbons that furans, most carboxylic acids except n-decanoic acids, and alcohols, were generally not harmful to fuel stability. Hazlett et al.<sup>87</sup> showed however, that carboxylic acids in aqueous solution increase deposit formation. Taylor and Frankenfeld<sup>89</sup> also demonstrated that carboxylic acid esters are only moderately harmful and their influence varies with structure. Peroxide compounds, regardless of structure, cause significant instability and may be classed as highly detrimental to stability. Interaction between some compound types was shown to cause instability. The two compounds showing the greater tendency to interact were 2,5-dimethylpyrrole and n-decanoic acid. These compounds interact with sulphur and unsaturated material. In contrast, interactions among purely oxygenated species were stabilising and tended to reduce deposit formation.

Of the oxygen compounds studied, Nixon<sup>4</sup> stated that phenols are the most likely to cause instability, whereas Offenhauer et al.<sup>85</sup> reported that most phenols

occurring in the fuel oil range are relatively harmless, with the exception of 1-naphthol. Hara et al.<sup>90</sup> have shown that phenolic- containing constituents present in coal derived liquids are involved in the sediment formation process. Oxidative coupling of phenols has been proposed as an ageing mechanism for coal liquefaction products in the presence and absence of metallic copper. Similarly, Cooney and Wechter<sup>40</sup> stated that oxygen containing species in the oil react preferentially to form higher molecular weight components, these components were phenols. White et al.<sup>52</sup> suggested that chemical hydrogenation of phenol to produce water and hydrocarbon or etherification of phenolic hydroxyl groups to form alkyl aryl ethers, might prevent or minimise these oxidative coupling reactions. Etherification does in fact improve product quality and makes the fuel more stable, less corrosive, less toxic and more compatible with other fuels.

A caustic extract of a light cycle oil obtained from an Australian crude with low sulphur content was shown by Hazlett and Power<sup>62</sup> to contain approximately 100 phenolic compounds with no other class of compound present. When added to a straight run automotive distillate oil or to a hydrotreated light cycle oil, this extract increased amounts of total insolubles obtained on thermal ageing. Phenolic oxidative coupling was considered to be the cause of the increased instability, based on infrared studies of the sediment produced. The hydrotreated fraction produced considerably less insolubles than the straight run distillate, which was attributed to the fact that the hydrotreated fraction is virtually free of unsaturated and other heteroatomic species which could act as gum precursors.

For most fuels, removal of molecular oxygen markedly lowered the rate of deposit formation. Nixon<sup>4</sup> reported that fuel stored in the absence of oxygen did not build up sediment. Frankenfeld and Taylor<sup>68</sup> also reported that dissolved oxygen plays a role. A combination of exclusion of light and deoxygenation reduce sediment formation by 87% over 60 days and by over 95% over 15 or 30 days. They also found that organic acids accelerate sediment formation with 2,5-dimethylpyrrole. The

details of these mechanisms are discussed in section 1.5.

#### 1.4.4 Effect of Nitrogen Compounds

It has been known for a long time that some nitrogen compounds contribute to diesel fuel instability<sup>4,7,20,26,29,47,51,57,68,88,91-94</sup> while others are inert. Several of the active nitrogen compounds are known to induce instability by promoting the formation of sediment deposition under storage conditions and during thermal stress. Others are not harmful by themselves, but by interaction with other compounds, such as those containing oxygen or sulphur.

A number of studies have been made of the nitrogen composition of diesel fuel<sup>68,95-102</sup>. The major compound types present are pyridines, pyrroles, amines, amides, anilines, indoles, carbazoles and quinolines. With regard to diesel fuel stability, most researchers agree that nitrogen containing aromatics (pyrroles, pyridines, indoles, quinolines) appear to be harmful. In contrast to these compounds, amines and amides have no deleterious effects, except if they interact with other chemicals.

Of the nitrogen compounds, the species most likely to cause fuel instability are alkylated heterocyclic nitrogen compounds, especially pyrroles. Removal of pyrroles from diesel fuel has been reported to increase its stability<sup>4,26,70,81,91,92,103-105</sup>. Although pyrroles represent only a small proportion of the nitrogen compounds present in diesel fuels, many studies have been reported<sup>26,30-32,39,53,57,68,70,76,81,91-94,104-106</sup> on the effect on stability of 2,5-dimethylpyrrole by several researchers for a number of reasons. This compound has been the subject of much work because it has been shown to promote the formation of insoluble materials in diesel fuel alone or by interaction with other compounds. It has been detected in middle distillate fractions rich in nitrogen and the pyrrolic functionality has been detected in gum and sediment which form in some unstable fuels<sup>53,68,104,107</sup>. Nixon<sup>4</sup>, Mushrush et al.<sup>105</sup>, Thompson et al.<sup>106</sup> and Frankenfeld et al.<sup>91</sup> reported that certain nitrogen heterocycles such as some



pyrroles and indoles are especially prone to form sediment, while other compounds are much less reactive. Thus, prediction of diesel fuel stability cannot be made on the basis of total nitrogen content alone, because the reactivity of nitrogen compounds depends upon their chemical structure. Therefore, it is extremely important to determine which nitrogen compounds will be deleterious, which types can be tolerated, and at what levels.

Worstell et al.<sup>103</sup> from their studies of deposit formation in diesel fuels concluded that nitrogen heterocycles increase the rate of deposit formation in diesel fuel under accelerated storage conditions by way of base catalysis. This increase in deposition rate is not seen when the highly polar constituents of the diesel fuel are removed. Therefore, the nitrogen base influence occurs in reactions in which highly polar fuel components are involved. Steric effects at the nitrogen atom are important. The nature of the deposited material is apparently dependent upon the presence of nitrogen compounds and on the temperature of deposition.

Thompson et al.<sup>81,106</sup> also reported that pyrroles caused the largest amounts of insoluble deposits; pyridines, while being detrimental, were less reactive. However, more recent work has indicated that alkyl indoles may play a greater role in diesel fuel gum formation than alkyl pyrroles<sup>30,31,39,86,106</sup>. Loeffler and Li<sup>57</sup> conducted accelerated ageing tests by stressing several liquid fuels in the presence of known amounts of nitrogen compounds at 50 °C. The sediments thus produced were characterised by solid state NMR, infrared and X-ray photoelectron spectroscopy. From these studies they concluded that 2,5-dimethylpyrrole is very detrimental to fuel stability. Interestingly, they also found that 2,5-dimethylpyrrole is much more potent than N-methylpyrrole and dimethylquinoline.

Jones et al.<sup>29</sup> collected sediment obtained from accelerated ageing of a shale derived diesel fuel with 2,5-dimethylpyrrole and thiophenol and showed that both pyrrole and thiophenol fragments exist in the sediment. Their results indicate that synergistic effects occur between 2,5-dimethylpyrrole and thiophenol when these

compounds are used to promote sediment formation at high temperatures in petroleum diesel fuel. In this storage study, light scattering was used to monitor particle development during the early stages of degradation. While working on storage stability of shale and petroleum derived fuels, they also concluded that 2,5-dimethylpyrrole is especially harmful to fuel stability. They placed relative reactivities of nitrogen heterocycles in the order 2,5-dimethylpyrrole followed by alkyl substituted, quinolines, pyridines and indoles.

Fookes and Walters<sup>78</sup> monitored pyrrole concentration in shale oil as a function of time and showed that in the presence of light and an oxygen blanket, the concentration dropped rapidly from 500 ppm initially to less than 10 ppm in less than 2 days in one instance. Their results indicated that at the stage when all the pyrrolic compounds had disappeared from the solution approximately 1% of the oil had been converted into gum. If the oil was allowed to mature further up to half of the oil became gum. The conclusion drawn was that although pyrroles were the most reactive compound identified they did not contribute significantly to overall sediment formation as the amounts involved were very small. It was also shown that the disappearance of pyrrolic nitrogen was very much slower under a blanket of argon.

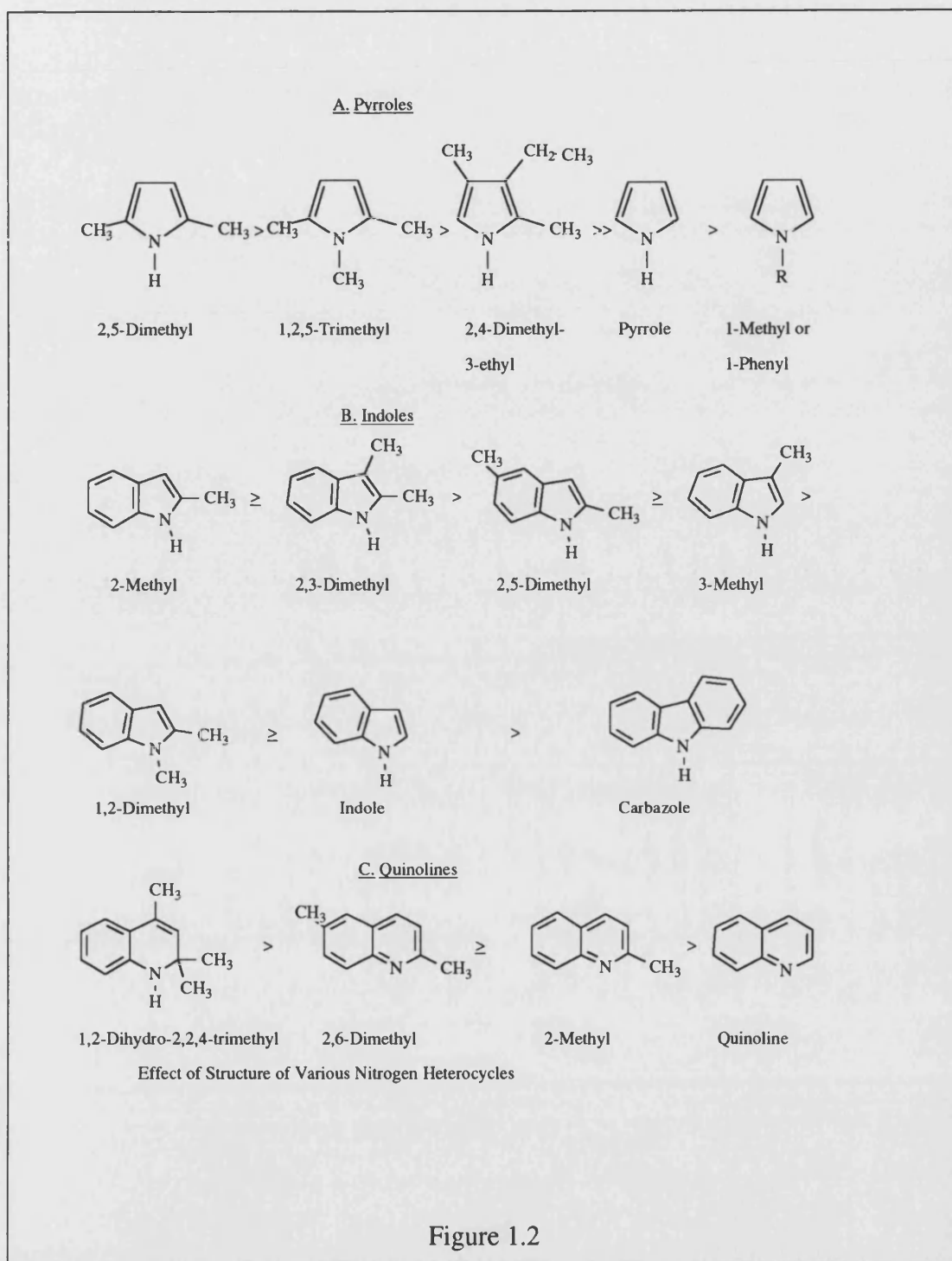
Frankenfeld et al.<sup>53,68,91,93</sup> have evaluated the relative tendencies of nitrogen compounds for promotion of sediment formation in liquid fuels under accelerated storage conditions in model systems. They found that the activities of the nitrogen compounds depend upon the structure. Non-basic nitrogen heterocycles with alkyl groups on a ring carbon adjacent to the nitrogen were highly reactive. The position of the alkyl group on the heterocyclic ring plays an important role. Alkylation on the carbon atom adjacent to the nitrogen atom activates the compound much more than on more remote positions, alkylation on the N position appears to retard sediment formation. It follows, thus, that alkylated pyrroles were the most reactive and many other nitrogen compounds had no effect on stability. From their studies on storage stability of synfuels from oil shale by using model fuel systems, Frankenfeld and

Taylor<sup>68,53</sup> concluded that the most reactive compounds were unsaturated nitrogen heterocycles with multiple alkyl groups, at least one of which being located on a carbon atom adjacent to the nitrogen atom. Amines or amides do not cause fuel instability. It appears that the most deleterious compounds were unsaturated and fall into a weak non-basic classification. They also grouped nitrogen compounds as strongly deleterious, moderately deleterious and relatively harmless with regard to their relative tendencies to form sediment in hydrocarbon fuels as shown in figure 1.1. These workers concluded that basic nitrogen compounds are much less prone to form sediment than non-basic compounds. Non-basic compounds with alkyl groups in positions 2 and 5 are especially reactive. The structural elements identified with the greatest reactivity were the compounds which have at least one double bond, an alkyl group at positions 2 or 5 and an unsubstituted carbon at position 3 or 4. They also concluded that interactions between nitrogen compounds can significantly effect sediment formation.



Figure 1.1

Amines which are considered harmless, can interact with other nitrogen compounds to either promote or inhibit sediment formation. Correlations between the chemical structure of various nitrogen heterocycles and their tendency toward sediment formation are given by Frankenfeld et al. and are shown in figure 1.2.



Beal et al.<sup>102</sup> as part of their studies on the mechanisms of syncrude/synfuel degradations, have examined in detail five classes of nitrogen compounds as dopant and co-dopants added to a stable shale derived diesel fuel. The compounds used were substituted pyridines, substituted quinolines, 2,5-dimethylpyrrole, 3-methylindole and

dodecahydrocarbazole. They concluded that a substituted pyridine and a substituted quinoline produced only a minor interaction with tert-butyl hydroperoxide, organic bases and weak organic acids, but formed large amounts of insolubles with a sulphonic acid. 2,5-Dimethylpyrrole interacted strongly with tert-butyl hydroperoxide and weak and strong organic acid to produce large amounts of sediment, but interacted weakly with organic bases. 3-Methylindole showed an interaction similar to that found for 2,5-dimethylpyrrole, but the positive interaction was significantly enhanced by venting the sample flasks. Dodecahydrocarbazole exhibited a distinctive pattern of behaviour; a strong positive increase of insolubles with tert-butyl hydroperoxide or tri-butylamine but a substantial decrease with acids, both carboxylic and sulphonic.

Most studies to date have concentrated on the role of nitrogen compounds from various sources on influencing diesel fuel stability. There is considerable disagreement however, as to which species are harmful and which mechanisms occur. It is an intention of this thesis to further investigate the influences that various nitrogen compounds have on diesel fuel stability and to develop a method for the prediction of fuel degradation by examination of simple systems and their reaction kinetics.

#### 1.4.5 Effect of Metals

The presence of only 1 part in  $10^9$  of some metals can sharply accelerate gum formation<sup>16,108</sup>. Schrepfer et al.<sup>16</sup> reported that copper will accelerate oxidation and esterification reactions to form insoluble gum. Jones and Li<sup>108</sup> found that metallic copper as copper foil or copper salt, accelerated ageing of coal derived liquids and the heavy end of petroleum products. Cu-N complexes were formed and these may accelerate certain ageing reactions. Li et al.<sup>109</sup> examined the role of the formation of copper complexes in fuel degradation in the presence of, phenol, 2,6-dimethylphenol, thiophenol and 2-methylpyridine. Copper was introduced in the form of powder, the

presence of copper in the sediment was confirmed using cyclic voltammetry and electron spin resonance. Li et al.<sup>28</sup> reported that the harmful effects of metals are in the order of  $\text{Cu} > \text{Al}, \text{Fe}$ . Beaver et al.<sup>110</sup> examined the ferric and cupric ion catalysed oxidation of indoles and the role of this process in the oxidative degradation of unstable diesel fuels. They reported that the presence of either of these ions effectively suppressed the action of hindered phenol antioxidants intended to prevent oxidative insoluble formation. The prediction they made based on their work and that of Pedley et al.<sup>111</sup> and Beranek et al.<sup>112</sup> was that an amine stabiliser and an efficient copper deactivator would be expected to significantly inhibit indole involvement in diesel fuel degradation. The results obtained at a later date by Dorbon et al.<sup>113</sup> supported this prediction.

#### 1.4.6 Effect of Storage Environment

Frankenfeld et al.<sup>53</sup> from their studies of storage stability of synfuel from oil shale concluded that light, either as sun or ultraviolet radiation, is a strong promoter of sediment formation. Model fuels containing 2,5-dimethylpyrrole stored in ultraviolet light or sunlight produced sediment up to 10 times faster than samples stored in the dark. However, the difference was greater early in the storage period. On the other hand, simply storing fuel in the dark is not sufficient to prevent sediment formation. Fookes and Walters<sup>78</sup> report that strict exclusion of oxygen from shale oil samples prevents gum formation at 45 °C for 7 weeks, even in light. From their studies of diesel fuel deterioration mechanism and additive inhibition, Lee and Stavinoha<sup>114</sup> concluded that natural sunlight has a noticeable effect on fuel deterioration.

Another important factor affecting the rate of sediment formation has been found to be the material from which storage vessels are made. White<sup>3</sup>, in studies of long term storage stability of marine distillates, found that fuels stored in metal cans developed deposits more rapidly than did those stored in either soft or Pyrex glass

bottles. He concluded that the use of tinned cans was unsuitable for long term storage because of corrosion of the can. Consequently, storage tests should not be conducted in such vessels. In addition, Christian et al.<sup>11</sup> from their studies of stability of diesel fuels during storage, concluded that soft glass has an inhibitory effect on the degradation of many fuels, but borosilicate glass is essentially inert. This effect is of obvious importance in that accelerated storage tests conducted in soft glass bottles may give erroneous results. Loeffler and Li<sup>57</sup> showed that, although soft glass has an inhibitory effect on ageing processes in relatively stable fuels, no significant differences exist between doped fuel in soft glass bottles and doped fuel in borosilicate flasks.

#### 1.4.7 Effect of Temperature and Pressure

Ritchie<sup>5</sup> and White<sup>3</sup> studied the effect of temperature on sediment formation in distillate fuel for ships and concluded that an increase in temperature increases the rate of oxidation reactions. This principle has been used in developing accelerated storage stability tests. The relation between the reaction rate and temperature follows the Arrhenius principle, which states that the logarithm of the rate constant for a reaction is proportional to the reciprocal of the absolute temperature at which that reaction takes place (section 1.7.1). Cooney, Beal and Hazlett<sup>104</sup> recommended that for tests to determine storage stability the test time should be doubled for each 10 °C decrease in temperature. This recommendation follows a rule of thumb which states that a 10 °C temperature increase will double the reaction rate. However, use of the Arrhenius equation gives a more accurate value of 1.7-3 times the rate of sediment formation per 10 °C rise<sup>115</sup>. The actual factor will of course depend upon the activation energy for the process under examination.

Nixon and Cole<sup>116</sup> studied the effect of temperature and pressure on sediment formation in jet fuel. The plot of the logarithm of the induction time against the reciprocal of the absolute temperature was found to be linear as implied by the



Arrhenius equation.

### 1.5 CHEMICAL REACTION MECHANISMS

A number of researchers have studied the reaction mechanisms of diesel fuel stability<sup>16,21,53,54,66,78-82,87,117</sup>. As detailed in section 1.4, storage instability of diesel fuel has been attributed to the formation of oxidation products of hydrocarbon components of the fuel and their subsequent reaction with sulphur, oxygen and nitrogen containing compounds<sup>66</sup>. The storage stability is also decreased due to the presence of easily oxidisable aromatic thiols and oxygen containing compounds<sup>79</sup>. The small difference between these two explanations of storage stability becomes significant when production of fuels from non-petroleum sources is considered. The differences in composition of fuels from alternative or petroleum sources will mean that either one mechanism or the other will predominate, thus affecting the final outcome. From studies of catalytically cracked distillates<sup>80</sup> Offenbauer et al. concluded that most sediment is formed through oxidation of part of the aromatic thiols present in the fuel to sulphonic acids, a reaction which, in the presence of air, leads to condensation of pyrroles.

There have been studies on the similarities or differences between the mechanisms of deposit formation on storage and on thermal stability. Dukek<sup>118</sup> stated that the initial reaction in both cases is the autoxidation of the hydrocarbon components of the fuel. In support of this, Smith<sup>119</sup> observed that during low temperature thermal stability tests the deposits were powdery and similar in appearance to storage deposits suggesting a similarity in mechanism of formation. In addition, elemental analysis yielded similar results. At higher temperatures the deposits were found to be firmly bonded to the surfaces of the storage vessels, indicating that cracking may be the primary cause of deposit formation under oxidative conditions.

Schrepfer et al.<sup>16</sup> reported that instability of middle distillates is primarily due

to three separate reactions; acid base reactions in which organic acids plus nitrogen compounds produce sediment, oxidative gum reactions in which alkenes plus oxygen produce gums and esterification reactions in which aromatic hydrocarbons plus heterocyclic nitrogen compounds and benzenethiols produce sediment in a multistep process.

The first reaction is common and most frequently occurs when product streams are blended from separate processes. The second is an autoxidation and/or a polymerisation reaction. Unsaturates contribute to fuel instability by this reaction. The increased severity of cracking processes now utilised has led to higher levels of unsaturated components able to participate in this reaction. The presence of oxygen is not needed for the initiation of this reaction. However, once contaminated with oxygen a fuel will undergo oxidative gum reactions very quickly. Investigations have shown that the major cause of instability is the esterification reaction. Some of the typical compounds identified in sediment formed by esterification are reported by Schrepfer et al.<sup>16</sup>.

Mayo and Lan<sup>54</sup> reported that most gum and deposit formation is associated with oxidation by molecular oxygen and that the rate of oxidation is not a measure of the rate of gum formation. Their results showed that the first deposits are often rich in oxygen, and that alkenes, especially conjugated alkenes increase gum and deposit formation. They concluded that oxidation is essential for the formation of soluble and insoluble gums except at pyrolysis temperatures. From this study they suggested that gum originates from two main sources, one from a chain termination mechanism, and the other from coupling of fuel molecules by peroxides in the absence of oxygen. An older alternative mechanism for gum formation is condensation by radicals from pyrolysis of hydroperoxides.

Bamford and Tipper<sup>120</sup> have explained the mechanism of low temperature liquid phase oxidation of pure hydrocarbon types found in distillate fuels as shown in figure 1.3. The mechanism is a free-radical chain reaction involving the generation of

an alkyl radical as the initiation step. This alkyl radical reacts rapidly with molecular oxygen to form a peroxide radical. Subsequently, this peroxide radical can react with more of the initial hydrocarbon substrate to generate another alkyl radical, thus continuing the chain reaction. Alternatively, peroxide radicals can combine with each other to form a stable product and terminate the chain reaction.

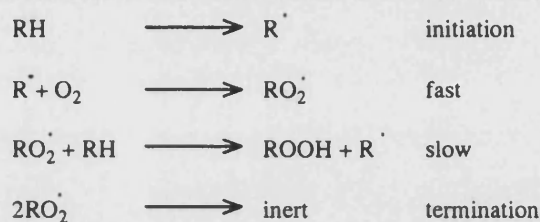


Figure 1.3

For a fixed initiation and termination rate, the rate of oxidation is controlled by the rate of the propagation step. Alkanes and cycloalkanes containing relatively strong secondary and tertiary alkyl carbon hydrogen bonds will oxidise more slowly than aromatics with weak benzylic carbon hydrogen bonds and alkenes with weak allylic carbon hydrogen bonds. Therefore, gum formed in this manner would be expected to contain a higher proportion of the unsaturated components of the fuel.

Luria<sup>121</sup> conducted studies on storage stability of gasoline, jet fuel and diesel fuel. He used 60-100 months under actual ambient conditions and found that for long periods of time oxidation stabilities of these fuels were found to have cyclic characteristics; that is, the rate of oxidation was not constant with time. For the whole period, no linear or exponential degradation was found. Similar results were shown by Le Pera and Sonenburg<sup>75</sup>.

From studies of storage stability of synfuels from oil or shale Frankenfeld and Taylor<sup>53,91</sup> reported that addition of pure nitrogen compounds to a model petroleum derived fuel system, produced sediment formation (section 1.4.4). The rate of sediment formation is dependent on the presence of nitrogen compounds, the nature

of the diluent employed and the storage conditions. Sediment formation is strongly accelerated by air, increased temperature, dissolved oxygen and light, but moisture has been found to have a variable effect. The sulphur or oxygen compounds used in this study did not produce sediment during storage at ambient conditions when tested by themselves, but interaction between pairs of nitrogen and sulphur or oxygen compounds caused both accelerating and inhibiting effects. This is in agreement with results reported by other workers. Bowden and Brinkman<sup>74</sup> together with Mayo and Lan<sup>54</sup> showed that some sulphur and nitrogen compounds increase deposit formation and some do not.

Bhan et al.<sup>21</sup> from their studies of storage stability of marine diesel fuels, suggested that oxidation of neutral compounds to polar intermediates may be a major pathway for sediment formation and darkening of marine diesel fuels. Considerable loss of polar compounds to produce sediments, both from those originally present and those newly formed, was also found. Within a compound class, the more aromatic, higher molecular weight members were observed to be the most active in sediment formation. Several fuels were aged at 65 °C for various periods and both aged and unaged fuel samples were separated chromatographically into acid, base and neutral fractions and the fractions subjected to detailed analysis. The conclusion was that oxidation of indigenous compounds in middle distillate fuels is the initial step of instability and that these or secondary oxidation products combine with indigenous polar compounds present to form gums and sediments. Thus, the compounds susceptible to oxidation actually promote or cause instability; the majority of polar compounds in the fuel passively participate in sediment and gum formation by way of various types of chemical bonding, including hydrogen bonding.

Sauer et al.<sup>83</sup> performed an experimental study of the kinetics of sediment formation in heating oils in the presence of aromatic thiols at 212 °F (100 °C). An examination of the kinetics revealed an induction period of 8-10 hours before a significant amount of sediment was formed. They also detected the presence of

oxygen in ester type linkages in the sediment. On the basis of experimental facts they were able to postulate a mechanism of sediment formation. Thiophenols catalyse the reaction of unstable hydrocarbon and oxygen to form hydroperoxides. These hydroperoxides are partially decomposed by splitting of water to form aldehydes. The aldehyde reacts with other peroxides to form monomeric oxidation products, such as acids and high molecular weight esters. Further oxidation and condensation of these products leads to the formation of insoluble gums. Mayo and Lan<sup>54</sup> have also reported that in the absence of a known initiator or catalyst, rates of oxygen absorption and gum formation in hydrocarbon fuels depend on peroxide already present or generated by light, by traces of metals or by initial slow oxidation.

Beaver et al.<sup>122</sup> reviewed some of the postulated mechanisms for alkyl pyrrole promoted sediment formation in liquid fuels. The oxidation of 2,5-dimethylpyrrole was termed an electron transfer initiated oxidation and it was considered that any electron rich organic molecule could undergo such a reaction and thus promote sediment formation. Beaver and co-workers also stated that certain metals could catalyse the oxidation reaction.

## 1.6 THE NATURE OF ULTRASOUND

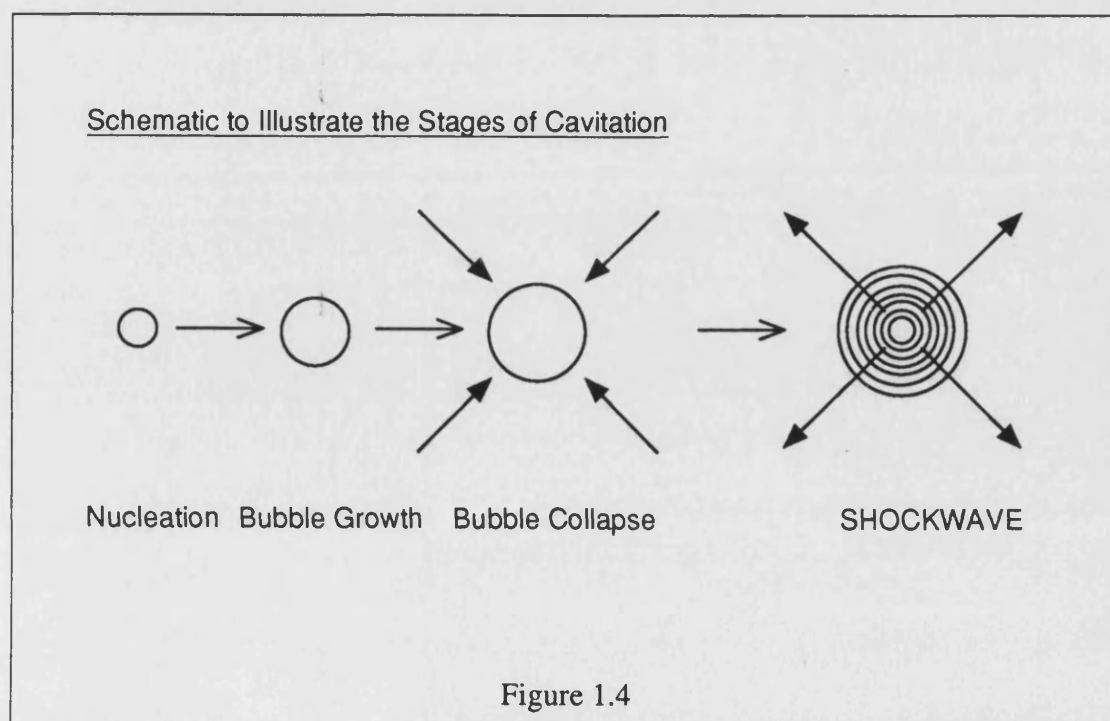
As described in section 1.4.7, increases in temperature and pressure have been shown to have an accelerating effect on the rate of degradation reactions. Therefore, alternative methods of achieving elevated temperatures and pressures should, where possible, be investigated as techniques for the assessment of fuel stability.

Ultrasonication is a method of obtaining very high instantaneous temperatures and pressures and as such was anticipated to have an accelerating effect on diesel fuel degradation and to have a deleterious effect on diesel fuel stability. Not only can ultrasound be utilised to generate high temperatures and pressures, but ultrasound can also be used to generate free radicals<sup>123,124</sup> which will then undergo free radical reactions of the types summarised in section 1.5<sup>120</sup>. The applicability of this effect to the degradation of diesel fuels, has been shown by ESR measurements done in relation to fuel stability<sup>56</sup>. It was shown that in a range of fuels, the highest free radical concentrations occurred in the fuels with the lowest storage stability.

Ultrasound is a technique which has not previously been applied to the area of fuel degradation. One aspect of the work contained in this thesis examines the utilisation of ultrasound as a fuel degradation method both directly and in model systems.

Ultrasound is the name given to sound waves having frequencies higher than those to which the human ear can respond. The upper limit of ultrasonic frequency is not sharply defined but is usually taken to be 5 MHz for gases and 500 MHz for liquids and solids. The use of ultrasound may be divided into two broad areas, low amplitude propagation and high energy propagation. A sound wave is a series of compressions and rarefactions in a medium. Low amplitude propagation involves a smaller pressure difference between these compressions and rarefactions than high energy propagation. High energy propagation may also involve more compressions and rarefactions passing through unit volume of the medium per second. The vast majority of chemical reactions studied in the presence of ultrasound are carried out in the liquid phase under either homogeneous<sup>125</sup> or heterogeneous conditions.

Under the influence of a pressure wave the average distance between the molecules in a liquid will vary as the molecules oscillate about their mean position. If the acoustic pressure on rarefaction is sufficiently large enough, the liquid will break down, and voids will be created. Figure 1.4 depicts the process of void nucleation, growth and collapse. These voids are termed cavitation bubbles. The collapse of a cavitation bubble produces a shockwave which has been estimated by calculation to generate pressures and temperatures in the range of 1000 bar and 4000 K respectively. The cooling rates calculated to go with these extremes are of the order of  $10^9 \text{ K s}^{-1}$ . To put these figures in context, the temperatures are as high as those found on the sun's surface, the pressures of deep oceanic trenches and cooling rates equivalent to molten metal being splatted onto a liquid helium cooled surface. As early as 1917 Lord Raleigh<sup>126</sup> predicted temperatures of 10000 K and 10000 atmospheres for cavitation collapse in an incompressible liquid. It is the presence of such high instantaneous temperatures and pressures in the medium which has brought about the widespread application of ultrasound to so many different areas of chemistry<sup>127-129</sup>, e.g. chemical synthesis, structural determinations, kinetic studies and polymer degradations.



For many chemical reactions the application of high power ultrasound has led to substantial improvements in both the reaction rate and product yield. This must be a result of one or another or a combination of the following:-

1. Reaction in the actual cavitation bubble, within which there are very high temperatures and pressures.
2. Reaction as a result of secondary reactions taking place at the gas liquid interface of the bubbles.
3. Reaction as a result of the enormous pressures released on bubble collapse.

The question of the precise origin of these enhancements has not been fully resolved, but what is certain is that all of the above are consequences of cavitation. Despite the many investigations of ultrasonic chemical reactions, few of these contained any detailed kinetic study of the effects of variations in irradiation frequency or intensity, the type of gas in the system or its concentration, or the solvent type and its solvent vapour pressure.

Although ultrasound has not been applied to the area of degradation of complex fuels, it has been utilised peripherally to this area. Suslick et al.<sup>130</sup> undertook a cursory examination of the effects of ultrasound on n-decane, which has been used by other workers<sup>91</sup> as a model fuel. Therefore, there is obviously a need for a more detailed examination of the use of ultrasound in the area of fuel stability. Preliminary results from this novel area are presented in chapter three.



### 1.7 KINETICS AND COMPUTERS

The burning of a candle, the operation of a petroleum cracking column and the behaviour of the ozone layer have much in common to a chemical kineticist. Each may be described as a chemical reactor involving very large numbers of individual chemical reactions taking place sequentially and simultaneously. The prediction of the behaviour of complex reaction systems is important in industry and in the laboratory, so it has been necessary to find ways of simulating such systems realistically with computer modelling. Computers have been used in this thesis for the analysis of kinetic data obtained from the fuel systems studied, and for the prediction of fuel dopant concentration change with time.

Modelling of detailed reaction mechanisms consisting of sets of elementary chemical reactions, with appropriate rate data, requires expression of the time dependence of the amounts of reactants, products and any intermediates throughout the reaction. These are based on well established theories of reaction kinetics, which provide rules to enable the conversion of an elementary chemical reaction equation into an expression for the time dependence of reactant and product concentrations.

Perez Pla et al.<sup>131</sup> have presented a multipurpose program for kinetics, OPKINE. OPKINE is designed for the study of reaction mechanisms and multicomponent analysis in dynamic conditions. The integration of differential equations is performed by means of the Runge-Kutta-Fehlberg method. The use of simulated experiments showed that complex kinetic mechanisms and mixtures of a large number of analytes could be managed with good results.

Of perhaps more pertinence is the modelling reported by Tam et al.<sup>132</sup>. They performed kinetic modelling of the oxidation reaction during desulphurisation of fuel oil by oxidation and extraction. The model describes the kinetics of sulphur removal in the oxidation of Arabian atmospheric gas oil. The kinetic model so derived can also predict the sulphur removal and residue yields from oxidation for a given space time.

From the literature it can be seen quite clearly that the modelling of kinetic systems using microcomputers is a powerful tool in the laboratory and once the kinetics of a system have been successfully modelled, reactant concentrations can be predicted without resort to experiment. As computers and languages develop or evolve, these modelling systems will become faster, more versatile and even more easily utilised.

### 1.7.1 Determination of Reaction Order, Rate Constants, Activation Energies and Pre-exponentials

In a kinetic study of a reaction the concentration,  $C$ , of a reactant,  $R$ , or product,  $P$ , is measured at various times in order to determine the rate. If this measured concentration is plotted against the time then in the cases where the order of reaction is not zero, a curve should be obtained. If the order of reaction is zero this plot will yield a straight line.

The slope of these curves at any time, is the rate of the reaction at that time. The manner in which the rate of reaction varies with the concentrations of the reacting substances can sometimes be indicated by stating the order of the reaction. The order of a reaction is strictly an experimental quantity and provides information about the way in which the rate depends upon concentration. The rate of a chemical reaction can be expressed as follows:-

$$\text{Rate} = dC_P/dt = -dC_R/dt = k(C_R)^n$$

where  $k$  is the rate constant for the reaction and  $n$  is the order of the reaction.

A commonly employed method for determining rate constants and orders of reactions involves deriving expressions relating the concentration to the time for reactions of various orders, and fitting the appropriate expression to the experimental data. If there is a good fit it can be concluded that the equation chosen is applicable and the rate constant can be obtained.

The rate constant thus obtained can be confirmed by performing the reaction

under study at differing starting reactant concentrations, and predicting the reactant concentration with time using the measured rate constant and the chosen rate expression. If the predictions are matched by the actual reactant concentration then this confirms that the measured rate constant is accurate.

In the cases examined in this thesis, rate equations for zero, first and second order kinetics were compared with the experimental data. The integrated forms of these equations are shown in table 1.1.

Table 1.1

<u>Order</u>	<u>Differential Form</u>	<u>Integrated Form</u>
Zero	$-(dC/dt)=k$	$-k=(C/t)$
First	$-(dC/dt)=kC$	$k=(1/t)(\ln(C_0/C))$
Second	$-(dC/dt)=kC^2$	$k=(1/t)((C_0-C)/(CC_0))$

In this table the symbol  $C_0$  is the initial concentration of the reactant i.e. the concentration of the reactant at time zero.

### Activation Energies

The Arrhenius law relates rate constants to activation energy and temperature and may be written as :-

$$k=Ae^{-(E/RT)}$$

where A is a constant usually known as the frequency factor, and where  $e^{-(E/RT)}$  is recognised as the Boltzmann expression for the fraction of systems having energy in excess of the value E (the activation energy). Taking logs on both sides of this equation yields a linear equation of the form :-

$$\ln(k)=- (E/RT) + \ln(A)$$

such that a plot of  $\ln(k)$  against the reciprocal of the absolute temperature

should yield a straight line of intercept  $\ln(A)$  and gradient  $-E/R$ , so that the activation energy ( $E$ ) and pre-exponential factor ( $A$ ) can be calculated.

### 1.7.2 Modelling of Reactant Concentration.

Micromodeller is a commercial software package supplied by IRL Press Ltd., compatible with IBM hardware and is designed for the integration and graphical representation of differential equations. The method used by micromodeller to solve these differential equations is the Runge-Kutta integration method. This is an iterative method that performs stepwise calculations across a range of the equation in question by breaking the range into a number of equal steps and treating the area below the curve as a series of trapezoids that it sums together. This process is repeated until the difference between two successive integrations is less than a pre-specified limit of acceptable error.

If the activation energy of a reaction is known, then micromodeller can be used to calculate rate constants at particular temperatures. These rate constants can then be used in a differential rate expression to calculate reactant concentrations with time.

In order to model a reaction pathway it is not only necessary to know the initial concentration of the reactant and the rate constant for the reaction, it is also necessary to know the order of the reaction and derive an expression for the way in which the reactant is consumed with time, that is, a differential rate equation. When the rate equation, the rate constants and the initial concentrations are known, it is possible to use micromodeller to calculate the reactant concentration with time, and having done so, to then view the resultant graph.

If the reactant profile so calculated is in agreement with observed reaction data, then the model used to calculate the profile may be a good representation or a good approximation of the real state of affairs.

For the purposes of this thesis, micromodeller has been used to integrate

differential rate equations and to predict the concentration change with time of reactants in the model systems studied. Curves generated from these calculations have been compared to the real data from which they were derived. This software has also been used to predict plots of concentration from simple rate constants derived from doped fuel systems and systems treated with ultrasound.

### 1.8 AIMS AND OBJECTIVES

This chapter has attempted to set out what a diesel fuel is and to detail some of the salient work being carried out in the area of diesel fuels. One area of primary importance is the assessment of fuel stability and a number of methods for determining this have been included. Work carried out in this thesis began with an attempt to establish the stability of a commercially available fuel, using techniques similar to those of other workers. Following this, attempts to destabilise the same fuel were made, based on the observations of other researchers. The introduction of various dopants to the fuel in conjunction with heat and ultraviolet irradiation, was examined. In addition, the use of ultrasound as a reaction accelerator for fuel degradation was investigated for the first time.

It is evident from the literature that at the present time there is no technique which has universal acceptance for predicting the instability of fuels from different sources. The innovation of introducing ultrasound to the area of fuel stability studies was undertaken in order to investigate a possible replacement for accelerated thermal tests.

The use of computers as an aid in modelling fuel degradation processes is an area which may be expected to rapidly develop. The derivation of a kinetic model for simple degradation processes was attempted, in order to enable the prediction of fuel stability from a single analysis. The following two chapters detail the experiments that have been performed and present a discussion of the results.

## Experimental

## INTRODUCTION

The experimental chapter contains details of general practical procedures used throughout the course of the work. Subsequent sections detail specific experiments carried out with diesel fuel and model fuel systems. The treatments to which these systems were subjected include thermal degradation, addition of free radicals, ultra-violet irradiation and addition of heterocyclic nitrogen compounds. A preliminary investigation into the applicability of ultrasound to the area of fuel stability studies is also included. The analytical techniques applied to these studies are covered in the final sections of this chapter.

## 2.1 GENERAL PRACTICAL DETAILS

### 2.1.1 Chemicals

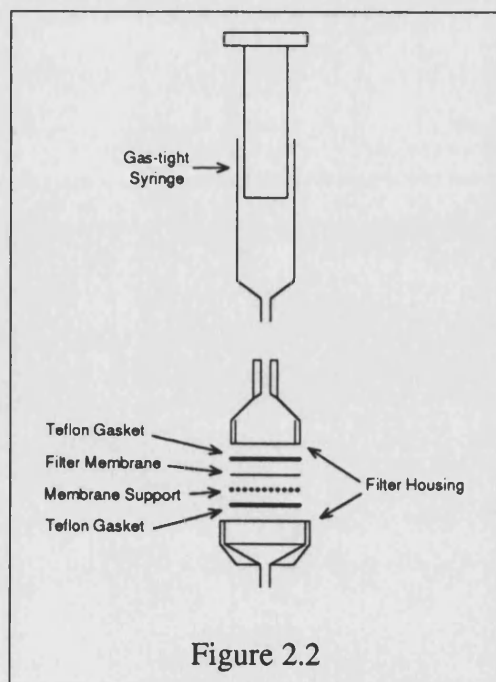
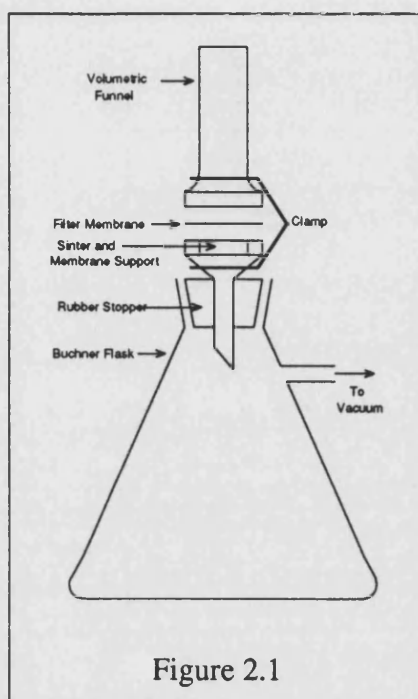
All diesel fuel used in the following experiments was a commercially available fuel purchased from a ESSO outlet and was filtered before use. The chemicals listed below were purchased from commercial sources and used as received:

n-Dodecane, n-hexane, n-tetradecane,  
Dibenzoyl peroxide, azo-bis-isobutyronitrile,  
Toluene, tetrahydrofuran,  
2,5-Dimethylpyrrole, 1,2,5-trimethylpyrrole.

### 2.1.2 Filtration

Except where stated otherwise, all filtrations performed in the course of this research were carried out in the following manner. The filters used were Whatman cellulose nitrate filter membranes of 0.45  $\mu\text{m}$  pore diameter and, depending on the scale of the filtration, either 13 mm or 25 mm membrane diameter. Before use each membrane was washed with n-hexane (HPLC grade) and dried in an oven at 118 °C for 10 minutes. After washing and drying the filter was accurately weighed.

Larger scale filtration was carried out using a Buchner flask and a water vacuum pump as shown in figure 2.1. Smaller scale filtration was performed with the aid of a gastight syringe and a special fitting as depicted in figure 2.2.





After sample filtration the filter cake was washed with n-hexane (3x20 ml aliquots) and dried in an oven at 118 °C for 10 minutes. When dry, the filter cake was removed from the oven, allowed to cool and weighed on the membrane.

## 2.2 EXPERIMENTS ON DIESEL FUEL: STABILITY TESTING

### 2.2.1 Long Term Thermal Degradation of Diesel

Before any investigation of the fuel in question was undertaken it was necessary to determine whether it was suitably stable for the tests intended.

As a preliminary stability test, 60 cm<sup>3</sup> of filtered diesel fuel was placed in a brown glass screw top bottle and kept in dark storage at 70 °C for a period of six months. It has been shown<sup>115</sup> that these conditions are equivalent to an ambient storage period of approximately sixteen years. At the end of the storage period the fuel was analysed gravimetrically for sediment content.

### 2.2.2 Thermal Degradation with Free Radical Initiators

Free radical initiators were introduced to the fuel with the intention of investigating the resistance of the fuel to effects or conditions known to cause instability. The presence of free radicals has been correlated with fuel instability<sup>56</sup> and free radical concentration has been shown to have a linear relationship with sediment formation. More specifically, the presence of peroxides in fuels has been shown to have a direct bearing on the stability of diesel fuels<sup>83,88,89,102</sup>. The free radical initiators chosen for this experiment were dibenzoyl peroxide and azo-bis-isobutyronitrile, as the former is a readily available peroxide and the latter is a commonly used free radical initiator.

#### **Short Term Experiment**

Fifteen 5 ml ampoules were weighed, filled with diesel fuel and reweighed. Six of the ampoules received approximately 0.5 wt % of dibenzoyl peroxide and six

received approximately 0.5 wt % of azo-bis-isobutyronitrile. The remaining three ampoules were blanks. After sealing, the ampoules were placed in dark storage in ovens set at temperatures of 25, 50, and 75 °C for sixteen days. At the end of the storage period, the ampoules were cracked open and their contents filtered. The ampoules were flushed with n-hexane and these washings were also filtered using the same membranes. The membranes were weighed before and after filtration.

### **Long Term Experiment**

Four 100 ml round bottomed flasks were cleaned, weighed and each filled with 100 ml of diesel. Two of the flasks had 0.5 wt % dibenzoyl peroxide added to them and the other two received 0.5 wt % azo-bis-isobutyronitrile. These flasks were placed in dark storage at 50 °C for 24 weeks. At the end of the storage period the flask contents were filtered, the flasks were washed with n-hexane and the washings were also filtered. After drying at 118 °C for 1 hour, both the flasks and filters were weighed in order to determine both filterable and adherent residue weights.

### **2.2.3 Ultra-violet Degradation with Free Radical Initiators**

#### **Initiator Degradation**

Before attempting to degrade diesel fuel with ultra-violet radiation and free radical initiators it was necessary to determine the conditions required to fully degrade the free radical initiators.

Saturated solutions of dibenzoyl peroxide and of azo-bis-isobutyronitrile were made up in carbon tetrachloride. The ultraviolet absorbance spectrum of each solution was recorded using a Unicam SP800B Ultra-violet Spectrophotometer. A sodium chloride solution cell was used to contain the solutions.

The absorbance maximum of azo-bis-isobutyronitrile was observed to be in the region of the cut off point for ultra-violet transmission through pyrex glass, so azo-bis-isobutyronitrile was judged to be unsuitable for this experiment.

The infra-red transmission spectrum of the dibenzoyl peroxide solution was recorded and the carbonyl peak intensities and positions noted. A high pressure mercury vapour lamp was used to irradiate the solution for periods of five minutes. After each period the infra-red spectrum of the solution was measured. The ultra-violet irradiation was continued until the carbonyl peak in the infra-red had diminished to a constant value. The time taken to achieve this was then used as the minimum irradiation time necessary for complete cleavage of the initiator in the diesel fuel.

### **Diesel Fuel Degradation**

Four round bottomed 100 ml flasks were weighed, filled with diesel fuel and reweighed. Two of the flasks received 0.5 wt % dibenzoyl peroxide. The flasks were irradiated together for thirty minutes using a high pressure mercury vapour lamp and placed in dark storage for a period of 24 hours.

After the storage period the contents of each flask were filtered, the flasks being flushed with n-hexane. The filters and flasks were dried at 118 °C for 1 hour, allowed to cool and weighed.

## **2.3 THERMAL DEGRADATION EXPERIMENTS ON PYRROLE DOPED DIESEL AND MODEL FUELS**

From work by other researchers it has been shown that pyrroles especially those substituted in either the 2 and 5 positions or the 1,2 and 5 positions are a major contributing factor to the instability of diesel fuels where they are found to be present.

### **2.3.1 2,5-Dimethylpyrrole in Diesel**

The thermal degradation of 2,5-dimethylpyrrole in diesel was the first system investigated, with the intention of showing the applicability of this approach to model fuel systems. Two aluminium foil wrapped 100 ml round bottomed flasks were each

filled with a mixture of 2,5-dimethylpyrrole (5500 ppm (N)) in diesel. These flasks were then placed in dark ambient storage for a period of up to 900 hours. Samples were taken from these flasks over this period and analysed using capillary gas chromatography to determine the concentration of the 2,5-dimethylpyrrole. It had been found that at concentrations below 1000 ppm (N) the 2,5-dimethylpyrrole peaks were obscured by other components in the diesel, which made accurate measurement very difficult. Therefore, an initial concentration of 5500 ppm (N) was chosen for this experiment.

### 2.3.2 The Model Systems

2,5-Dimethylpyrrole in toluene and dodecane was the first model system studied. The C:H:N ratios of this system were adjusted to give similar values to that found in doped diesel. The experimental procedure, conditions and analysis used were similar to those used for the diesel system described above. The time period for which this system was monitored was reduced to 600 hours as this was sufficient to obtain the relevant degradation data.

In depth studies were performed on 2,5-dimethylpyrrole, 1,2,5-trimethylpyrrole and a mixture of both 2,5-dimethylpyrrole and 1,2,5-trimethylpyrrole in dodecane. A concentration, temperature matrix for these three simple model fuel systems was studied in order to determine rate constants and activation energies for these systems.

Reaction mixtures were made up by weight in 10 ml sample vials covered in aluminium foil, and measured by weight into aluminium foil covered, screw top vials with teflon backed rubber septa. These reaction mixtures were placed into ovens at 40, 52, 65 and 70 degrees centigrade and the contents were sampled via the septa using a 0.5  $\mu$ l SGE syringe and analysed using gas chromatography as detailed in section 2.5.2. The temperature was maintained for periods of up to 2800 hours. At the end of the isothermal storage period, each sample vial was opened, the contents

filtered and the sediments submitted for elemental analysis. A sampling of these sediments was also submitted to gel permeation chromatography to investigate the possibility of polymer formation.

The data obtained from this concentration, temperature matrix were submitted to a detailed kinetic investigation in order to determine rate constants, reaction orders, activation energies and ultimately to enable computer modelling of the systems.

## **2.4 ULTRASONIC EXPERIMENTS**

Where reference is made to the energy of the ultrasonic irradiation, these being low and high, low energy irradiation is that delivered by the bath and high energy is that delivered by the probe. These are differentiated from each other by the power intensity of the output, measured in  $\text{Wcm}^{-2}$ .

### **2.4.1 General Experimental Details for Ultrasonic Experiments**

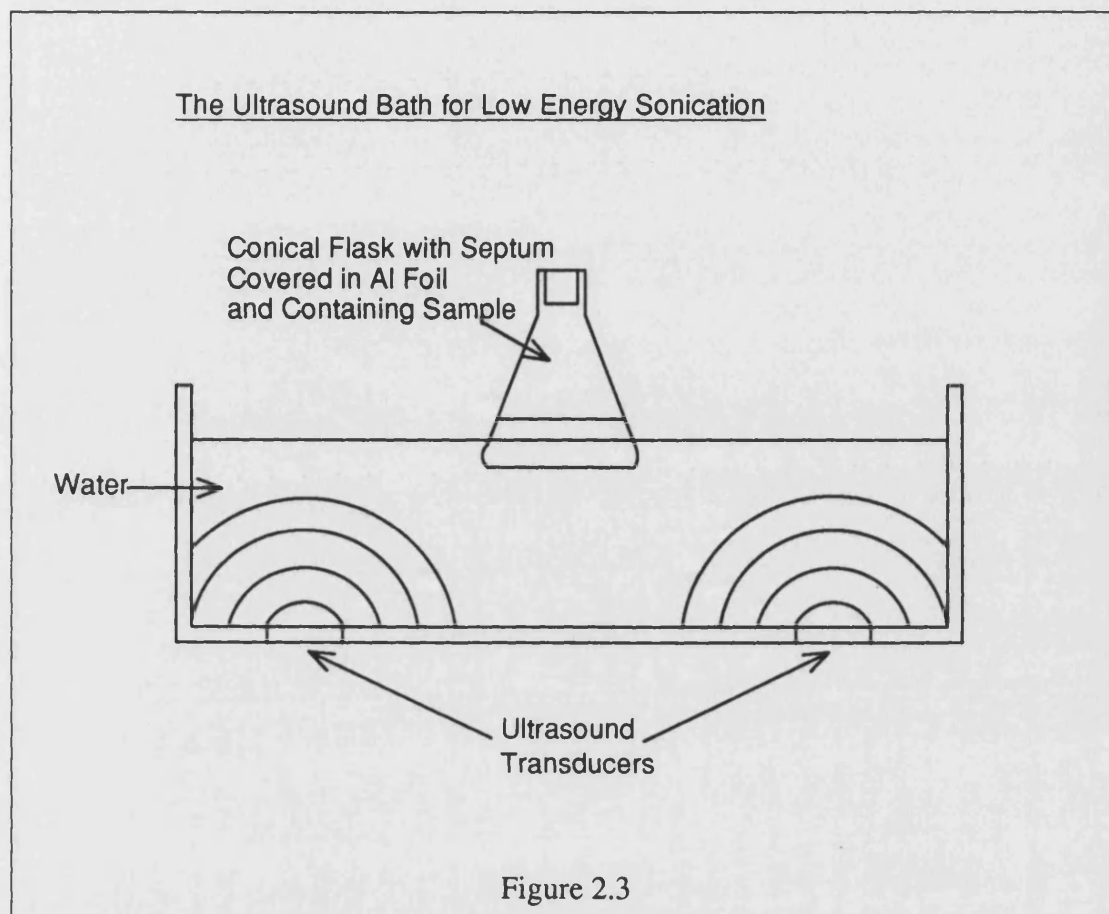
#### **Vessel Preparation**

All vessels for use with ultrasonic apparatus were prepared in the following manner. The reaction vessel was soaked in chromic acid, washed with copious amounts of distilled water and then with acetone. After air drying with compressed air, the vessel was then dried in an oven at  $118^{\circ}\text{C}$  for 1 hour. The vessel was then allowed to cool and weighed before use.

#### **The Ultrasound Bath**

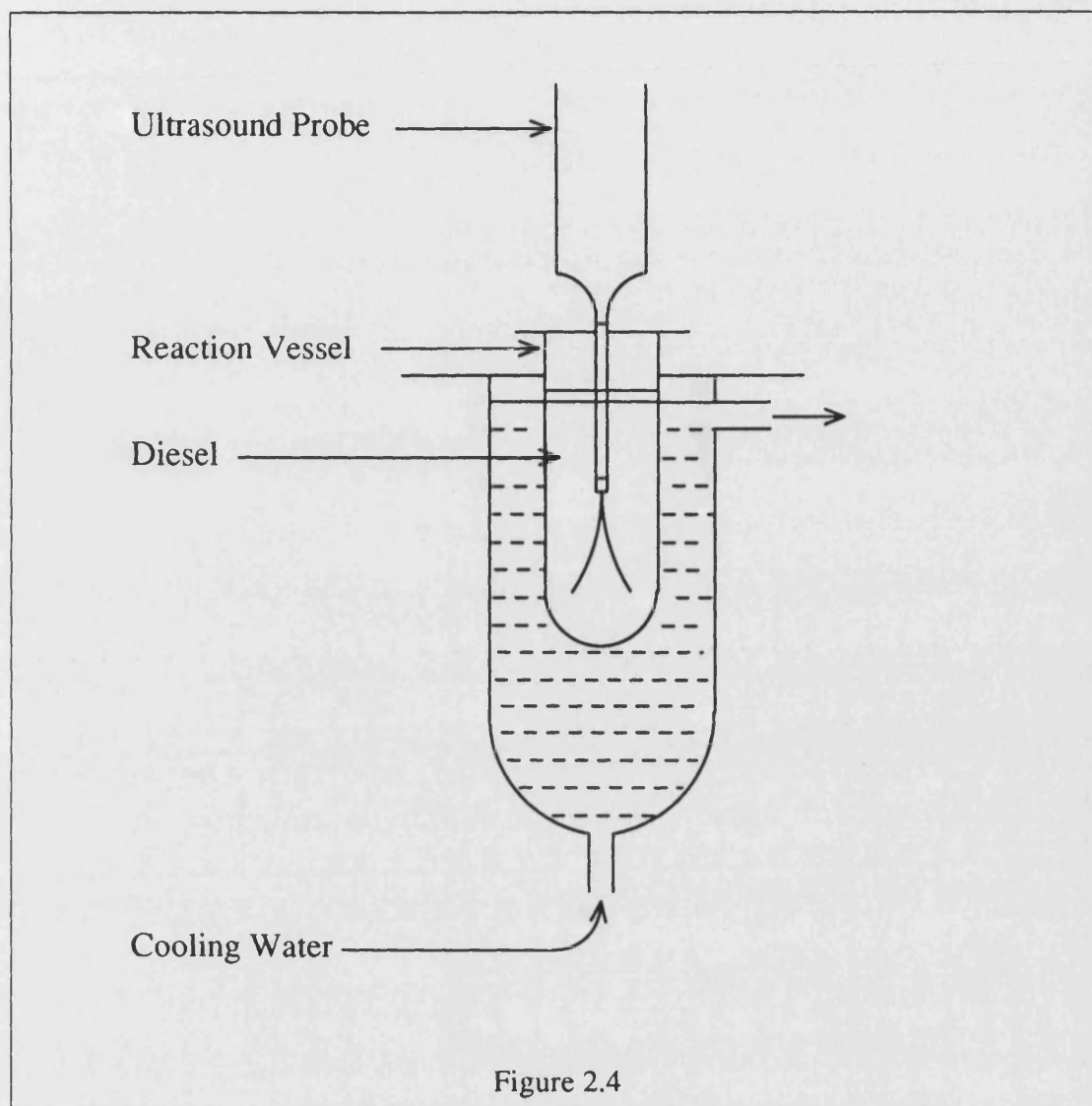
These experiments were carried out in a Kerry Pulsatron 325 (500 W) ultrasound bath. Except where stated otherwise reactions were performed in 100 ml conical flasks covered in aluminium foil to prevent ultra violet interference. The flasks were stoppered with rubber septa after being filled with reaction mixture, and partially immersed below the surface of the water in the bath. Conical flasks were chosen for use in the bath to give a large surface area to volume ratio for better

ultrasound transmission. Mason et al.<sup>133</sup> cover the experimental details for best use of an ultrasound bath.



### Ultrasonic Probe

All high energy ultrasonic irradiations were carried out with a collimated 23 kHz beam from a titanium alloy amplifying horn driven by a Sonics and Materials Inc. Vibra Cell VC600 with a variable power output and a maximum of 600 W. The probe calibration showed a power intensity of  $152 \text{ Wcm}^{-2}$  at the horn's surface with the output set to 10. Reactions were carried out using the apparatus shown in the diagram (figure 2.4).



The reaction vessel was cooled by immersion in a continuous flow water reservoir which was covered in aluminium foil to prevent interference by ultra-violet radiation. The temperature of the reaction vessel contents was continually monitored using a thermocouple.

### **Ultrasonic Probe Calibration**

In order to determine the power intensity being delivered by the ultrasound probe for a particular combination of output and pulse settings, and a particular vessel, it is necessary to calibrate the probe.

The probe was calibrated by setting up the apparatus as in the diagram (figure 2.4), and filling the reaction vessel with water equal in volume to the volume of reactant which was to be sonicated. Coolant was not used in this case so that the heating effect of the ultrasound could be measured without any interfering effects. The probe was then switched on and the temperature of the water was monitored with time. This procedure was repeated a number of times with different probe settings allowing the water to cool to the same starting temperature between sonications. With the results obtained heating curves were plotted for the heating action of the ultrasound on the water.

The whole procedure was then repeated using a heating coil in place of the sonic probe. Current consumption and voltage requirements were monitored for the heating coil with time, so that the coil power consumption, power output and energy output could be calculated. Thus, by comparison of the heating curves and a knowledge of the heating coil energy output, a power output for the probe tip was calculated.

Table 2.1 shows the heating rate of water in the sonication vessel when heated with an electrical heater. The voltage and current for these measurements were 28.1 V and 0.29 A respectively. A graph of these results, shown in figure 2.5, provides a rate of increase of temperature of  $0.514 \text{ K min}^{-1}$ .



Table 2.1

Time (min)    Temperature (°C)

<u>t</u>	<u>T</u>
0	18.9
7	20.4
10	24.3
15	25.9
20	28.0
25	29.8
30	33.0
35	36.4

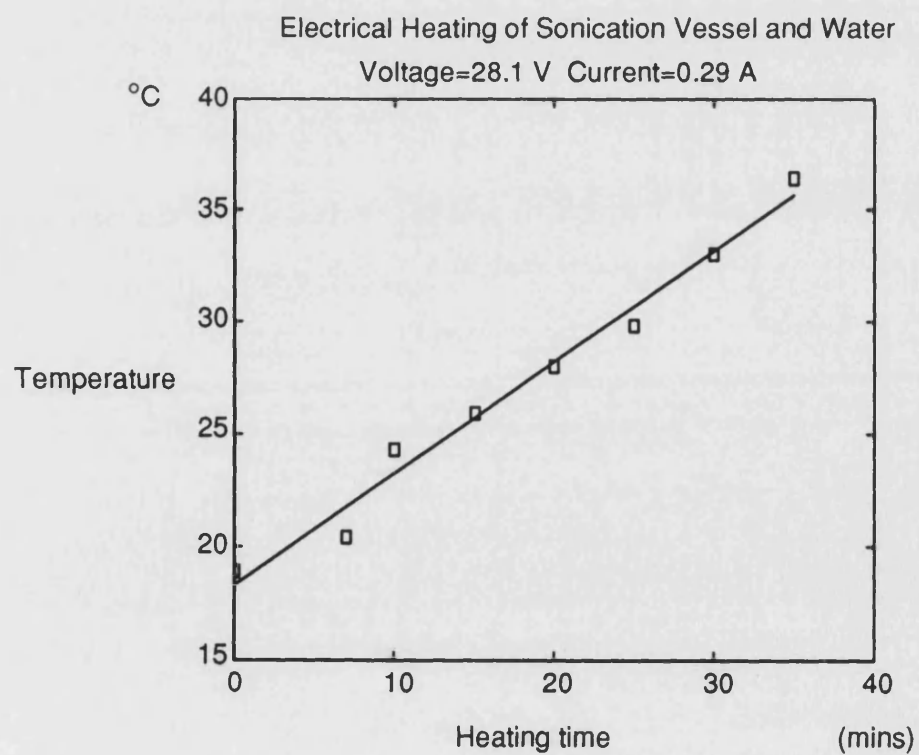


Figure 2.5

Table 2.2 below shows the change in temperature of the water with different probe power settings.

Table 2.2				
<u>Intensity Settings</u>	<u>2.5</u>	<u>5</u>	<u>7.5</u>	<u>10</u>
<u>Time t (s)</u>	<u>Temperature T (°C)</u>			
0	23.0	22.0	28.0	22.1
15	-	-	30.0	-
30	24.5	-	31.8	25.7
45	-	-	33.7	-
60	26.0	26.5	35.0	31.0
75	-	-	36.9	-
90	26.9	-	38.5	34.5
120	28.0	31.2	42.1	41.5
150	-	-	45.3	45.2
180	30.3	35.4	49.5	49.5
240	33.4	40.4	54.2	-
300	34.3	43.1	-	-
360	36.4	-	-	-

A graph of these results, shown below, provides rates of increase of temperature of  $0.036 \text{ K s}^{-1}$  at a power setting of 2.5,  $0.070 \text{ K s}^{-1}$  at 5,  $0.110 \text{ K s}^{-1}$  at 7.5 and  $0.160 \text{ K s}^{-1}$  at 10.0. From these results the actual power output of the probe tip can be calculated at different settings.

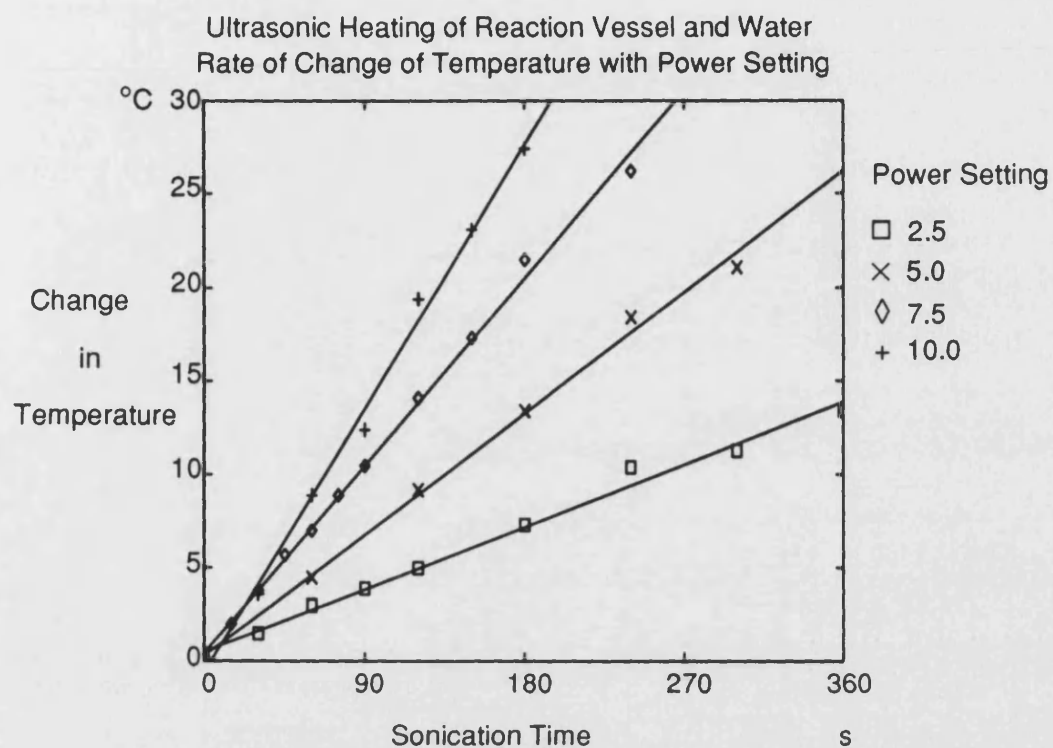


Figure 2.6

The Heat Capacity of the Apparatus ( $c$ ) is calculated as follows.

$$c = \frac{0.29 \times 28.1 \times 60}{0.514}$$

yielding a value of  $c = 951.25 \text{ J K}^{-1}$

At the different power settings the power output can then be calculated as the temperature change per second multiplied by the heat capacity of the apparatus.

These calculated values are shown in table 2.3.

Table 2.3

<u>Intensity Setting</u>	<u>Power Output (W)</u>
2.5	35
5.0	67
7.5	105
10.0	153

A graph of these values (figure 2.7) demonstrates the linear relationship between the intensity setting and the power output of the probe and can be used to predict power output values at intermediate intensity settings.

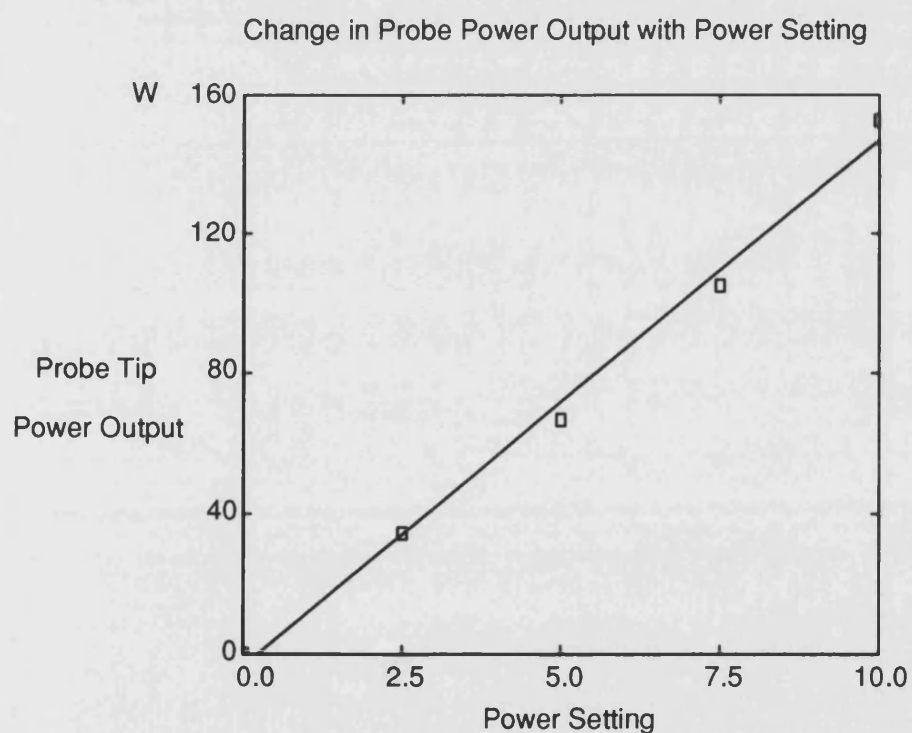


Figure 2.7

#### 2.4.2 Low Energy Sonication and Storage of Diesel Fuel

Two 100 ml round bottomed flasks were cleaned and weighed. Each flask was filled with 100 ml of diesel fuel. The contents of both of these flasks were subjected to an hour of low energy ultrasound and subsequently placed in dark ambient storage.

After a period of 24 hours the flasks were removed from storage and their contents filtered, each flask being flushed with n-hexane. The flasks and the filters were dried in an oven at 118 °C for 1 hour, allowed to cool and weighed.

A similar experiment was also performed using dibenzoyl peroxide, a free radical initiator, in conjunction with the ultrasound. The initiator was present at a concentration of 0.5 wt %.

#### 2.4.3 Ultra-violet and Low Energy Ultrasonic Degradation: A Comparison

Ten 100 ml round bottomed flasks were cleaned and weighed. Each flask received a combination of diesel, 2,5-dimethylpyrrole, 1,2,5-trimethylpyrrole and dibenzoyl peroxide, giving a total of five duplicated mixtures each of 100 ml volume.

One half of the mixtures were subjected to 30 minutes of ultra-violet irradiation from a high pressure mercury vapour lamp. The other half of the mixtures were each subjected to a 15 minute period of low energy ultrasound. The flasks were then placed in dark ambient storage for 1 week.

After storage, the contents of each flask were filtered. Each flask was then flushed with n-hexane and the washings also filtered. After drying, both the filters and the flasks were weighed.

10 ml of combined washings and diesel from each experiment were put back into dark ambient storage for later examination.

#### 2.4.4 Low Energy Sonication of 2,5-Dimethylpyrrole Doped Model Fuel

The systems studied in this experiment contained 2,5-dimethylpyrrole in dodecane in concentrations of 1032, 1480, 1818 and 2006 ppm (N). The units of concentration (ppm (N)) are defined as the mass of nitrogen in mg per litre of dodecane. Sample volumes were 40 ml and samples were made up by weight. The samples were sonicated for a total of approximately 900 hours and samples were taken for analysis approximately every 35 hours. Samples for analysis were removed via the septa using a 0.5 µl SGE syringe and analysed by gas chromatography as detailed in the chromatography section. The bath temperature was monitored using a simple mercury in glass thermometer and was found to stabilise at 44 °C.

Degradation data were corrected using the previously determined calibration curve. The data were subsequently manipulated using the "As-Easy-As" spreadsheet program.

#### 2.4.5 High Energy Sonication of n-Dodecane (a Simple Model Fuel)

Using the previously described apparatus, where the reaction vessel was a brown glass bottle of 1.0 l capacity, 900 ml of dodecane were measured into the vessel and sonicated for periods of 40 hours to a total of 280 hours with the acoustic power set to an output of 50% and a pulse rate of 50%. At the end of each sonication period two 2 ml aliquots of dodecane were taken from the vessel and transferred to screw top sample vials covered with aluminium foil. These were placed in a refrigerator at 4 °C for later analysis by gas chromatography as detailed in section 2.5.3.

#### 2.4.6 High Energy Sonication of Diesel for Sedimentation Kinetics

Using the apparatus described previously, where the reaction vessel was a 200 ml centrifugation tube, three 50 ml aliquots of diesel were measured into the reaction vessel to make a total of 150 ml. The diesel was then subjected to ultrasonic

irradiation for a preset period of time with the acoustic power set to full intensity and an uninterrupted signal i.e. no pulsing. The contents of the vessel were then filtered, dried and weighed, with the vessel being flushed with three 20 ml aliquots of n-hexane (HPLC grade). The vessel was weighed before and after the experiment and was cleaned between sonications after each weighing.

The time periods used for sonication began with six hours and were increased in increments of six hours to a total of thirty six hours.

After drying and weighing, the sediment obtained was analysed by elemental analysis for carbon, hydrogen and nitrogen content (C:H:N). A sample of the final sediment was also analysed for polymer content, by dissolution in tetrahydrofuran and gel permeation chromatography.

The filtered diesel was put into brown glass bottles and stored in the dark for examination after one years storage at ambient temperature. After this storage period the diesel was filtered and the amount of sediment that had been formed was determined gravimetrically.

#### 2.4.7 High Energy Sonication of Diesel, The Effect on Alkane Distribution

Using the apparatus described for sonication by probe, 900 ml of diesel fuel was sonicated in a brown glass bottle in the same manner as described for sonication of n-dodecane. This sonication was maintained for a total time of 360 hours with samples being taken every 40 hours, resulting in ten sets of samples including a blank. These samples were analysed using Gas Chromatography/Mass Spectroscopy (GCMS). The final product was filtered and the sediment submitted for elemental analysis and also analysed for polymer content using gel permeation chromatography.

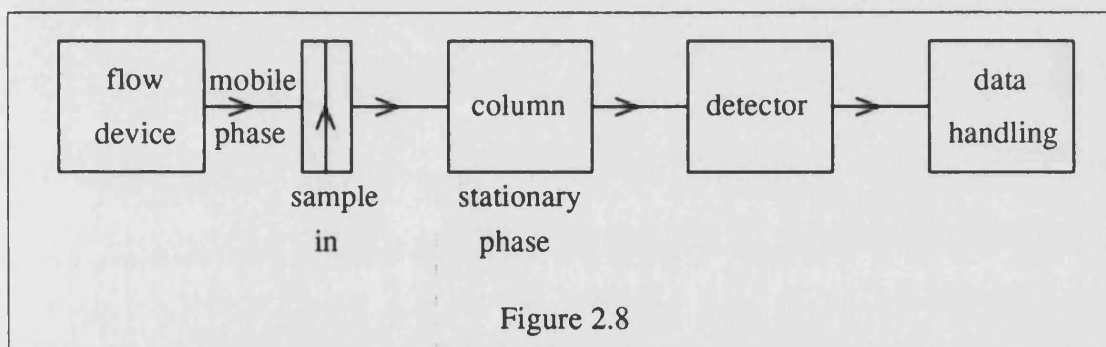
## 2.5 ANALYTICAL TECHNIQUES

### 2.5.1 Elemental Analysis

Elemental analysis was performed by courtesy of the University of Bath analytical services on a Carlo-Erba Strumentazione Elemental Analyzer (Mod. 1106) with a ICL DRS M30 Data Station.

### 2.5.2 Chromatography

Chromatography is a separation technique and is, in its various forms, the most widespread and useful analytical method available. It can be used for qualitative and quantitative analysis, for preparative separations and for physicochemical measurements. A simple schematic of a chromatographic system is represented in figure 2.8.



### 2.5.3 Gas Chromatography

Gas chromatography is probably the most widespread of the routine analytical techniques. The sample is carried along the column using a gas as a mobile phase. The stationary phase can be liquid or solid. The carrier gas is fed to the columns via regulators and flow valves to ensure a constant flow rate. The most accurate way to measure flow rate is by using a soap bubble flowmeter. Flow rate can also be measured by injecting a compound which does not interact with the column and determining its retention time. Thus, knowing the characteristics of the column i.e.



length and cross sectional area, volumetric or linear flow rate can be calculated.

Volatile samples, are injected through a septum, using very small sample amounts in the range 0.5-1  $\mu\text{l}$ . Gases and vapours are usually injected via a sample valve as in liquid chromatography, (see size exclusion chromatography).

The chromatography column is usually contained in an oven, the temperature is kept constant to plus or minus half a degree centigrade for isothermal use. For samples containing a number of components, temperature programming is more common.

Packed columns are generally 1/8" to 1/2" diameter, tubes of coiled glass or stainless steel, of 2-3 meters in length. They can be packed with an active solid or an involatile liquid spread onto an inert solid. Gas Solid Chromatography (GSC) is generally used for analysis of gases or low boiling and low molecular weight materials. In Gas Liquid Chromatography (GLC) a large number of liquids are generally available as stationary phases, these number over 400. The solid support has a very important effect and needs to be of a high surface area, of uniform pore size, strong and inert.

Capillary columns achieve high surface area by using long 10-100 meter tubes of 0.1-0.5 mm diameter, usually made of glass, stainless steel or fused silica. Originally, capillary columns had to utilise very thin (1-2  $\mu\text{m}$ ) films of liquid, as thicker films were unstable, but now the liquid can be bonded to the inner surface of the capillary, or this surface can be coated with a polymer, which can then be crosslinked, so that films of 5-10  $\mu\text{m}$  can be used.

The disadvantages of capillary columns include the low flow rate, the use of a special injector and a high sensitivity detector, and of course by their very nature, capillary columns are fragile. The advantages include the very high efficiencies of the technique and the small sample sizes (at the nanogram level), as well as far better resolution, leading to lower analysis times.

Many types of detector are used in gas chromatography, including some that

are specific for particular elements. Ionisation detectors are a series of detectors that cause the sample to ionise and measure the extent of the ionisation, usually by measuring the current between two charged plates. The most common type of ionisation detector is the flame ionisation detector (FID). The carrier gas is mixed with hydrogen and air and this is burned. Combustion causes formation of ions and hence generates a current between the plates. This type of detector is especially good for organic compounds. The FID is the most common form of detector in use and is very sensitive, down to  $10^{-11}$  grammes of alkanes or the parts per billion range. It is also insensitive to column temperature, so it is good for temperature programmed work.

Chromatographs have also been coupled to various spectroscopic techniques. Mass spectroscopy is a spectroscopic technique that has proved particularly useful in the qualitative analysis of complex mixtures when coupled to capillary chromatography.

### **The Use of Gas Chromatography**

The main instrument used in this investigation was a PYE 204 gas chromatograph fitted with a flame ionisation detector and connected to a Spectra-Physics model SP4270 integrator. A stainless steel 5 m column with 4 mm internal diameter packed with 10% SE30 on a diatomite support was used in this work.

The injected sample volumes were 0.5  $\mu$ l. Dry, oxygen free nitrogen was the carrier gas and its volumetric flow rate was measured using a bubble flow meter. The injector port was set at a temperature of 250 °C and the detector oven was set at 300 °C. The oven temperature and the carrier gas flow rate were set according to the requirements of the system under study.

### **2,5-Dimethylpyrrole and 1,2,5-Trimethylpyrrole**

Thermal and ultrasonic degradation of 2,5-dimethylpyrrole and of 1,2,5-trimethylpyrrole in dodecane were monitored using an oven temperature of 155 °C and a carrier flowrate of 60 cm<sup>3</sup>/minute.

### **Dodecane**

Ultrasonic degradation of dodecane was monitored using a carrier flow rate of 40 cm<sup>3</sup>/minute and a column temperature of 155 °C. Peak identification was performed with the aid of a calibration mixture (supplied by Phase Sep) containing a range of n-alkanes. Peak retention time was the identifying criterion for unknown peaks in the sonicated dodecane.

### **Gas Chromatograph Calibration**

In order to make measurements of the concentration of a species in a mixture by gas chromatography, it is necessary to calibrate the detector. This is done by making up mixtures of the species to be measured in the solvent system being used, covering a range of concentrations which may be expected during an experiment, and adding a known amount of a reference species, an internal standard, to which the reactant species is referred. These calibration mixtures are then injected onto the column and analysed using the same conditions as would be used for the analysis of a reaction mixture. The results obtained from these analyses are then used to calculate response factors with respect to the internal standard, and these response factors are plotted against the actual concentration of the reactant in the reaction mixture to obtain a calibration curve.

### GC Calibration for Analysis of Doped Model Fuel Systems

The following calibration curves were determined for 2,5-dimethylpyrrole in dodecane and 1,2,5-trimethylpyrrole in dodecane. These plots were used throughout this thesis where concentrations of either dopant were required.

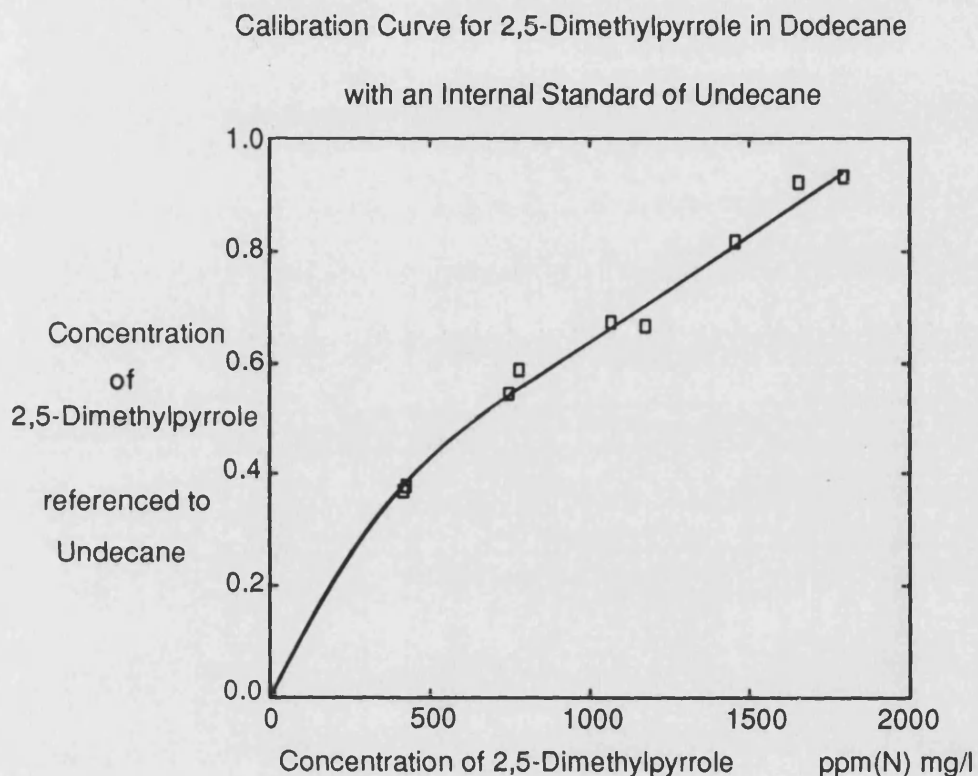


Figure 2.9

2,5-Dimethylpyrrole in dodecane produces a linear response when analysed using gas chromatography and a flame ionisation detector. The equation of the calibration plot is of the form  $y=mx+c$  and it is a simple exercise to use this equation to transform raw analysis data into concentration values measured in ppm(N) mg/1000 ml.

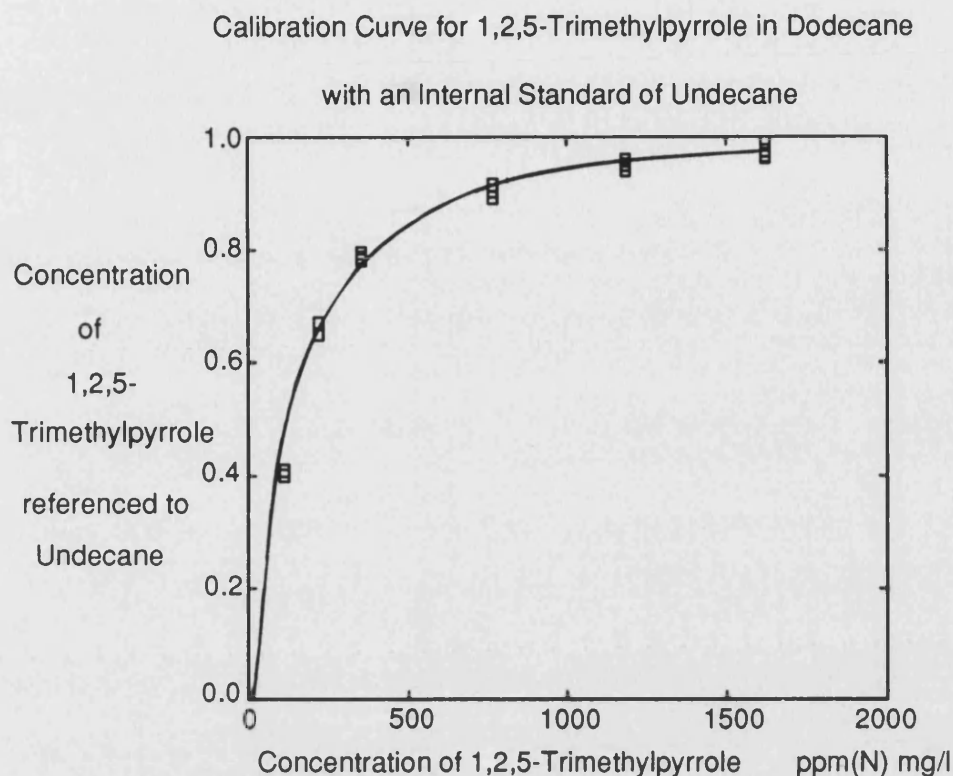


Figure 2.10

1,2,5-Trimethylpyrrole in dodecane does not produce a linear response when analysed using gas chromatography and a flame ionisation detector. This introduces a small amount of difficulty to the process of transforming raw data into concentration values, because fitting an equation to a non-linear data set is more problematical than fitting data to a linear equation. The equation which was found to give the best fit for the calibration data, was of the form  $y = x^{-0.5} + c$ . This equation when found proved suitable for transforming raw data.

#### 2.5.4 Gas Chromatography/ Mass Spectrometry

A GC/MS system was used to monitor the changes in composition during sonication of diesel fuel. The instrument used was a Hewlett Packard Gas Chromatograph/ Mass Spectrometer (HP 59970C GCMSD) with a split-splitless injector and a HP 7673A Autosampler. A 25 m fused silica, open tubular column of

0.33 mm internal diameter coated with a 0.15  $\mu\text{m}$  film of immobilised OV101 was used in this work. The injected sample volumes were 1  $\mu\text{l}$  splitless with a carrier gas of clean dry hydrogen at an average linear velocity of 20  $\text{cm s}^{-1}$ . The injector port was set at a temperature of 300  $^{\circ}\text{C}$ , while the temperature of the column oven was programmed from 80  $^{\circ}\text{C}$  to 250  $^{\circ}\text{C}$  at 4  $^{\circ}\text{C min}^{-1}$  with an initial pause of 3 minutes and a final pause of 4 minutes. This system was also used to perform analysis of unsonicated diesel fuel.

Diesel fuel samples were diluted in n-hexane by a factor of six before injection onto the column to avoid overloading of the mass spectrometer. Peak identification was aided using the calibration mixture mentioned earlier. However, the main mode of peak identification was the library of fragmentation patterns supplied as a data package for comparison purposes in a Hewlett Packard data handling package.

#### 2.5.5 Capillary Chromatography

A Hewlett Packard Gas Chromatograph with a split-splitless injector, flame ionisation detector and an integrator printer unit was used for analysis of 2,5-dimethylpyrrole in diesel and in a dodecane toluene system. A 25 m fused silica open tubular column of internal diameter 0.33 mm coated with a 0.15  $\mu\text{m}$  film of immobilised OV101 was used in the chromatograph.

The injected sample volumes were 0.5  $\mu\text{l}$  with no split. The carrier gas was clean, dry, oxygen free nitrogen at an average linear velocity of 20  $\text{cm s}^{-1}$ . The injector port and the detector were both set at a temperature of 300  $^{\circ}\text{C}$  while the temperature of the column oven was programmed from 80  $^{\circ}\text{C}$  to 250  $^{\circ}\text{C}$  at 4  $^{\circ}\text{C/min}^{-1}$  with an initial and final time of 10 minutes.

### 2.5.6 Gel Permeation Chromatography

Size exclusion chromatography or gel permeation chromatography (GPC) is a relatively recent method developed for measuring a range of polymer characteristics, covering the number average molecular weight, the weight average molecular weight, the Z average molecular weight and the polydispersity, which is a measure of the spread in the chain lengths of the polymer.

GPC is a high performance liquid chromatography (HPLC) technique, the difference lying in the actual column packing. A pumping system that can deliver clean, dust free, degassed solvent against very large pressures is required. This system must also supply a constant pulse free and accurate flowrate. The pressures generated in this type of system are in the hundreds of atmospheres, obviously a syringe cannot supply the sample against pressures of this magnitude. A switching valve is used, where a loop is filled with the sample in solution at atmospheric pressure and the flow is then switched through the loop.

A number of types of detectors are used which fall into two classes. The first type utilise a property of the sample not shared with the solvent, such as, ultra-violet absorbance, fluorescence or conductivity. The second type utilises a difference in bulk property between the solvent and the sample, such as refractive index.

The stationary phase consists of a porous packing, such as silica or a crosslinked polymer, with organic solvents and dextrans "Sephadex" for aqueous polymers. The separation mechanism as suggested by the name, size exclusion chromatography, is that small molecules can enter the pores in the packing matrix and are retained on the column, whereas large molecules cannot enter the matrix and are eluted before the small molecules.

GPC is a secondary method, this means that it requires calibration with known standards. Calibration is done by taking a series of polymers with very low polydispersity and known molecular weight and running chromatograms to get a calibration curve. Usually calibration is performed with commercially available

polymers prepared by anionic polymerisation, polymers such as polystyrene, polymethylmethacrylate and polyethyleneoxide.

### **Experimental Aspects**

Gel permeation chromatography was carried out on a Bruker pumping system with a Bruker LC21/41 system. The mobile phase was HPLC grade tetrahydrofuran. The column was 'PL Gel' 60 cm 'linear' crosslinked polystyrene divinylbenzene resin. The sample was introduced to the mobile phase via a sampling valve as a single 50  $\mu$ l injection of 5 wt/vol % sediment in THF. The sample was filtered prior to injection.

Mobile phase flow rate was 2 ml/minute and inlet pressure was 60 bar. Data handling was performed using an Epsom data station. Peaks were detected using a Bischoff differential refractive index detector and a Bruker ultra-violet fixed wavelength detector arranged in series. System calibration was performed using polystyrene reference polymers of known molecular weight and polydispersity.



## Results and Discussion

### 3.1 INTRODUCTION

This chapter details the results obtained from the experiments on diesel and model fuels described in the experimental section. Thermal and ultra-violet degradation techniques were used in conjunction with free radical initiators and heterocyclic nitrogen compounds. The thermal and ultra-violet studies, some in the presence of free radical initiators, were performed to test the stability of the diesel. The heterocyclic nitrogen compounds were studied for their potential use as model dopants since literature studies have shown them to be important in promoting diesel degradation.

The results obtained from model fuel experiments using 2,5-dimethylpyrrole and 1,2,5-trimethylpyrrole as dopants have been subjected to a detailed kinetic analysis. The raw data are represented graphically in the appendix and the analysis of the data is reported in this chapter. This analysis includes some computer modelling of the system with the intention of predicting fuel degradation.

The use of ultrasound for the degradation of diesel fuel has not previously been reported. Results from the novel experiments in this area are also detailed in this chapter. This method showed the possibility of being developed as a new test for fuel stability with several advantages over existing tests. As ultrasound is a new technique in this area there is obviously potential for a vast amount of further research.

### 3.2 EXPERIMENTS ON DIESEL

These initial experiments were intended to investigate the stability of the diesel fuel used throughout this thesis. The stability of the fuel was assessed in terms of the propensity of the fuel to form sediments under various conditions. The conditions chosen were ones known to promote the formation of sediment in a manner considered to be analogous to long term ambient storage.

### 3.2.1 Long Term Storage of Undoped Diesel

This early experiment involved the storage of the diesel fuel at an elevated temperature in order to simulate the effects of long term ambient storage. The diesel showed no evidence of sediment formation after storage at a temperature of 70 °C for a period of six months. On filtration a slight discolouration of the filter membrane was noted, but no residue was found. There was also found to be no residual gum or adherent residue detectable by weight difference of the storage vessel.

Use of the Arrhenius equation gives a value of 1.7-3 times the rate of sediment formation per 10 °C rise<sup>115</sup>. Six months storage at 70 °C is, therefore equivalent to at least 16 years storage at an ambient temperature of 20 °C, assuming a doubling of reaction rate with each 10 degree increase in temperature. This assumes an activation energy of approximately 50 kJ mol<sup>-1</sup>. The volume of diesel fuel used in this experiment was 60±0.1 ml and weighing was performed to an accuracy of 0.1±0.05 mg, so any degradation that had occurred was on a scale of less than 2 ppm or mg/l.

This figure compares well with results obtained by Pedley et al.<sup>50</sup> for ambient storage of a Middle Eastern straight run diesel which formed an estimated mass of sediment of 0.8 mg dm<sup>-3</sup> (ppm) after sixteen months of storage. The fuel used by Pedley et al. was termed, by them, a stable fuel. From this result it can safely be concluded that the diesel used in these experiments is, under normal conditions, a stable fuel. After demonstrating the thermal stability of the fuel it was necessary to investigate the effects of other possible methods of fuel degradation by use of various dopants and accelerating conditions with those dopants.

### 3.2.2 Thermal Degradation of Free Radical Initiator Doped Diesel

As has been discussed earlier, the presence of free radicals in diesel has been correlated with fuel instability<sup>56</sup>. In particular peroxide radicals have been shown to have a deleterious affect on the integrity of fuel<sup>83,88,89,102</sup>. An investigation of these effects on the fuel used in this thesis was carried out using dibenzoyl peroxide and

azo-bis-isobutyronitrile as free radical initiators.

### **Short Term Experiment**

The results from the short term (380 hours) experiment yielded no detectable residues or sediments. This would indicate that, in the short term, the fuel used in these experiments is resistant to the presence of free radicals. However, this may have been due to the low sample volumes used in the experiment. In order to confirm that the results from this experiment were not due simply to the low volumes used, a similar experiment for a longer period of time, utilising larger volumes, was performed.

### **Long Term Experiment**

As the short term experiment did not yield detectable sediments, larger volumes (100 ml) and a longer storage period (4030 hours) were used in this follow up experiment. Surprisingly, the formation of sediments was again undetected, suggesting once again that the fuel being used in this investigation was stable even to the presence of free radicals, which have been found by other groups<sup>54,56,88,89,102</sup> to either be the cause of instability or to be present in larger amounts in less stable fuels. It was noted, however, that the fuel used was discoloured after the storage period, but the filterability characteristics remained unchanged.

### **3.2.3 Ultraviolet Degradation of Doped Diesel Fuel**

#### **Ultraviolet Degradation Conditions**

The ultra-violet absorption of dibenzoyl peroxide occurs at a wavelength of approximately 230 nm. A saturated solution of dibenzoyl peroxide in carbon tetrachloride was irradiated with a high pressure mercury vapour lamp. An irradiation period of thirty minutes was found to be sufficient to cleave all of the dibenzoyl peroxide to radicals. Therefore, in the following experiment, an irradiation period of

thirty minutes was considered to be adequate for complete breakdown of the initiator to radicals.

### **Diesel Fuel Degradation with Dibenzoyl Peroxide Initiator**

Fuel was irradiated for thirty minutes in the presence of dibenzoyl peroxide and then placed in dark storage for twenty four hours. After filtration of the flask contents and washing of the flasks, sediment gum and adherent residue were not detected. If any filterable solids had been produced during degradation of the diesel fuel they were on a scale of less than 2 ppm or mg/l since this is the lowest limit of detection for the conditions used.

It was noted that immediately after irradiation and before commencement of dark ambient storage, the diesel fuel had undergone a colour change and darkened appreciably. This colour change was also observed if the doped fuel was left to stand in direct sunlight. Although the dibenzoyl peroxide apparently does not cause sedimentation to occur in the fuel, the colour change would indicate that some fuel degradation had occurred. A peroxy radical chain oxidation mechanism<sup>134</sup> has been suggested for the mechanism of fuel degradation by the presence of peroxides, but evidence would suggest<sup>47</sup> that the situation is more complex than this. The action of sunlight and ultra-violet irradiation have both been shown to accelerate the formation of insolubles during ambient storage of diesel fuels<sup>53</sup> which confirms that some degradation is occurring in this case. However, this degradation would not be of the type to impair fuel filterability characteristics unless the viscosity of the fuel had also increased. As the area of interest for this thesis is sedimentation in fuel degradation, the lack of sediment was taken as further evidence for the stability of the diesel fuel under investigation.

Having shown that the diesel was a stable fuel, it was then doped with a chemical known to cause instability which has been found to be present in unstable fuels. This was carried out with the intention of examining the dopant for the purpose

of a kinetic study using model fuel systems.

#### 3.2.4 Thermal Degradation of 2,5-Dimethylpyrrole Doped Diesel

As described in the introduction, it has been shown that pyrroles, especially those substituted in either the 2 and 5 positions or the 1,2 and 5 positions, are a major contributing factor to the instability of diesel fuels where they are found to be present.

Before investigating the degradation of 2,5-dimethylpyrrole in a model fuel, the kinetics of degradation were investigated in actual diesel. This was performed in order to show the applicability of a model fuel system in demonstrating the behaviour of real systems. The necessity for this approach arose from the complexity of diesel fuels as observed when they are analysed using gas chromatography. A great many chromatographic analysis techniques have been developed to examine the various components of fuels. Of these, most have been aimed at identification of hydrocarbon or aromatic groups within the fuel<sup>135-146</sup>. Other techniques<sup>147-150</sup> have examined the heterocyclic components of the fuels, but regardless of the focus of the analysis, the analytical techniques have been complicated and involved. As the main thrust of this thesis is not concerned with the actual techniques of chromatographic analyses for fuels, the adoption of one of these analysis techniques was not considered. Figure 3.1 shows an example of an analysis of diesel fuel using capillary gas chromatography, the graph is a Total Ion Chromatogram of the analysed fuel. The complexity of the fuel can be clearly seen.

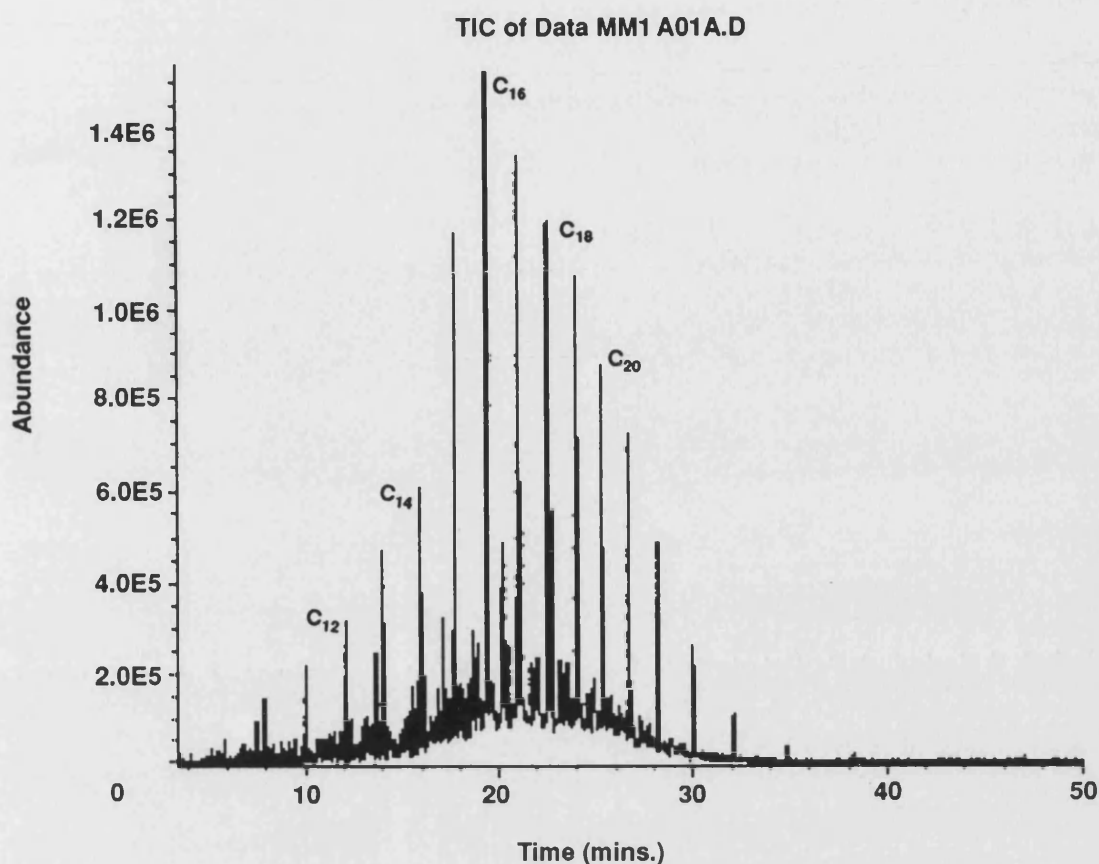


Figure 3.1

Diesel doped with 2,5-dimethylpyrrole (5500ppm (N)) was stored at ambient temperature for a period of 900 hours and the dopant concentration was measured periodically.

The graph (Figure 3.2) shows that 2,5-dimethylpyrrole in diesel degrades exponentially with time. This is indicative of a first order reaction and can be confirmed by a linear fit with a first order plot.

The log plot of  $C_0/C_t$  against time (Figure 3.3) clearly shows a linear relationship again indicative of first order kinetics. The gradient of this line is  $0.0015 \text{ h}^{-1}$  which is the rate constant for the disappearance of 2,5-dimethylpyrrole in diesel when stored at an ambient temperature of  $20^\circ\text{C}$ .

## Thermal Degradation of 2,5-Dimethylpyrrole in Diesel

at ambient temperature

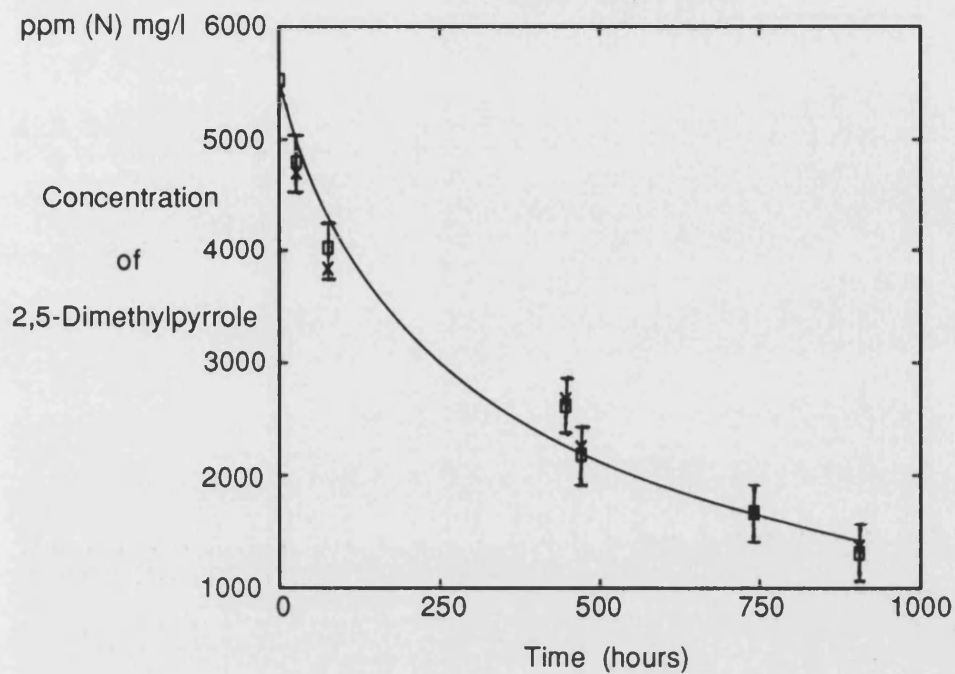


Figure 3.2

## Thermal Degradation of 2,5-Dimethylpyrrole in Diesel

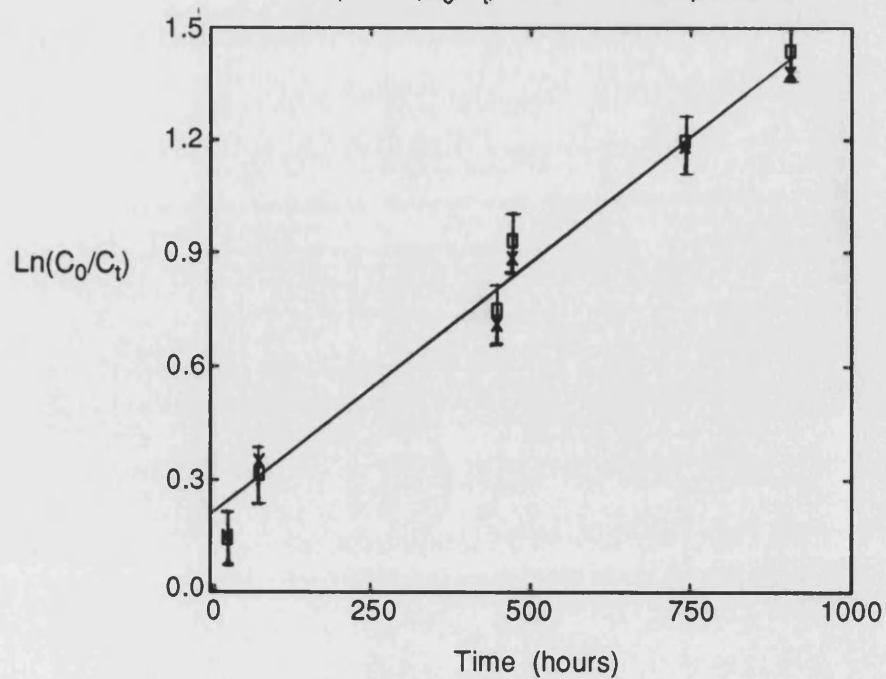
Ln plot  $\ln(C_0/C_t)$  at ambient temperature

Figure 3.3



These results demonstrated that an alkyl pyrrole in the fuel will degrade. This is confirmed by the work of other groups where it has been shown that at ambient temperature, 2,5-dimethylpyrrole will degrade in diesel fuel. However, these workers have not gone as far as quoting actual degradation rate constants. Frankenfeld et al.<sup>53</sup> have quoted activation energies for the degradation of 2,5-dimethylpyrrole in various media, but without pre-exponential values for these figures, it is not possible to calculate rate constants for comparison. Many other workers have quoted sediment values found after specific time periods and it is possible to calculate similar values from the work in this thesis for the purposes of comparison. The calculation was performed with the aid of the micromodeller package, details of which are given in section 1.7.2. An ambient reaction of 2,5-dimethylpyrrole (750 ppm (N)) in diesel should yield a loss of 477 ppm (N) mg/l of dopant after four weeks storage, if it is assumed that this loss of nitrogen from the fuel translates to formation of sediment then this value can be manipulated to make it suitable for direct comparison with values found by Frankenfeld et al.<sup>53</sup>. For a comparison to be made this sediment value must be converted to a figure in mg/100 cm<sup>3</sup>, which yields a value of 47.7 mg/100 cm<sup>3</sup>. The results obtained by Frankenfeld et al. were found at a temperature of 43.3 °C after four weeks storage. If a temperature correction factor of 1.7 per 10 °C rise in temperature<sup>115</sup> is used to recalculate the rate constant, then the final value predicted from results in this thesis is one of 138 mg/100 cm<sup>3</sup>, which compares well with a value of 141 mg/100 cm<sup>3</sup> at a storage temperature of 43.3 °C found by Frankenfeld et al.<sup>53</sup>.

Performing this experiment was the initial step in obtaining degradation data from a model system. The next step was to reduce the complexity of the fuel system under study.

### 3.3 EXPERIMENTS ON MODEL SYSTEMS

#### 3.3.1 Thermal Degradation of 2,5-Dimethylpyrrole in Dodecane and Toluene

After demonstrating the effects of the dopant in a real system, a model system with the same carbon:hydrogen ratio as diesel fuel was investigated. The model system used for this was a combination of dodecane and toluene (30 % toluene in dodecane).

Thermal Degradation of 2,5-Dimethylpyrrole in Dodecane and Toluene  
at ambient temperature

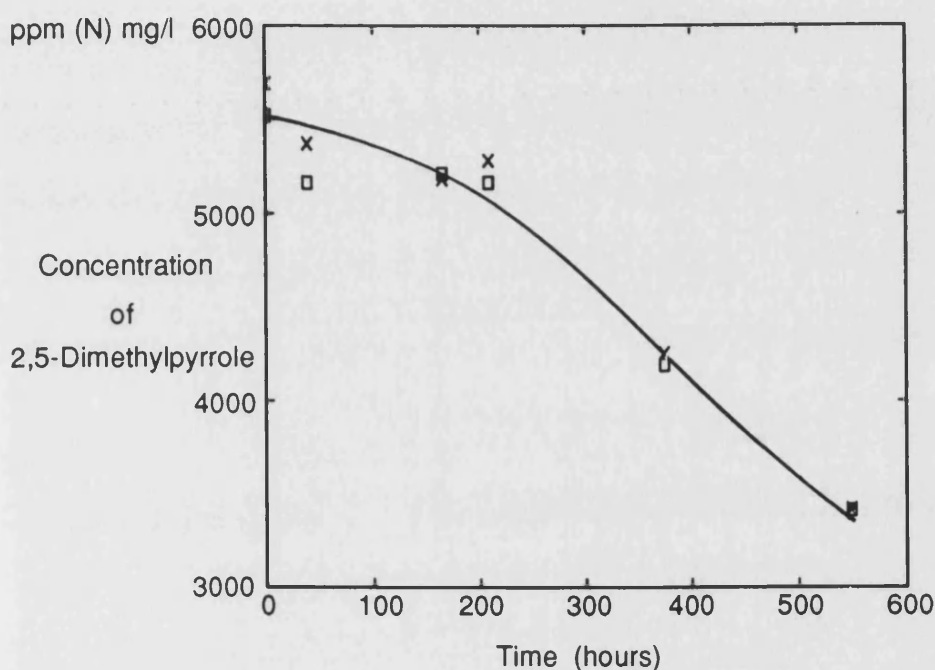


Figure 3.4

Figure 3.4 displays autoxidation. There exists on the plot an induction time where the reaction proceeds at a slower rate. After the initial induction period, the reaction proceeds with the dopant concentration decreasing at a greater rate. The induction period is the stage of the reaction where an intermediate is being formed. This intermediate is suspected to be an oxidation product caused by the autoxidation of the pyrrole, which is supported by the findings of other workers. Bhan et al.<sup>21</sup>

found that oxidation of compounds in distillate fuels was the initial step of instability and that these oxidation products combine with indigenous polar compounds to form gums and sediments. Beaver et al.<sup>122</sup> have postulated mechanisms for alkyl pyrrole promoted sediment formation. The oxidation of 2,5-dimethylpyrrole was termed an electron transfer initiated oxidation, which would thus promote sediment formation. The presence of this oxidation product causes an acceleration in the rate of disappearance of 2,5-dimethylpyrrole. Oxygen dissolved in the model fuel is responsible for this autoxidation reaction. However, it may be that the intermediate and the final product are chemically indistinguishable and it is the presence of the final product which accelerates the reaction. Kinetic analyses of subsequent systems were successfully treated as though the final product accelerates the degradation reaction while also taking part in it.

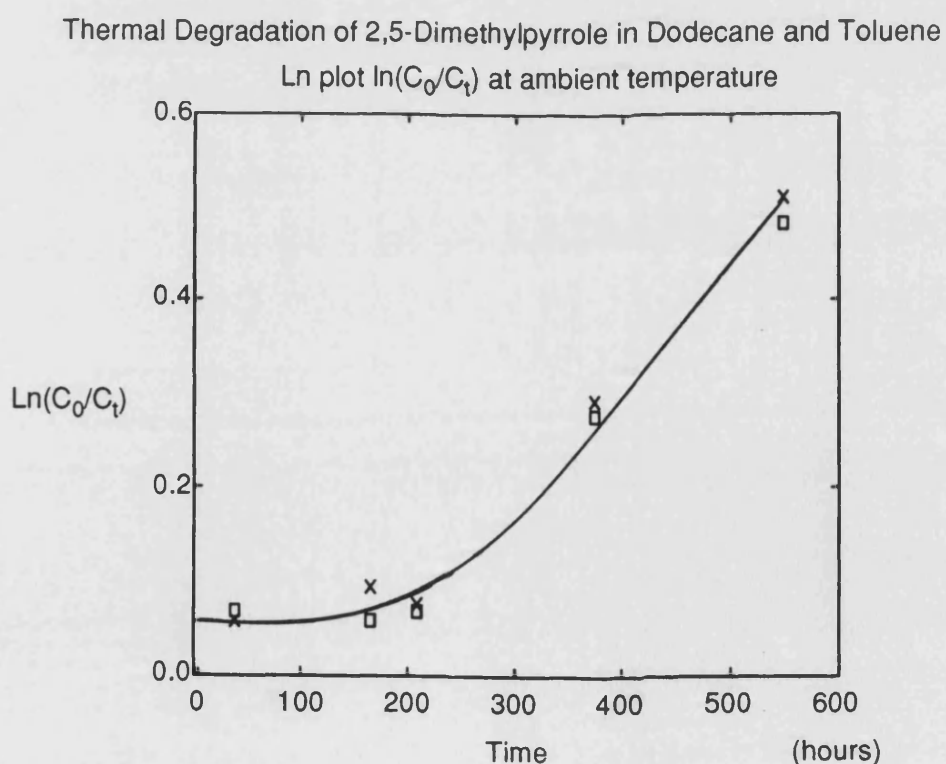


Figure 3.5

The log plot of initial concentration of 2,5-dimethylpyrrole divided by the concentration at time  $t$  reveals two linear portions on the curve (figure 3.5). The gradients for these portions yield two different values which are rate constants for two different modes of dopant consumption. The values for these constants are:- for the induction period  $0.00022 \text{ h}^{-1}$  and for the latter part of the reaction  $0.0012 \text{ h}^{-1}$  which obviously compares favourably with a degradation rate in diesel of  $0.0015 \text{ h}^{-1}$ .

This experiment confirmed that the use of a model system to demonstrate fuel degradation gives a good approximation to real systems.

### 3.3.2 Thermal Degradation of 2,5-Dimethylpyrrole and of 1,2,5-Trimethylpyrrole in Dodecane

The approach described in the previous section was extended to include a range of temperatures and starting concentrations, sufficient to provide data for a kinetic analysis of the systems studied. The systems that were investigated included 2,5-dimethylpyrrole, 1,2,5-trimethylpyrrole and also a combination of the two dopants. Data analysis was performed using a spreadsheet package on an IBM personal computer.

#### **The Order of Reaction**

Plots of log of initial concentration divided by concentration at time  $t$  yielded data suitable for rate constants to be calculated. From this it was deduced that the reactions under study approximated to a first order rate equation. The plots obtained (shown in the appendix) each contained two regions in which a linear equation could be fitted in a similar way to that shown in the previous section. This made simple calculation of one rate constant from the plots impossible. Between these two regions there exists a section of the graph in which the apparent rate constant of the reaction gradually increases to a higher but constant value. The complexity of the data led to the calculation of two rate constants ( $k_1$  and  $k_2$ ) for each plot. Both of these rate

constants were used in the final rate equation which was as follows:-

$$(dC/dt) = -k_1 C_t - k_2 C_t (1 - C_t)$$

From the shape of the raw data plots (shown in the appendix) and of the  $C/C_0$  plots it was deduced that there was some autoxidation occurring during the course of the reaction. An example raw data plot is depicted in figure 3.6. This again parallels the results of the previous section, where 2,5-dimethylpyrrole was degraded in a mixture of dodecane and toluene. Therefore, it was again concluded that either some intermediate, or the final product itself, was catalysing the reaction and causing the rate of dopant consumption to increase during the course of the reaction.

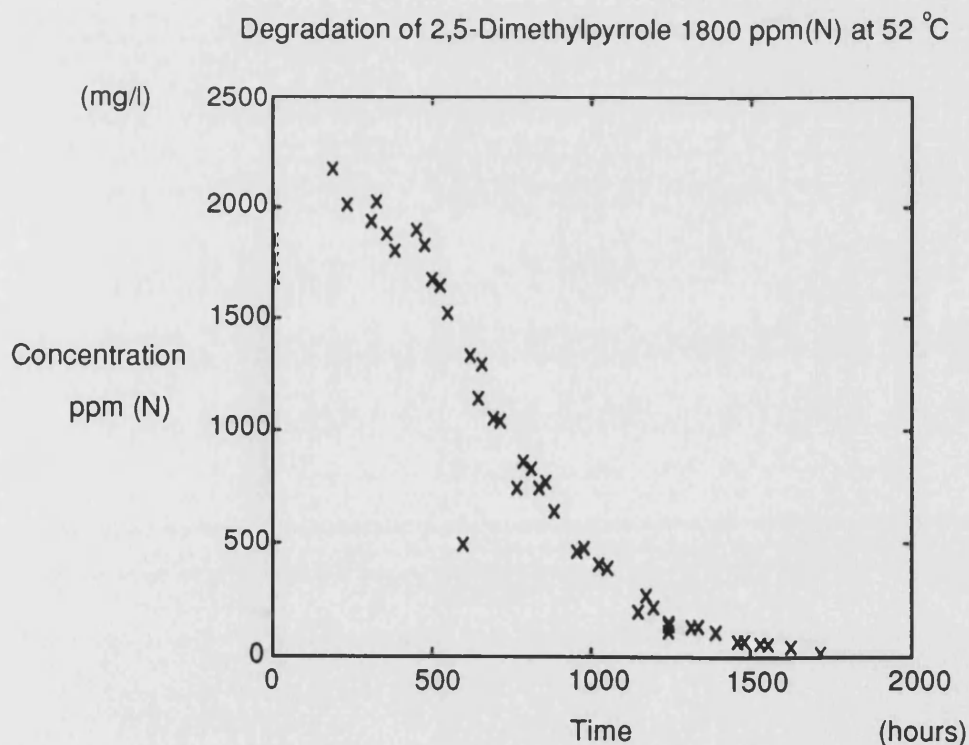


Figure 3.6

Figure 3.6 shows a graph typical of a reactant which undergoes autoxidation. The data shown in the graph is taken from one of the experiments performed in this

thesis and is also present in the appendix.

The graph (figure 3.7) shows an example of a first order plot of a data set which clearly demonstrates the two linear regions in the plot. It is from graphs such as this, that the gradient of the linear regions is taken to use in activation energy calculations.

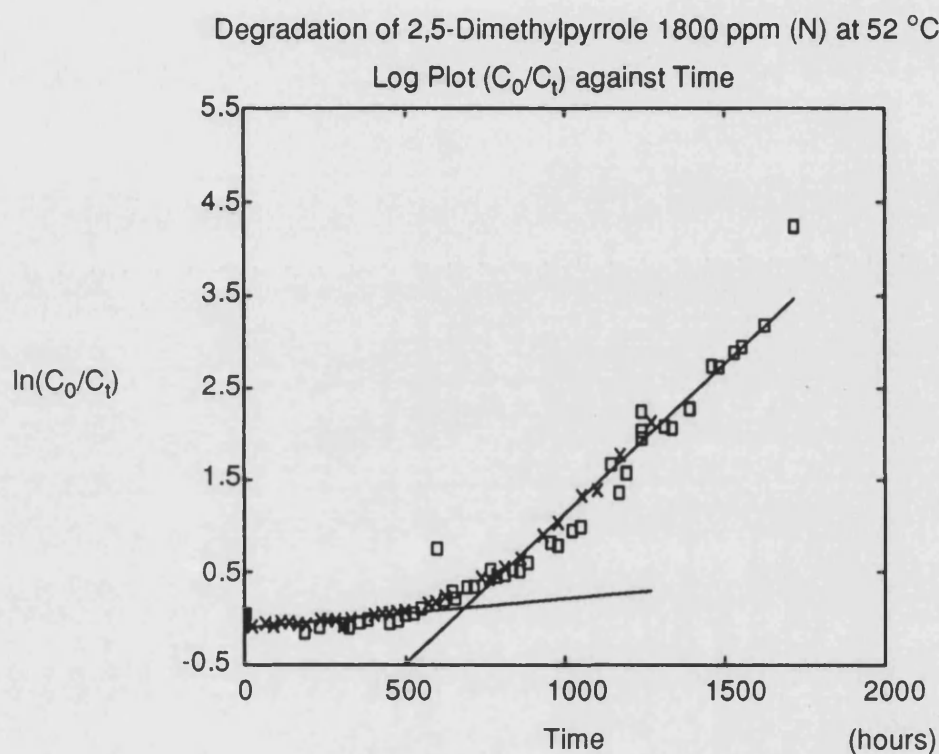


Figure 3.7

The lines fitted to this data have equations of:-

$$(k_1) \quad y = 0.00032(x) - 0.10$$

$$(k_2) \quad y = 0.0032(x) - 2.11$$

The intercepts of these lines are unimportant for use in Arrhenius plots, the gradients are the rate constants used in the Arrhenius plots. The equation for  $k_1$  for

this set of data yields a rate constant for the initial reaction rate of 2,5-dimethylpyrrole in dodecane, which will be referred to as  $k_{1\text{DMP}}$ . The equation for  $k_2$  yields a value which will be referred to as  $k_{2\text{DMP}}$ , the rate constant for the final reaction rate of 2,5-dimethylpyrrole in dodecane. Similar treatment for the 1,2,5-trimethylpyrrole system yields the values  $k_{1\text{TMP}}$  and  $k_{2\text{TMP}}$ .

### Activation Energies

The following tables show the rate constants calculated from first order plots of degradation data. The number (No.) column in both tables 3.1 and 3.2 denotes the code assigned to a particular experiment and also the temperature at which that experiment was performed. For example a code of 3-60 denotes experiment number 3 which was carried out at a temperature of 65 °C. Some of the figures in the table are clearly anomalous.

Table 3.1					
No.	$k_{1DMP} \text{ h}^{-1}$	$k_{2DMP} \text{ h}^{-1}$	No.	$k_{1DMP} \text{ h}^{-1}$	$k_{2DMP} \text{ h}^{-1}$
1-40	0.00098	0.0026	3-60	0.00013	0.0059
5-40	0.00023	0.0027	7-60	0.00041	0.0038
9-40	0.00021	0.0026	11-60	0.00050	0.0039
13-40	0.00020	0.0025	15-60	0.00042	0.0038
17-40	0.00018	0.0026	19-60	0.00425	0.0042
21-40	0.00020	0.0026	23-60	0.00420	0.0039
25-40	0.00020	0.0024	27-60	0.00052	0.0038
29-40	0.00024	0.0027	31-60	0.00050	0.0035
33-40	0.00021	0.0026	37-60	0.00046	0.0038
34-40	0.00021	0.0025	38-60	0.00116	0.0038
2-50	0.00092	0.0034	4-70	0.00066	0.0041
6-50	0.00028	0.0031	8-70	0.00067	0.0042
10-50	0.00032	0.0031	12-70	0.00058	0.0042
14-50	0.00032	0.0031	16-70	0.00061	0.0040
18-50	0.00030	0.0031	20-70	0.00455	0.0046
22-50	0.00032	0.0031	32-70	0.00054	0.0041
26-50	0.00028	0.0030	28-70	0.00475	0.0043
30-50	0.00034	0.0031			
35-50	0.00031	0.0031	39-70	0.00066	0.0042
36-50	0.00032	0.0032	40-70	0.00066	0.0041

In table 3.1 experiments 1 to 8 and 33 to 40 were performed at concentrations of approximately 1800 ppm (N), 9 to 16 at 1100 ppm (N), 17 to 23 at 750 ppm (N) and 25 to 32 at 410 ppm (N). In table 3.2 experiments 41 to 48 were performed at a concentration of 1650 ppm (N), 49-56 at 1290 ppm (N), 57-64 at 750 ppm (N) and 65-72 at 350 ppm (N).



Table 3.2					
No.	$k_{1TMP} \text{ h}^{-1}$	$k_{2TMP} \text{ h}^{-1}$	No.	$k_{1TMP} \text{ h}^{-1}$	$k_{2TMP} \text{ h}^{-1}$
41-40	0.00016	0.00117	45-60	0.00077	0.00252
42-40	0.00015	0.00111	46-60	0.00073	0.00259
49-40	0.00014	0.00113	53-60	0.00061	0.00255
50-40	0.00014	0.00113	54-60	0.00077	0.00259
57-40	0.00016	0.00112	61-60	0.00074	0.00306
58-40	0.00017	0.00112	62-60	0.00116	0.00303
65-40	0.00015	0.00113	69-60	0.00077	0.00260
66-40	0.00016	0.00116	70-60	0.00080	0.00260
43-50	0.00036	0.00176	47-70	0.00103	0.00304
44-50	0.00034	0.00170	48-70	0.00101	0.00303
51-50	0.00032	0.00175	55-70	0.00098	0.00314
52-50	0.00035	0.00173	56-70	0.00105	0.00302
59-50	0.00037	0.00172	63-70	0.00101	0.00301
60-50	0.00036	0.00171	64-70	0.00103	0.00306
67-50	0.00035	0.00173	71-70	0.00102	0.00306
68-50	0.00034	0.00173	72-70	0.00105	0.00306

Having calculated these rate constants it was then possible to obtain activation energies using the Arrhenius relationship as described in section 1.7.1. The graphs (figures 3.8, 3.9, 3.12 and 3.13) are Arrhenius plots for the two model systems studied, using 2,5-dimethylpyrrole and 1,2,5-trimethylpyrrole as dopants. Each plot has a number of points at each temperature, these points represent the experiments performed at different concentrations and duplicated experiments. Regression lines fitted to this data are fitted using all of the points on each plot.

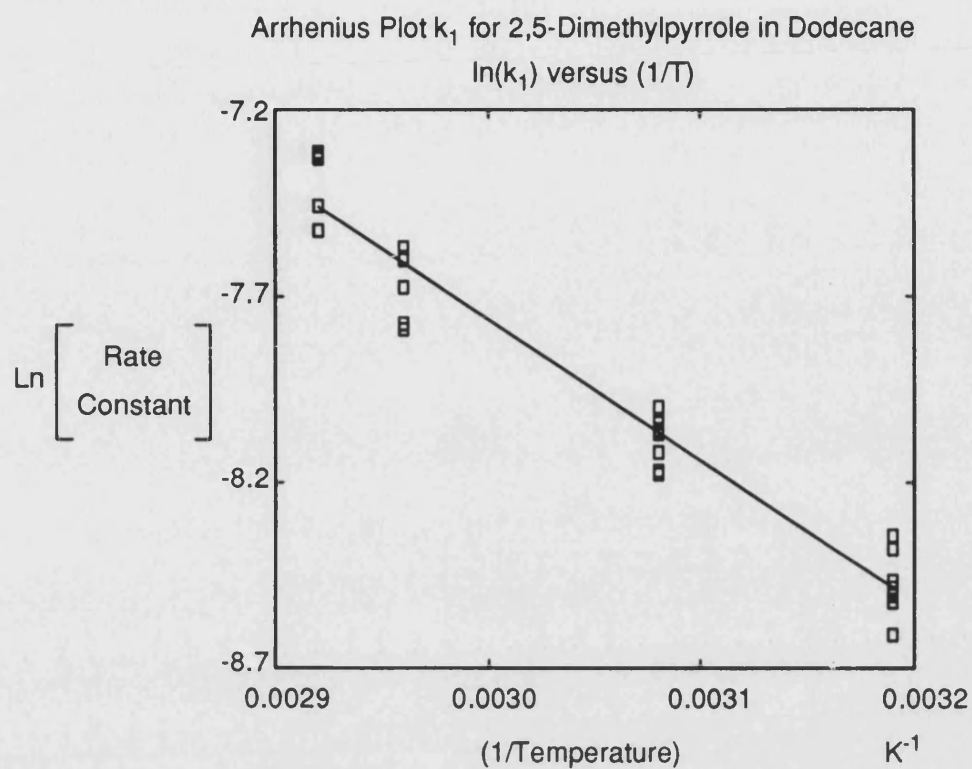


Figure 3.8

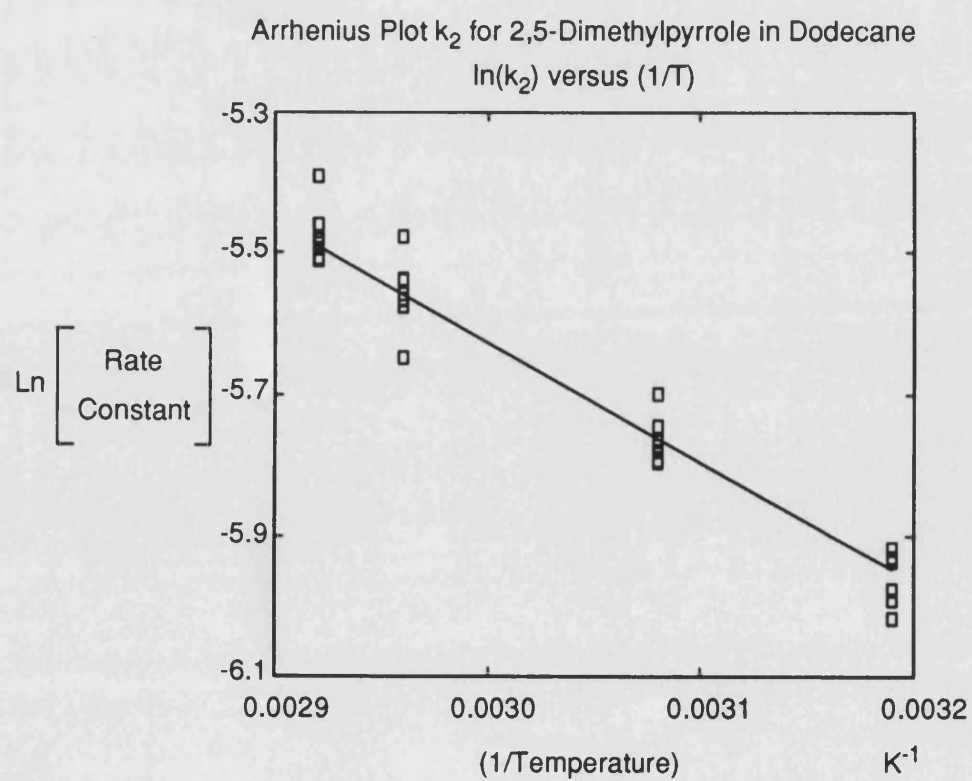


Figure 3.9

These two graphs (figures 3.8 and 3.9) show the relationship between the log of the rate constant and the reciprocal of the temperature for 2,5-dimethylpyrrole in dodecane. The gradient of these two lines is a function of the activation energy for each part of the reaction. From the gradient the activation energy (E) can be calculated as:-

$$E = \text{gradient} \times R$$

where R = the gas constant ( $8.314 \text{ J mol}^{-1} \text{ K}^{-1}$ )

For 2,5-dimethylpyrrole in dodecane the activation energy for the rate constant  $k_{1\text{DMP}}$  which represents the initial rate of consumption of 2,5-dimethylpyrrole can be calculated as follows:-

The gradient of the best fit line, fitted to all of the points on the plot (figure 3.8) is -3790 K and the intercept is 3.61 which is the logarithm of the pre-exponential factor. From this the activation energy is then  $-(-3790 \times 8.31) = 31.5 \text{ kJ mol}^{-1}$ .

Therefore, the equation for the line of best fit is:-

$$\ln(k) = 3.61 - 31500/(RT)$$

For  $k_{2\text{DMP}}$  the calculation is as follows:-

The gradient of the best fit line is -1690 K and the intercept on the y-axis is -0.56 which is the logarithm of the pre-exponential factor. From this the activation energy is then  $-(-1690 \times 8.31) = 14.0 \text{ kJ mol}^{-1}$ .

Therefore, the equation for the line of best fit is:-

$$\ln(k) = -0.56 - 14000/(RT)$$

In order to examine the range of error in the calculation of the activation energies from the Arrhenius plots, lines were fitted to the extreme points on the plots. The graphs generated in this manner are shown in figures 3.10 and 3.11.

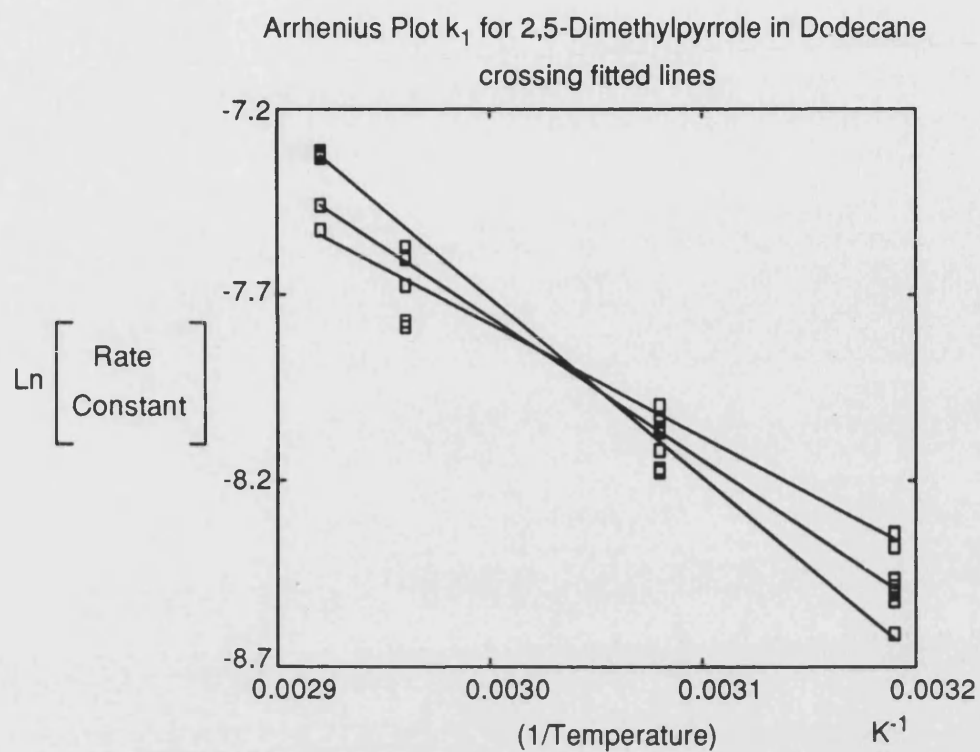


Figure 3.10

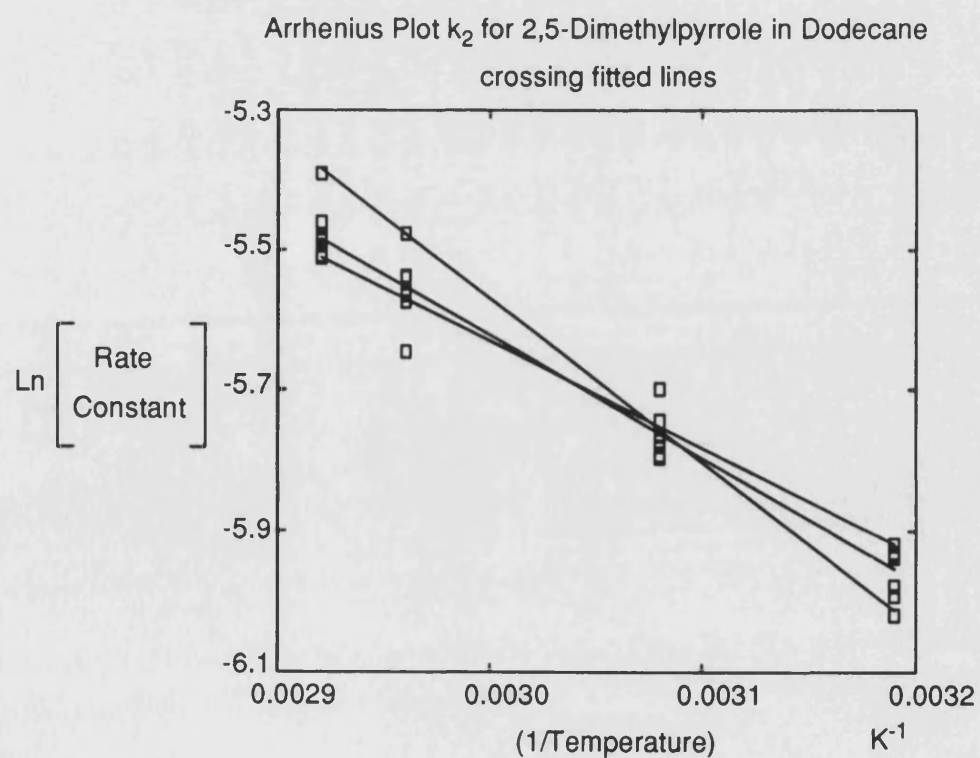


Figure 3.11

These lines yielded gradients and intercepts (logarithms of the pre-exponential factors), from which activation energies could be calculated. For the initial consumption of 2,5-dimethylpyrrole, the maximum and minimum values of gradient with their respective intercepts were:-

maximum gradient=-3030 K, intercept=1.31

minimum gradient=-4810 K, intercept=6.72.

For the later part of the degradation process the maximum and minimum values were:-

maximum gradient=-1500 K, intercept=-1.11

minimum gradient=-2320 K, intercept=1.39.

A similar analysis was applied to the 1,2,5-trimethylpyrrole system and the following two graphs (figures 3.12 and 3.13) are the plots obtained for this system. These two graphs show the Arrhenius relationship for 1,2,5-trimethylpyrrole in dodecane. The gradient of these two lines is a function of the activation energy for each part of the reaction. From the gradient the activation energy (E) can be calculated in a similar manner to that used previously for the 2,5-dimethylpyrrole system.

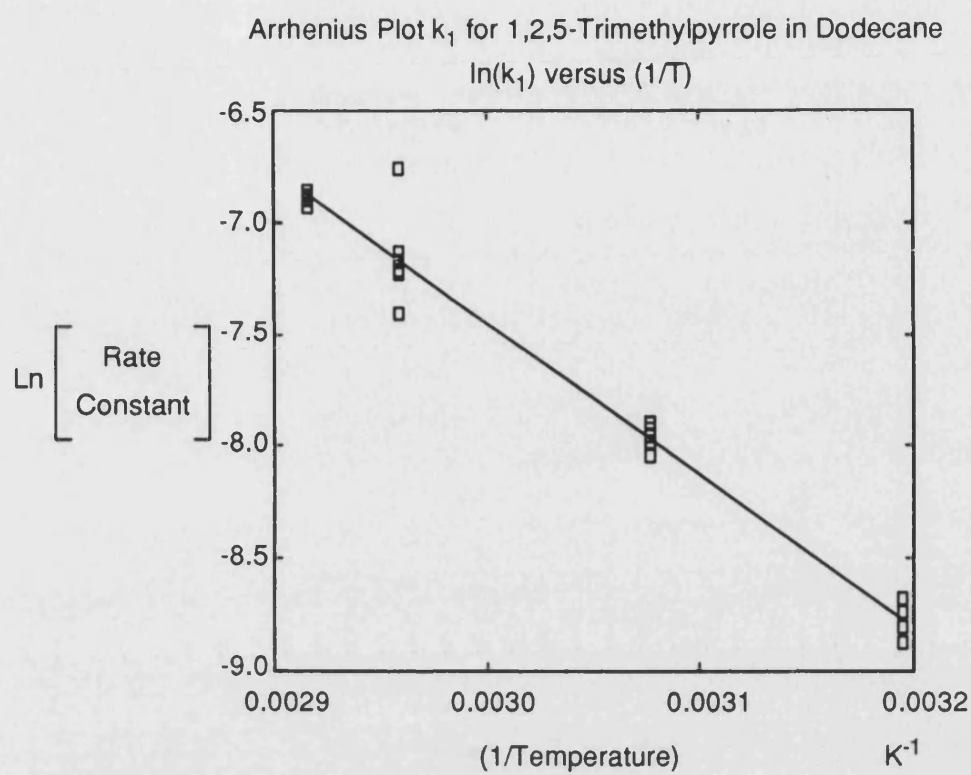


Figure 3.12

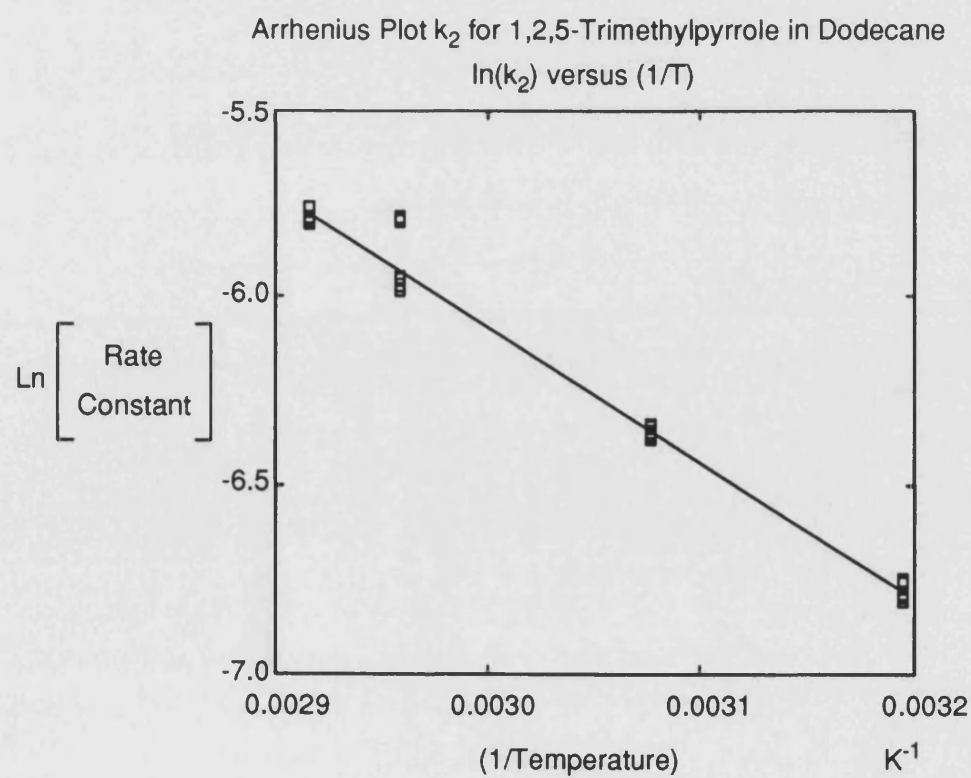


Figure 3.13

The values calculated from these graphs are as follows:-

For  $k_{1\text{TMP}}$  the gradient is -6800 K and the value of the intercept is 12.95. This yields an activation energy of  $-(-6800 \times 8.31) = 56.5 \text{ kJ mol}^{-1}$ .

Therefore, the equation for the line of best fit is:-

$$\ln(k) = 12.95 - 56500/(RT)$$

In the case of  $k_{2\text{TMP}}$  the gradient is -3580 K and the value of the intercept is 4.67. This yields an activation energy of  $-(-3580 \times 8.31) = 29.7 \text{ kJ mol}^{-1}$ .

Therefore, the equation for the line of best fit is:-

$$\ln(k) = 4.67 - 29700/(RT)$$

The same error range calculations were performed for the 1,2,5-trimethylpyrrole system and the plots generated are shown in figures 3.14 and 3.15.

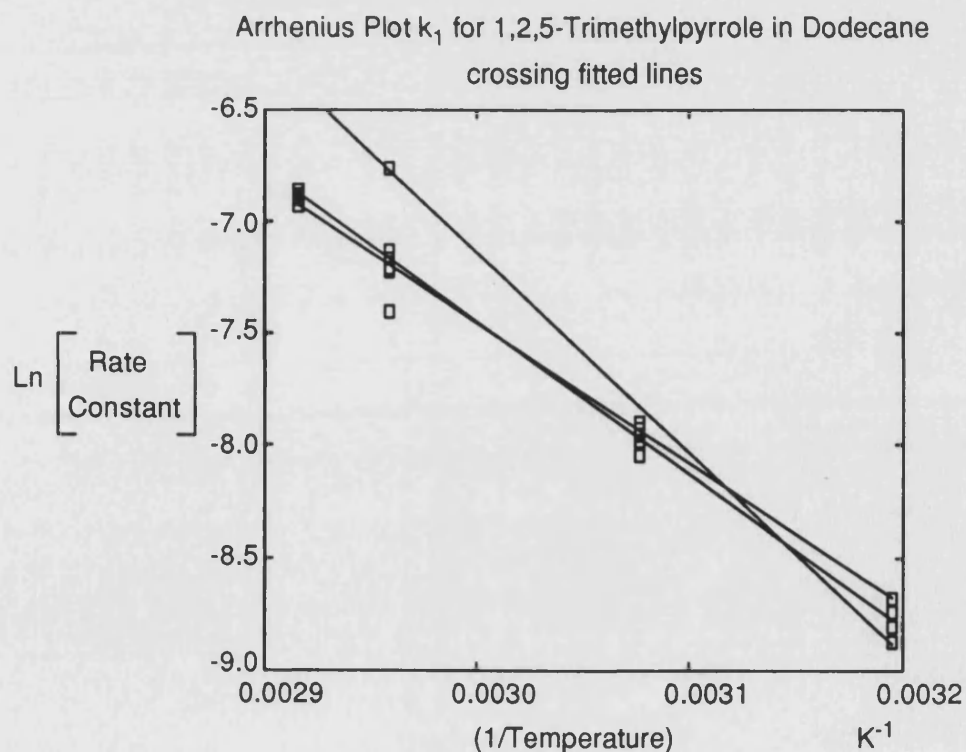


Figure 3.14

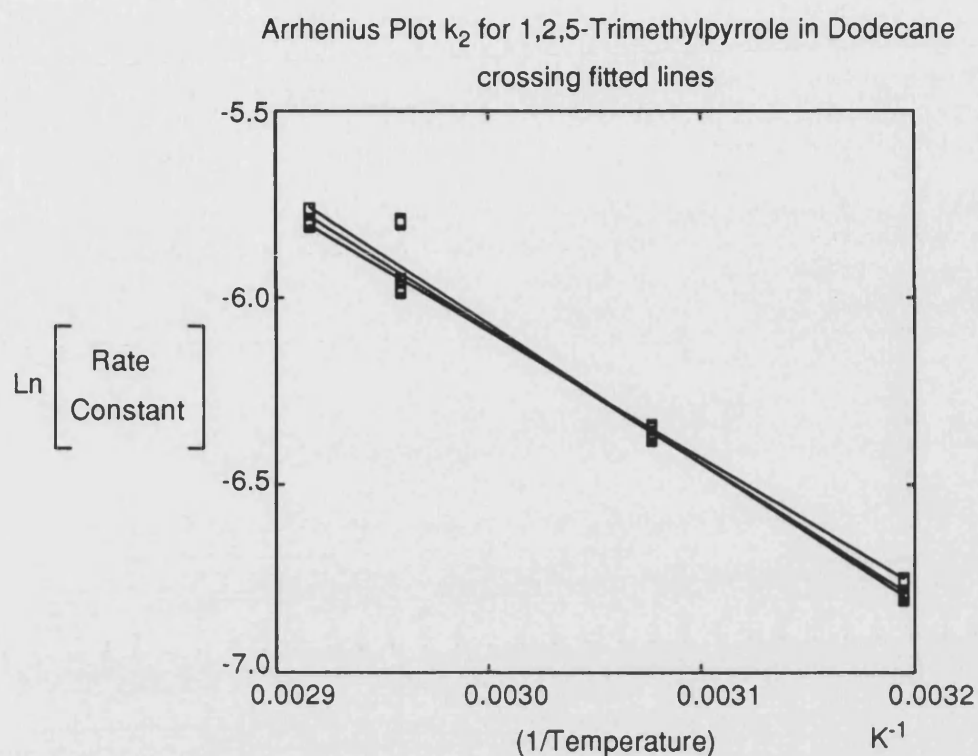


Figure 3.15

Analysis of these graphs yielded the following values:-

Initial reaction rate,

maximum gradient=-6268 K, intercept=11.35

minimum gradient=-8950 K, intercept=19.71.

For the later part of the degradation process the values were:-

maximum gradient=-3380 K, intercept=4.05

minimum gradient=-3720 K, intercept=5.09.



It was realised that the use of these values while yielding a good range for the error in the activation energies would not yield the best error range when used to recalculate the rate constants for the modelling exercise. Where the fitted lines cross each other on the Arrhenius plots the width of the error is obviously narrower. The lines fitted cross at a position corresponding to a temperature of approximately 54 °C. This results in a very narrow error for the curves modelled at a temperature of 52 °C. In order to overcome this problem a second set of lines were fitted to the Arrhenius plots. These lines were fitted in such a way that they did not cross each other in the temperature range that was being examined. The graphs generated in this manner are shown in the figures 3.16 to 3.19.

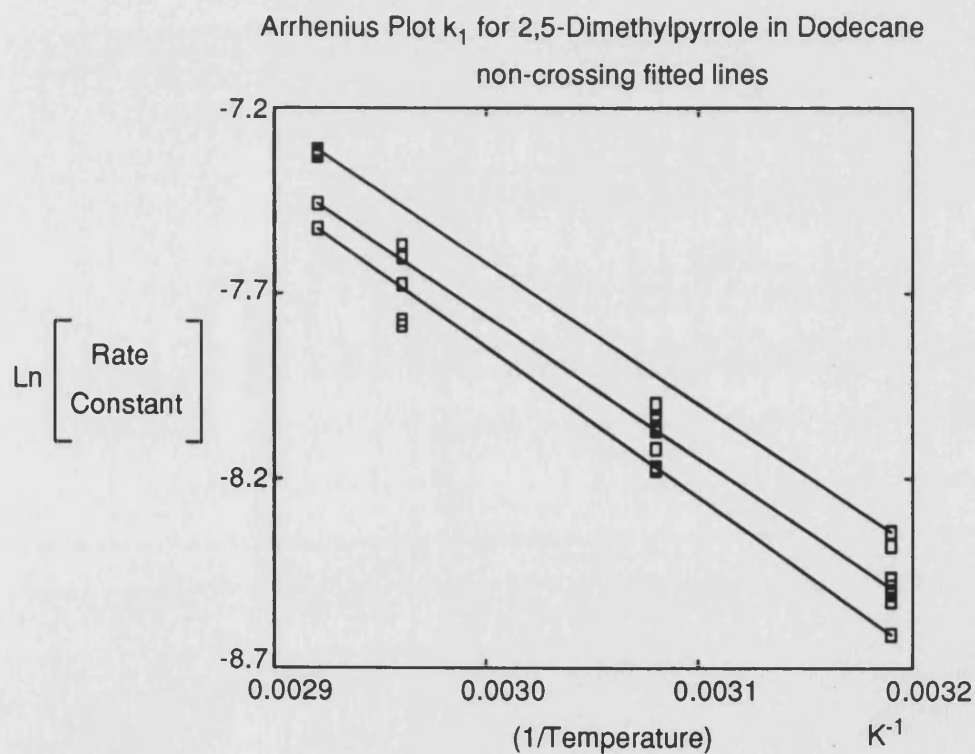


Figure 3.16

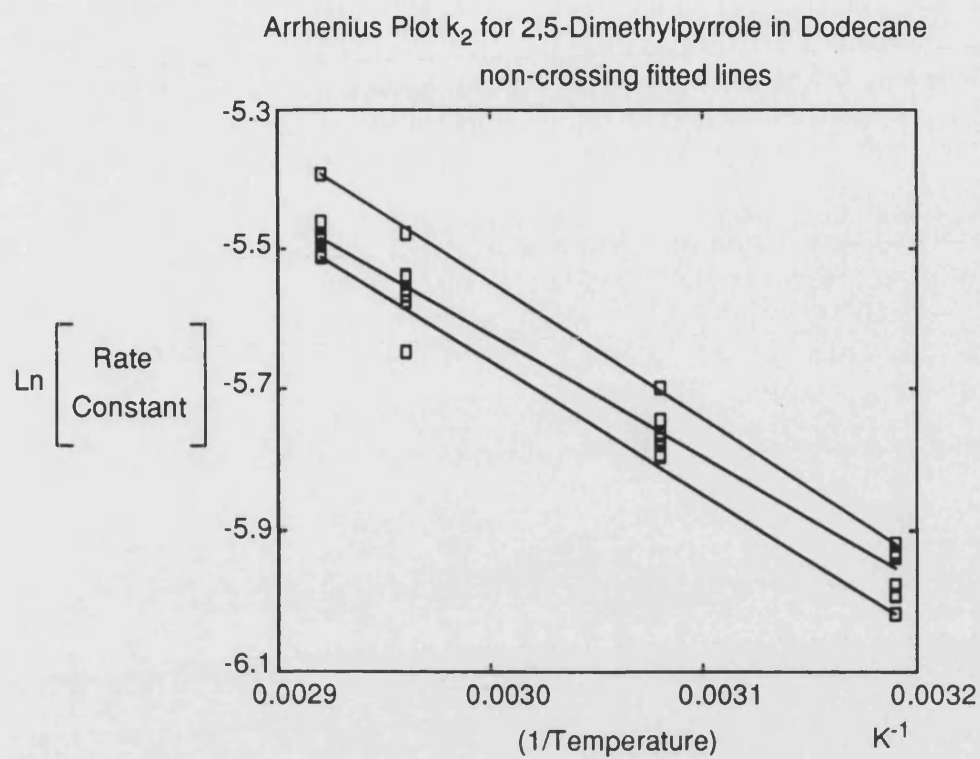


Figure 3.17

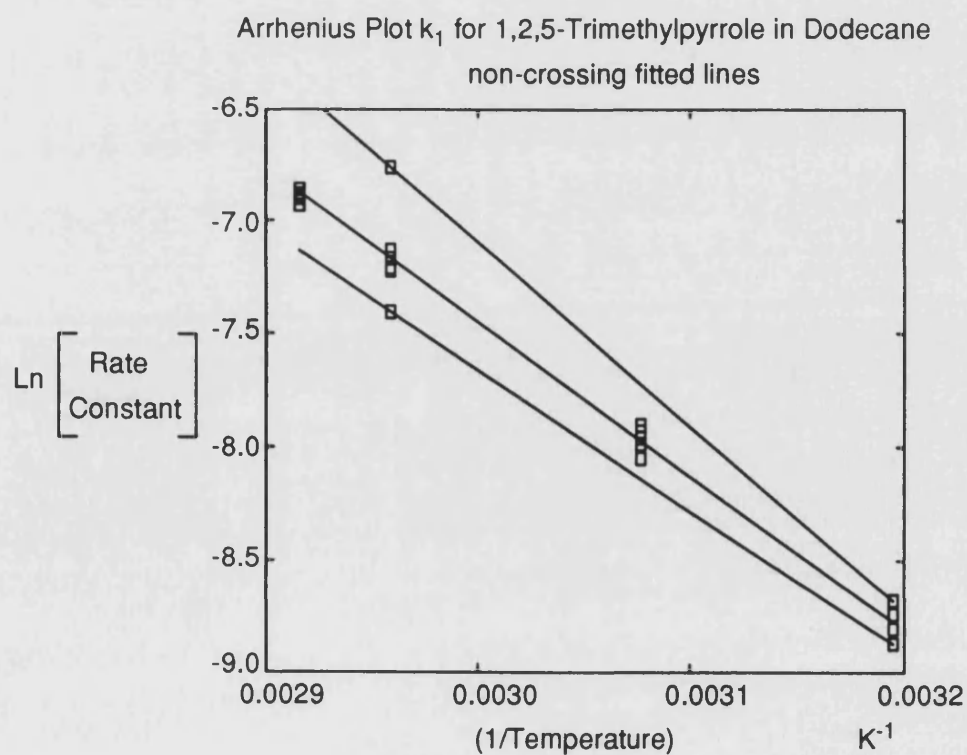


Figure 3.18

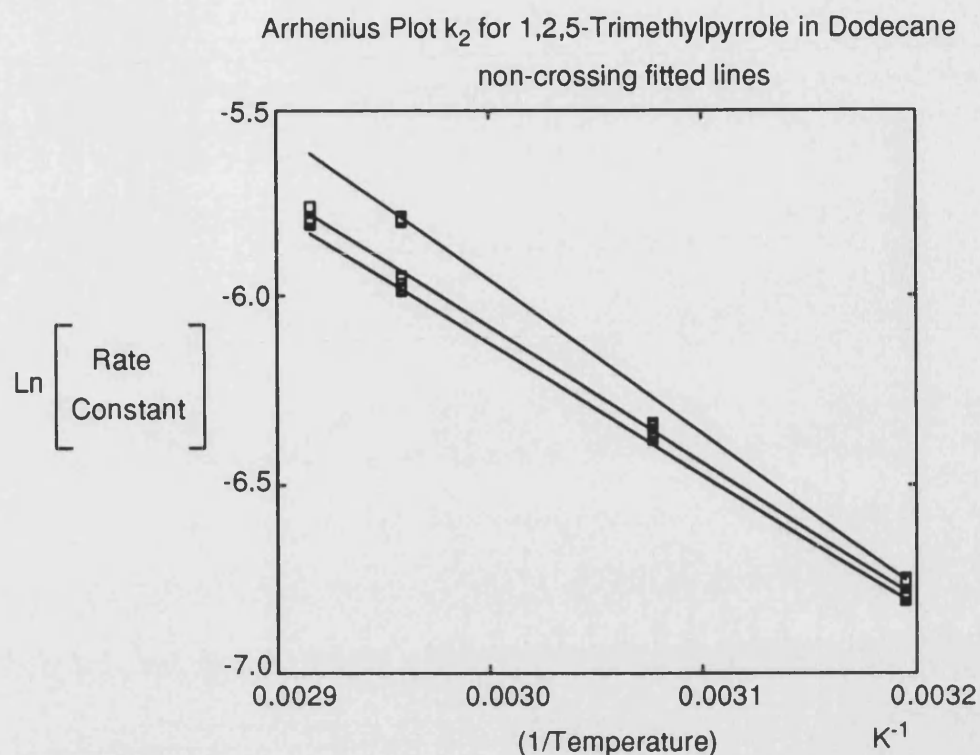


Figure 3.19

The values of gradient and intercept generated from figures 3.8 to 3.15 were used to calculate highest and lowest activation energies for each part of each system studied. The activation energies and their pre-exponential factors are shown in table 3.3.

The values of gradients and intercepts generated using figures 3.16 to 3.19 were used to calculate a second set of activation energies and pre-exponential values. This second set of values is shown in table 3.4. These values would be expected to yield rate constants with a more consistent breadth of error.

Table 3.3

Activation Energies Calculated from Best, Highest and Lowest Fitted Lines

<u>System</u>	<u>Initial Reaction</u>			<u>Final Reaction</u>		
	<u>Low</u>	<u>Best</u>	<u>High</u>	<u>Low</u>	<u>Best</u>	<u>High</u>
<u>2,5-Dimethylpyrrole</u>						
Activation Energy kJ mol <sup>-1</sup>	25.2	31.5	40.0	12.5	14	19.3
Ln(Pre-exponential Factor)	1.31	3.61	6.72	-1.11	-0.56	1.39
<u>1,2,5-Trimethylpyrrole</u>						
Activation Energy kJ mol <sup>-1</sup>	52.1	56.5	74.4	28.1	29.7	30.9
Ln(Pre-exponential Factor)	11.35	12.95	19.71	4.05	4.67	5.09

Table 3.4

Alternative Activation Energies Calculated from Non-Crossing Fitted Lines

<u>System</u>	<u>Initial Reaction</u>		<u>Final Reaction</u>	
	<u>Low</u>	<u>High</u>	<u>Low</u>	<u>High</u>
<u>2,5-Dimethylpyrrole</u>				
Activation Energy kJ mol <sup>-1</sup>	31.7	33.5	15.6	16.2
Ln(Pre-exponential Factor)	3.80	4.23	-0.03	0.31
<u>1,2,5-Trimethylpyrrole</u>				
Activation Energy kJ mol <sup>-1</sup>	51.8	67.6	28.8	33.8
Ln(Pre-exponential Factor)	11.02	17.28	4.28	6.25

From an examination of the two tables (3.3 and 3.4) the best fitted activation energies in table 3.3 do not all lie between the values fitted in table 3.4. This can be

easily understood by an examination of the graphs used to calculate the values of activation energies.

Frankenfeld, Taylor and Brinkman<sup>53</sup> have quoted values for apparent activation energies for sediment formation with 2,5-dimethylpyrrole in a variety of fuel systems (decane, jet fuel and diesel). The measurements that they performed were calculated upon the basis of sediment formed. The values they quote lie in the range 8.4 to 12.7 kcal mol<sup>-1</sup>, which translates to a range of 35.3 to 53.3 kJ mol<sup>-1</sup>. For 2,5-dimethylpyrrole in decane they reported an activation energy of 8.4 kcal mol<sup>-1</sup> (35.3 kJ mol<sup>-1</sup>), so the value of 31.5±8.5 kJ mol<sup>-1</sup> found for 2,5-dimethylpyrrole in dodecane in this thesis is in good agreement with the work of other groups. Differences in these values may arise from the fact that Frankenfeld et al.<sup>53</sup> have calculated their values on the basis of sediment formed, whereas the values calculated in this thesis are on the basis of dopant consumed. The assumption being made, in order to compare these values of activation energies, is that the reaction of 2,5-dimethylpyrrole is equivalent to the formation of sediment. As the values of activation energy are so similar this assumption may be justified. Frankenfeld et al.<sup>53</sup> have also stated that the hydrocarbon profile of the fuel used has little effect on the level of sediment formation with 2,5-dimethylpyrrole. Thus, when pure dodecane is used as a model fuel there are no compounds present in the fuel which will affect the rate of reaction of the pyrrole. The results obtained for ambient reaction of 2,5-dimethylpyrrole in diesel and also in toluene and dodecane provide comparable rate constants of 0.0015 h<sup>-1</sup> and 0.0012 h<sup>-1</sup> respectively. The figures calculated here can be used to predict an ambient rate constant of 0.0018 h<sup>-1</sup> for the latter part of the reaction process. This figure compares well with the value found in this thesis for 2,5-dimethylpyrrole disappearance in diesel.

Values for the activation energies for the 1,2,5-trimethylpyrrole system have not been found in the work of other groups. However, looking again at the work of

Frankenfeld et al.<sup>53</sup>, these results lie just outside those calculated by that group for 2,5-dimethylpyrrole in decane, so it is not unreasonable to suggest that these values are reasonably accurate.

### 3.3.3 C:H:N Analysis of the Sediments from the Model Systems

The sediments obtained from the thermal experiments with 2,5-dimethylpyrrole and 1,2,5-trimethylpyrrole were submitted for C:H:N analysis. These results were examined by plotting nitrogen:carbon ratio found in the sediment against temperature at which that sediment was formed. It was interesting to note that, when examined graphically, the sediment had a trend of increasing nitrogen content with temperature. As the temperature of the storage conditions rose, then so did the amount of nitrogen found in the sediment formed during storage. This was found to be true of both of the systems examined. These observations would imply that as the temperature of storage increases the mechanism by which sediment is formed changes. Plots of this data are shown in figures 3.20 and 3.21 with regression lines fitted to the data.

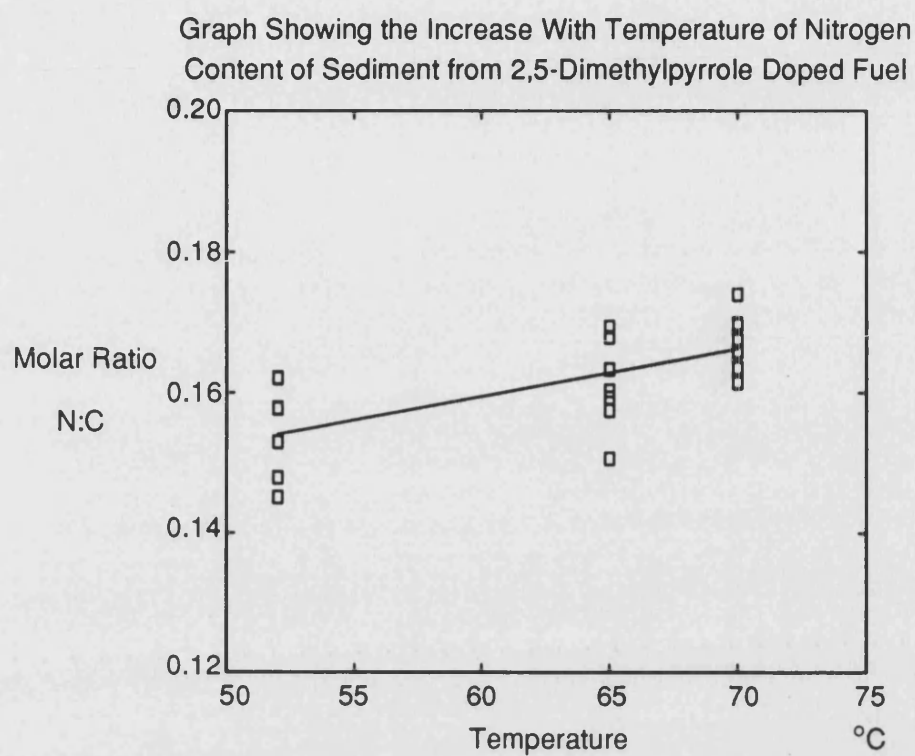


Figure 3.20

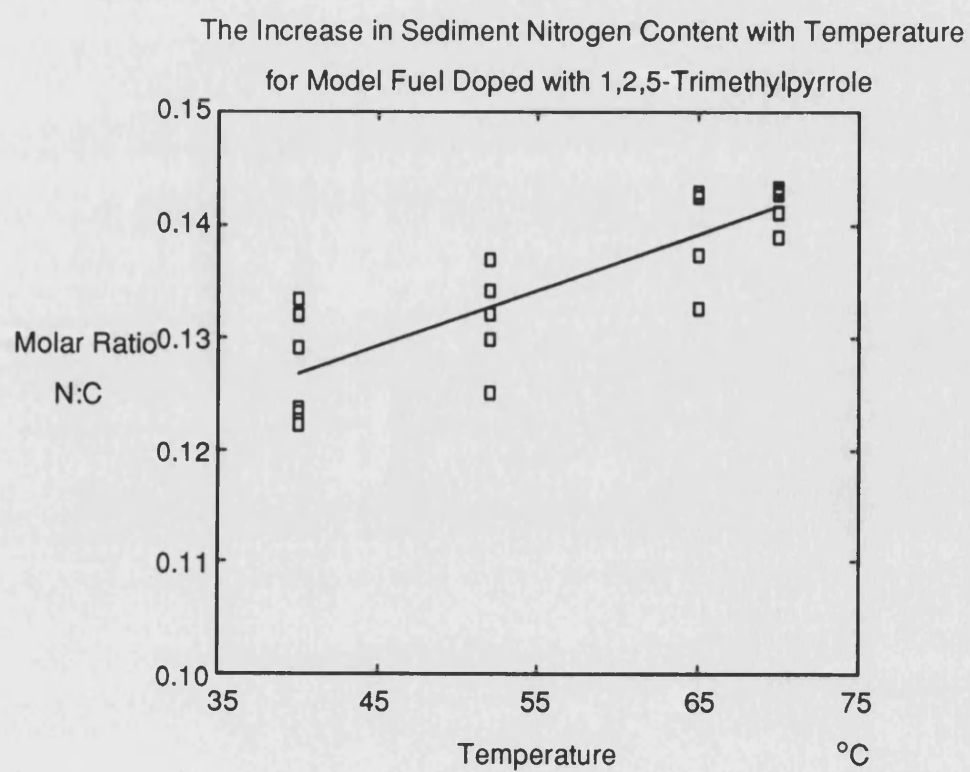


Figure 3.21

### 3.4 COMPUTING RESULTS

The following calculations and concentration curves were performed using Micromodeller. Micromodeller is a commercial software package, designed for integration and graphical representation of differential equations. Further details for this software are given in the computing section 1.7.2.

#### 3.4.1 Modelled Concentration Curves for 2,5-Dimethylpyrrole and for 1,2,5-Dimethylpyrrole

Using the activation energy values (E) and the pre-exponential values (A) from the best fit equations given in section 3.3.2, rate constants at specific absolute temperatures (T) were calculated using the following relationship:-

$$k = Ae^{-(E/RT)}$$

The rate constants generated in this manner are shown in table 3.5.

Table 3.5					
<u>Temperature</u>		<u>k<sub>1DMP</sub></u>	<u>k<sub>2DMP</sub></u>	<u>k<sub>1TMP</sub></u>	<u>k<sub>2TMP</sub></u>
<u>°C</u>	<u>K</u>	<u>h<sup>-1</sup></u>	<u>h<sup>-1</sup></u>	<u>h<sup>-1</sup></u>	<u>h<sup>-1</sup></u>
40	313.15	0.00020	0.00259	0.00015	0.00113
52	322.15	0.00032	0.00316	0.00035	0.00173
65	338.15	0.00050	0.00386	0.00077	0.00265
70	343.15	0.00059	0.00415	0.00104	0.00309

These rate constants for both the 2,5-dimethylpyrrole and the 1,2,5-trimethylpyrrole systems, were used in a differential rate equation of the form:-

$$(dC_v/dt) = -k_1 C_t - k_2 C_t (1 - C_v)$$

Where the reactant concentration at time t, is expressed as a fraction of the initial reactant concentration:-

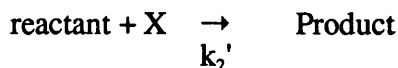


$$C_t = \frac{\text{(Concentration at time t)}}{\text{(Initial Concentration)}}$$

The rate equation was derived with the following assumptions. The dopant consumption is a two stage process, with the initial stage being an autoxidation and the second stage being a reaction of the dopant and the product. This assumption was based on the results obtained in sections 3.3.1 and 3.3.2 where two distinct linear regions were observed in the first order plots of reactant concentration. From this two reaction equations were postulated, the first one being autoxidation of the reactant with a rate constant of  $k_1$  and yielding an intermediate designated as X.



The second reaction equation involves reaction of reactant with the intermediate X, with X possibly acting as a catalyst and with the end product being chemically indistinguishable from X.



Where  $k_2 = (C_0)(k_2')$  and  $k_2'$  is a second order rate coefficient.

With these assumptions the differential rate equation can then be derived as follows:-

For step 1

$$d(\text{reactant concentration})/dt = -k_1(\text{reactant concentration})$$

For step 2

$$d(\text{reactant concentration})/dt = -k_2(\text{reactant concentration})(\text{concentration of X})$$

Then step 1 becomes

$$d(C_t)/dt = -k_1 C_t$$

and step 2 becomes

$$d(C_t)/dt = -k_2 C_t X_t$$

where, if  $X_t$  and the product are chemically indistinguishable,  $X_t$  is now also the

product concentration at time  $t$ .

Summing the two steps together for the overall rate of reactant consumption the equation becomes

$$d(C_t)/dt = -k_1 C_t - k_2 C_t X_t$$

At  $t=0$ ,  $C_t=1$ , therefore, assuming a 1:1 conversion  $X_t=1-C_t$ . Therefore the equation has a final form of

$$d(C_t)/dt = -k_1 C_t - k_2 C_t (1-C_t)$$

When plotted, the data generated in this manner provided a series of curves for the single dopant simple model fuel systems, which are applicable for any reasonable dopant concentration (0-2500 ppm(N) mg/l). These curves are shown in the following graphs (figures 3.22 and 3.23).

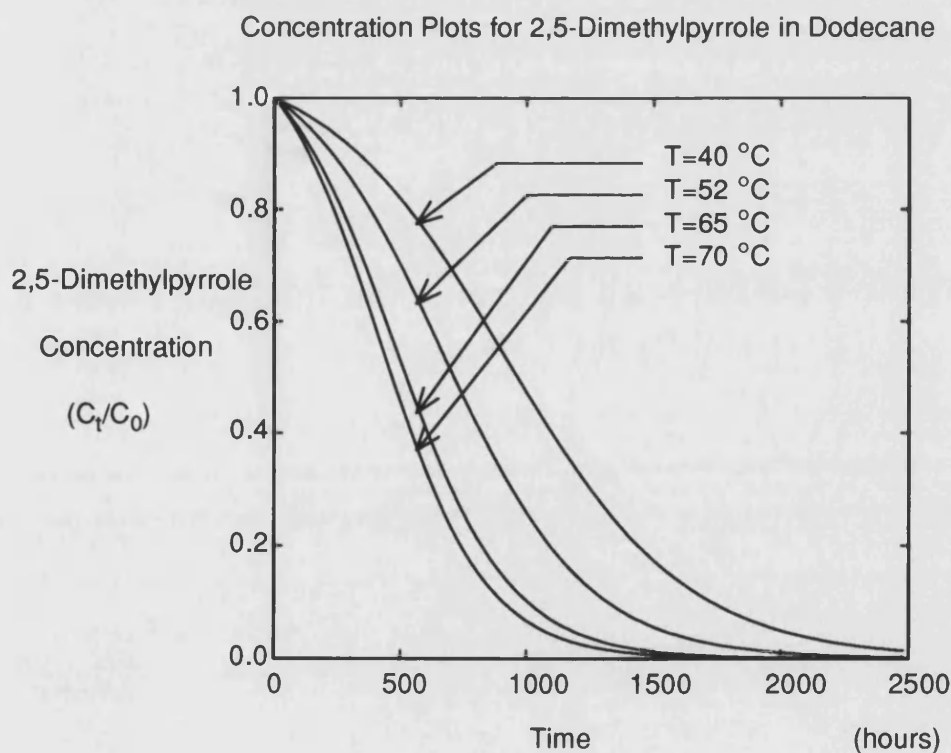


Figure 3.22

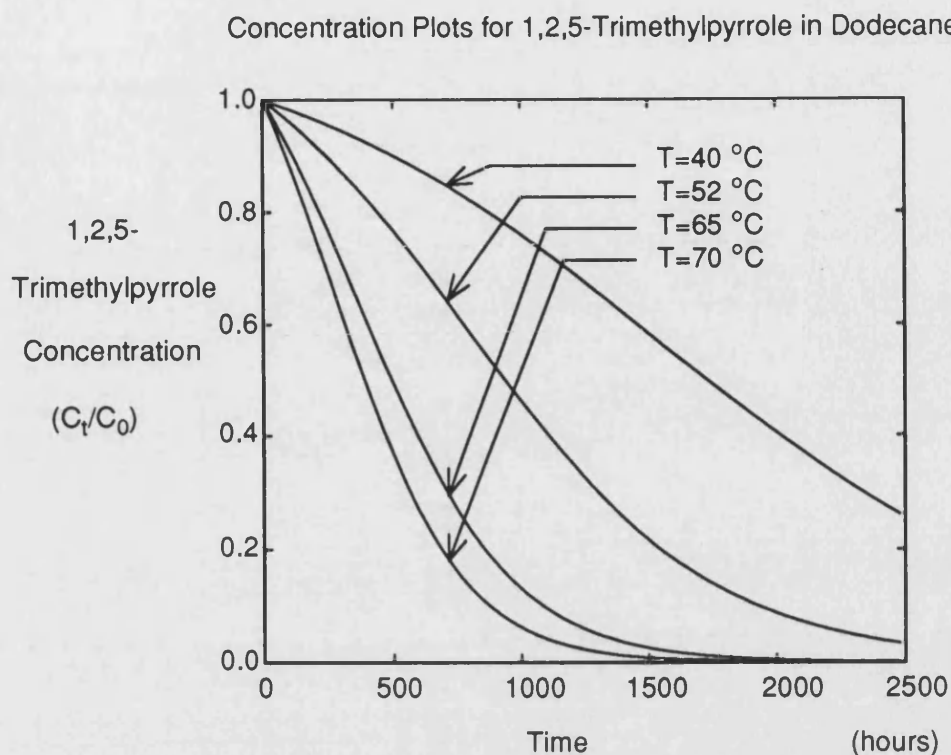


Figure 3.23

These curves (figures 3.22 and 3.23) and those generated from the highest and lowest values of  $E$  and  $A$  with the crossing fitted lines (figures 3.24 to 3.31) and from rate constants calculated using the non-crossing fitted lines (figures 3.32 to 3.39) were compared with the degradation data for the single dopant, simple model fuel systems shown in the appendix. The comparisons were made by scaling degradation data to fit a range between 0 and 1 and plotting this data on the same axes as the predicted degradation curves.

Graph Depicting the Concentration Plot Modelled for 2,5-Dimethylpyrrole at 40 °C using the Extreme Values of Activation Energies

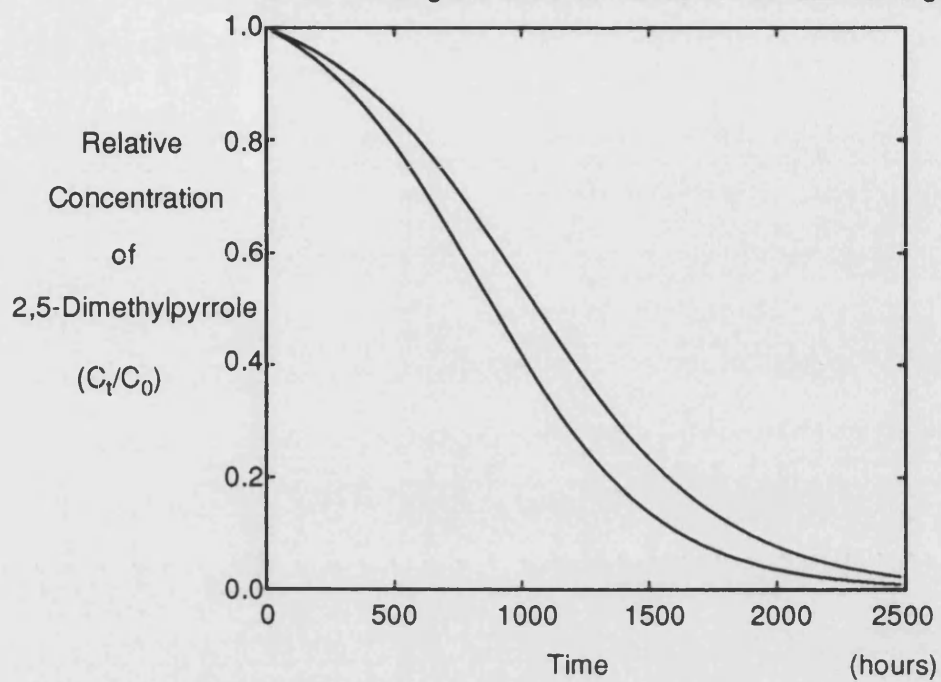


Figure 3.24

Graph Depicting the Concentration Plot Modelled for 2,5-Dimethylpyrrole at 52 °C using the Extreme Values of Activation Energies

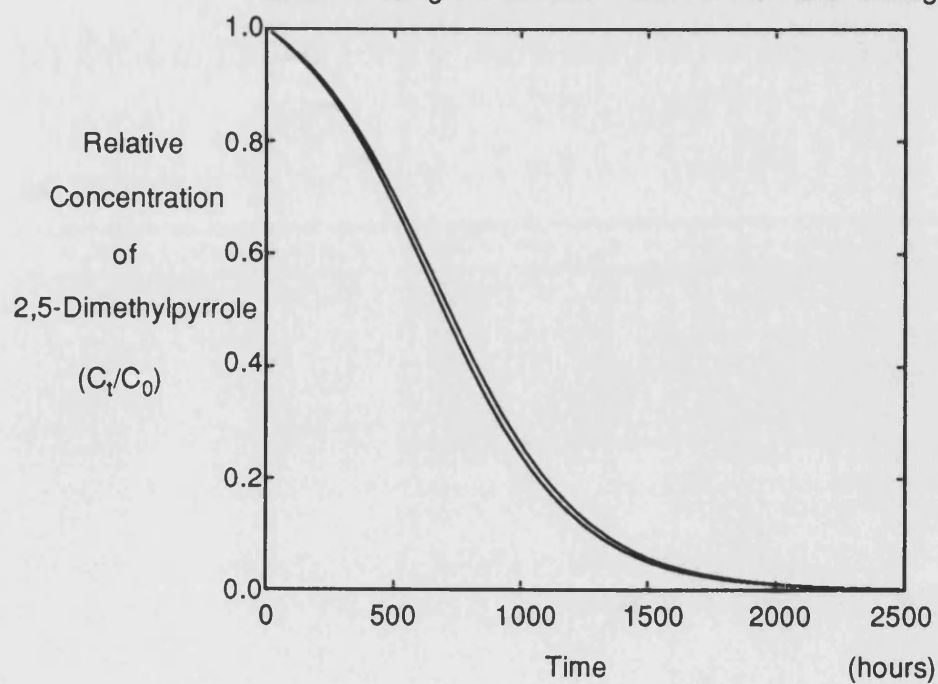


Figure 3.25

Graph Depicting the Concentration Plot Modelled for 2,5-Dimethylpyrrole at 65 °C using the Extreme Values of Activation Energies

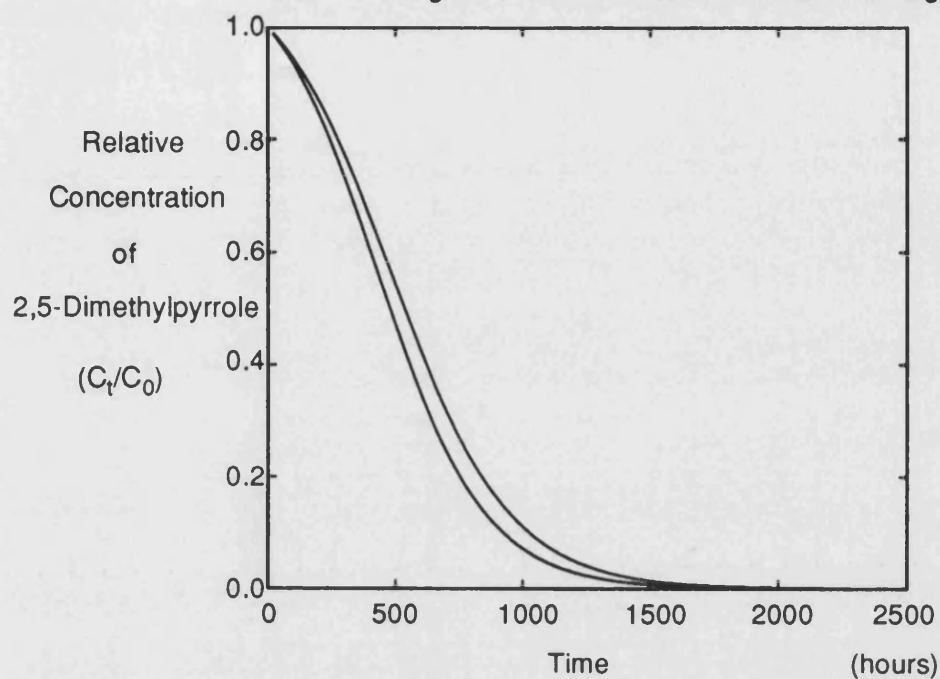


Figure 3.26

Graph Depicting the Concentration Plot Modelled for 2,5-Dimethylpyrrole at 70 °C using the Extreme Values of Activation Energies

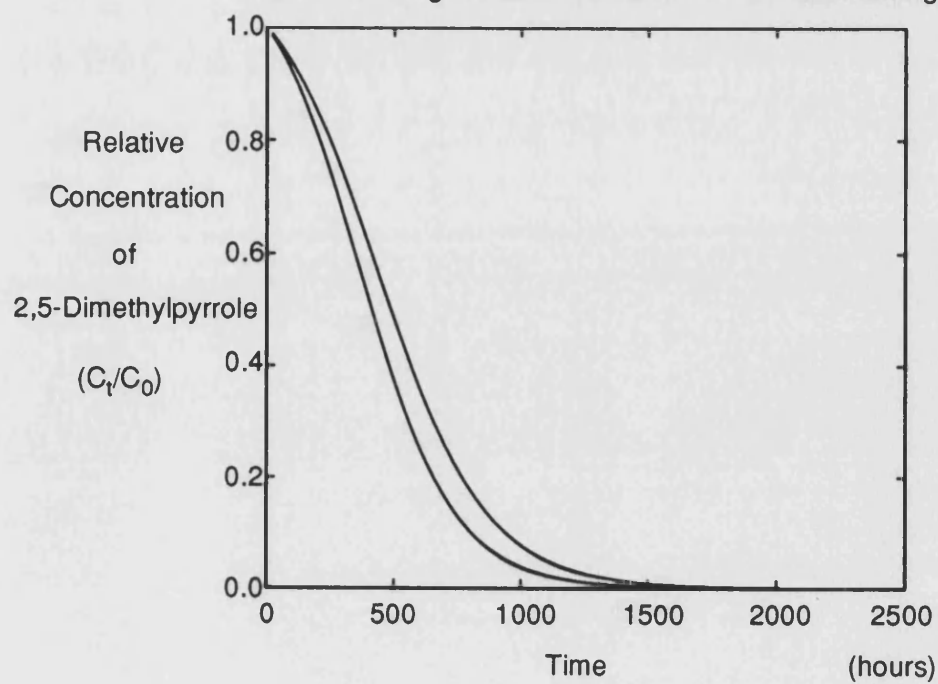


Figure 3.27

Graph Depicting the Concentration Plot Modelled for 1,2,5-Trimethylpyrrole at 40 °C using the Extreme Values of Activation Energies

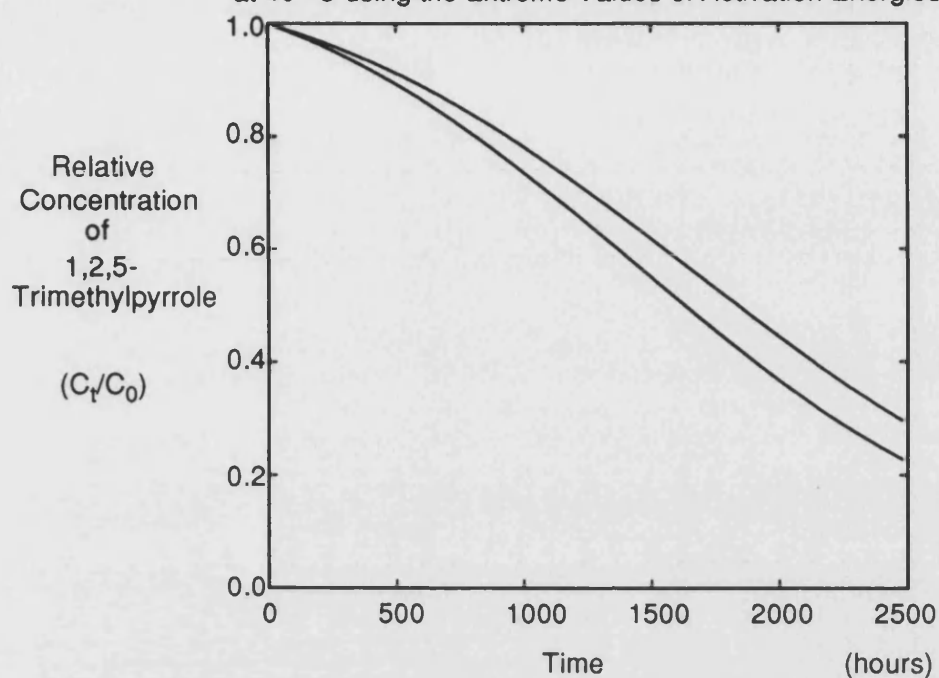


Figure 3.28

Graph Depicting the Concentration Plot Modelled for 1,2,5-Trimethylpyrrole at 52 °C using the Extreme Values of Activation Energies

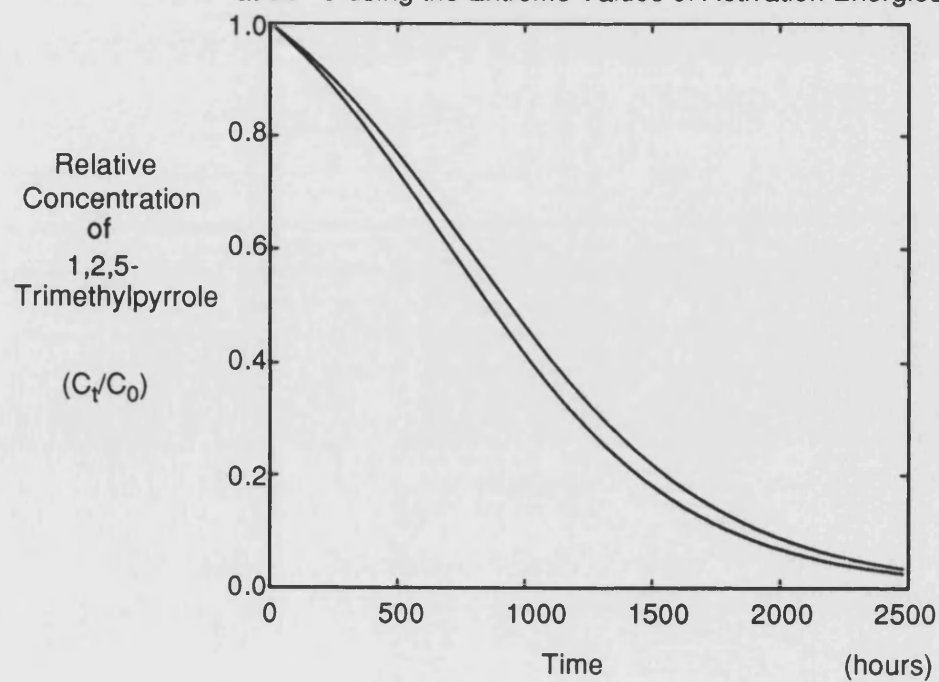


Figure 3.29

Graph Depicting the Concentration Plot Modelled for 1,2,5-Trimethylpyrrole  
at 65 °C using the Extreme Values of Activation Energies

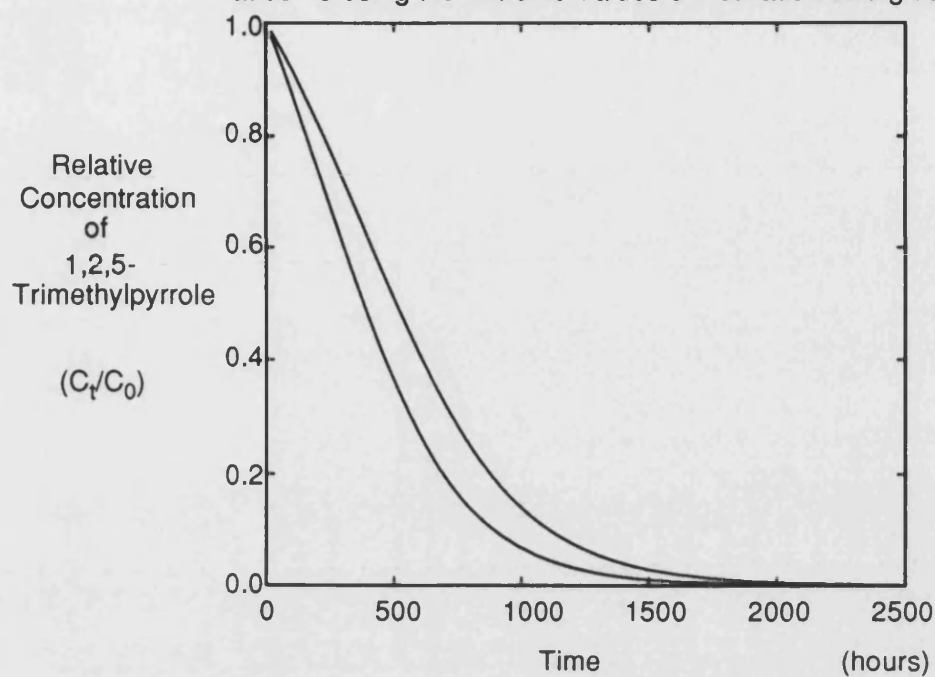


Figure 3.30

Graph Depicting the Concentration Plot Modelled for 1,2,5-Trimethylpyrrole  
at 70 °C using the Extreme Values of Activation Energies

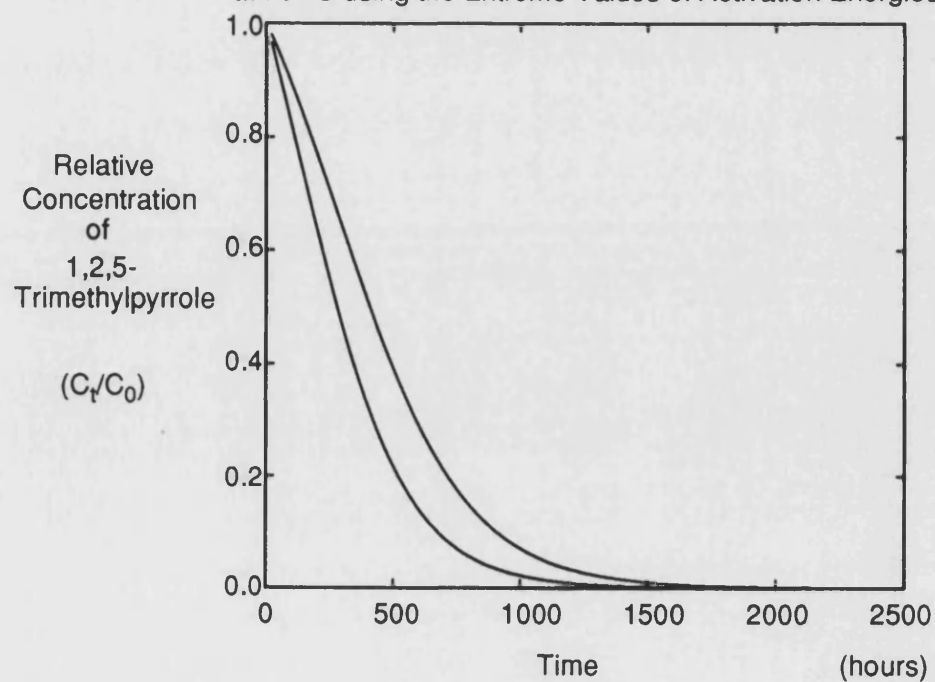


Figure 3.31

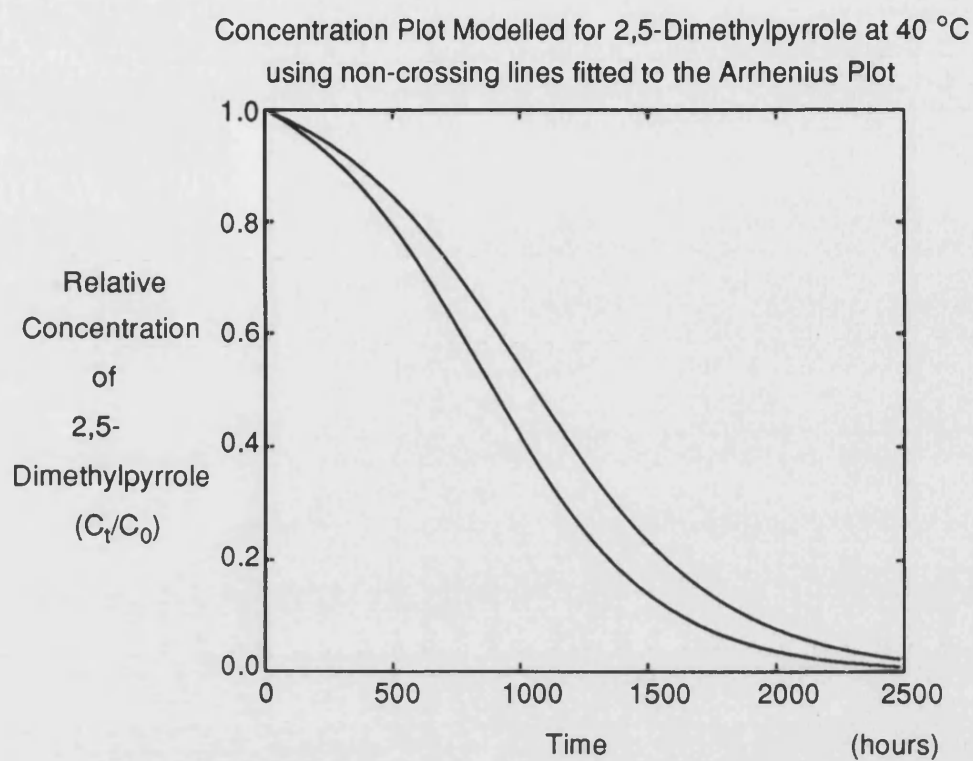


Figure 3.32

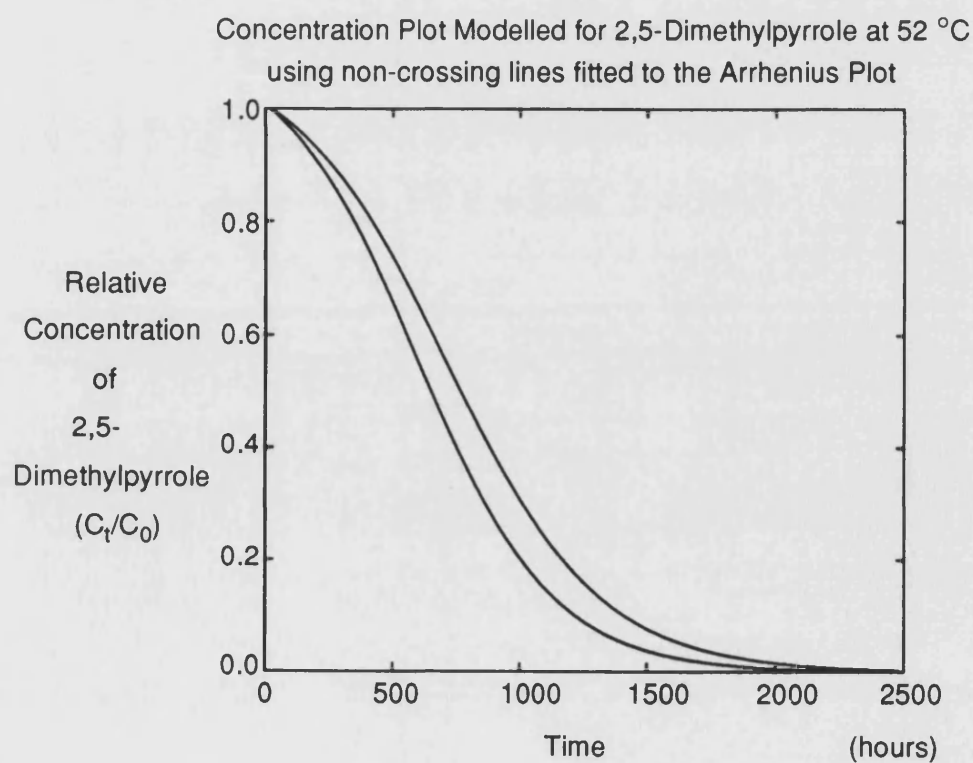


Figure 3.33



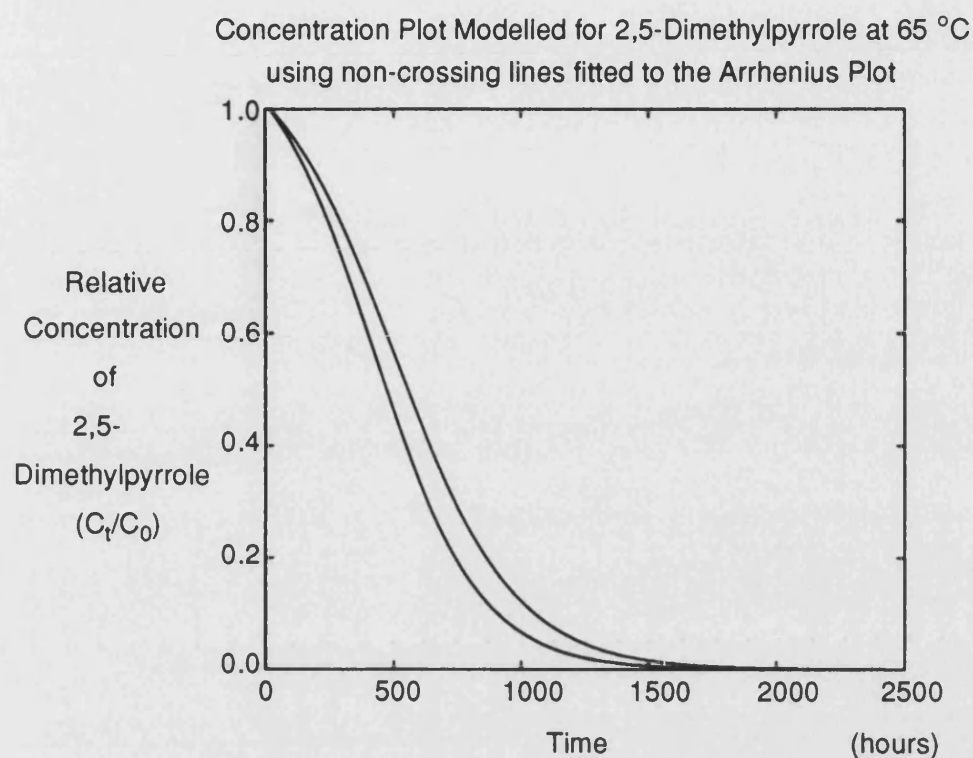


Figure 3.34

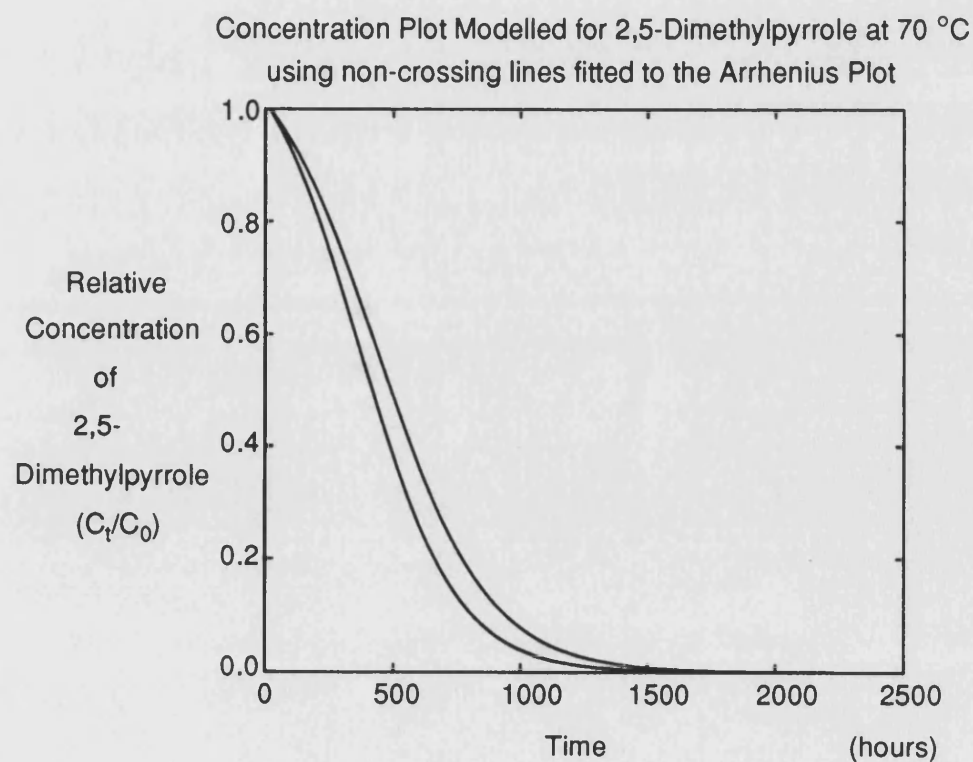


Figure 3.35

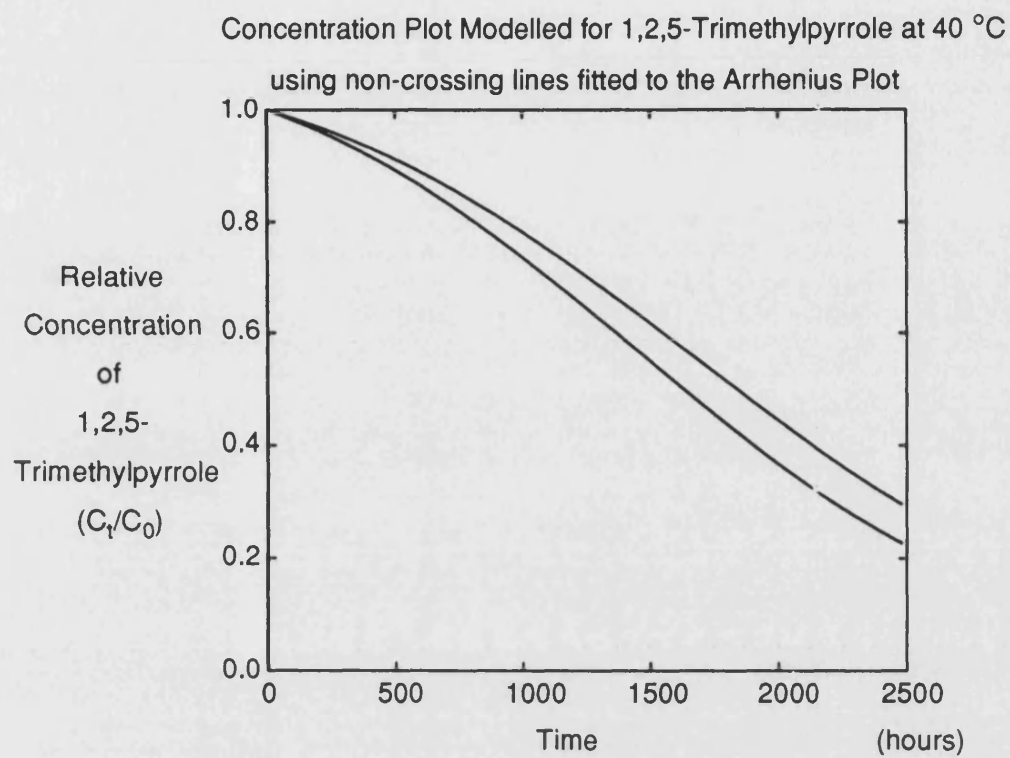


Figure 3.36

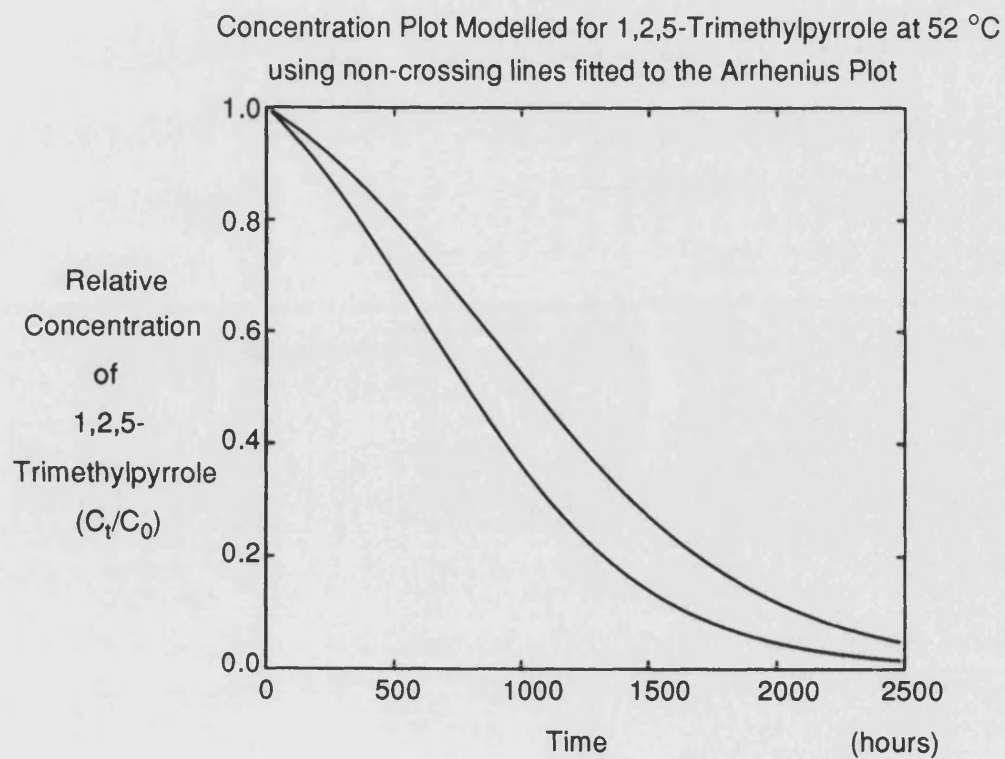


Figure 3.37

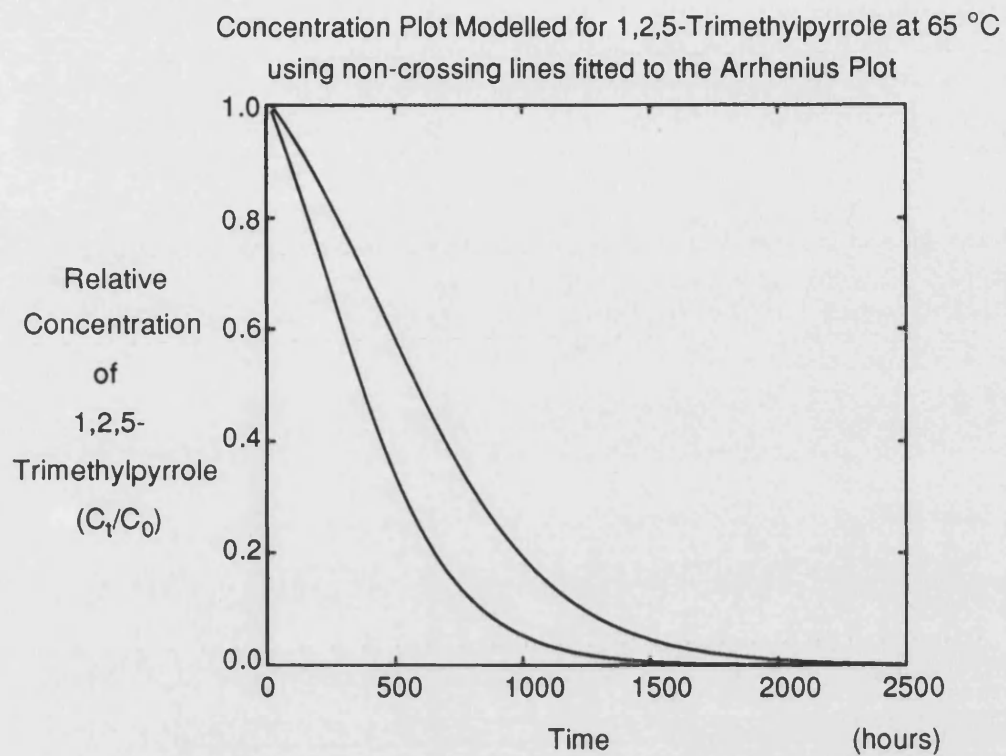


Figure 3.38

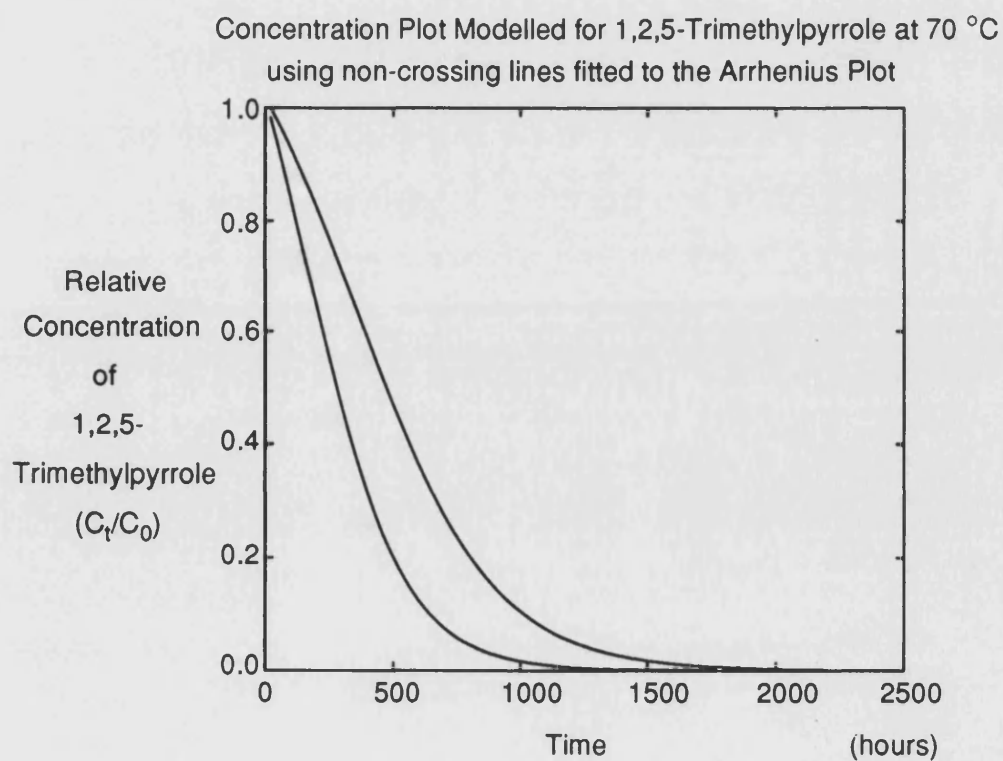


Figure 3.39

As can clearly be seen from the graphs shown (figures 3.40 to 3.42), there is good agreement between the actual degradation data and the modelled concentration plots. The two lines fitted to this data are those curves generated from the highest and lowest values of the rate constants.

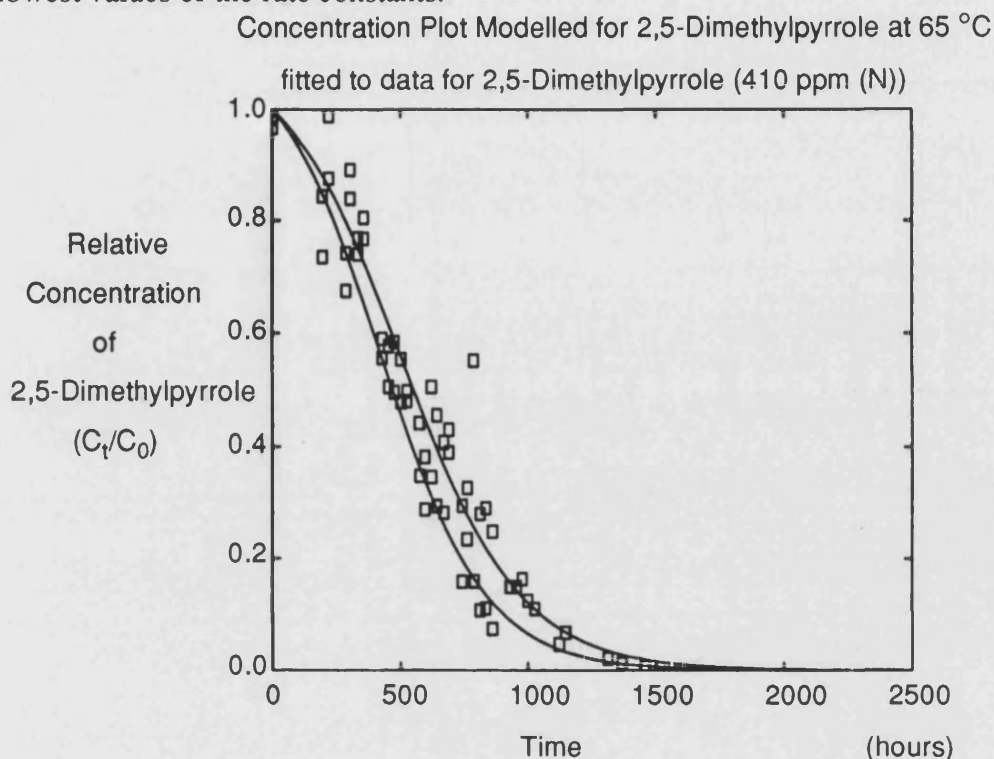


Figure 3.40

In the case of 1,2,5-trimethylpyrrole the modelled concentration plots give good agreement at low pyrrole concentration, but as the concentration increases these modelled curves begin to deviate from the experimental data. The deviation that occurs with 1,2,5-trimethylpyrrole may be due simply to the effects of the calibration curve for 1,2,5-trimethylpyrrole. As the concentration of the dopant increases, the error on the curve also increases, until at very high concentrations a small change in analysis result yields a large change in reactant concentration. However, the results would still appear to suggest that the predicted rate equations are a good approximation to the actual degradation process in both the 2,5-dimethylpyrrole and 1,2,5-trimethylpyrrole cases.

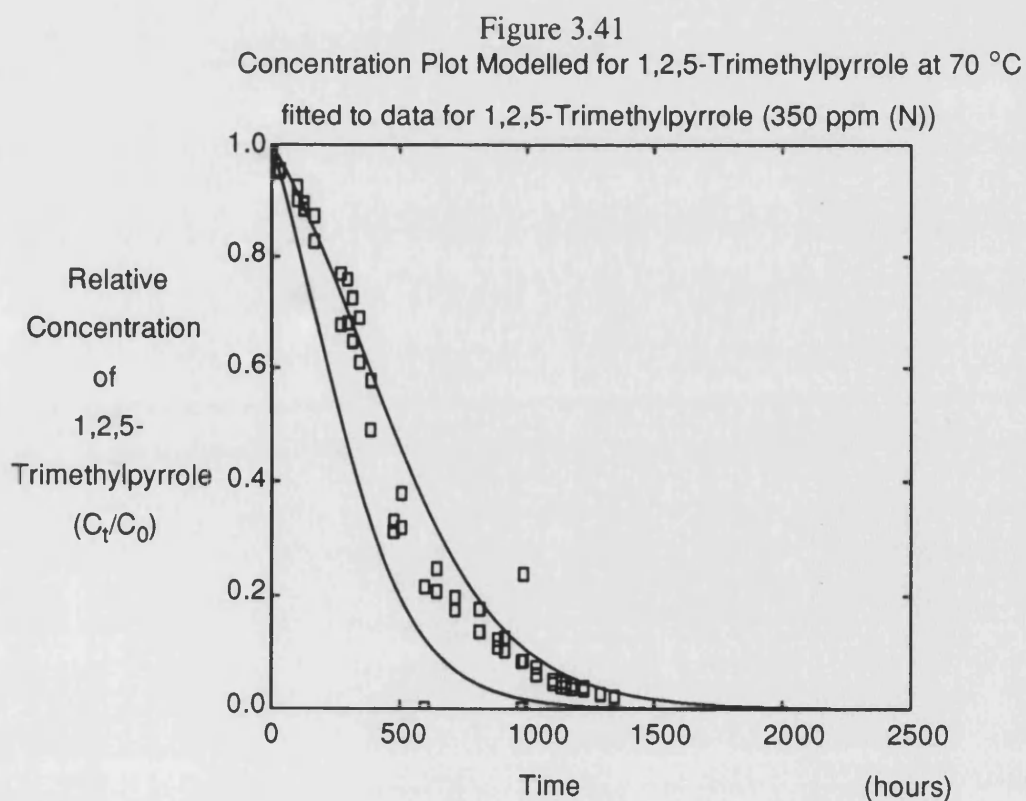
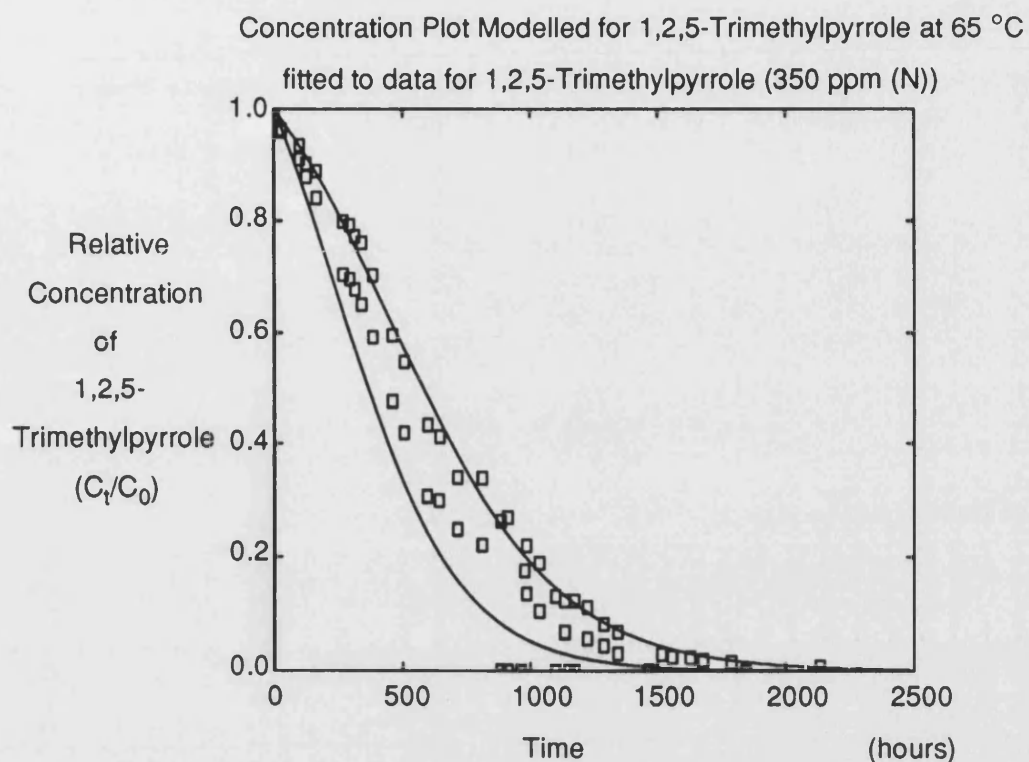


Figure 3.42

It should be noted that curves modelled by micromodeller may suffer an error when a large step size is chosen for the integration. When a comparison was made with results from an integration based on ten steps or one hundred steps for 2,5-dimethylpyrrole at ambient temperature, final fractions of the original concentration of 0.15 and 0.16 respectively were predicted after 2500 hours. This is a difference of approximately 7 %. All calculations performed with micromodeller were based on 125 steps in the integration.

#### 3.4.2 The Combined Dopant System

The data for this system are presented graphically in the appendix. A detailed analysis of the kinetics of this system proved not to be possible. A graphical examination of the degradation data obtained for the combined dopant system revealed a more complicated picture than was initially expected. In order to perform a detailed kinetic analysis of this system more measurements are required, but some comments and conclusions can be made from the data available.

When these profiles were compared with the measured degradation data for the combined dopant simple model fuel systems, a marked difference was noted. The major dopant 2,5-dimethylpyrrole was observed to follow much the same reaction profile, with only a slight increase in the overall rate of dopant consumption. The minor dopant 1,2,5-trimethylpyrrole was observed to deviate greatly from the predicted reaction profile, not, as might be expected by an increase in consumption rate, but by a drastic decrease in the rate of consumption. At low concentration, the reaction order with respect to the minor dopant tends towards zero.

An explanation for this behaviour can be based on the rates of reaction being dependent on the presence of oxygen, which is required for the autoxidation reaction. If 2,5-dimethylpyrrole can react easily and preferentially with the oxygen then this would make oxygen unavailable for autoxidation with the 1,2,5-trimethylpyrrole. The result of this would be that, the 1,2,5-trimethylpyrrole would not degrade

noticeably, and its degradation would be even less than that predicted by the first half of its normal rate equation due to the lack of oxygen for the autoxidation reaction.

This explanation depends of course on the assumption that oxygen is in short supply for the reaction. This assumption is supported by the fact that the reaction vessels are sealed with teflon lined screw top septa. Seals of this type have been suggested by Bhan et al.<sup>21</sup> to pass oxygen into or out of the container during ageing tests.

The explanation suggested for this behaviour is supported by the conclusions reached by Frankenfeld, Taylor and Brinkman<sup>53</sup>, who observed that 2,5-dimethylpyrrole is, apparently, much more reactive than other nitrogen bearing species and competes successfully for available oxygen.

#### 3.4.3 Concluding Comments on Modelling

The work performed up to this point has been an examination of two compounds found in diesel fuel and known to be very deleterious to fuel stability, namely 2,5-dimethylpyrrole and 1,2,5-trimethylpyrrole. The kinetic analyses of these systems has shown good correlation with the degradation data measured for the model systems. In addition, rate constants predicted by the kinetic studies compare well with those obtained from the doping of a real fuel, both in this thesis and by other workers. Although kinetic analyses of such systems have previously been performed, modelling on such a detailed scale has not been attempted and therefore, comparison of these two systems with real fuel systems can only be made on a qualitative basis at the present time. In view of the success in predicting concentration plots for dopants, there is obviously a need for similar analyses on other deleterious compounds to be carried out. This would then allow the assembly of a more complete picture of fuel degradation kinetics and the construction of a kinetic model applicable to a wider range of fuel types on a more quantitative basis.

Pedley et al.<sup>50</sup> performed an ambient study on three fuels, one a stable fuel and

the other two containing 10 % catalytically cracked stock. The temperature range for the study was between -5 °C and 25 °C. For one of the unstable fuels containing 63 ppm of nitrogen, 2.9 % of this nitrogen was found in sediment after a storage period of thirteen months. Using the kinetic model developed in this thesis a storage period of one month within this temperature range yields the same nitrogen loss with the 2,5-dimethylpyrrole as a dopant. However, the 1,2,5-trimethylpyrrole system predicts a period of six months to attain the same nitrogen loss. These two compounds are obviously highly deleterious to fuel stability and the predictions made are based on the nitrogen content of the fuel being composed solely of these components. In a real fuel the nitrogen composition would contain far less of these components and more of the less harmful nitrogen heterocycles. Therefore, a knowledge of exact fuel composition and of the kinetic behaviour of the fuel constituents would enable a more accurate prediction of sedimentation rates.

In conclusion, the results obtained during this kinetic study have provided a valuable method of predicting the behaviour of various systems. There is obviously great potential for the development of this approach to a wider range of fuel types and systems.



### 3.5 RESULTS FROM LOW ENERGY ULTRASOUND EXPERIMENTS

The introduction details some of the fuel degradation techniques which are currently in use for assessing fuel stability. Although ultrasonic irradiation has been applied in many areas of chemistry, it has not until now been applied to fuel stability studies. The remainder of this chapter is concerned with detailing results of the initial work carried out in this novel area. This has proved to be a fruitful and interesting field of study and initial results indicate that further investigation should yield data of significant value.

#### 3.5.1 Low Energy Ultrasonic Degradation of Diesel Fuel

In order to assess the utility of low energy ultrasonic irradiation as a technique for testing fuels for their stability characteristics, samples of diesel fuel were subjected to irradiation for 1 hour. The fuel was then filtered after a dark ambient storage period of 24 hours. After filtration there was found to be no detectable residue. There was also found to be no residual gum or adherent residue detectable by weight difference of the storage vessel. Therefore, if degradation had occurred during storage, it was on a scale of less than 2 ppm or mg/l. This again confirms the stability of the fuel, as indicated by the thermal and ultra-violet tests, or the inability of low energy ultrasound to degrade it.

#### 3.5.2 Low Energy Ultrasonic Degradation Initiation and Storage of Diesel

Having discovered that low energy ultrasound was, by itself, insufficient to cause fuel degradation, a free radical initiator was included in the reaction. It has been shown that ultrasound can cause reaction of free radical initiators. Apart from the presence of a free radical initiator the conditions used in this experiment were the same as those described in the previous experiment. After filtration, no sedimentation or gum formation was found to have occurred and no adherent residue was detected. Any solid formation was thus on a scale of less than 2 ppm or mg/l. It would

therefore appear that low energy ultrasound, even in conjunction with a free radical initiator, was insufficient to destabilise the fuel.

### 3.5.3 Ultra-violet and Ultrasonic Degradation: A Comparison

A series of experiments were carried out to compare the relative effects of ultra-violet irradiation and low energy ultrasonication. The compositions of the mixtures examined are shown in table 3.6.

It was immediately obvious that the ultra-violet irradiation had produced a significant darkening of all of the fuel samples so treated. However, treatment with ultrasound produced no visible change.

These samples were placed in dark ambient storage for a period of one week and then filtered. The table clearly shows that ultra-violet irradiation produced a mass of sediment which was directly proportional to the concentration of dopant in the original mixture. In contrast, the ultrasonic experiments although showing detectable amounts of sediment, showed no significant difference between differently doped samples.

Table 3.6

<u>No.</u>	<u>ppmDBP</u>	<u>ppmDMP</u>	<u>ppmTMP</u>	<u>Treatment</u>	<u>Sediment Weight</u> g
1	0	0	0	U.V.	0.0044
2	0	0	0	U.S.	0.0044
3	0	250	250	U.V.	0.0128
4	0	250	250	U.S.	0.0055
5	25	250	250	U.V.	0.0082
6	25	250	250	U.S.	0.0051
7	0	500	250	U.V.	0.0102
8	0	500	250	U.S.	0.0069
9	25	500	250	U.V.	0.0126
10	25	500	250	U.S.	0.0058

U.V.= Ultra-violet irradiation  
U.S.= Ultrasonic irradiation  
DBP = Dibenzoyl peroxide  
DMP = 2,5-Dimethylpyrrole  
TMP = 1,2,5-Trimethylpyrrole

The diesel and washings were put back into dark ambient storage where they continued to degrade. It appeared that under these experimental conditions the ultra-violet irradiation had destabilised the fuel to a greater extent than the low energy ultrasonic treatment.

### 3.5.4 Ultrasonic Degradation of 2,5-Dimethylpyrrole Doped Model Fuel

The results from the thermal study on the 2,5-dimethylpyrrole doped dodecane are detailed in section 3.3. In order to compare low energy ultrasonic degradation with thermal degradation, an experiment was performed in which the same system was treated with ultrasonic irradiation. This experiment was necessitated by the need to assess ultrasonic irradiation as a potential fuel stability characterisation technique. Therefore, with this aim in mind, this experiment allowed a comparison between the two methods to be made. Four different starting concentrations of 2,5-dimethylpyrrole were examined. The concentrations chosen were between 1032 and 2006 ppm (N) mg/l, these values being in a range similar to that used in the thermal studies. The following graphs (figures 3.43 to 3.46) show the change in concentration of 2,5-dimethylpyrrole in dodecane during sonication.

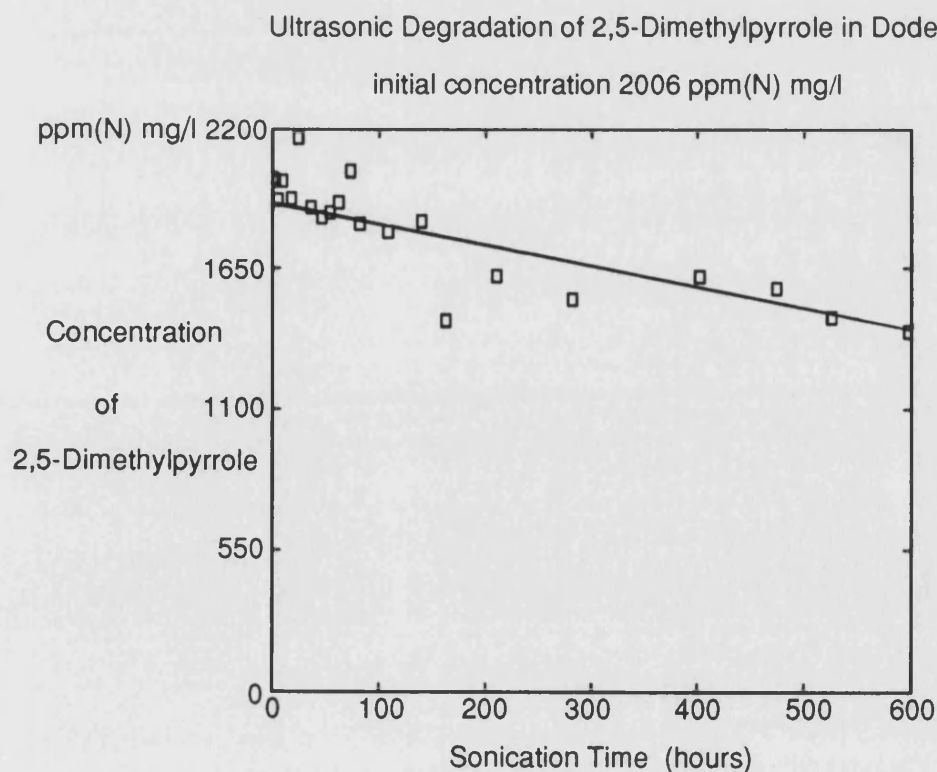


Figure 3.43

## Ultrasonic Degradation of 2,5-Dimethylpyrrole in Dodecane

initial concentration 1818 ppm(N) mg/l

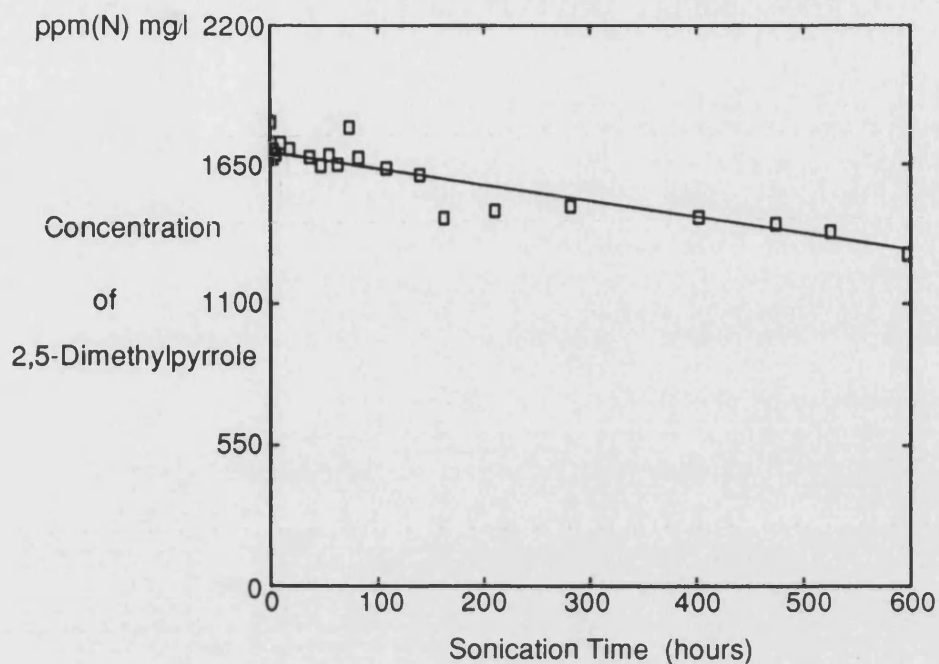


Figure 3.44

## Ultrasonic Degradation of 2,5-Dimethylpyrrole in Dodecane

initial concentration 1480 ppm(N) mg/l

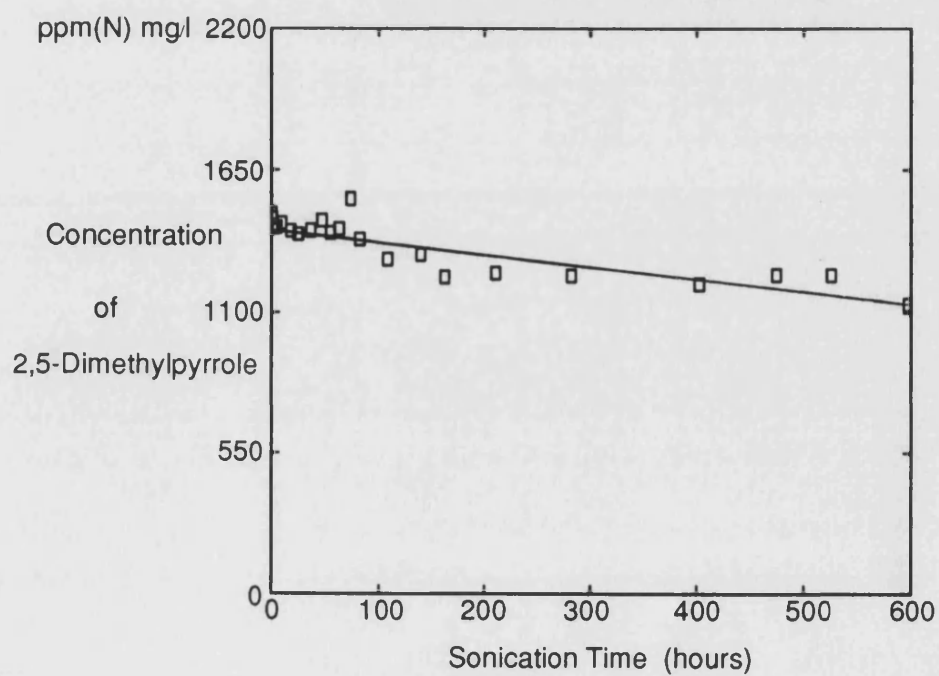


Figure 3.45

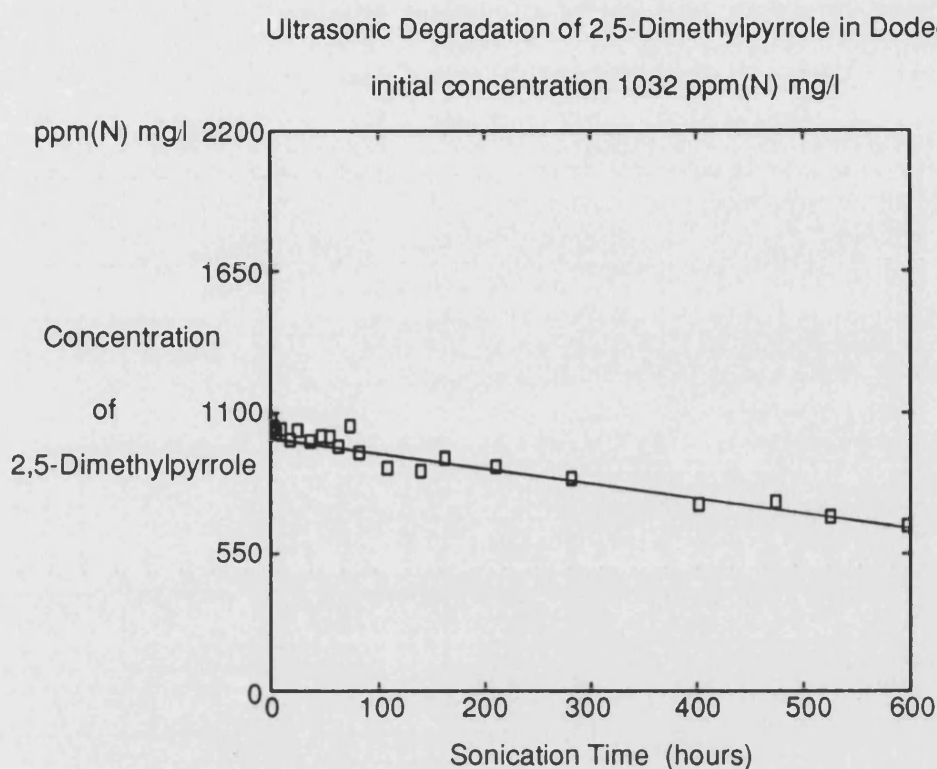


Figure 3.46

The three higher concentration plots (figures 3.43 to 3.45) (1480, 1818 and 2006 ppm (N)) of 2,5-dimethylpyrrole in dodecane appear to show a linear relationship with sonication time. This indicates that the rate of reaction is possibly a zero order process. The lowest concentration plot (1032 ppm (N)) (figure 3.46) also indicates, after cursory examination, a zero order process. However, an examination of the first order plots of these curves (figures 3.47-3.50) reveals the involvement of a higher order process in the overall kinetics.

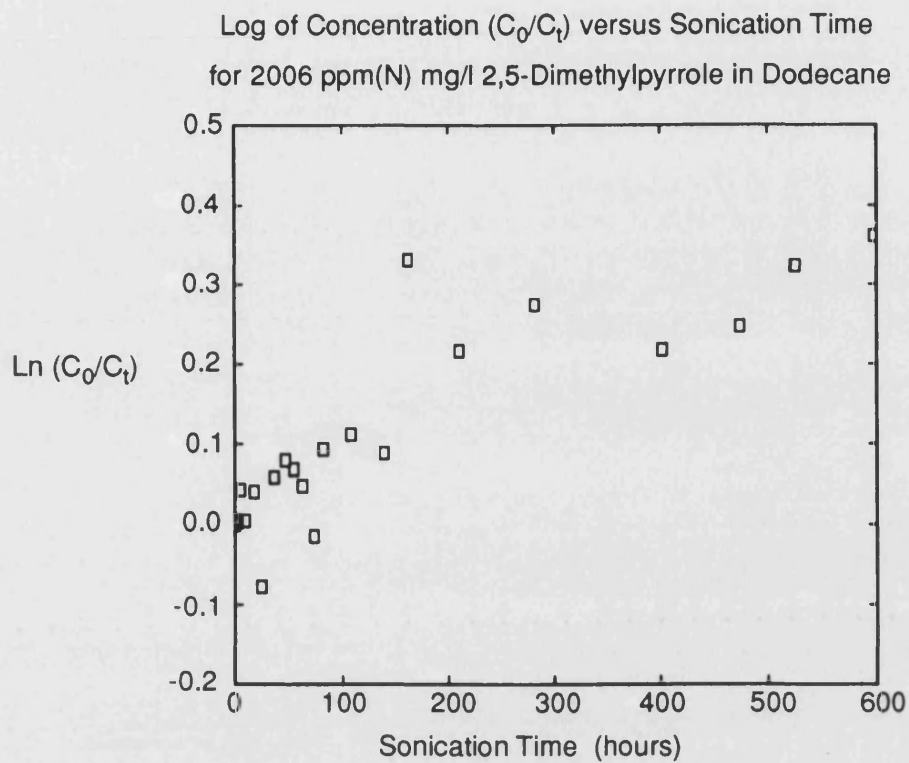


Figure 3.47

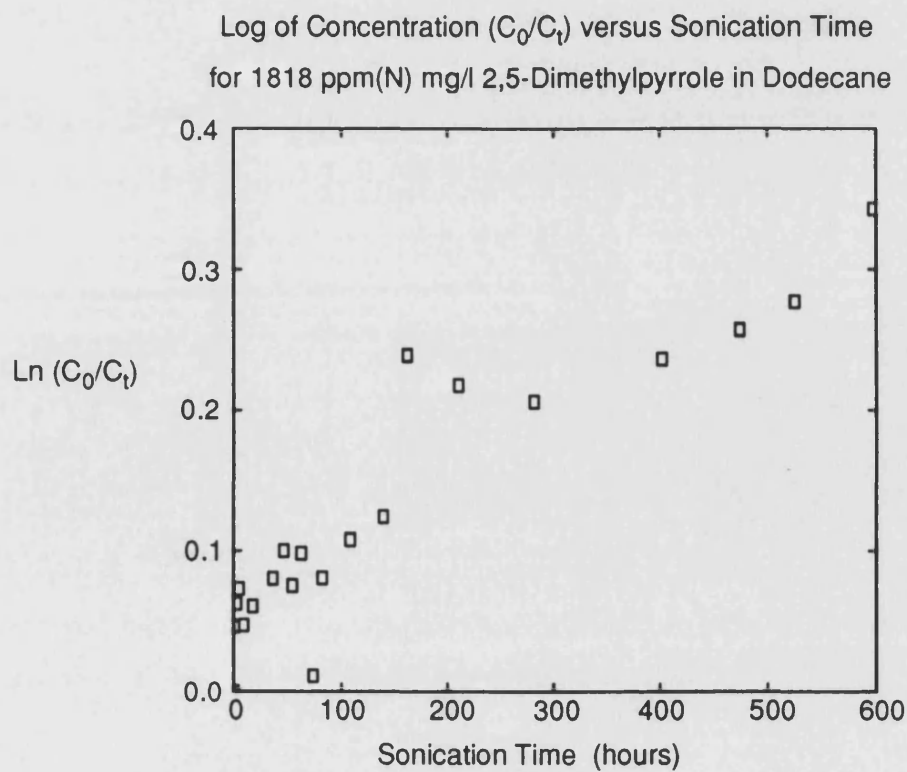


Figure 3.48

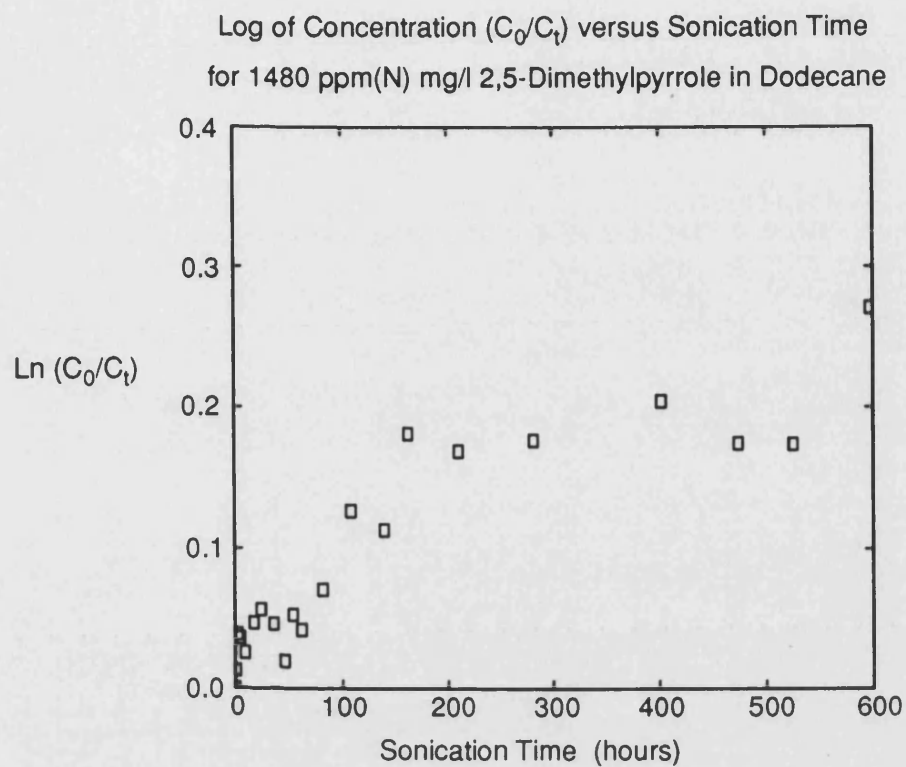


Figure 3.49

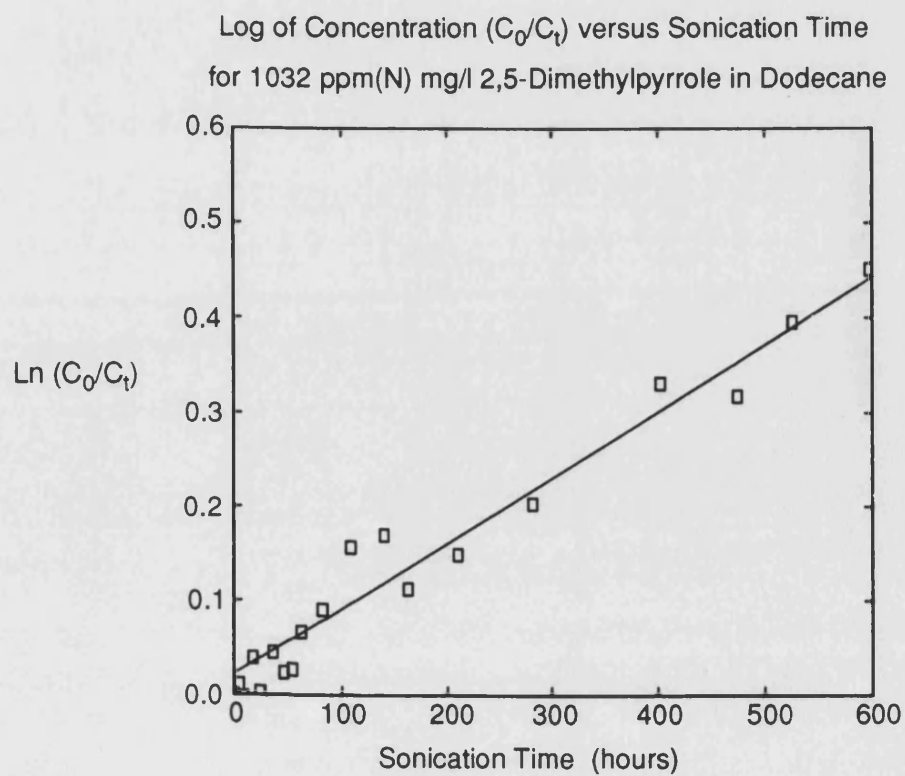


Figure 3.50



The first order plot (figure 3.50) of the lowest concentration of 2,5-dimethylpyrrole in dodecane against sonication time, shows linear characteristics. A linear fit for this plot indicates that the reaction approximates to a first order process in which the rate of 2,5-dimethylpyrrole consumption is directly proportional to its concentration. This is in keeping with the character of the reactions observed when 2,5-dimethylpyrrole is degraded thermally in dodecane.

While the lowest concentration of 2,5-dimethylpyrrole indicates a first order process, the results obtained for the higher dopant concentrations are in conflict with this. These appear not to follow simple first order kinetics. As the concentration of the dopant is increased it is no longer a controlling factor in the rate of reaction. It is possible that this is a simple saturation effect and that the fractional change in the higher dopant concentrations during the reaction is so small as to be negligible. A contributing factor to the difference in these results could also be due to the position of the conical flasks in the ultrasound bath. The intensity of ultrasound in a bath varies with position. This is due to the pattern in which the transducers are laid out. Further from the transducers the ultrasound is weaker.

The first order process yields a rate constant of  $0.00040 \text{ h}^{-1}$  and the temperature of the ultrasonic bath was found to stabilise at  $44^\circ\text{C}$ . Calculations performed using micromodeller would yield a sediment value of  $9.2 \text{ mg}/100 \text{ cm}^3$  after 14 days sonication from a starting dopant concentration of  $750 \text{ ppm (N) mg/l}$ . This figure can be compared with a prediction from the modelled degradation curves calculated at a temperature of  $44^\circ\text{C}$ . At this temperature the calculated values for  $k_{1\text{DMP}}$  and  $k_{2\text{DMP}}$  are  $0.00024 \text{ h}^{-1}$  and  $0.0028 \text{ h}^{-1}$  respectively. These values would yield a sediment value of  $9.0 \text{ mg}/100 \text{ cm}^3$  after a storage period of 14 days. From these results it can be seen that low energy ultrasonication appears to exert a small accelerating effect upon the reaction rate of 2,5-dimethylpyrrole in dodecane.

### 3.6 RESULTS FROM HIGH ENERGY ULTRASOUND EXPERIMENTS

The investigation of low energy ultrasound, while producing some interesting results, did not show the promise of applicability as a fuel stability assessment technique. The use of high energy ultrasound was, therefore, investigated to examine its utility for this purpose.

#### 3.6.1 Ultrasonic Degradation of Dodecane (a Model Fuel)

Before using high energy ultrasonic irradiation on diesel fuel to investigate the effects on fuel stability and sedimentation in particular, it was obviously necessary to investigate the effects on the actual alkanes in the diesel. Therefore, the effects of high energy ultrasonication on dodecane were investigated. A sample of dodecane was sonicated and periodically analysed using gas chromatography to determine the rates of production of hydrocarbon fragments from the dodecane. Work similar in nature to this has been performed by Suslick et al.<sup>130</sup> on decane.

The analyses of sonicated dodecane revealed the production of lighter alkanes during the irradiation. By comparison with a calibration mixture containing a wide range of straight chain alkanes, these lighter alkanes were identified as n-heptane, n-octane, n-nonane and n-decane. If alkanes below n-heptane were being formed and remained in solution, they were below the detection limits for the equipment.

Undecane is an impurity which was found to be present in the dodecane used throughout this thesis and has proved to be a useful internal reference. As the concentration of undecane in the dodecane is low it was assumed that any fragments arising from undecane sonication would also be of a very low concentration and would thus, not noticeably affect the overall results. The peak areas for dodecane fragments were expressed as fractions of the peak area of undecane. These values were plotted against sonication time and are shown in the graphs figures 3.51-3.54.

## Growth of Heptane in Dodecane During Sonication

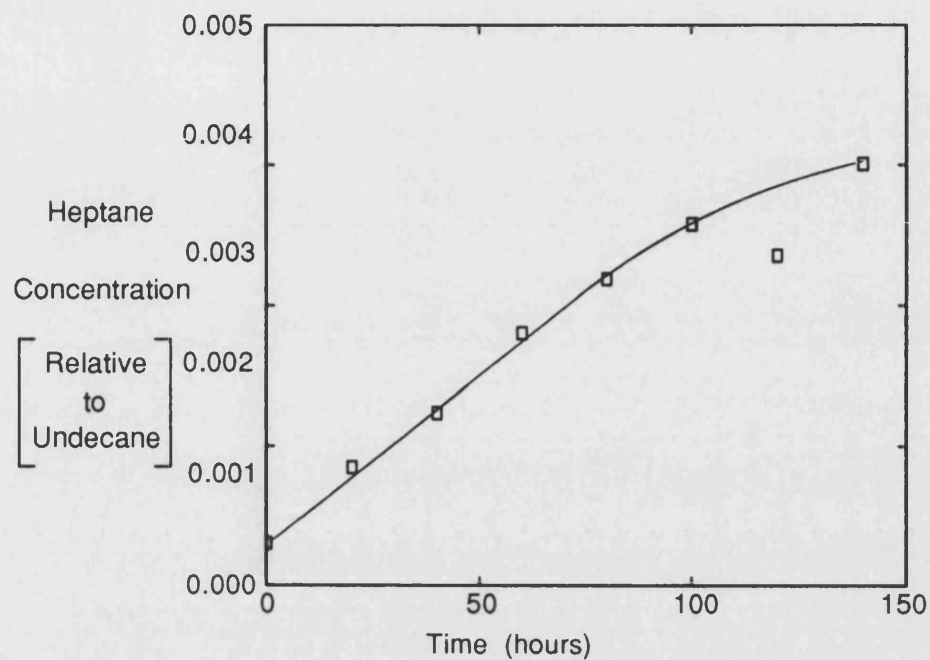


Figure 3.51

## Growth of Octane in Dodecane During Sonication

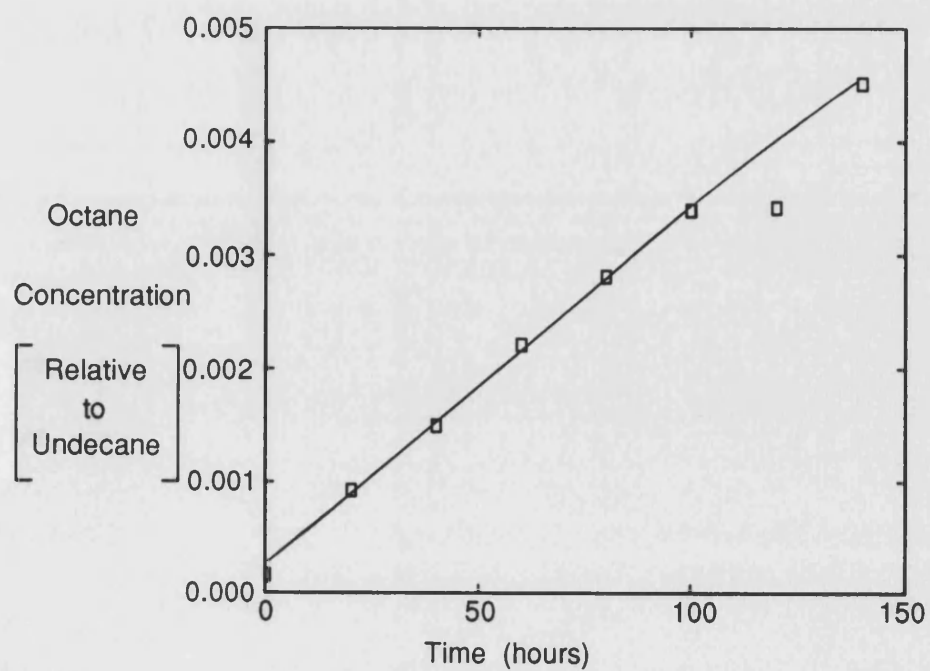


Figure 3.52

Growth of Nonane in Dodecane During Sonication

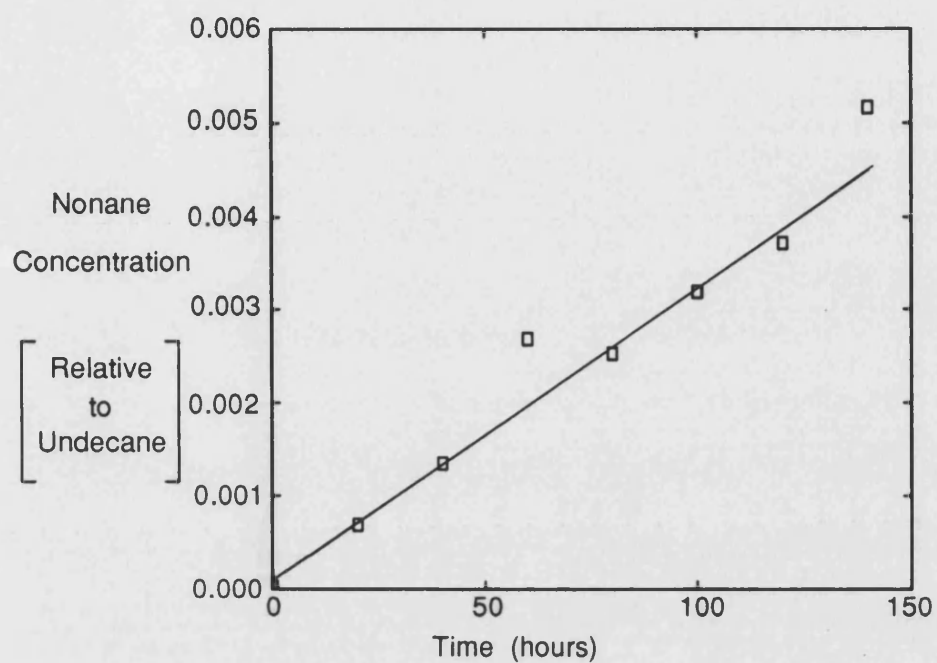


Figure 3.53

Growth of Decane in Dodecane During Sonication

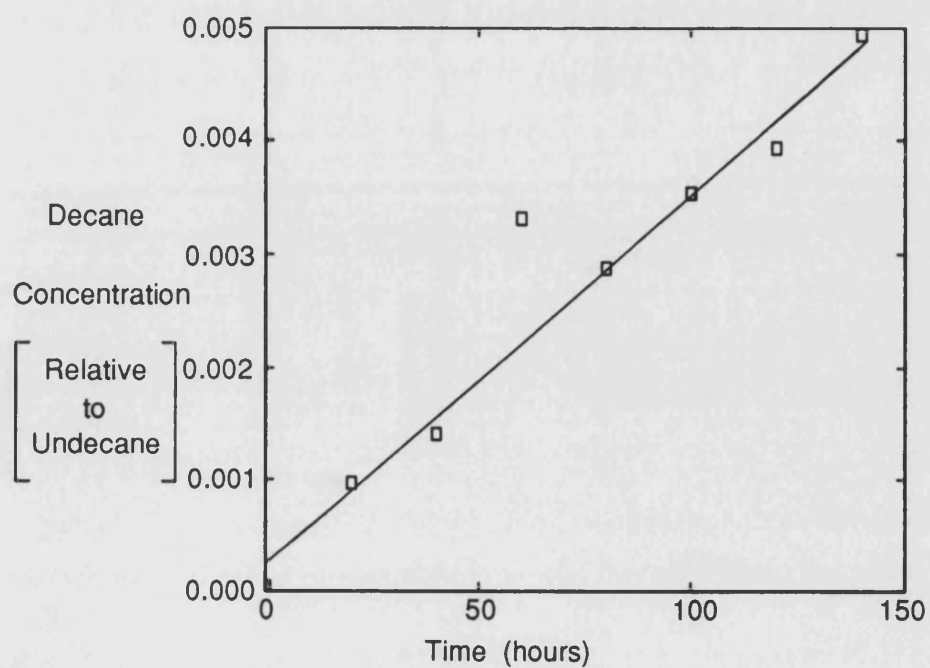


Figure 3.54

Sonication of dodecane causes fragmentation of the alkane chains. For all four plots there is an increase in  $C_7$  to  $C_{10}$  with sonication time. Initially, the concentration of heptane in dodecane increases linearly. However, there appears to be an upper limit to this and the plot apparently begins to flatten out after 100 hours sonication. Confirmation of this would require a duplicate experiment for a longer total sonication period. A possible explanation for this behaviour could be related to the increased ease of stripping the volatile heptane from the dodecane as its concentration increases. In addition to this effect, as the heptane concentration increases, the effect of its volatilising into cavitation sites will become more pronounced, cushioning to some extent the collapse of the cavitation sites. This cushioning reduces the effects of the ultrasound and the rate of increase of heptane begins to decrease.

Octane follows much the same changes in concentration as heptane. The major difference being that the rate of production of octane does not appear to decrease within the time period of the experiment. The growth of nonane also follows a linear pattern. The rate of production of nonane is very similar to the rate of production of those alkanes with shorter chain lengths. Decane shows the same characteristics as nonane and reaches a very similar relative concentration in the same amount of time. The rate constants for the formation of n-heptane, n-octane, n-nonane and n-decane are shown in table 3.7. The units of the rate constant are calculated on the basis of alkane concentration relative to n-undecane and thus only have the value of  $h^{-1}$ . In this format the rate constants cannot be related to work by other researchers and must thus be transformed to a more usable format.

The effect observed for n-heptane may also occur for the other alkanes formed, but was not observed during the 150 hour sonication. It may be that the deviations from linearity observed for the formation of n-heptane is due in part to experimental error. Confirmation of these results could be obtained by performing the sonication of dodecane for a longer time period.

Table 3.7

<u>Alkane</u>	<u>Rate Constant</u>
n-Heptane	0.00018 h <sup>-1</sup>
n-Octane	0.00029 h <sup>-1</sup>
n-Nonane	0.00033 h <sup>-1</sup>
n-Decane	0.00032 h <sup>-1</sup>

The implications of this experiment for degradation of chain molecules using ultrasound are obvious. As the rates of production of the alkanes in this experiment are all very similar, this would imply that a chain molecule is equally likely to fragment at any of the carbon carbon bonds along its length.

Suslick et al.<sup>130</sup> performed a study of the effect of ultrasonic irradiation on n-decane and drew a parallel between this and other high energy processes such as pyrolysis. They showed linear rates of production for less volatile products and some diminution of observed rates for volatile products. This is in agreement with the results observed in this thesis. The following table (table 3.8) shows a comparison between the results of Suslick et al. and the recalculated results from this thesis assuming that the concentration of undecane in the dodecane is approximately 10% and that the signal is directly proportional to the mass of alkane and converted to an equivalent dodecane volume of 10 ml (assuming a dodecane density of 1). The calculation is as follows:- For heptane the rate =  $0.18 \times 10^{-3}$  g (density of 1) h<sup>-1</sup>, this is converted to a fraction of the dodecane by dividing by 10 (10% undecane in dodecane) to yield a value of  $18 \times 10^{-4}$  h<sup>-1</sup>. This value can then simply be converted to a value in moles per minute which yields a value of  $3 \times 10^{-7}$  mol min<sup>-1</sup> for 150 ml of dodecane. This must then be divided by 15 to correct to a volume of 10 ml as used by Suslick to yield a final value of 20 nmoles min<sup>-1</sup>. If all of the other results are treated in like fashion then the calculated values are as shown in the table.

Table 3.8

<u>Alkane</u>	<u>Rate Constant (this work)</u>	<u>Rate Constant (Suslick et al.)<sup>131</sup></u>
Heptane	20 nmoles m <sup>-1</sup>	16 nmoles m <sup>-1</sup>
Octane	28 nmoles m <sup>-1</sup>	9 nmoles m <sup>-1</sup>
Nonane	29 nmoles m <sup>-1</sup>	3 nmoles m <sup>-1</sup>

An examination of the compared values in the table shows the results obtained in the thesis are in the same range as those rate constants found for the formation of the same alkanes when Suslick et al. sonicated decane. There are noticeable differences between the two sets of results. Suslick et al. used a smaller reaction cell (10 ml) and the acoustic output of their probe was less (100 Wcm<sup>-2</sup>), compared to 150 ml and a power output of 152 Wcm<sup>-2</sup>. There is a noticeable volume effect when using ultrasound, so the different volumes utilised will produce different results. Also the difference in power output will produce different results. These two effects will cancel out to some extent, the higher power cancelling out the effect of a larger volume, but a difference in results would still be expected.

An interesting conclusion that they reached was that as solvent volatility is reduced, the intensity of cavitation collapse, the maximum temperature reached and the rate of reaction, all increase. So as ambient temperature increases, sonochemical reaction rates decrease, due to increased solvent vapour pressure. The pertinence of this to the sonication of dodecane and of diesel should be clear. Sonication at lower temperatures should yield higher amounts of sonication products over the same time period and as the sonication proceeds and volatile components are driven off the reaction rates should increase which will to some extent balance the effect of the loss of the volatile components.

### 3.6.2 High Energy Sonication of Diesel Fuel

As has been discussed earlier in section 1.6, ultrasound has various effects on the sonication medium. These effects include the generation of very high instantaneous temperatures and pressures and also the production of free radicals in the medium. The effects of temperature<sup>3,5,104,115</sup>, pressure<sup>116</sup> and free radicals<sup>56</sup> in relation to sedimentation in diesel fuel have all been studied. Ultrasound is a technique which might be expected to draw all three of these together.

This experiment was intended to investigate the degrading effects of ultrasound on diesel fuel in terms of sedimentation. The results from this investigation are shown in table 3.9 and except where stated otherwise, sample volume for sonication was 150 ml and the probe output was set at 100% with no pulsing of the signal.

Table 3.9

<u>Sonication Time</u>	<u>Sediment Weight</u>	<u>N Content</u>	<u>N Weight</u>
<u>hours</u>	<u>mg/l</u>	<u>%</u>	<u>mg/l</u>
0	0.0	0	0
6	46.0	2.6†	1.20†
12	72.0	0.48	0.35
18	76.7	1.79	1.37
24	114.7	1.12	1.28
30	154.7	0.94	1.45
36	213.3	0.84	1.79
440‡	244.0	2.57	6.27
† C:H:N operator quoted this analysis as unreliable.			
‡ Sample volume is 900 ml probe conditions are 50% output 50% pulse rate.			

The following graph (figure 3.55) displays the amount of sediment formed



with time, during the sonication of samples of diesel.

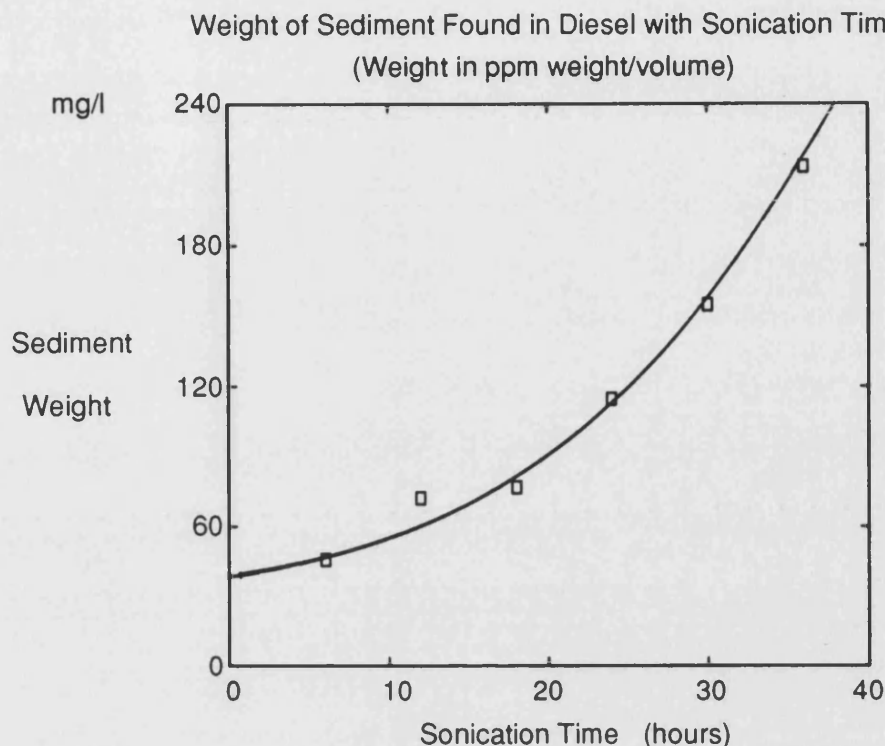


Figure 3.55

The plot clearly shows that the rate of sediment formation increases with sonication time. This observation can be related to work carried out by Suslick et al.<sup>130</sup>. As volatiles are driven out of solution by the sonication, the collapse of sonication cavities is no longer cushioned and the intensity of the shockwave, produced by their collapse, increases. It could be expected that a higher rate of reaction would be found at the start of sonication due to the presence of more reactive species in the diesel. As these species degraded the rate would slow slightly, accounting for the non-zero intercept on figure 3.55. However, there are reasons why degradation does not stop entirely. As has already been stated, the effect of the ultrasound increases with the removal of volatiles. Also, ultrasound is known to produce free radicals which cause instability<sup>56</sup> and to produce instantaneous

temperatures and pressures of a very high order, which have been shown<sup>3,5,116</sup> to have a deleterious effect on fuel stability.

Figure 3.56 depicts the linear relationship for a plot of log of sediment weight found against sonication time.

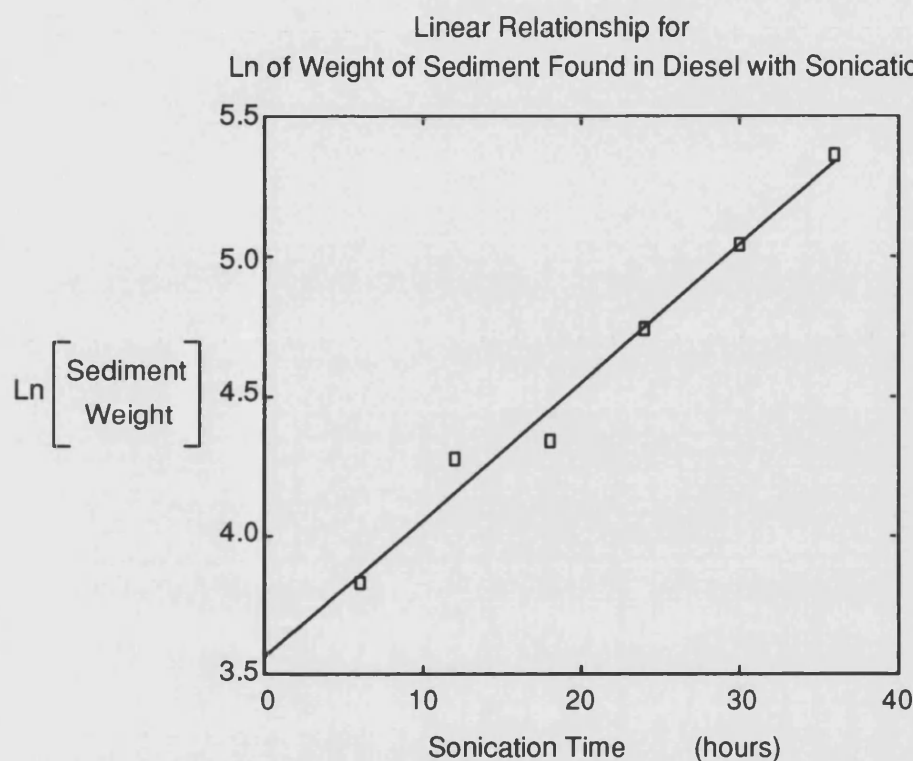


Figure 3.56

The graph unequivocally shows a linear relationship, thus confirming the first order nature of the sedimentation process for which the rate constant is  $0.05 \text{ h}^{-1}$ . The best fitted lines to this data be utilised by micromodeller to predict a sediment value of  $34.6 \text{ mg/l}$  after 1.2 hours sonication. Pedley et al.<sup>50</sup> found  $2.2 \text{ mg/l}$  of sediment after 28 days storage at  $50^\circ \text{C}$ . If it can be assumed that the diesel used in this thesis and the Bahrain straight run distillate used by Pedley et al. are of comparable stabilities, then one hours sonication under the conditions utilised for this experiment, is approximately equivalent to a storage period of 420 days at  $50^\circ \text{C}$ . It would be

expected that other fuels would produce plots of a very similar nature. However, for less stable fuels a larger gradient would be expected. The gradient of such a plot could therefore be a measure of the stability of a fuel.

Out of interest the nitrogen contents of these sediments were examined. These percentage nitrogen contents and the calculated weights of nitrogen precipitated are shown in table 3.9. It was significant that the values of nitrogen content found in the sediment were noticeably higher than the nitrogen content of the fuel (0.25 %). This indicated that the nitrogen components of the fuel were, as might be expected, the major destabilising compounds involved in sediment formation. A plot of nitrogen content in the sediment against sonication time is shown in figure 3.57.

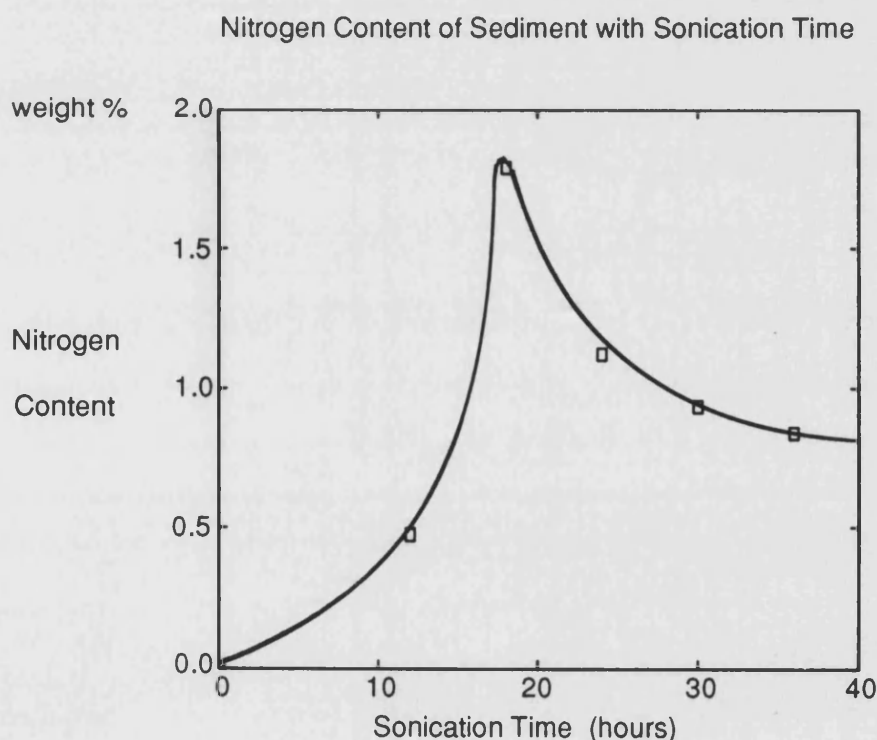


Figure 3.57

The graph (figure 3.57) shows an initial rapid increase in nitrogen content to a maximum of 1.8 %, followed by an exponential dilution of the nitrogen in the

sediment. This can be explained by the presence of a nitrogen bearing component of the fuel. This component reacts rapidly at the start of the sonication. Once this component becomes concentrated into the sediment the less reactive components in the fuel, which may not contain nitrogen, play a more significant role in the sedimentation process and dilute the nitrogen content of the sediment.

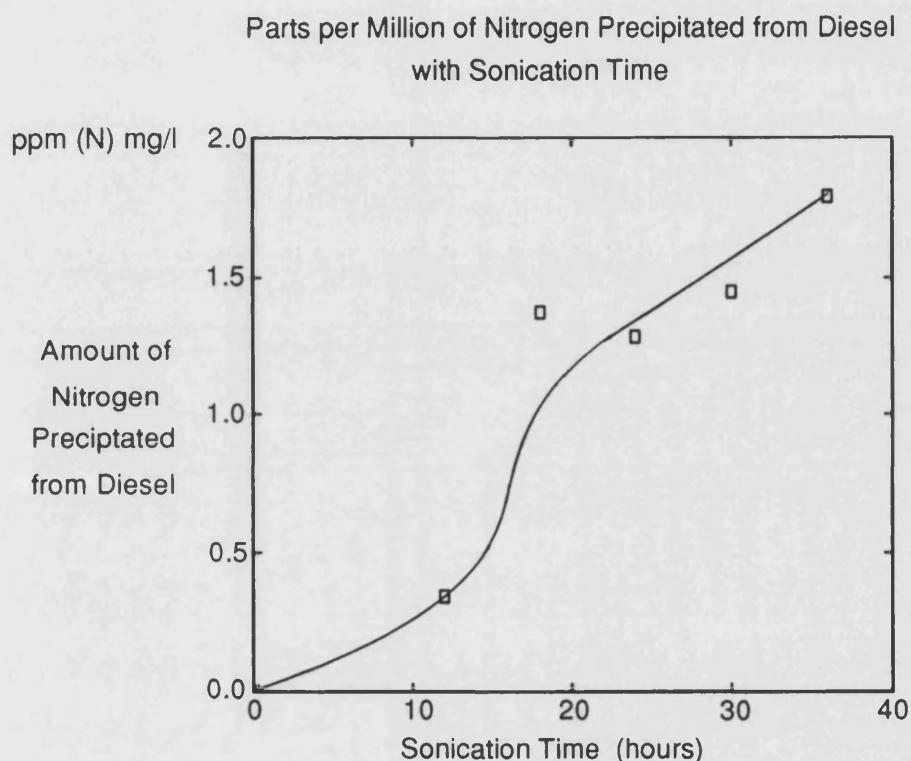


Figure 3.58

This graph (figure 3.58) shows the actual weight of nitrogen precipitated from 150 ml of diesel with time, expressed as parts per million of nitrogen in  $\text{mg l}^{-1}$  of diesel fuel. Apart from the initial slow increase in nitrogen, which is followed by an acceleration, the nitrogen content of the sediment increases in a linear fashion with time. This curve shape indicates that there may be some autoacceleration occurring during the sonication. After the autoaccelerated part of the process there is a continual and constant depletion of the nitrogen bearing components of the fuel. A

line fitted to these points yields an intercept of 0.02 ppm (N) and a gradient of 0.051 ppm (N) h<sup>-1</sup>. Using these values in conjunction with micromodeller yields a value of 149 mg/100 cm<sup>3</sup> nitrogen precipitated after nine and a half days sonication. Frankenfeld et al.<sup>53</sup> found a sediment value of 141 mg/100 cm<sup>3</sup> (mg of nitrogen) at a storage temperature of 43.3 °C after a period of four weeks. The fuel used by Frankenfeld et al. was doped with 2,5-dimethylpyrrole which obviously enhanced the rate of nitrogen precipitation in their fuel. However, the precipitation rate of nitrogen found using ultrasound is still ten times faster than that found by Frankenfeld et al.<sup>53</sup>. If it is assumed that all of the nitrogen which is in the fuel (0.25 %) is consumed in the formation of the sediment, then a total weight of nitrogen of 0.28 g should be precipitated from a 150 ml volume of diesel. This value converts to one of 1.875 g/l or 1875 ppm (N) mg/l. Thus, it might be expected that sonication for longer time periods should yield much higher amounts of sediment with a higher nitrogen content.

After filtration the fuel samples were placed in dark ambient storage for one year. The following table gives the results of gravimetric analyses for these fuel samples after the storage period. Table 3.10 shows that ultrasonic irradiation of diesel destabilises the fuel and degradation can continue after ultrasonication has ceased. This behaviour might be expected from the ability of ultrasound to produce changes in the sonication medium in the form of free radicals in solution. It has been shown<sup>56</sup> that the presence of free radicals in a fuel correlates with the instability of that fuel.

Table 3.10

<u>Sonication Time</u>	<u>Free Sediment</u>	<u>Adherent Residue</u>	<u>Total Sediment</u>
<u>Hours</u>	<u>mg</u>	<u>mg</u>	<u>mg</u>
6	5.3	3.5	8.8
12	4.9	4.3	9.2
18	8.4	4.5	12.9
24 <sup>1</sup>	20.3	7.5	27.8
30 <sup>2</sup>	9.0	-	-
36	8.4	4.8	13.2
1	The hexane washings were mistakenly included in the diesel during the storage period for this sample.		
2	Adherent residue for this sample was lost.		

Repeating this particular experiment proved to be impractical due to the long storage period.

Taking into account the anomalous results, it can be seen from the table that there is a trend of increasing sediment weights with sonication time. The increase is not very large and as the initial sonication time increases the increase in sediment weight decreases. This implies some upper limit to the amount of sediment formed. This upper limit may be related to the sonication conditions and may also be related to the duration of the initial sonication period. Treatment with ultrasound would be expected to remove some of the more deleterious compounds from the fuel into the sediment, but this effect would be balanced by the destabilising effect of the ultrasound itself. Sonication, therefore, does destabilise the fuel and the degree of the destabilisation appears to be dependent upon the duration of the initial irradiation. There must also be a minimum sonication time below which destabilisation does not occur. This minimum sonication time would of course vary with the nature of the fuel being tested and would be expected to be a measure of the stability of the fuel.

### 3.6.3 High Energy Long Term Sonication of Diesel

A sonication was performed over a period of 440 hours with samples of diesel fuel being taken every 40 hours. This was carried out with the intention of examining the change in alkane distribution in the diesel fuel with sonication. An examination of the final sediment was also undertaken.

GC/MS analysis of the sonicated diesel fuel showed, as would be expected, a loss of the more volatile components. There was also observed to be a change in the distribution of the remaining n-alkanes, with the component present in the highest concentration (hexadecane) increasing as a percentage of the overall fuel composition. The longest chain length components did not appear to change in any noticeable way.

The following graphs (figures 3.59 to 3.62 and 3.65 and 3.66) show the concentrations of alkane components in the fuel with sonication time. These concentrations are calculated by summing the percentages of the alkanes and expressing each component as a percentage of this summed total.

## Disappearance of n-Decane and n-Undecane During Sonication of Diesel Fuel

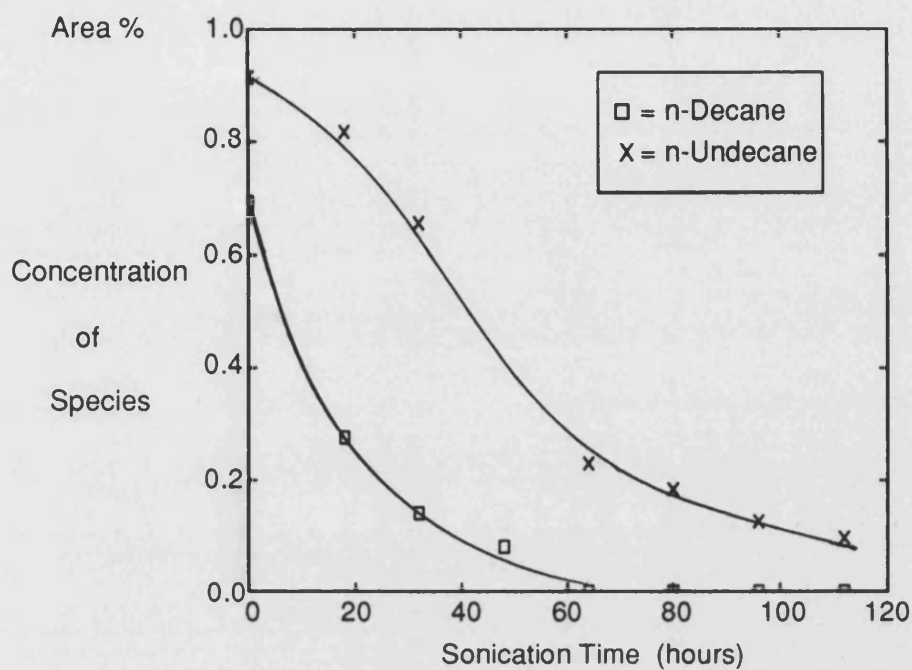


Figure 3.59

## Disappearance of n-Dodecane and n-Tridecane During Sonication of Diesel Fuel

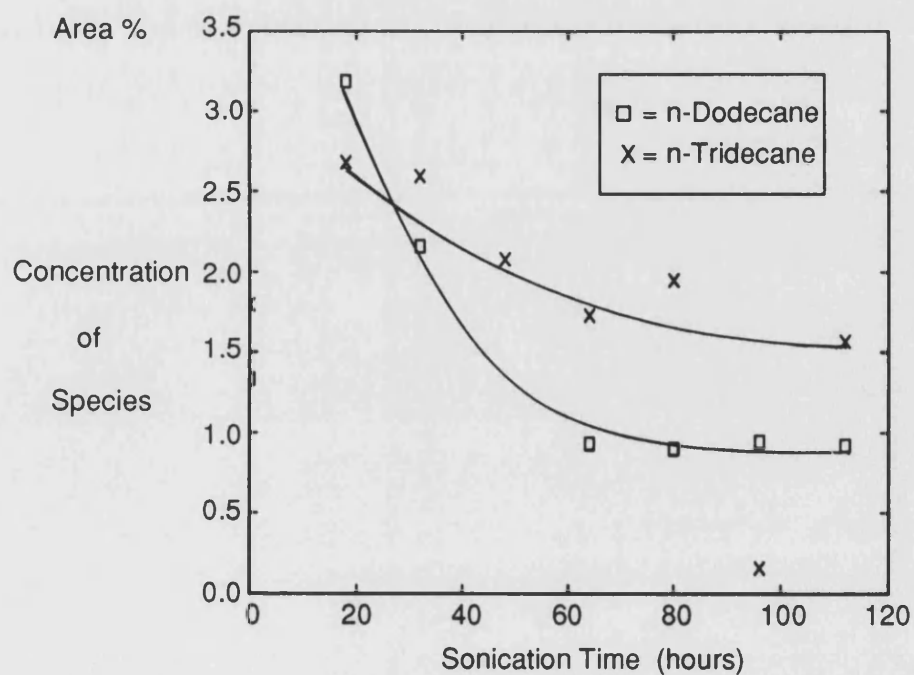


Figure 3.60



## Disappearance of n-Tetradecane During Sonication of Diesel Fuel

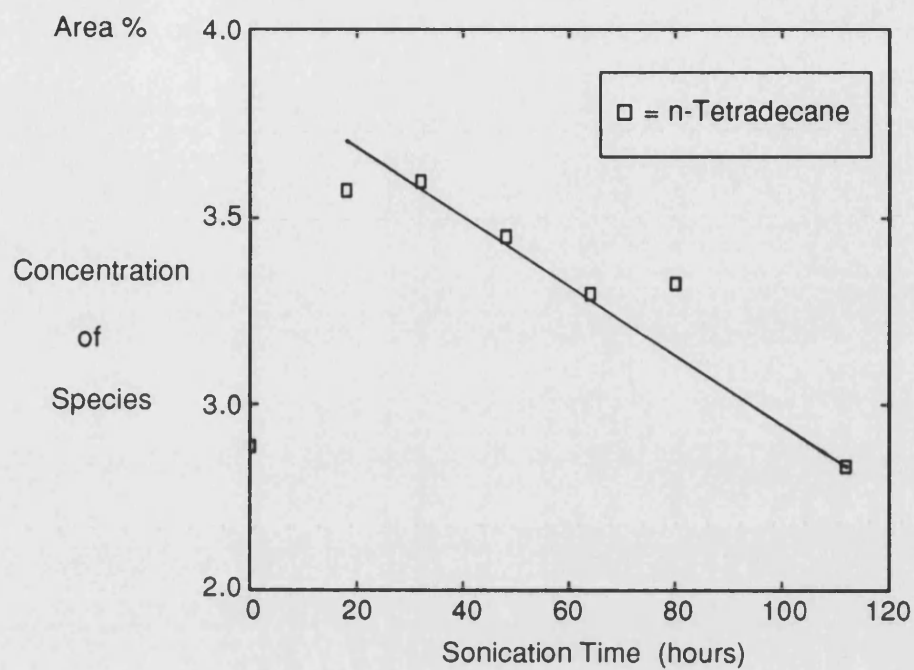


Figure 3.61

## Disappearance of n-Pentadecane During Sonication of Diesel Fuel

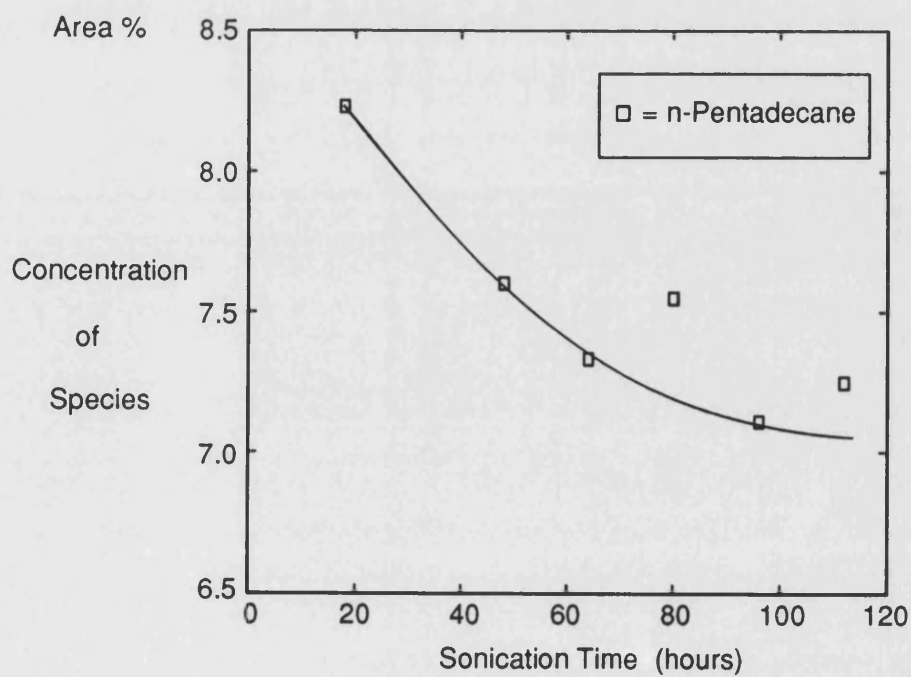


Figure 3.62

The alkanes in diesel with a chain length of less than sixteen provide an exponential reaction profile when their concentrations are plotted as a percentage of total alkane content against sonication time. This implies that the rate of disappearance of these alkanes is dependent on their concentration as well as on the ultrasound. In order to confirm this, the first order plots of these components were examined. The plots for n-tetradecane and n-pentadecane were found not to obey any distinct order. However, an examination of the plots for n-tridecane and n-dodecane showed a tendency to follow first order kinetics and n-undecane and n-decane showed clear linear fits for the first order plots. This indicates that the shorter alkanes with higher volatilities have their disappearance controlled mainly by their volatility, whereas, the longer alkanes having lower volatilities are not subject to this to the same degree. This is again in agreement with results found earlier in this thesis during the sonication of n-dodecane, and also in agreement with the findings of Suslick et al.<sup>130</sup> during their sonication of n-decane. The first order plots for the disappearance of the alkanes n-decane to n-tridecane are shown in figures 3.63 and 3.64.

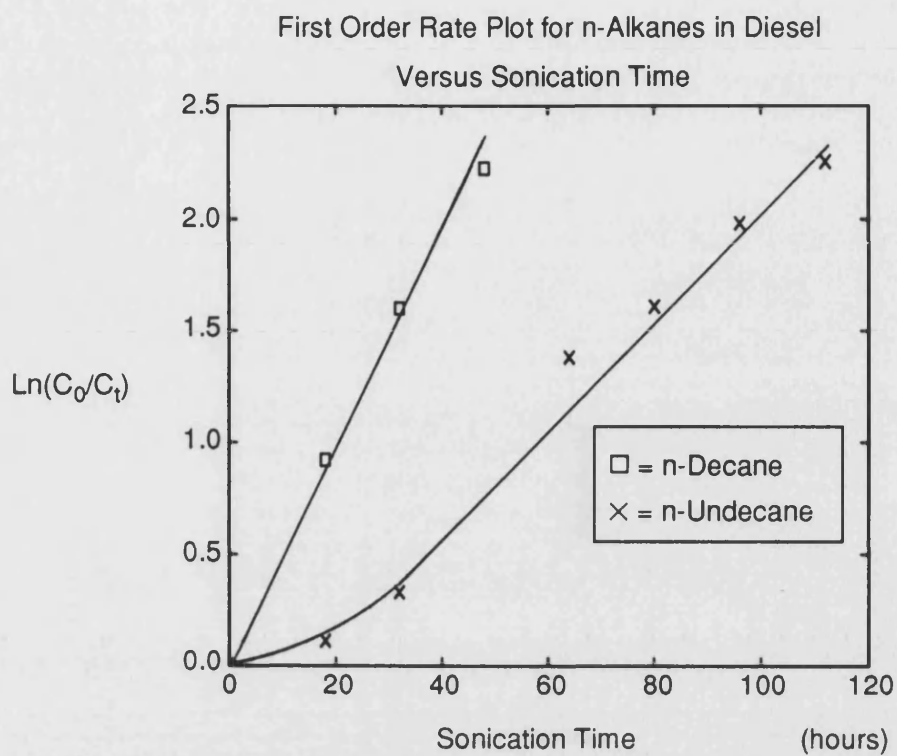


Figure 3.63

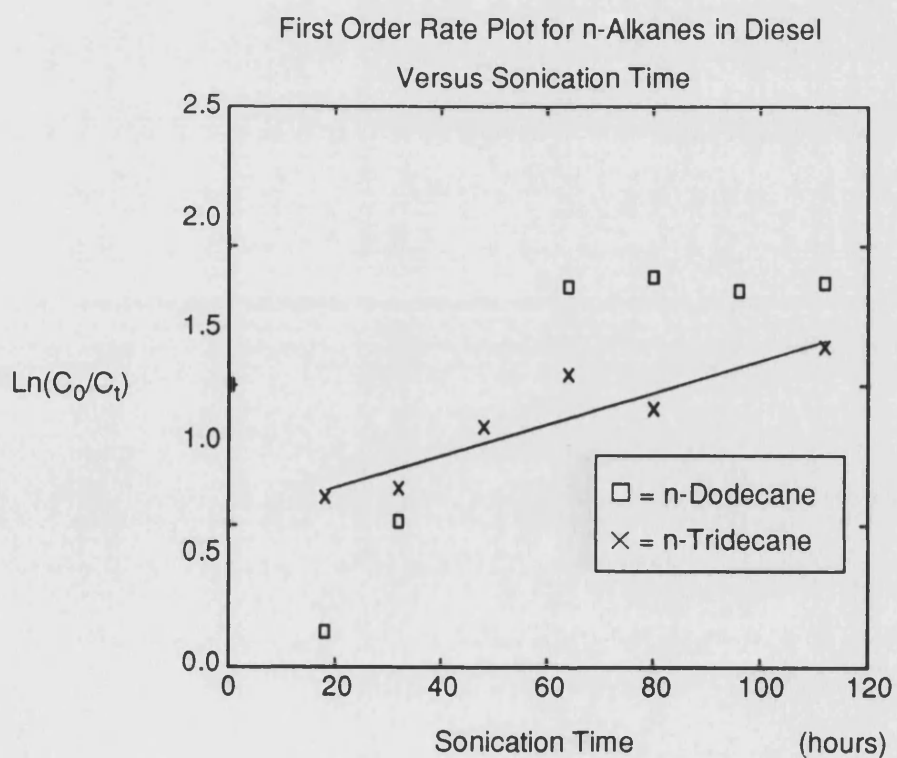


Figure 3.64

After an examination of the fuel components lighter than n-hexadecane it was obviously necessary to examine n-hexadecane and heavier components. The following graphs (figures 3.65 and 3.66) show the concentrations of these species with sonication time.

#### Disappearance of n-Hexadecane and n-Heptadecane During Sonication of Diesel Fuel

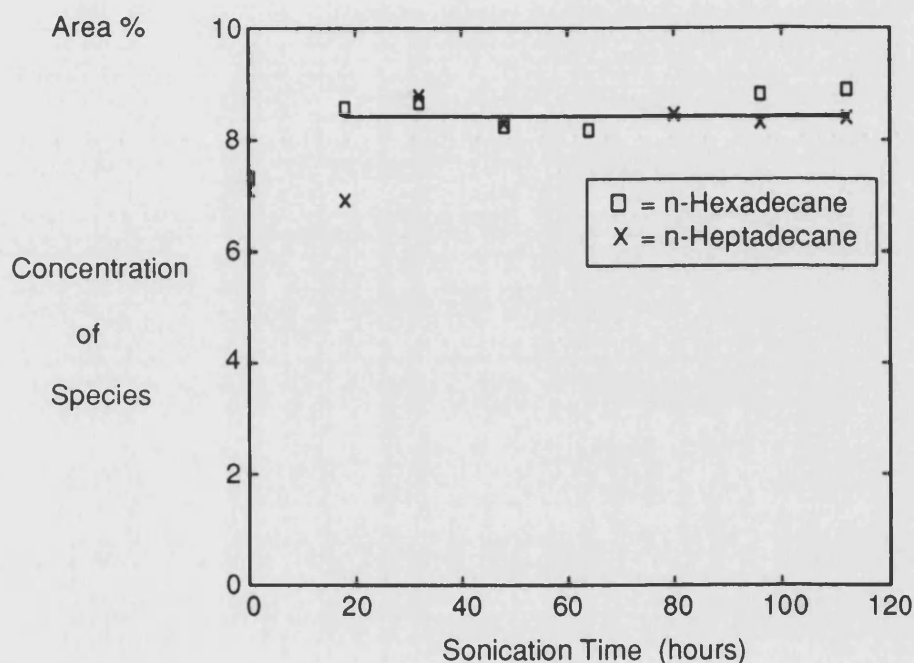


Figure 3.65

It is clear from the graphs that n-hexadecane and heavier components are not noticeably affected by the sonication methods used. The relative concentrations of these species did not change noticeably during sonication. The lighter fuel alkanes are lost from the medium during sonication whilst the relative concentrations of the heavier components remained constant. Therefore, the absolute concentrations of the heavier components increases during sonication. In conclusion, sonication of diesel fuel will increase the average chain length of the component alkanes in that fuel.

## Change in Concentration of n-Alkanes in Diesel with Sonication

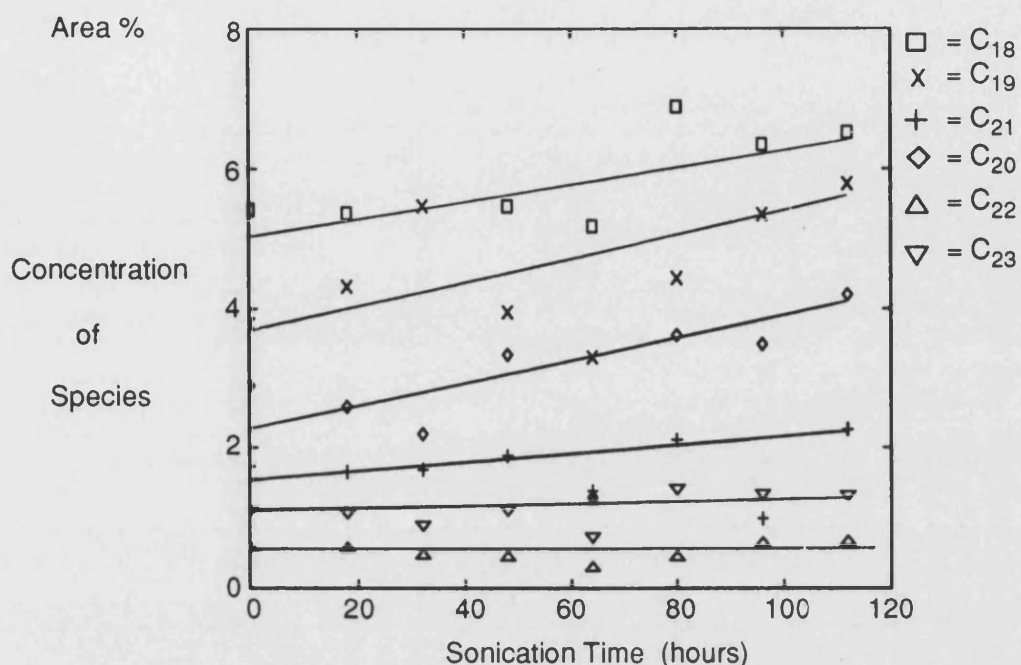


Figure 3.66

**Sediment Analysis**

After the 440 hours sonication period, the diesel fuel was filtered and the resultant sediment was analysed using elemental analysis and gel permeation chromatography.

Analysis of the sediment showed a significantly higher nitrogen content than that of the fuel. The nitrogen content of the fuel was at the lower level of the limits of detection at about 0.25 % whereas the nitrogen content of the sediment was 2.57 %. This sediment nitrogen content is higher than that found during the short term sonication of the fuel and a possible explanation for this may be found in the sonication conditions and simply the duration of the sonication. The conditions for this experiment are far less severe, an intensity of  $66.6 \text{ Wcm}^{-2}$  and a volume of 900 ml, compared to an intensity of  $152 \text{ Wcm}^{-2}$  and a volume of 150 ml. However, the sonication period was extended over 440 hours allowing a longer time for nitrogen to

be removed from the diesel. This result is in agreement with the work of other researchers in this area, that nitrogenous compounds can cause fuel instability and are concentrated into any sediment formed.

This sediment was found to be soluble in THF and ultra-violet analysis of this solution showed absorbance maxima at 234 and 272 nm. When analysed using GPC the sediment was shown to contain polymeric components with a molecular weight of about 40000 relative to polystyrene. The graph (figure 3.67) shows the chromatogram obtained from the analysis of this sediment.

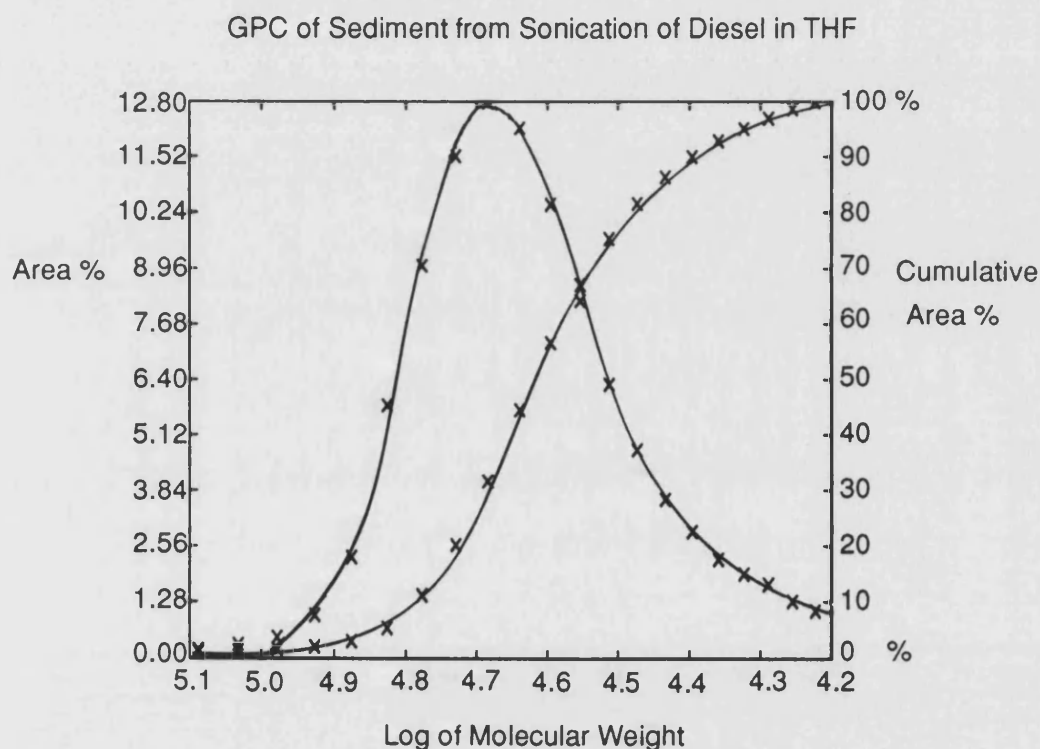


Figure 3.67

This is an important result which shows that it is possible to obtain polymeric residues from diesel fuels using ultrasonic irradiation of an intense nature. This also compares with results found by Frankenfeld et al.<sup>53</sup> who doped fuels with 2,5-dimethylpyrrole and found that after thermal degradation the residues produced

contained polymeric components. Pedley et al.<sup>50</sup> also detected the presence of polymeric material in the sediments that they produced at ambient storage over a period of sixteen months using fuel volumes of up to 2000 gallons. If it can be shown that the nature of sediments produced by these two different techniques is similar, then this indicates that ultrasound shows great promise as a new test to determine the stabilities of fuels in a relatively short time period. There is obviously much more work possible in this area to fully assess the potential of ultrasound in the area of fuel studies.

## Conclusion



#### 4 Conclusion

The results and calculations presented in the previous chapter have afforded some valuable information on assessment of diesel fuel stability. By various techniques it was shown that the diesel fuel used throughout this thesis was a stable fuel suitable for commercial use. The fuel was shown to be stable to the effects of heat, ultra-violet irradiation and free radical initiators as illustrated by sedimentation being undetected. The former two techniques have been used by other workers to promote degradation in diesel fuels. Alkyl pyrroles are known to be deleterious to fuels and addition of these to diesel was subsequently shown to cause loss of these pyrrolic components in the form of sediment. This has been shown by other workers to be a manifestation of fuel instability.

The main work in this area was concerned with using alkyl pyrroles as dopants in model fuel systems in order to determine the reaction kinetics of these degradation processes. This approach was found to afford data suitable for the successful modelling of the kinetics, enabling the prediction of concentration versus time relationships for a particular dopant at a given starting temperature and concentration. This type of modelling has not previously been applied to these types of systems and shows the utility of this method for the prediction of fuel stability based on a knowledge of the fuel components and their kinetic behaviour.

The rest of the work was centred around the development of ultrasound as a technique for the assessment of fuel stability. This study was the first to apply ultrasound to the area of fuel degradation. Two methods of ultrasound delivery were used, an ultrasound bath and an ultrasonic probe. Low energy ultrasound delivered by the bath was shown to have no deleterious effect on the diesel fuel used. However, when used in conjunction with a model fuel system, the reaction of the dopant was found to be slightly accelerated by the ultrasound. The use of high energy ultrasound delivered by the probe yielded some interesting results. A comparison with work done on fuels by other workers showed that high energy sonication for one hour on a

small volume of fuel was approximately equivalent to a storage period of 420 days at 50 °C for a similar fuel. While further work is needed to develop the full potential of this method, it is a significant result and demonstrates that ultrasound will prove to be a valuable technique for assessing fuel stability.

## References

### References

- 1) May, H.; Tausk, H.J.; Oblaender, K.; Reglitzky, A.A. *Proc. World Pet. Congr.* **1987**, 12<sup>th</sup> (Vol. 4), 187-201.
- 2) Van Winkle, T.L.; Affens, W.A.; Beal, E.J.; Mushrush, G.W.; Hazlett, R.N.; De-Guzman, J. *Fuel* **1987**, 66, 974-953.
- 3) White, E.W. *ASTM STP* **1973**, 531, 143-166.
- 4) Nixon, A.C. Autoxidation and Antioxidants of Petroleum. In *Autoxidation and Antioxidants*; Lundberg, W.O., Ed.; Interscience: New York, 1962; Vol. II, Chapter 17, pp 696-856.
- 5) Ritchie, J. *J. Inst. Pet.* **1965**, 51, 296-307.
- 6) Halsall, R. In *Proceedings of The 2nd International Conference on Long Term Storage Stabilities of Liquid Fuels*; Stavinocha, L. L., Ed.; 1986; pp 722-737. Also *ASTM STP* **1988**, 1005, 63-81.
- 7) Johnson, J.E.; Chiantella, A.J.; Carhart, H.W. NRL Report 4422, Fuels Branch, Chemistry Division, Naval Research Laboratory, Washington, DC, 1954.
- 8) Stavinocha, L.L. In *Proceedings of the 3rd International Conference on Stability and Handling of Liquid Fuels*; Hiley, R.W., Penfold, R.E., Pedley, J.F., Eds.; 1988; pp 1-11.
- 9) Kite, Jr., W.H.; Stephens, G.G. Fuel Oils, Including Domestic Heating Oils, In *Criteria for Quality of Petroleum Products*; Allinson, J.P., Ed.; Wiley: New York, 1973; Chapter 9, pp 152-173.
- 10) Por, N.; Brauch, R.; Brodsky, N.; Diamant, R. In *Proceedings of the 3rd International Conference on Stability and Handling of Liquid Fuels*; Hiley, R.W., Penfold, R.E., Pedley, J.F., Eds.; 1988; pp 12-23.
- 11) Christian, J.G.; Chiantella, A.J.; Johnson, J.E.; Carhart, H.W. *Ind. Eng. Chem.* **1958**, 50, 1153-1156.

- 12) Garner, M.Q.; White, E.W. *ASTM STP* **1981**, *751*, 34-46.
- 13) Stavinocha, L.L.; Westbrook, S.R. *ASTM STP* **1981**, *751*, 3-21.
- 14) Chiantella, A.J.; Johnson, J.E. "Comparative Studies of Some Accelerated Ageing Tests for Distillate Fuels"; Naval Research Laboratory, NRL Problem C 01-03, 1959.
- 15) Smith, R.J.; Palmer, L.D. In *Proceedings of The 2nd International Conference on Long Term Storage Stabilities of Liquid Fuels*; Stavinocha, L.L., Ed.; 1986; pp 875-886.
- 16) Schrepfer, M.W.; Arnold, R.J.; Stansky, C.A. *Oil Gas J.* **1984**, Jan. 16, 79-84.
- 17) American Society for Testing and Materials. *Annual Book of ASTM Standards*, Vol. 05.03, 1989.
- 18) Hardy, D.R.; Hazlett, R.N.; White, E.W. In *Proceedings of The 2nd International Conference on Long Term Storage Stabilities of Liquid Fuels*; Stavinocha, L.L., Ed.; 1986; pp 887-901.
- 19) Stavinocha, L.L.; Westbrook, R.; Brinkman, D.W. "Accelerated Stability Test Techniques for Middle Distillate Fuels"; US Department of Energy Report No. DOE/BC/10043-12, 1980. Also "Optimization of Accelerated Stability Test Techniques for Diesel Fuels"; US Department of Energy Report No. DOE/BC/10043-25, 1981.
- 20) Henry, C.P. *ASTM STP* **1981**, *751*, 22-33.
- 21) Bhan, O.K.; Brinkman, D.W.; Green, J.B.; Carley, B. *Fuel* **1987**, *66*, 1200-1214.
- 22) American Society for Testing and Materials. *Annual Book of ASTM Standards*, Vol. 05.02, 1989.
- 23) Lee, G.H. II.; Stavinocha, L.L. In *Proceedings of The 2nd International Conference on Long Term Storage Stabilities of Liquid Fuels*; Stavinocha, L.L., Ed.; 1986; pp 663-678.
- 24) White, E.W. In *Proceedings of The 2nd International Conference on Long*

- Term Storage Stabilities of Liquid Fuels*; Stavinoha, L.L., Ed.; 1986; pp 646-662.
- 25) White, E.W.; Bowen, R.J. In *Proceedings of the 3rd International Conference on Stability and Handling of Liquid Fuels*; Hiley, R.W., Penfold, R.E., Pedley, J.F., Eds.; 1988; pp 659-687.
  - 26) Cooney, J.V.; Beal, E.J.; Hazlett, R.N. *Prepr. Pap. - Am. Chem. Soc., Div. Fuel Chem.* **1983**, 28(5), 1139-1144.
  - 27) American Society for Testing and Materials. *Annual Book of ASTM Standards*; Vol. 05.01, 1989.
  - 28) Li, N.C.; Chang, H.; Wang, S.M.; Huang, P.J.; Tzou, J.. In *Proceedings of the 3rd International Conference on Stability and Handling of Liquid Fuels*; Hiley, R.W., Penfold, R.E., Pedley, J.F., Eds.; 1988; pp 596-608.
  - 29) Jones, L.; Hazlett, R.N.; Li, N.C.; Ge, J. *Fuel*, **1984**, 63, 1152-1156.
  - 30) Li, J.; Li, N.C. *Fuel* **1985**, 64, 1041-1046.
  - 31) Li, N.C.; Hazlett, R.N.; Ge, J.; Yaggi, N.F. *Fuel* **1984**, 63, 1285-1289.
  - 32) Jones, L.; Hazlett, R.N. *Prepr. Pap. - Am. Chem. Soc. Div. Fuel Chem.* **1983**, 28(1), 196-201.
  - 33) Berry, G.C. *J. Chem. Phys.* **1966**, 44(12), 4550-4563.
  - 34) Dandliker, W.B.; Kraut, J. *J. Am. Chem. Soc.* **1956**, 78, 2380-2384.
  - 35) Smith, E.B.; Jensen, H.B. *J. Org. Chem.* **1967**, 32, 3330-3334.
  - 36) Hardy, D.R.; Beal, E.J.; Hazlett, R.N.; Burnett, J.C. In *Proceedings of the 3rd International Conference on Stability and Handling of Liquid Fuels*; Hiley, R.W., Penfold, R.E., Pedley, J.F., Eds.; 1988; pp 647-658.
  - 37) Chiantella, A.J.; Johnson, J.E. "Diesel Fuel Stability Studies on Navy-CRC Barge Storage Fuels"; Naval Research Laboratory, 1956.
  - 38) Johnson, J.E.; Chiantella, A.J.; Christian, J.G. "Diesel Fuel Stability Studies"; Naval Research Laboratory; NRL Problem C 01-03, 1956.
  - 39) Yaggi, N.F.; Lee, S.H.; Ge, J. Li, N.C. *Prepr. Pap. - Am. Chem. Soc. Div. Fuel*

*Chem.* **1983**, *29*, 178-185.

- 40) Cooney, J.V.; Wechter, M.A. *Fuel*, **1986**, *65*, 433-436.
- 41) Solly, R.K.; Arfelli, W. In *Proceedings of The 2nd International Conference on Long Term Storage Stabilities of Liquid Fuels*; Stavinocha, L.L., Ed.; 1986; pp 453-467.
- 42) Irish, G.E.; Bell, K.L.; Dillon, D.M. In *Proceedings of The 2nd International Conference on Long Term Storage Stabilities of Liquid Fuels*; Stavinocha, L.L., Ed.; 1986; pp 441-452.
- 43) Bhan, O.K.; Tang, S.Y.; Brinkman, D.W. In *Proceedings of The 2nd International Conference on Long Term Storage Stabilities of Liquid Fuels*; Stavinocha, L.L., Ed.; 1986; pp 483-495.
- 44) Onion, G.; Bartlett, P.J. *J. Inst. Pet.* **1966**, *52*, 285-299.
- 45) Westbrook, S.R.; Stavinocha, L.L.; Barbee, J.G.; Bundy, L.L. In *Proceedings of The 2nd International Conference on Long Term Storage Stabilities of Liquid Fuels*; Stavinocha, L.L., Ed.; 1986; pp 111-124.
- 46) Hiley, R.W. In *Proceedings of The 2nd International Conference on Long Term Storage Stabilities of Liquid Fuels*; Stavinocha, L.L., Ed.; 1986; pp 426-440.
- 47) Pedley, J.F.; Hiley, R.W.; Hancock, R.A. *Fuel* **1988**, *67*, 1124-1130.
- 48) Cooney, J.V.; Beal, E.J.; Hazlett, R.N. *Ind. Eng. Chem. Prod. Res. Dev.* **1985**, *24*, 294-300.
- 49) Bhan, O.K.; Green, J.B.; Brinkman, D.W.; Carley, B. In *Proceedings of The 2nd International Conference on Long Term Storage Stabilities of Liquid Fuels*; Stavinocha, L.L., Ed.; 1986; pp 915-926. Also *ASTM STP* **1988**, *1005*, 48-62.
- 50) Pedley, J.F.; Hiley, R.W.; Hancock, R.A. *Fuel* **1987**, *66*, 1646-1651.
- 51) Pedley, J.F.; Hiley, R.W.; Hancock, R.A. *Fuel*, **1989**, *68*, 27-31.
- 52) White, C.M.; Jones, L.; Li, N.C. *Fuel* **1983**, *62*, 1397-1403.

- 53) Frankenfeld, J.W.; Taylor, W.F.; Brinkman, D.W. *Ind. Eng. Chem. Prod. Res. Dev.* **1983**, *22*, 608-614.
- 54) Mayo, F.R.; Lan, B.Y. *Ind. Eng. Chem. Prod. Res. Dev.* **1986**, *25*, 333-348.
- 55) Anderson, R.P.; Brinkman, D.W.; Goetzinger, J.W. In *Proceedings of The 2nd International Conference on Long Term Storage Stabilities of Liquid Fuels*; Stavinoha, L.L., Ed.; 1986; pp 25-38.
- 56) Wright, B.W.; Kalkwarf, D.R.; Smith, R.D.; Hardy, D.R.; Hazlett, R.N. *Fuel* **1985**, *64*, 591-593.
- 57) Loeffler, M.C.; Li, N.C. *Fuel* **1985**, *64*, 1047-1053.
- 58) Smith, R.D.; Utseth, H.R.; Hazlett, R.N. *Fuel* **1985**, *64*, 810-815.
- 59) Brinkman, D.W.; Bowden, J.N. *Fuel* **1982**, *61*, 1141-1148.
- 60) Finseth, D. "Isotopic Studies of the Storage Instability of Coal Derived Liquids"; US Department of Energy, 1988.
- 61) Power, A.J. *Fuel* **1986**, *65*, 133-137.
- 62) Hazlett, R.N.; Power, R.J. *Fuel* **1989**, *68*, 1112-1117.
- 63) Power, A.J.; Davidson, R.G. *Fuel* **1986**, *65*, 1753-1755.
- 64) Palmer, L.D.; Copson, B.V. In *Proceedings of The 2nd International Conference on Long Term Storage Stabilities of Liquid Fuels*; Stavinoha, L.L., Ed.; 1986; pp 902-914.
- 65) Powers, E.J.; Wotring, W.T. *ASTM STP* **1981**, *751*, 92-102.
- 66) Clinkenbeard, W.L. *ASTM STP* **1959**, *244*, 32-40.
- 67) Hiley, R.W.; Pedley, J.F. *Fuel* **1988**, *67*, 469-473.
- 68) Frankenfeld, J.W.; Taylor, W.F. "Fundamental Synthetic Fuel Stability Study"; US Department of Energy Report No. DOE/BC/10045-12, 1981.
- 69) Hogin, D.R.; Clinkenbeard, W.L. In *Petroleum Products Handbook*; Guthrie, V.B., Ed.; McGraw-Hill: New York, 1960: Chapter 7.
- 70) Taylor, W.F.; Frankenfeld, J.W. In *Proceedings of The 2nd International Conference on Long Term Storage Stabilities of Liquid Fuels*; Stavinoha, L.



L., Ed.; 1986; pp 496-511.

- 71) Brinkman, D.W.; Bowden, J.N.; Giles, H.N. "Crude Oil and Finished Fuel Storage Stability: An Annotated Review"; US Department of Energy Report No. DOE/BETC/RI-79/13, 1980.
- 72) Goetzinger, J.W.; Thompson, C.J.; Brinkman, D.W. "A Review of Storage Stability Characteristics of Hydrocarbon Fuels"; US Department of Energy Report No. DOE/BETC/IC-83/3, 1983.
- 73) Batts, B.D.; Fathoni, A.Z. *Energy & Fuels* **1991**, 5, 2-21.
- 74) Bowden, J.N.; Brinkman, D.W. *Hydrocarbon Process.* **1980**, 59(7), 77-82.
- 75) Le-Pera, M.E.; Sonenburg, J.G. *Hydrocarbon Process.* **1973**, 111-115.
- 76) Cooney, J.V.; Beal, E.J.; Beaver, B.D. *Fuel Sci. Technol. Int.* **1986**, 4(1), 1-18.
- 77) Malhotra, R.; Coggiola, J.; Young, S.E.; Tse, D.; Buttrill, S.E.Jr. *Prepr. Pap. - Am. Chem. Soc. Div. Fuel Chem.* **1985**, 30, 192.
- 78) Fookes, C.J.R.; Walters, C.K. In *Proc. 5th Austr. Workshop on Oil Shale* **1989**, 103-108.
- 79) Elmquist, E.A. *ASTM STP* **1959**, 244, 26-31.
- 80) Offenhauer, R.D.; Brennan, J.A.; Miller, R.C. *Prepr. - Am. Chem. Soc. Div. Pet. Chem.* **1956**, 1(3), 249-254.
- 81) Thompson, R.B.; Drudge, L.W.; Chenicek, J.A. *Ind. Eng. Chem.* **1949**, 41, 2175.
- 82) Hazlett, R.N.; Kelso, G. In *Proceedings of The 2nd International Conference on Long Term Storage Stabilities of Liquid Fuels*; Stavinocha, L.L., Ed.; 1986; pp 541-555. Also Hazlett, R.N. *Fuel Sci. Technol. Int.* **1988**, 6(2), 185-208.
- 83) Sauer, R.W.; Weed, A.F.; Headington, C.E. *Prepr. - Am. Chem. Soc. Div. Pet. Chem.* **1958**, 3(3), 95-113.
- 84) Dunn, F.R.; Sauer, R.W. *ASTM STP* **1959**, 244, 47-56.
- 85) Offenhauer, R.D.; Brennan, J.A.; Miller, R.C. *Ind. Eng. Chem.* **1957**, 49(8), 1265-1266.

- 86) Malhotra, R.; St. John, G.A. In *Proceedings of the 3rd International Conference on Stability and Handling of Liquid Fuels*; Hiley, R.W., Penfold, R.E., Pedley, J.F., Eds.; 1988; pp 525-537.
- 87) Hazlett, R.N.; Power, A.J.; Kelso, A.G.; Solly, R.K. "The Chemistry of Deposit Formation in Distillate Fuels." Department of Defence, Defence Science and Technology Organisation, Material Research Laboratories Report No. MRL-R-986, 1986.
- 88) Taylor, W.F.; Wallace, T.J. *Ind. Eng. Chem. Prod. Res. Dev.* **1969**, *8*, 375-380.
- 89) Taylor, W.F.; Frankenfeld, J.W. *Ind. Eng. Chem. Prod. Res. Dev.* **1978**, *17*, 86-90.
- 90) Hara, T.; Jones, L.; Li, N.C.; Tewari, K.C. *Fuel* **1981**, *60*, 1143-1148.
- 91) Frankenfeld, J.W.; Taylor, W.F.; Brinkman, D.W. *Ind. Eng. Chem. Prod. Res. Dev.* **1983**, *22*, 615-621.
- 92) Fortnagel, M.; Herbrick, B. *API Prepr.* No. 820-00012, 1984.
- 93) Frankenfeld J.W.; Taylor W.F.; Brinkman, D.W. *Ind. Eng. Chem. Prod. Res. Dev.* **1983**, *22*, 622-627.
- 94) Mushrush, G.W.; Beal, E.J.; Hazlett, R.N.; Hardy D.R. *Energy & Fuels* **1990**, *4*, 15-19.
- 95) Poulson, R.E. *Prepr. - Am. Chem. Soc. Div. Pet. Chem.* **1975**, *20*, 183-197.
- 96) White, C.M.; Schweighardt, F.K.; Shultz, J.L. *Fuel Process. Technol.* **1977**, *1*, 209-215.
- 97) Novotny, M.; Kump, R.; Merli, F.; Todd, L.J. *Anal. Chem.* **1980**, *52*, 401-406.
- 98) Burchill, P.; Herod, A.A.; Pritchard, E. *Fuel* **1983**, *62*, 20-29.
- 99) Del Bianco, A.; Zaninelli, M.; Girardi, E. *Fuel* **1987**, *66*, 55-57.
- 100) Ali, M.F.; Ali, M.A. *Fuel Sci. Technol. Int.* **1988**, *6*(3), 252-290.
- 101) Hardy, R.H.; Davis, B.H. *Fuel Sci. Technol. Int.* **1989**, *7*(4), 399-421.
- 102) Beal, E.J.; Cooney, J.V.; Hazlett, R.N.; Morris, R.E.; Mushrush, G.W.;

- Beaver, B.D.; Hardy, D.R. "Mechanisms of Syncrude/Synfuel Degradation"; US Department of Energy Report No. DOE/BC/10525-16, 1987.
- 103) Worstell, J.H.; Daniel, S.R.; Fraunhoff, G. *Fuel* **1985**, *64*, 485-487.
- 104) Cooney, J.V.; Beal, E.J.; Hazlett, R.N. *Liq. Fuels Technol.* **1984**, *2*(4), 395-426.
- 105) Mushrush, G.W.; Cooney, J.V.; Beal, E.J.; Hazlett, R.N. *Fuel Sci. Technol. Int.* **1986**, *4*(1), 103-125.
- 106) Thompson, R.B.; Chenicek, J.A.; Drudge, L.W.; Symon, T. *Ind. Eng. Chem.* **1951**, *43*, 935-939.
- 107) Frankenfeld, J.W.; Taylor, W.F.; Brinkman, D.W. "Fundamental Synthetic Fuel Stability Study - Final Report"; US Department of Energy Report No. DOE/BC/10045-23, 1982.
- 108) Jones, L.; Li, N.C. *Fuel* **1983**, *62*, 1156-1160.
- 109) Li, N.C.; Tzou, J.R.; Chang, H.; Wang, S.M. *J. Chin. Chem. Soc.* **1987**, *34*, 91-98.
- 110) Beaver, B.; Gilmore, C.; Veloski, G.; Sharief, V. *Energy & Fuels* **1991**, *5*, 274-280.
- 111) Pedley, J.F.; Hiley, R.W.; Hancock, R.A. *Fuel* **1989**, *68*, 27-31.
- 112) Beranek, L.A.; McVea, G.G.; O'Connell, M.G.; Solly, R.K. *Prepr. Pap. - Am. Chem. Soc., Div. Fuel Chem.* **1990**, 1117-1124.
- 113) Dorbon, M.; Bernasconi, C.; Gaillard, J.; Derris, J. *Prepr. Pap. - Am. Chem. Soc., Div. Fuel Chem.* **1990**, 1135-1155.
- 114) Lee, G.H. II.; Stavinocha, L.L. In *Proceedings of The 2nd International Conference on Long Term Storage Stabilities of Liquid Fuels*; Stavinocha, L.L., Ed.; 1986; pp 585-599.
- 115) Pedley, J. *Pet. Rev.* **1988**, *42*(503), 25-28.
- 116) Nixon, A.C.; Cole, C.A. *Prepr. - Am. Chem. Soc. Div. Pet. Chem.* **1954**, *31*, 5-18.

- 117) Beal, E.J.; Cooney, J.V.; Mushrush, G.W.; Hazlett, R.N. In *Proceedings of The 2nd International Conference on Long Term Storage Stabilities of Liquid Fuels*; Stavinoha, L.L., Ed.; 1986; pp 759-773.
- 118) Dukek, W.J. *J. Inst. Pet.* **1964**, *50*, 273.
- 119) Smith, J.D. *Ind. Eng. Chem. Process Des. Dev.* **1969**, *8*, 299-308.
- 120) Bamford, C.H., Tipper, C.F., Eds, *Comprehensive Chemical Kinetics*; Elsevier: New York, 1980; Vol. 16.
- 121) Luria, D. In *Proceedings of The 2nd International Conference on Long Term Storage Stabilities of Liquid Fuels*; Stavinoha, L.L., Ed.; 1986; pp 66-82.
- 122) Beaver, B.D.; Hazlett, R.N.; Cooney, J.V.; Watkins, J.M. *Fuel Sci. Technol. Int.* **1988**, *6*(2), 131-150.
- 123) Luche, J.L.; Einhorn, C.; Einhorn, J.; de Souza Barboza, J.C.; Petrier, C.; Dupuy, C.; Delair, P.; Allavena, C.; Tuschl, T. *Ultrasonics* **1990**, *28*, 316-321.
- 124) *Ultrasound, Its Chemical, Physical and Biological Effects*; Suslick, K.S.; **1988**; VCH pub., Weinheim RFA.
- 125) Suslick, K.S. *Science* **1990**, *247*, 1439-1445.
- 126) Lord Raleigh *Philos. Mag.* **1917**, *34*, 94.
- 127) Ley, S.V.; Low, C.M.R. *Ultrasound in Synthesis* **1989**, pub. Springer-Verlag., Berlin Heidelberg.
- 128) Mason, T.J. *Ultrasonics* **1986**, *24*, 245-253.
- 129) Goldberg, Yu; Sturkovich, R.; Lukevics, E. *Heterocycles* **1989**, *29*(3), 597-627.
- 130) Suslick, K.S.; Gawlenowski J.J.; Schubert P.F.; Wang H.H. *J. Phys. Chem.* **1983**, *87*, 2298-2301.
- 131) Perez Pla, F.; Baeza Baeza, J.J.; Ramis Ramos, G.; Palou, J. *Journal of Computational Chemistry* **1991**, *12*(3), 283-291.
- 132) Tam P.S.; Kittrell, J.R.; Eldridge, J.W. *Ind. Eng. Chem. Res.* **1990**, *29*, 324-329.

- 133) Mason, T.J.; Lorimer, J.P.; Moorhouse, J.P. *Education in Chemistry* **1989**, Jan., 13-15.
- 134) Fodor, G.E.; Naegeli, D.W.; Kohl, K.B. *Energy Fuels* **1988**, 2, 729-734.
- 135) Cookson, D.J.; Smith, B.E. *Anal. Chem.* **1985**, 57, 864-871.
- 136) Desideri, P.G.; Lepri, L.; Heimler, D.; Checcini, L.; Giannessi, S. *Journal of Chromatography* **1985**, 322, 107-116.
- 137) Ronchetti, M.; Cartoni, G.; Zoccolillo, L.; *Journal of Chromatography* **1985**, 348, 159-165.
- 138) Tameesh, A.H.H.; Hanna, M.H.; Komers, R. *Journal of Chromatography* **1985**, 328, 207-217.
- 139) Crisp, P.T.; Ellis, J.; de Leeuw, J.W.; Schenck, P.A. *Anal. Chem.* **1986**, 58, 258-261.
- 140) Kucchal, R.K.; Kumar, B.; Mathur, H.S.; Joshi, G.C. *Journal of Chromatography* **1986**, 361, 269-278.
- 141) Williams, P.T.; Bartle, K.D.; Mills, D.G.; Andrews, G.E. *Journal of High Resolution Chromatography and Chromatography Communications* **1986**, 9, 39-43.
- 142) Davies, I.L.; Bartle, K.D.; Andrews, G.E.; Williams, P.T. *Journal of Chromatographic Science* **1988**, 26, 125-130.
- 143) Wright, B.W.; Udseth, H.R.; Chess, E.K.; Smith, R.D. *Journal of Chromatographic Science* **1988**, 26, 228-235.
- 144) Davies, I.L.; Bartle, K.D.; Williams, P.T.; Andrews, G.E. *Anal. Chem.* **1988**, 60, 204-209.
- 145) Campbell, R.M.; Djordjevic, N.M.; Markides, K.E.; Lee, M.L. *Anal. Chem.* **1988**, 60, 356-362.
- 146) Woodrow, J.E.; Seiber, J.N. *Journal of Chromatography*, **1988**, 455, 53-65.
- 147) Rygle, K.J.; Feulmer, G.P.; Scheideman, R.F. *Journal of Chromatographic Science*, **1984**, 22, 514-518.

- 148) Tameesh, A.H.H.; Bender, A.O.; Sarkissian, T.M. *Journal of Chromatography*, **1985**, 321, 59-67.
- 149) Nishioka, M.; Bradshaw, J.S.; Lee, M.L.; Tominaga, Y.; Tedjamulia, M.; Castle, R.N. *Anal. Chem.* **1985**, 57, 309-312.
- 150) Cortes, H.J.; Richter, B.E.; Pfeiffer, C.D.; Jensen, D.E. *Journal of Chromatography* **1985**, 349, 55-61.

## Appendix

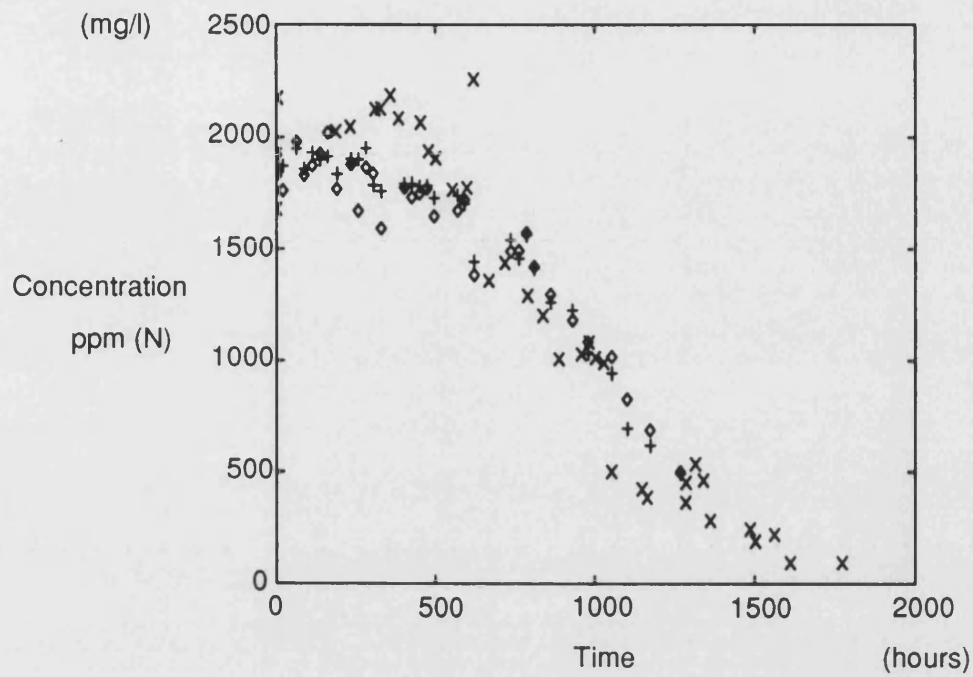
## Appendix

The graphs contained in this appendix depict the raw concentration plots of both 2,5-dimethylpyrrole and 1,2,5-trimethylpyrrole in the separately doped model fuel and also in the combined dopant system. First order rate plots of the degradation data is also given in this appendix. Any rate constants derived from this data are reported in the results section for the modelled fuel systems.

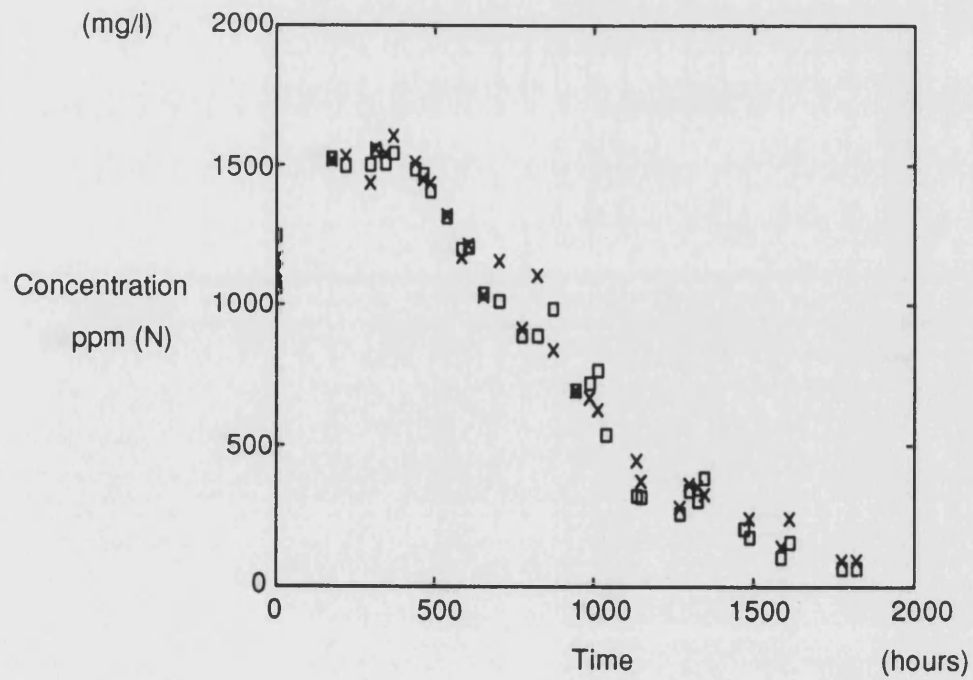


## Data from the 2,5-Dimethylpyrrole System

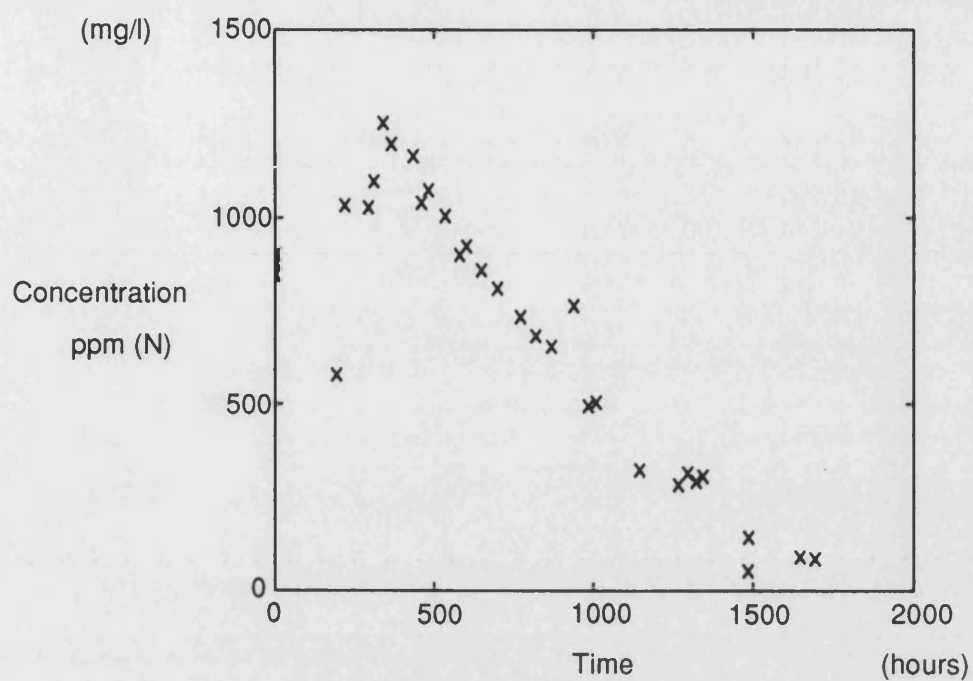
Degradation of 2,5-Dimethylpyrrole 1800 ppm(N) at 40 °C



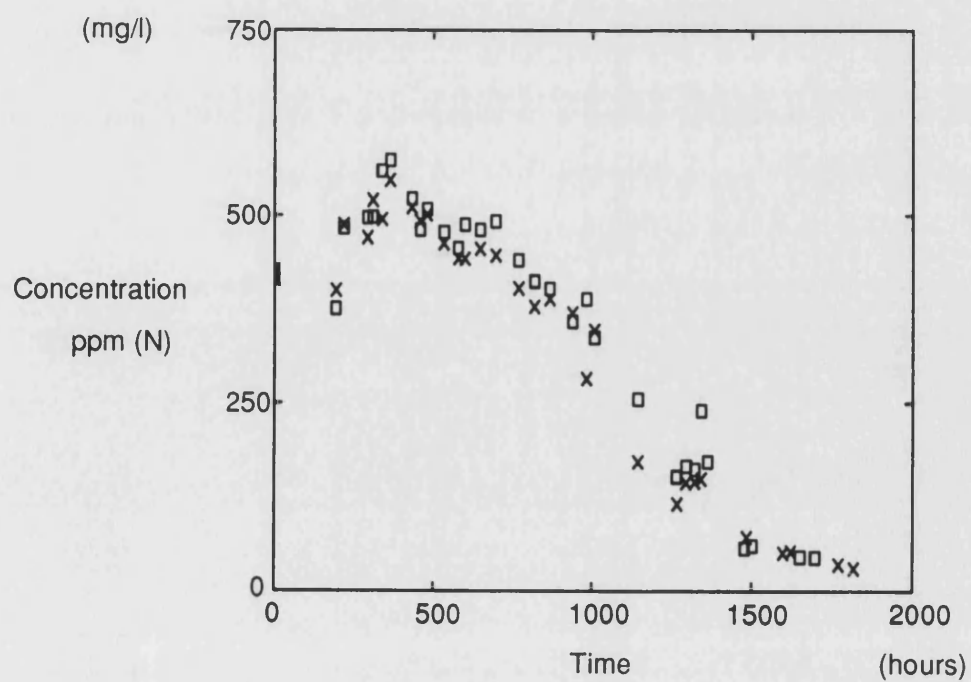
Degradation of 2,5-Dimethylpyrrole 1100 ppm(N) at 40 °C



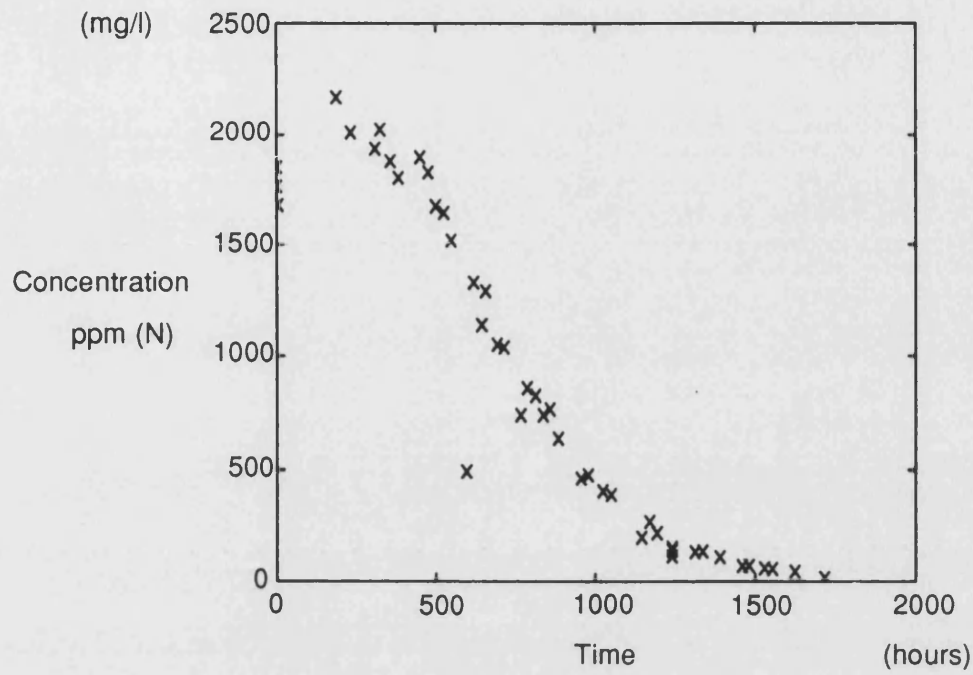
Degradation of 2,5-Dimethylpyrrole 750 ppm(N) at 40 °C



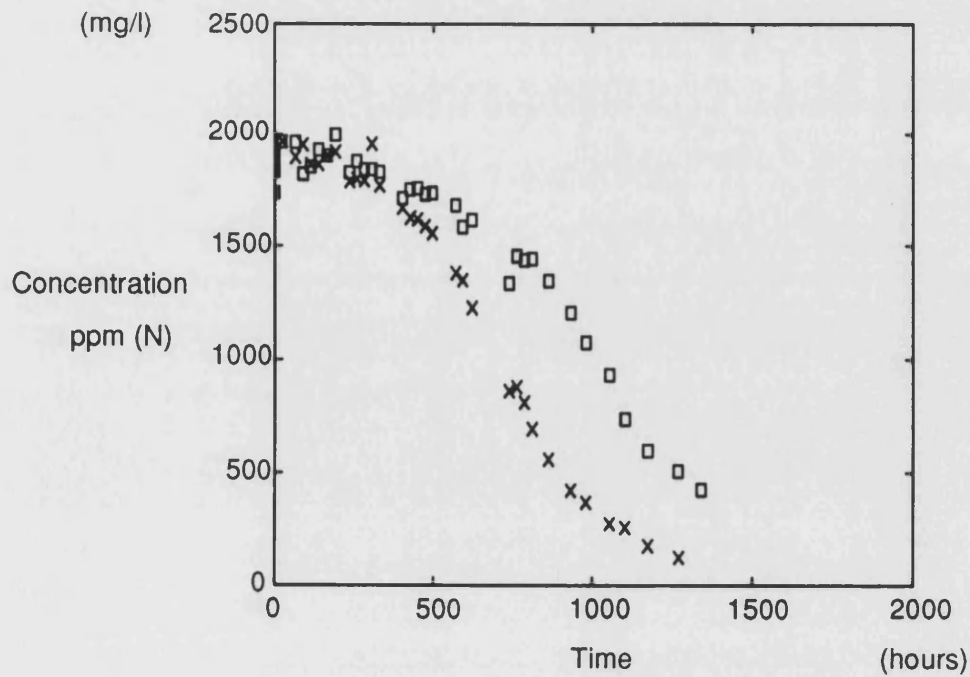
Degradation of 2,5-Dimethylpyrrole 410 ppm(N) at 40 °C



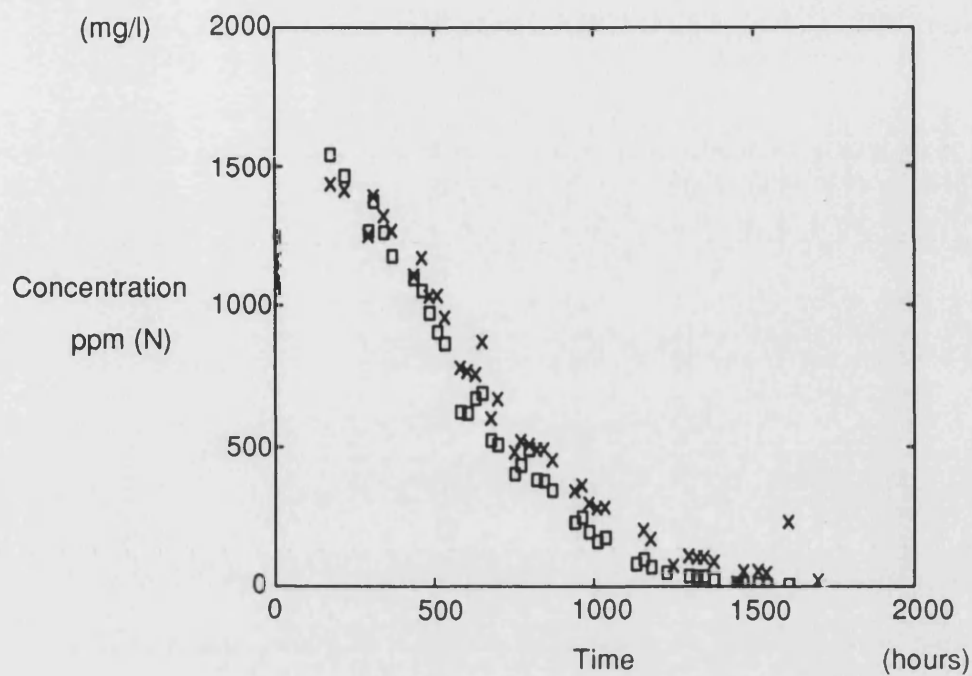
Degradation of 2,5-Dimethylpyrrole 1800 ppm(N) at 52 °C



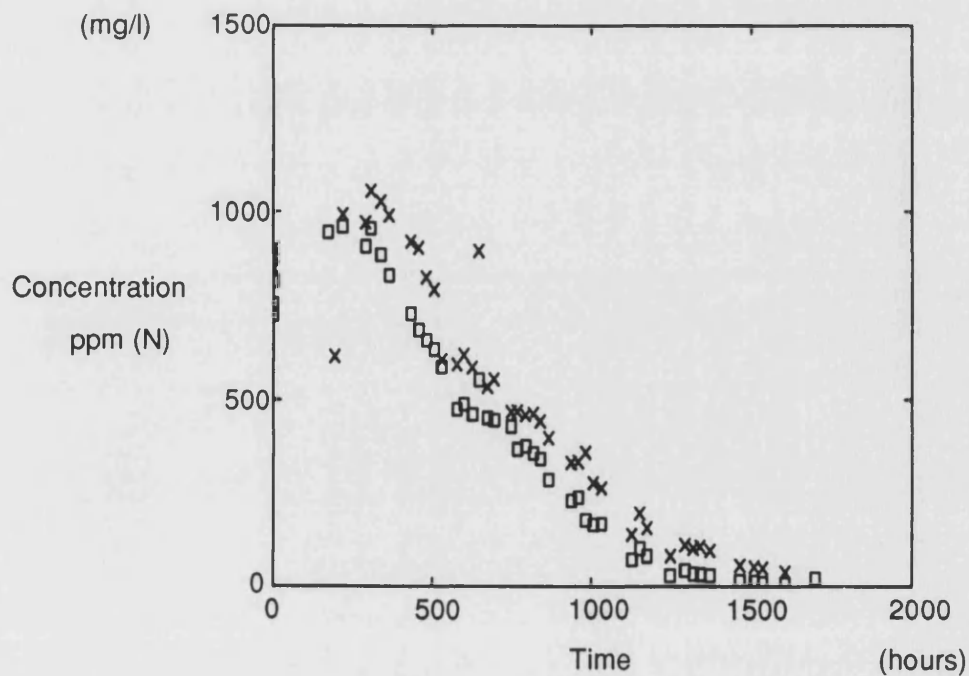
Degradation of 2,5-Dimethylpyrrole 1600 ppm(N) at 52 °C



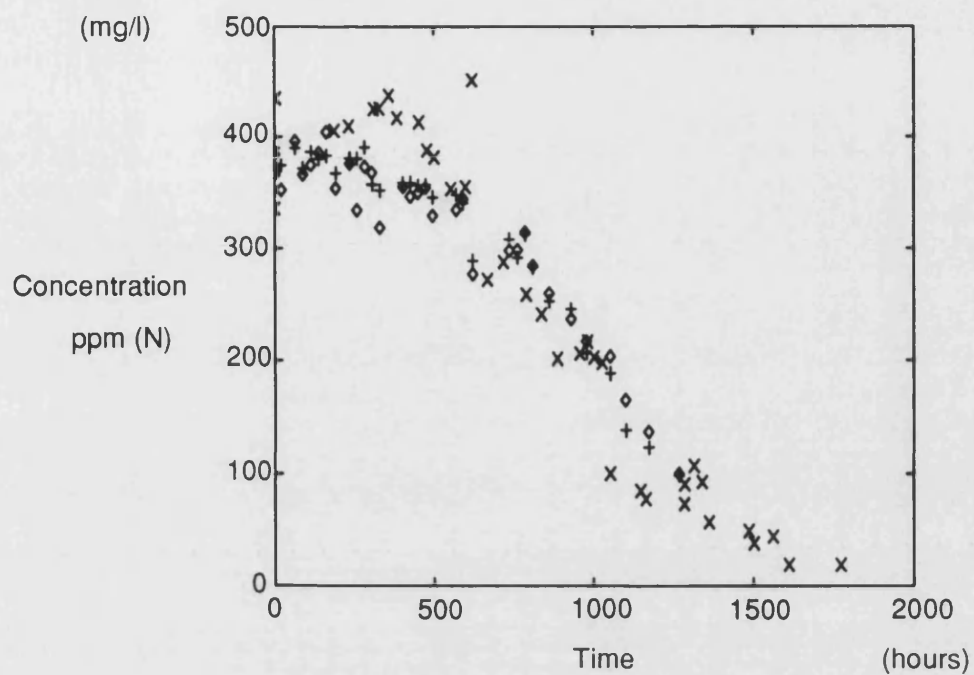
Degradation of 2,5-Dimethylpyrrole 1100 ppm(N) at 52 °C



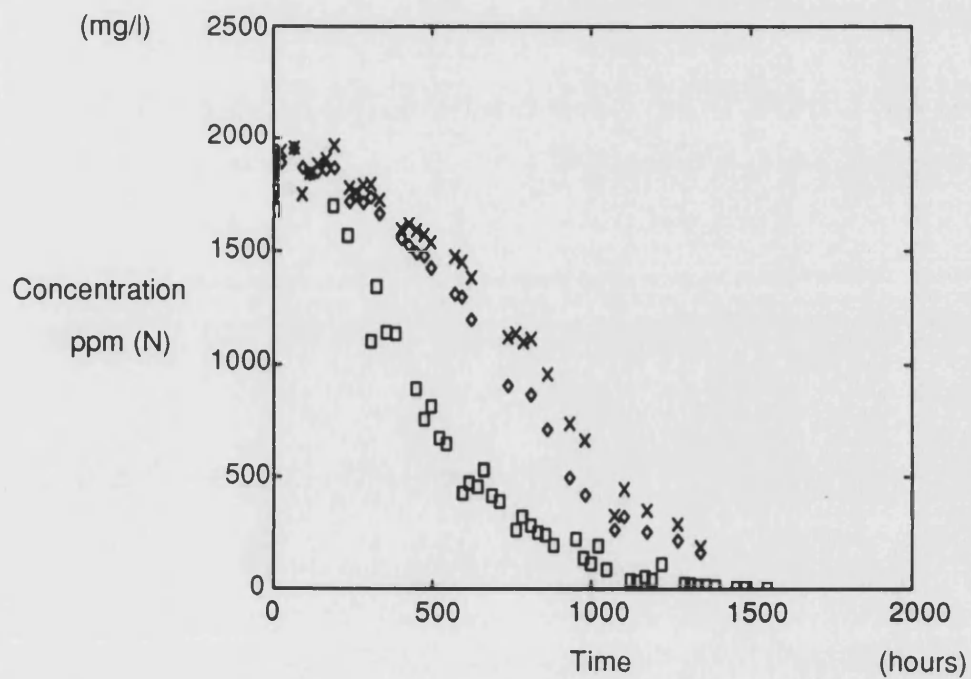
Degradation of 2,5-Dimethylpyrrole 750 ppm(N) at 52 °C



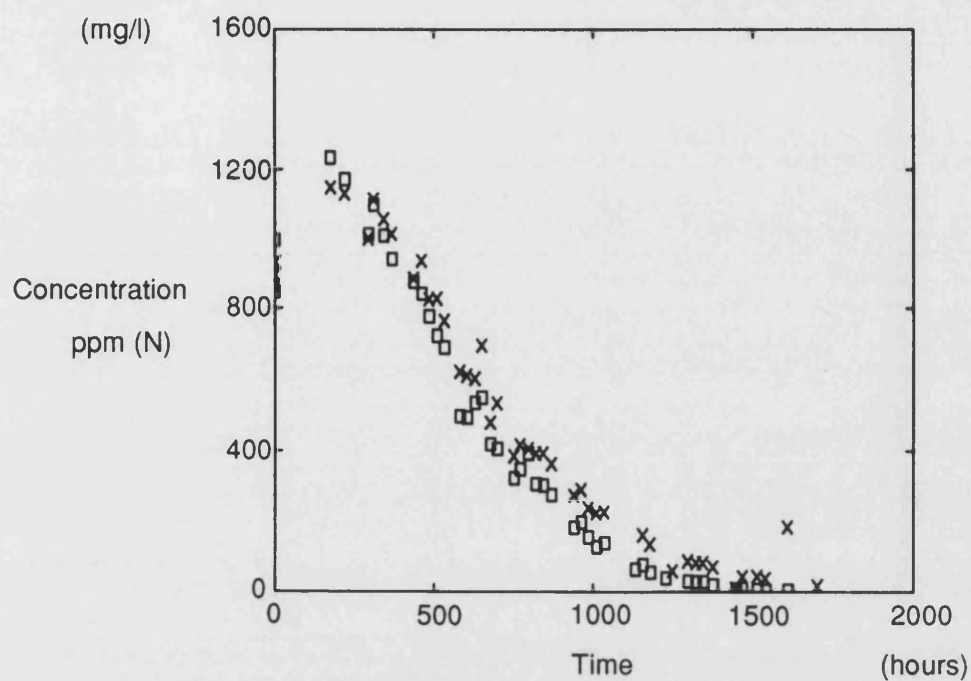
Degradation of 2,5-Dimethylpyrrole 410 ppm(N) at 52 °C



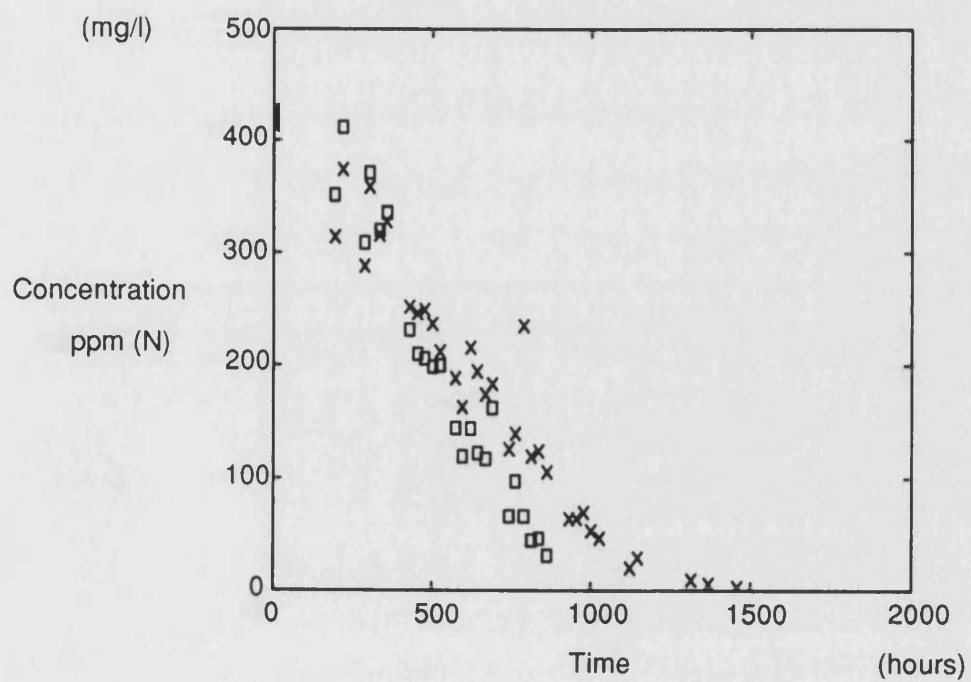
Degradation of 2,5-Dimethylpyrrole 1800 ppm(N) at 65 °C



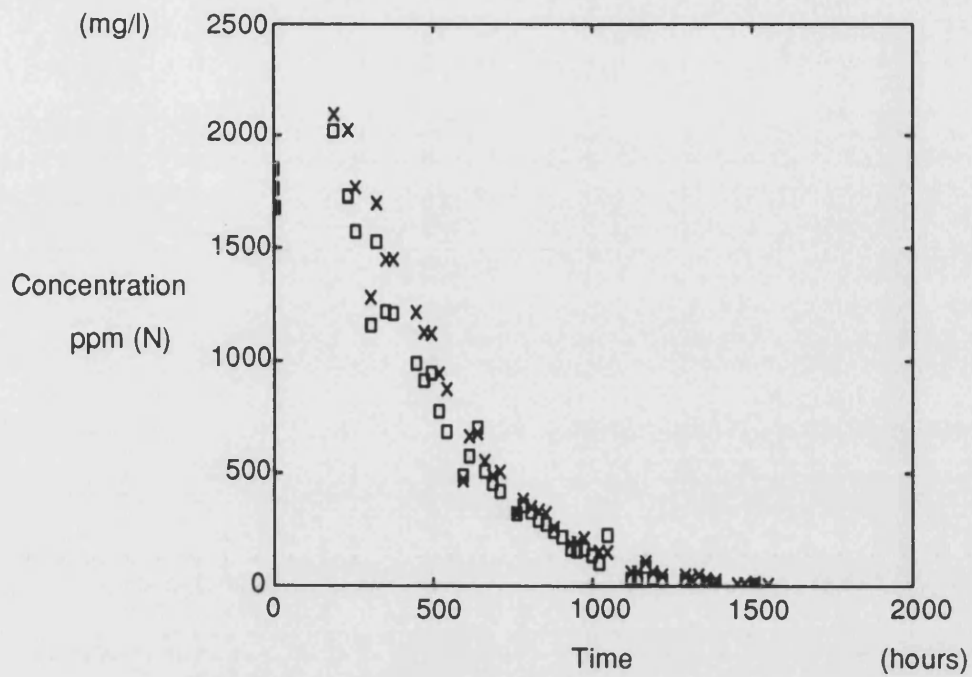
Degradation of 2,5-Dimethylpyrrole 1100 ppm(N) at 65 °C



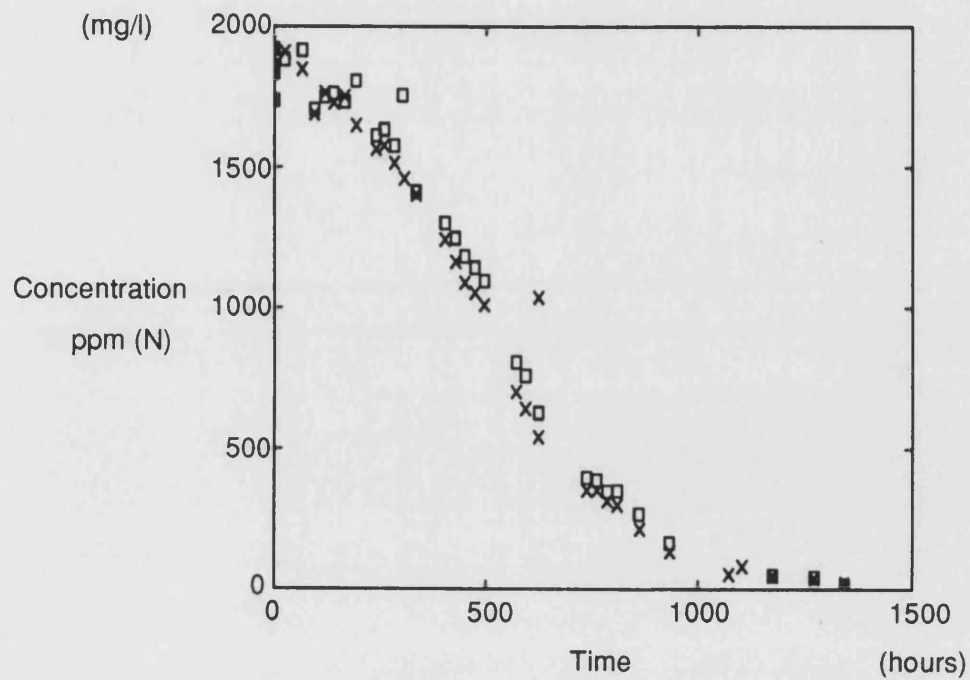
Degradation of 2,5-Dimethylpyrrole 410 ppm(N) at 65 °C



Degradation of 2,5-Dimethylpyrrole 1800 ppm(N) at 70 °C

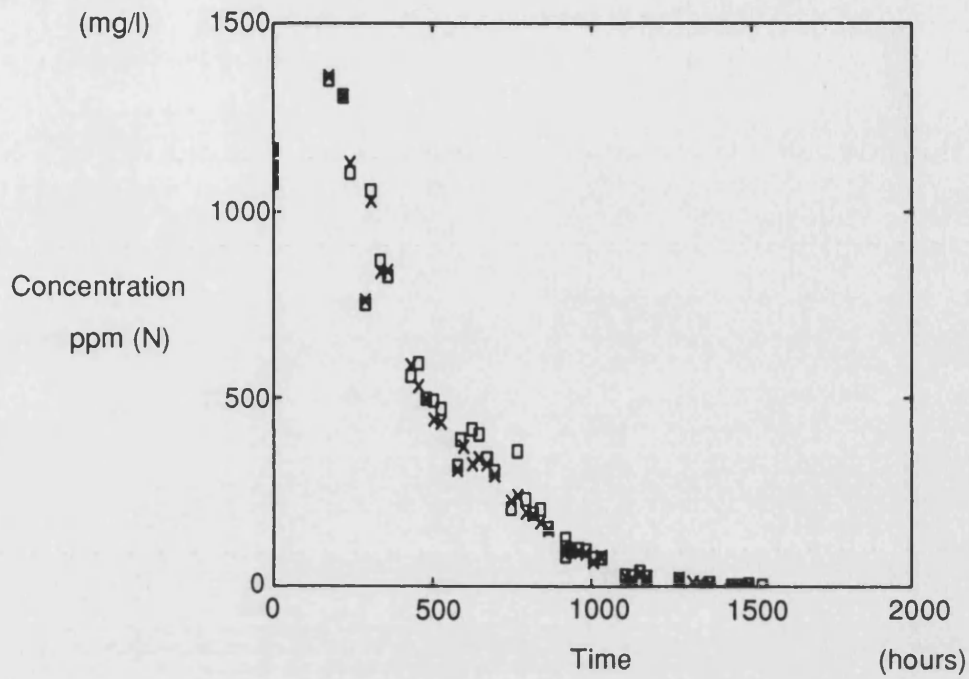


Degradation of 2,5-Dimethylpyrrole 1600 ppm(N) at 70 °C

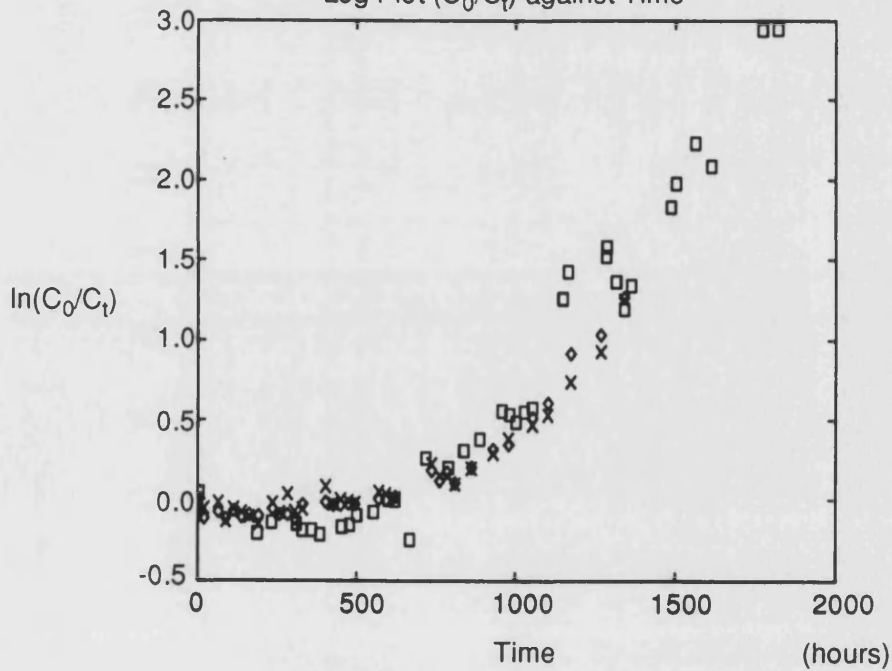




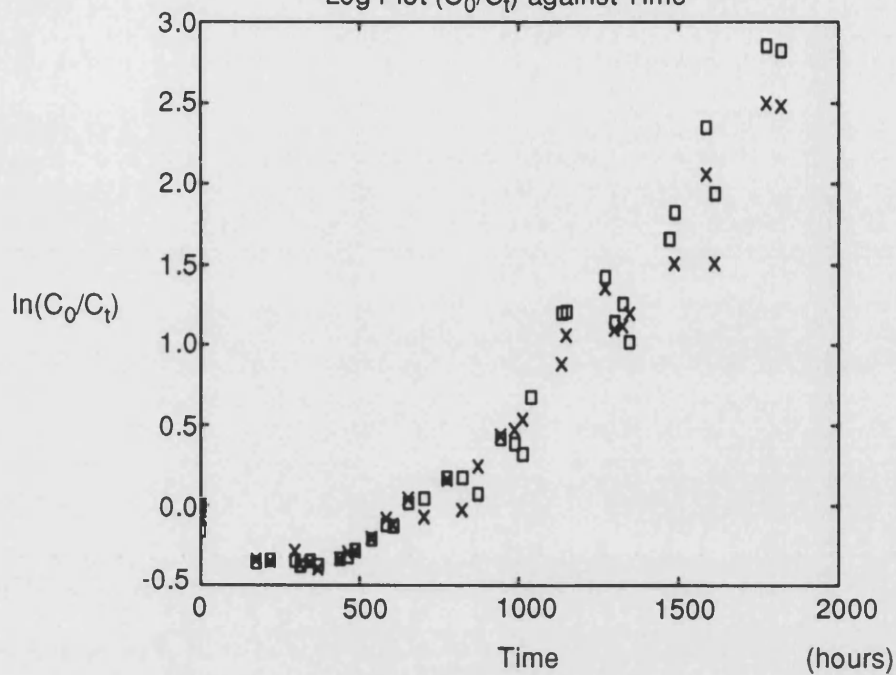
Degradation of 2,5-Dimethylpyrrole 1100 ppm(N) at 70 °C



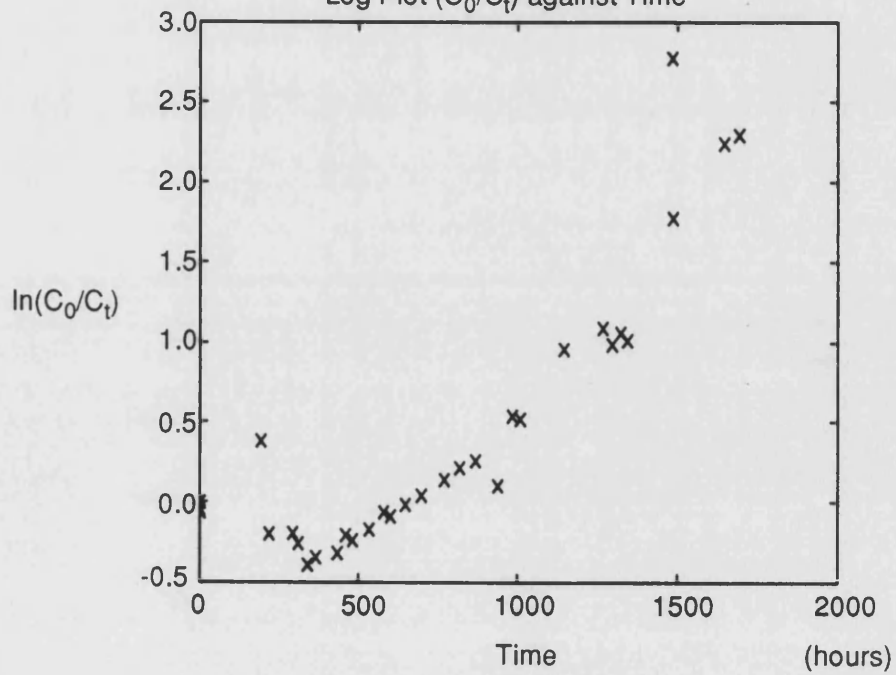
Degradation of 2,5-Dimethylpyrrole 1800 ppm(N) at 40 °C  
Log Plot ( $C_0/C_t$ ) against Time



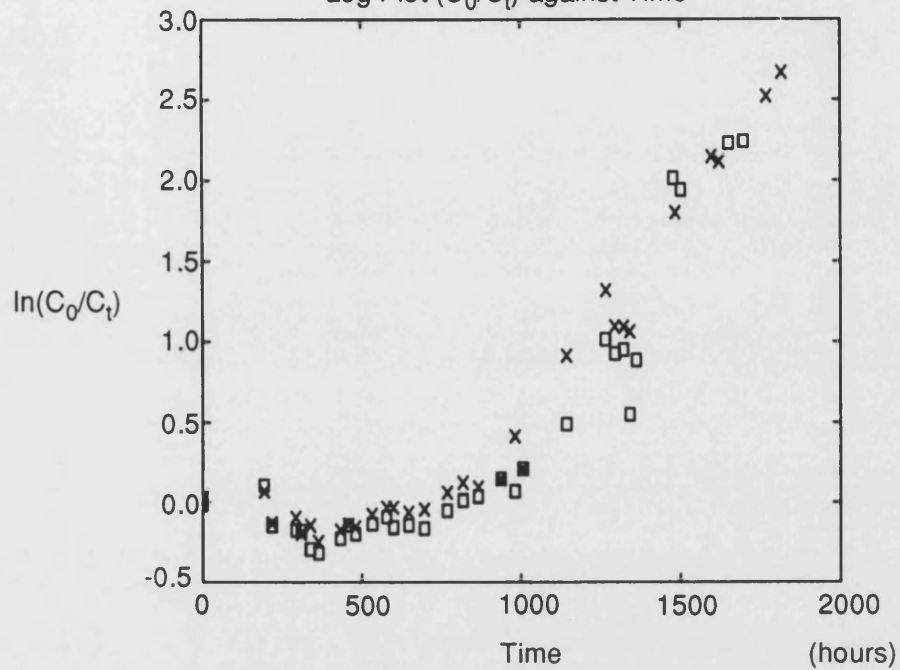
## Degradation of 2,5-Dimethylpyrrole 1100 ppm(N) at 40 °C

Log Plot ( $C_0/C_t$ ) against Time

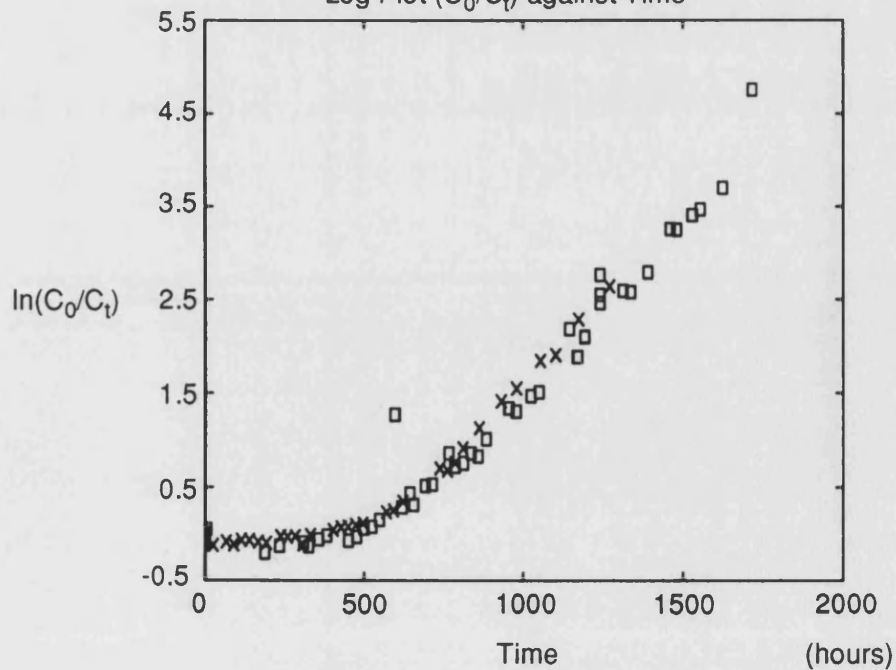
## Degradation of 2,5-Dimethylpyrrole 750 ppm(N) at 40 °C

Log Plot ( $C_0/C_t$ ) against Time

Degradation of 2,5-Dimethylpyrrole 410 ppm(N) at 40 °C  
Log Plot ( $C_0/C_t$ ) against Time

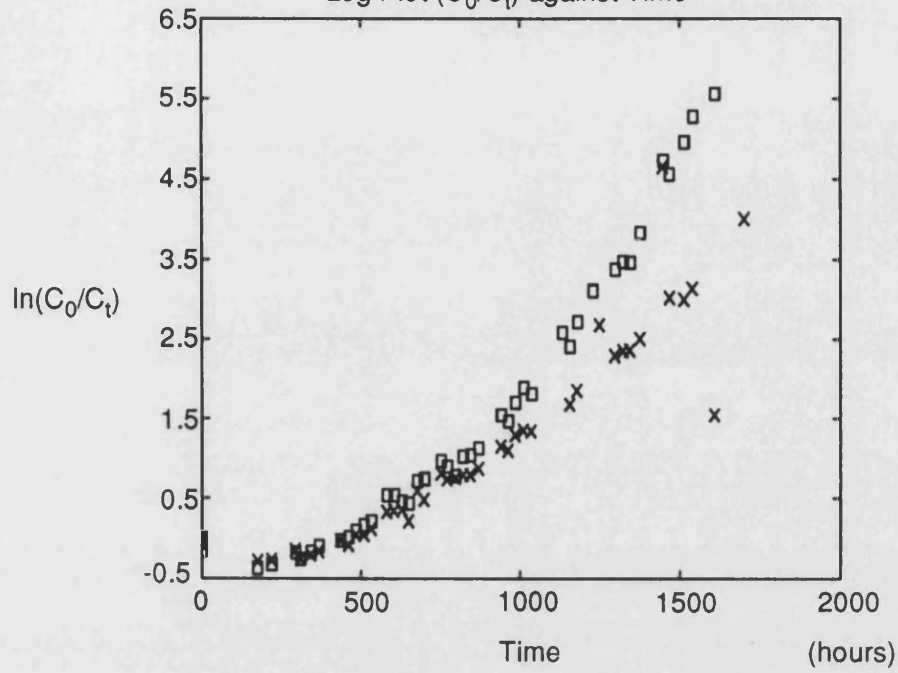


Degradation of 2,5-Dimethylpyrrole 1800 ppm(N) at 52 °C  
Log Plot ( $C_0/C_t$ ) against Time



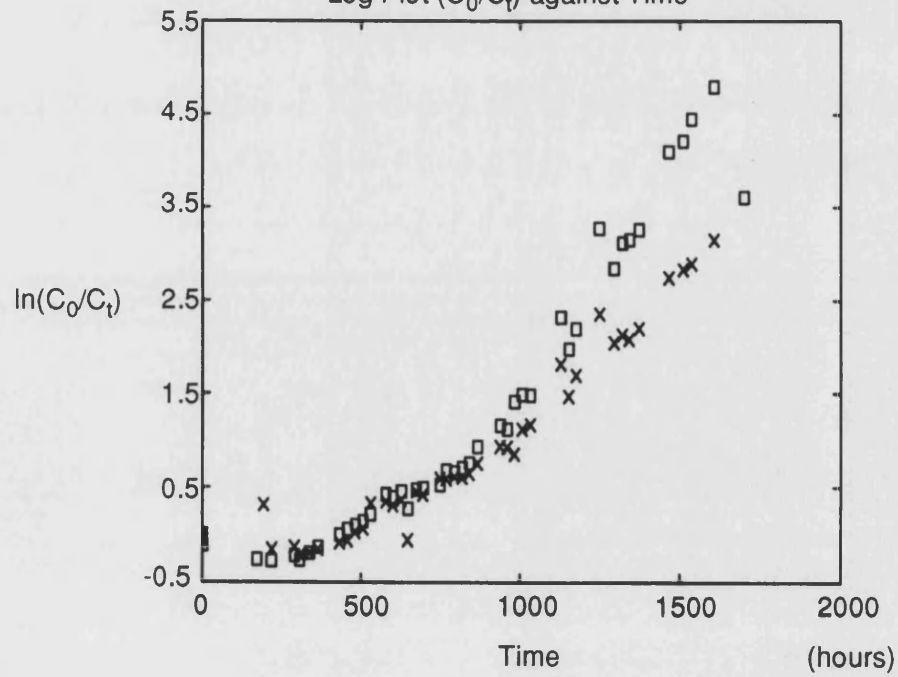
Degradation of 2,5-Dimethylpyrrole 1100 ppm(N) at 52 °C

Log Plot ( $C_0/C_t$ ) against Time



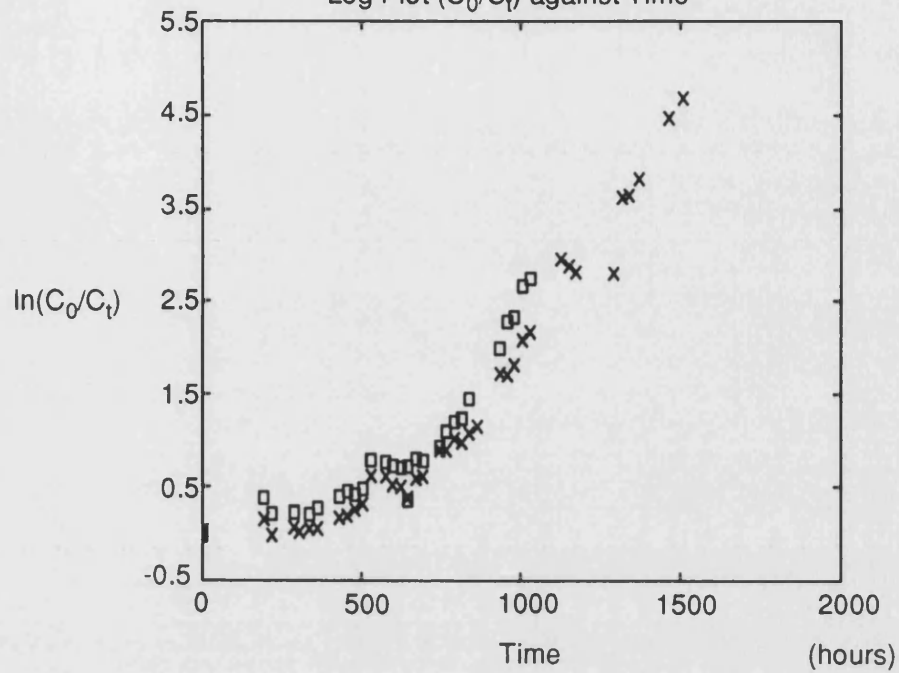
Degradation of 2,5-Dimethylpyrrole 750 ppm(N) at 52 °C

Log Plot ( $C_0/C_t$ ) against Time



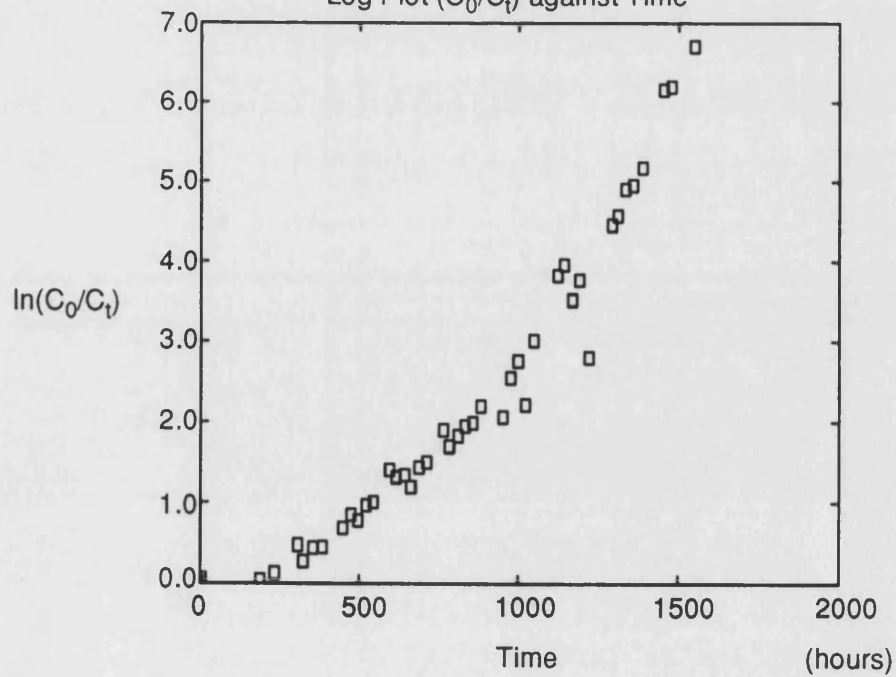
Degradation of 2,5-Dimethylpyrrole 410 ppm(N) at 52 °C

Log Plot ( $C_0/C_t$ ) against Time

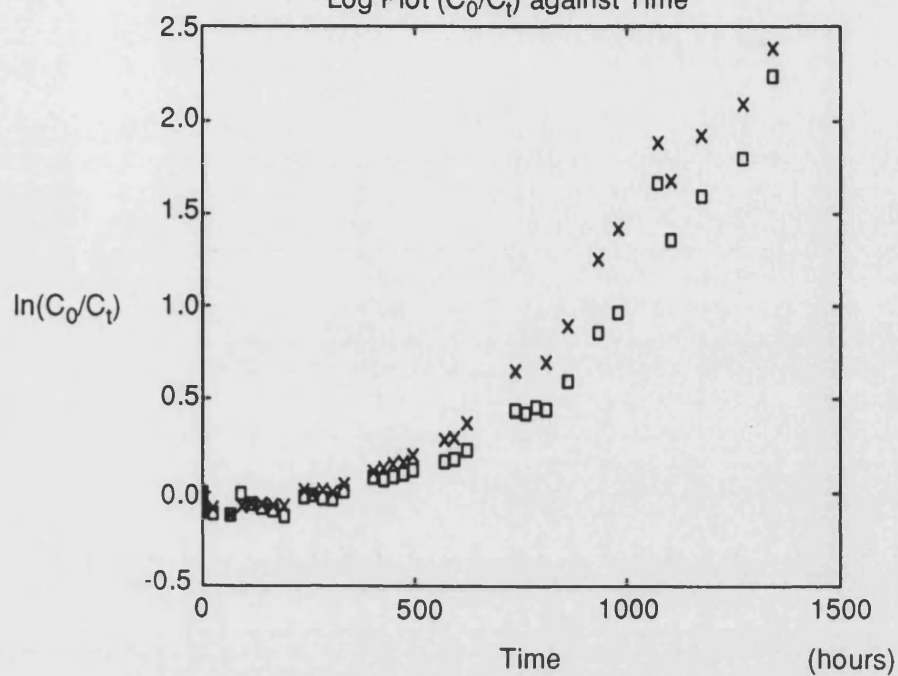


Degradation of 2,5-Dimethylpyrrole 1800 ppm(N) at 65 °C

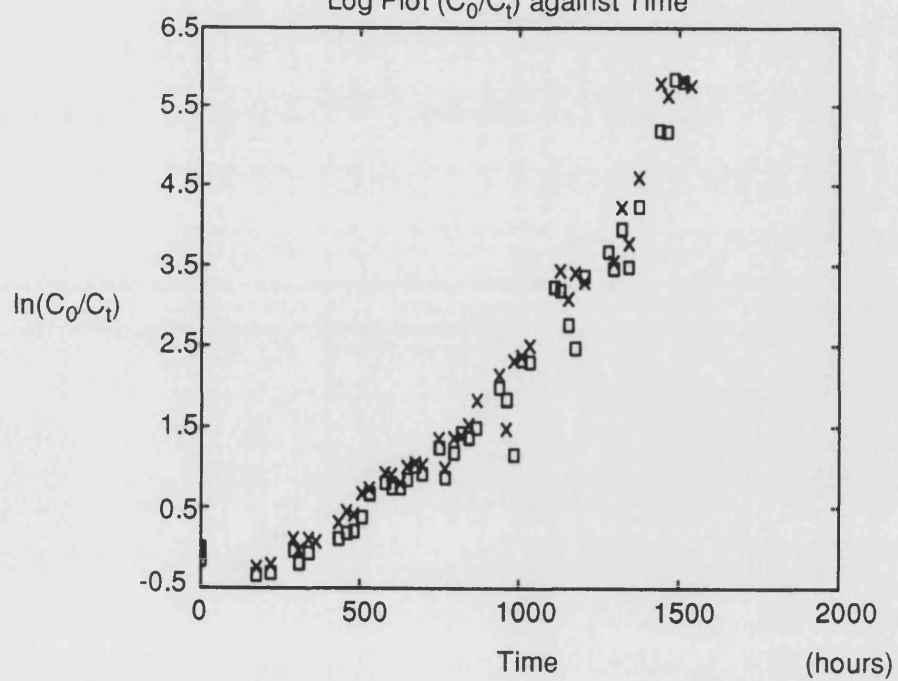
Log Plot ( $C_0/C_t$ ) against Time



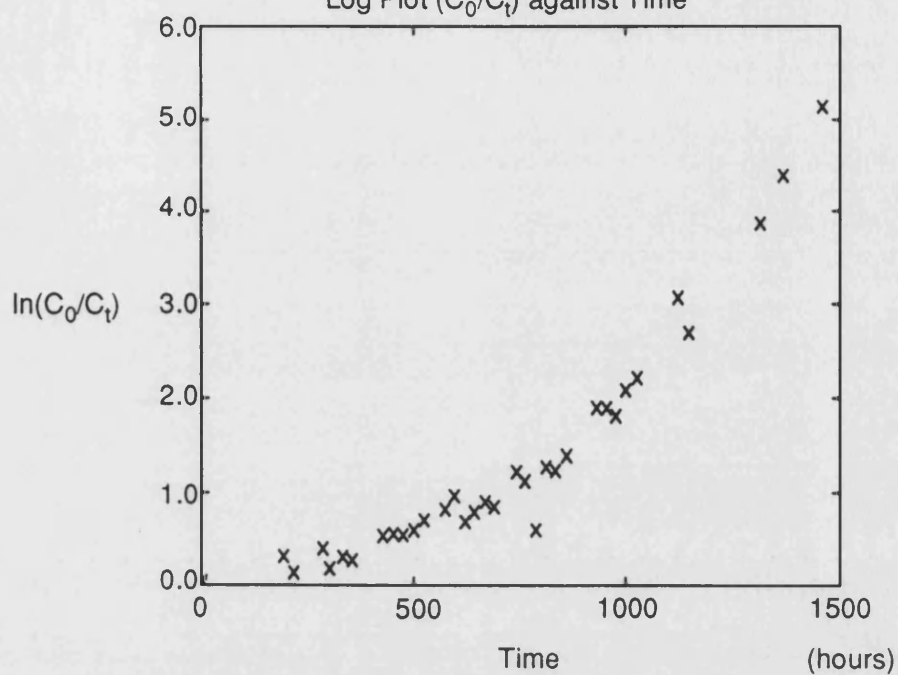
## Degradation of 2,5-Dimethylpyrrole 1600 ppm(N) at 65 °C

Log Plot ( $C_0/C_t$ ) against Time

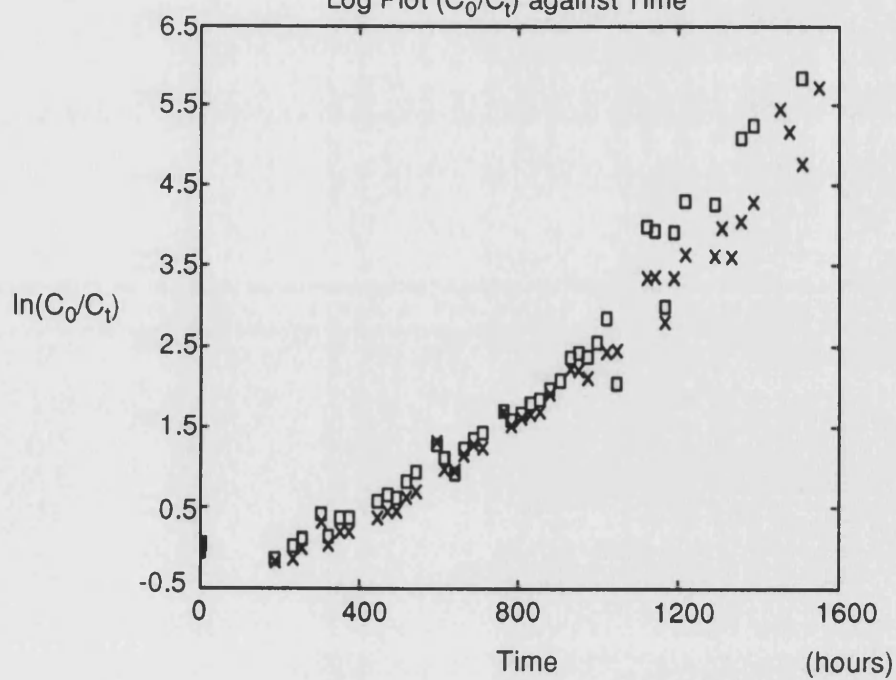
## Degradation of 2,5-Dimethylpyrrole 1100 ppm(N) at 65 °C

Log Plot ( $C_0/C_t$ ) against Time

Degradation of 2,5-Dimethylpyrrole 410 ppm(N) at 65 °C

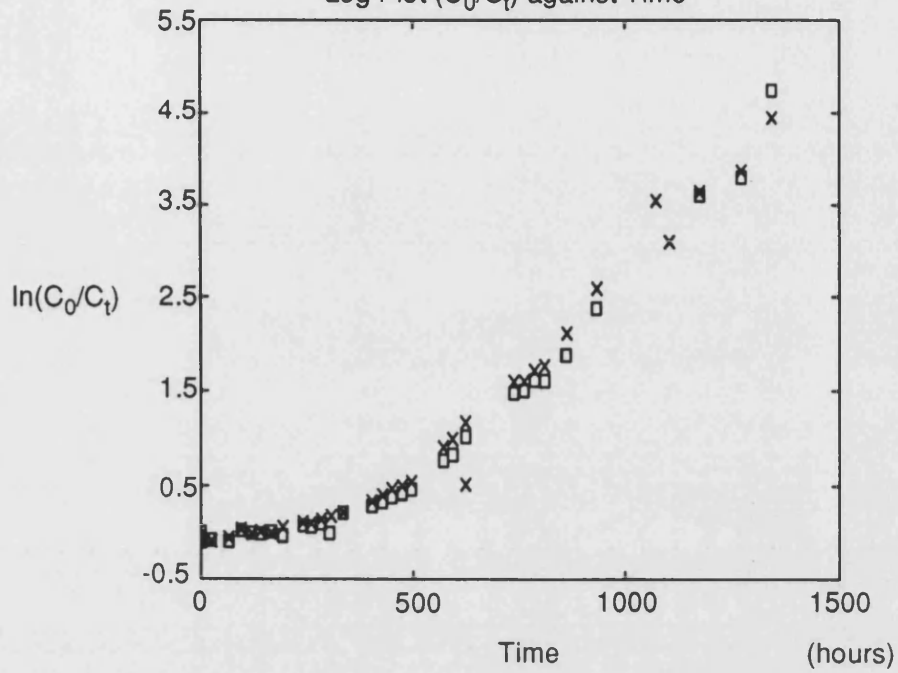
Log Plot ( $C_0/C_t$ ) against Time

Degradation of 2,5-Dimethylpyrrole 1800 ppm(N) at 70 °C

Log Plot ( $C_0/C_t$ ) against Time

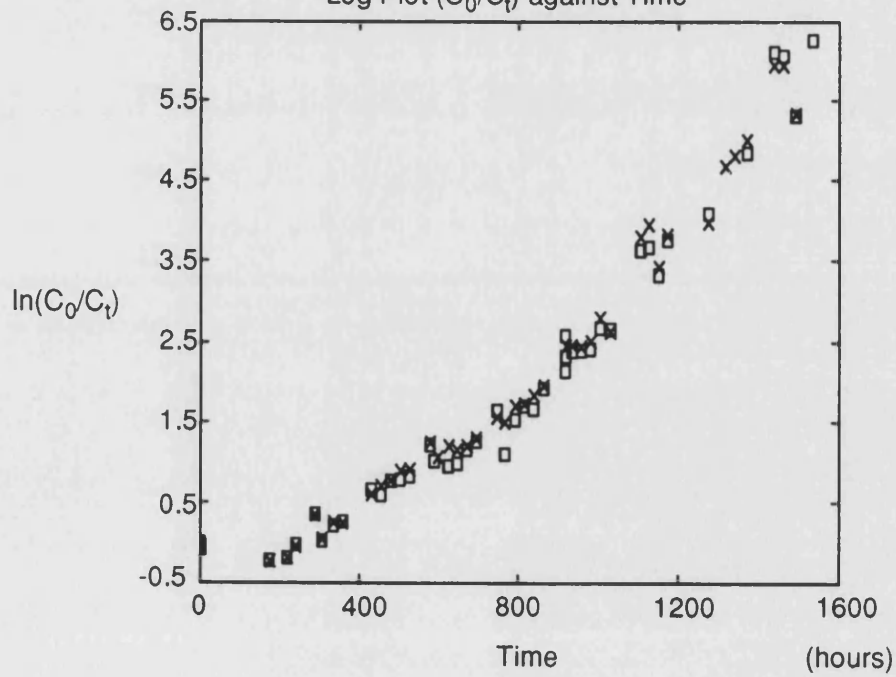
Degradation of 2,5-Dimethylpyrrole 1600 ppm(N) at 70 °C

Log Plot ( $C_0/C_t$ ) against Time



Degradation of 2,5-Dimethylpyrrole 1100 ppm(N) at 70 °C

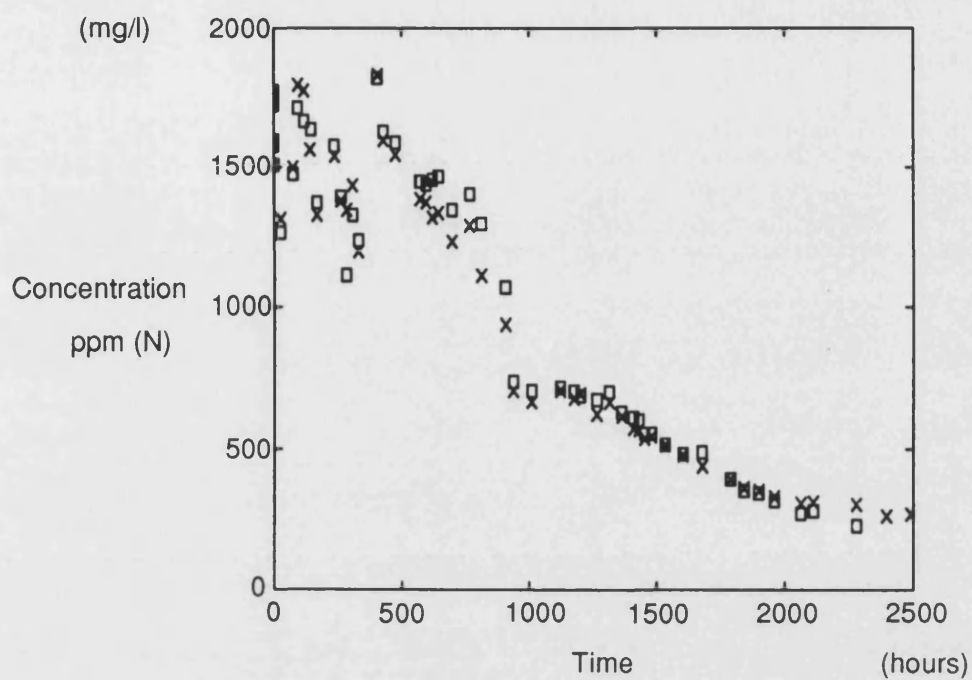
Log Plot ( $C_0/C_t$ ) against Time



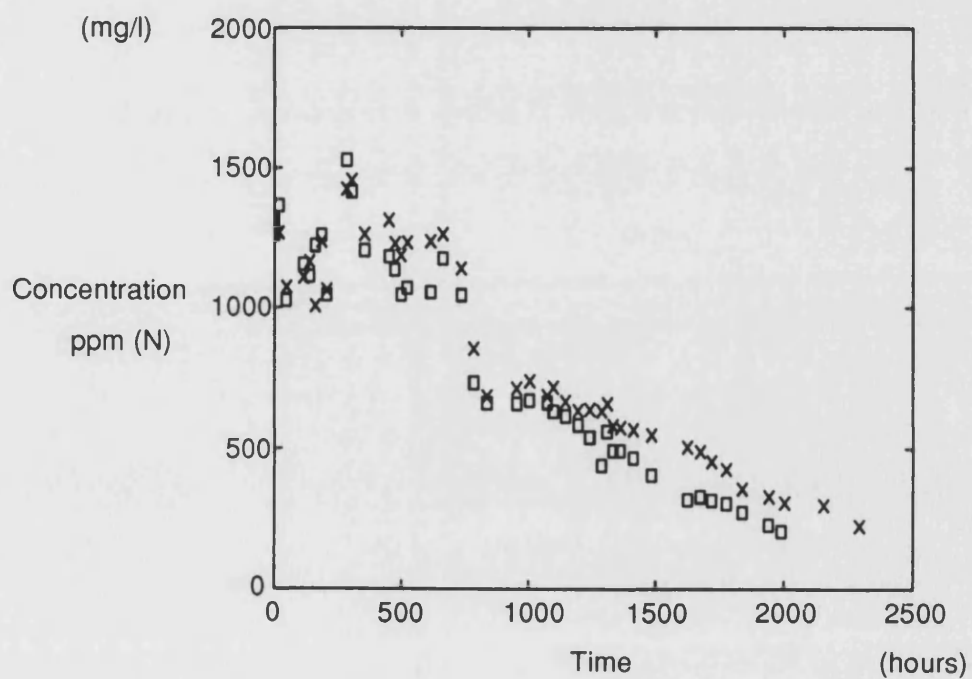


## Data from the 1,2,5-Trimethylpyrrole System

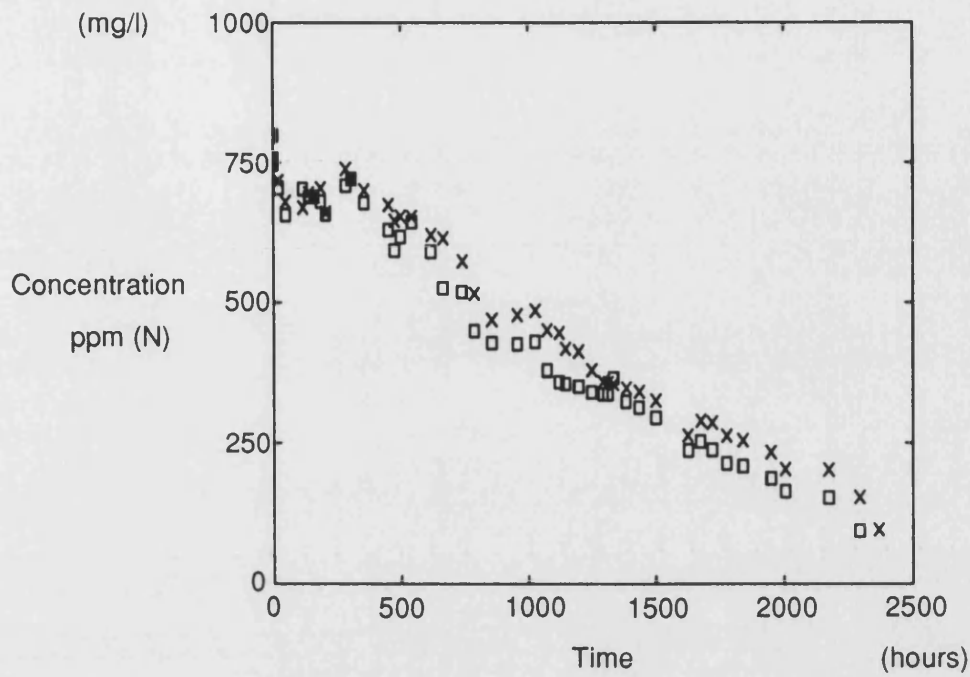
Degradation of 1,2,5-Trimethylpyrrole 1650 ppm(N) at 40 °C



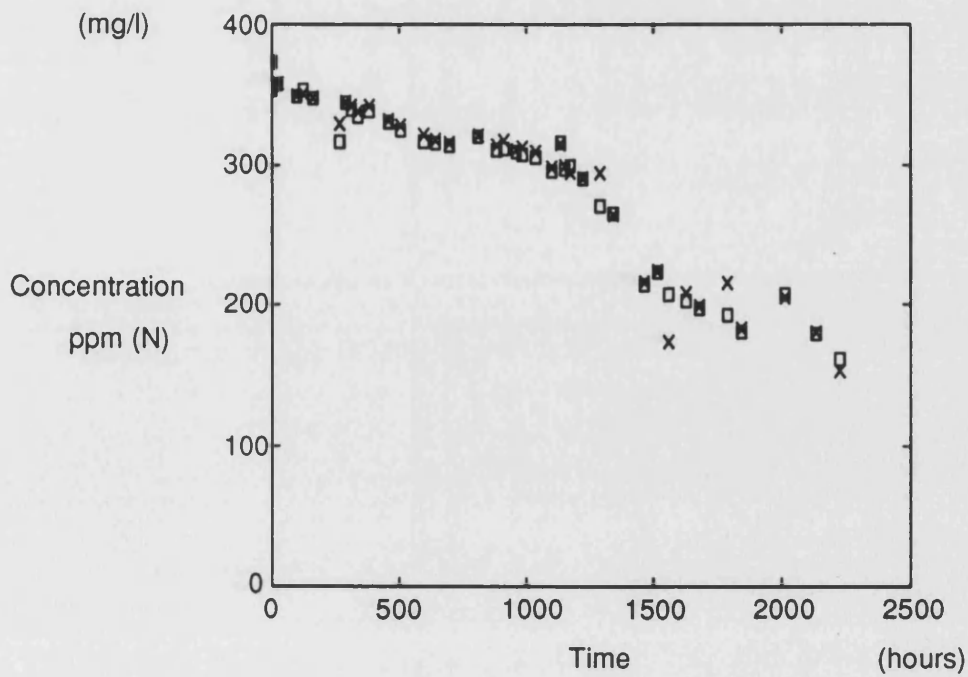
Degradation of 1,2,5-Trimethylpyrrole 1290 ppm(N) at 40 °C



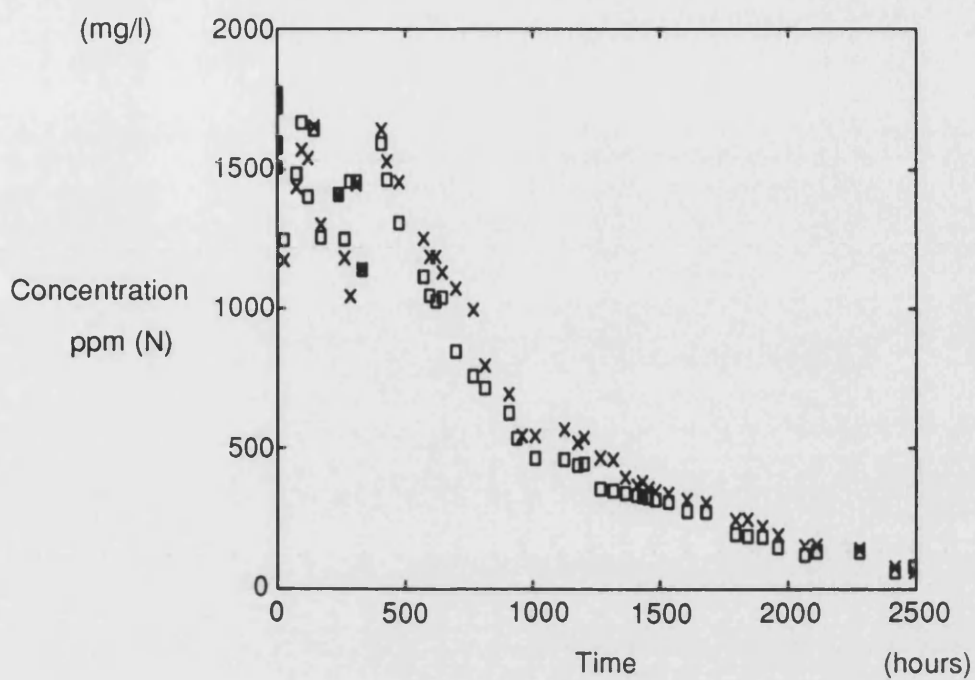
Degradation of 1,2,5-Trimethylpyrrole 750 ppm(N) at 40 °C



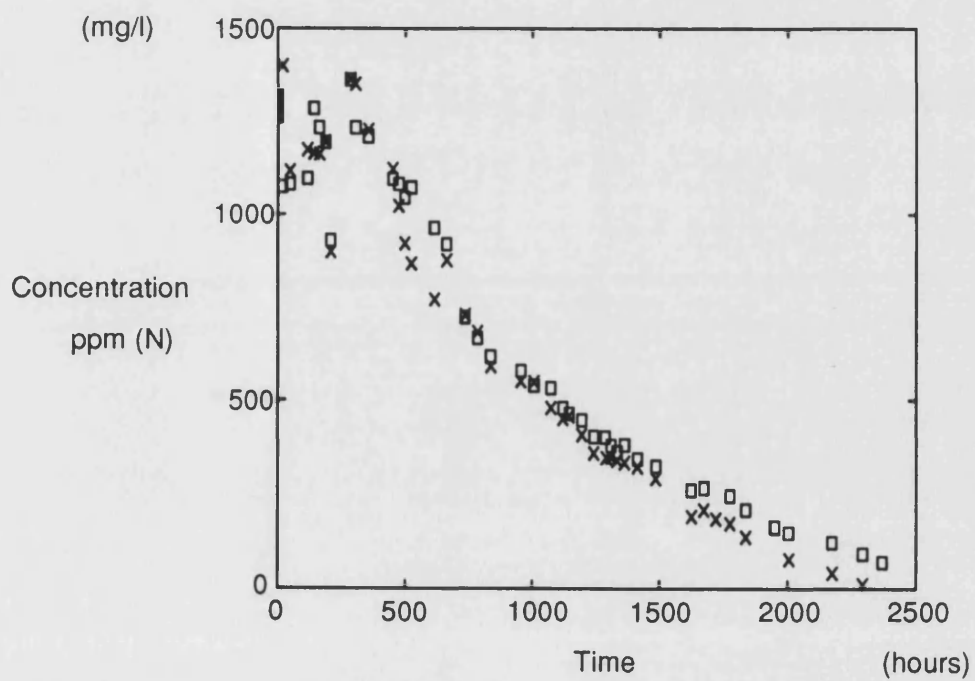
Degradation of 1,2,5-Trimethylpyrrole 350 ppm(N) at 40 °C



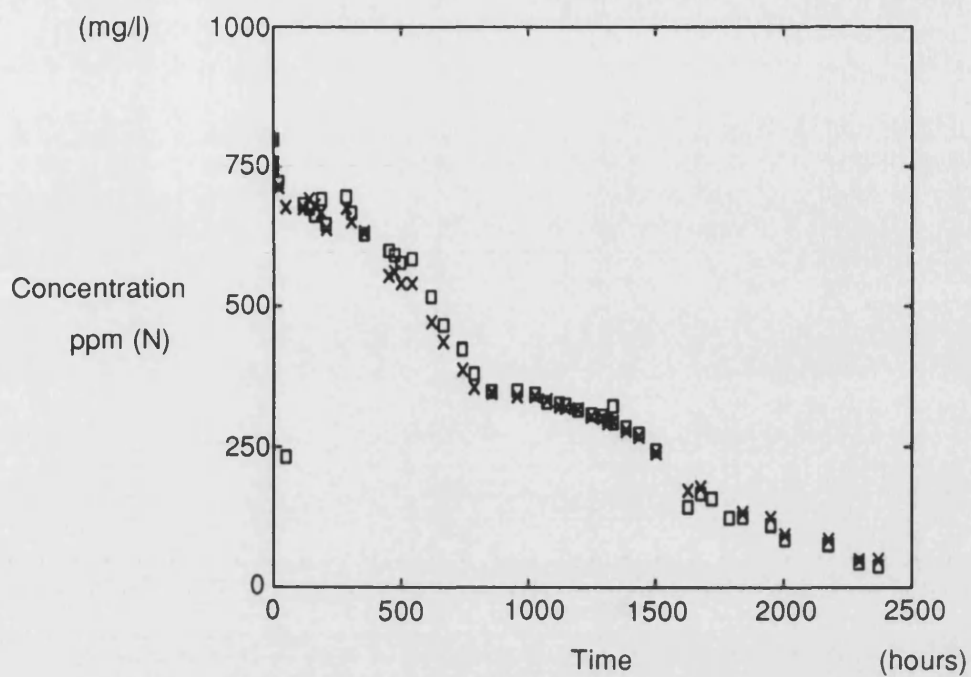
Degradation of 1,2,5-Trimethylpyrrole 1650 ppm(N) at 52 °C



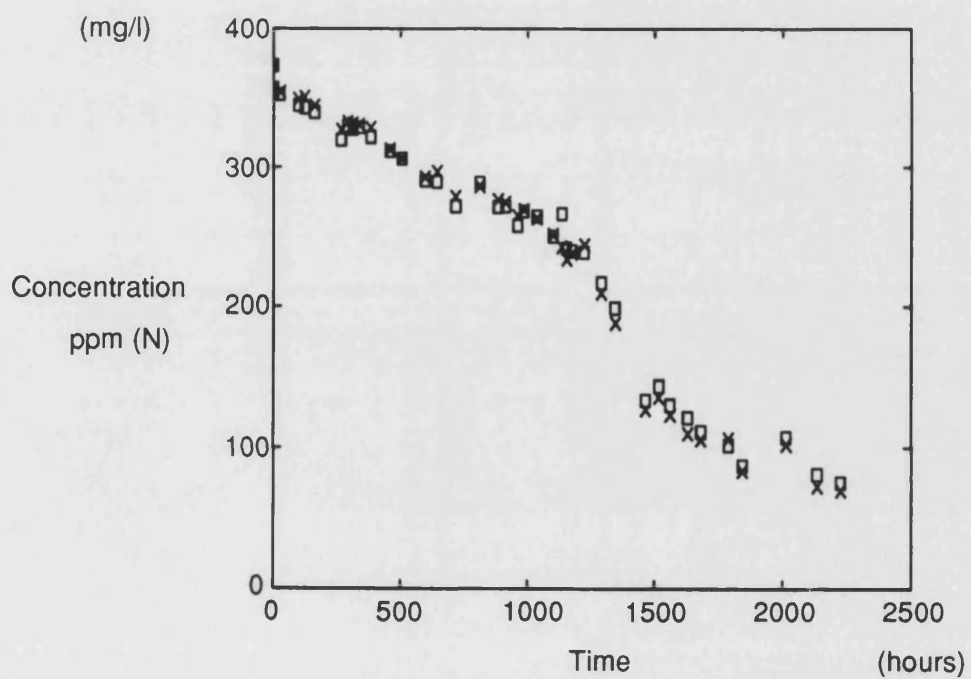
Degradation of 1,2,5-Trimethylpyrrole 1290 ppm(N) at 52 °C



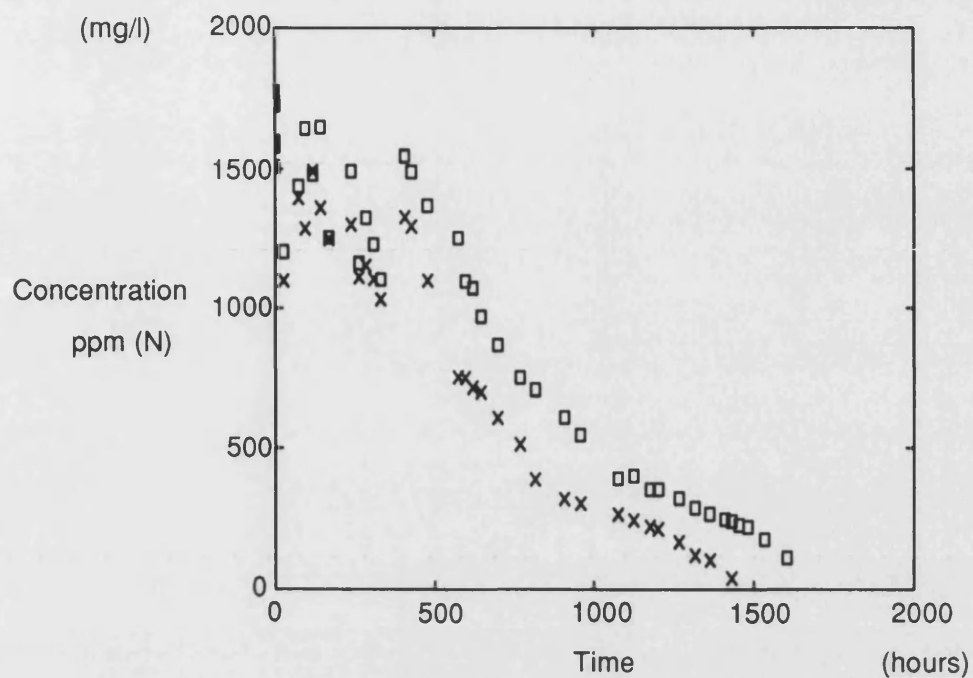
Degradation of 1,2,5-Trimethylpyrrole 750 ppm(N) at 52 °C



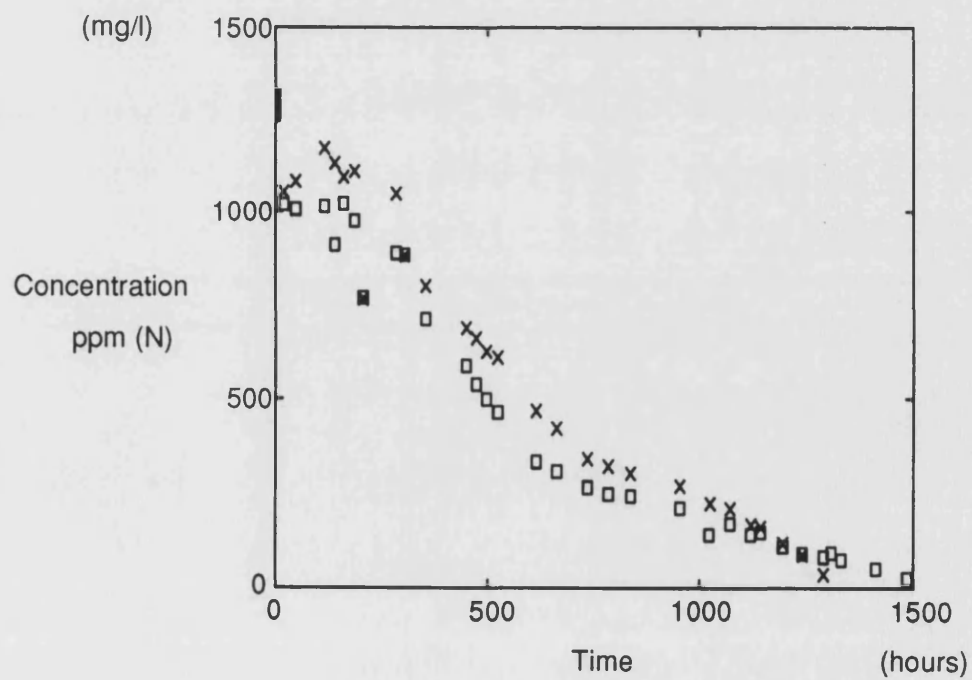
Degradation of 1,2,5-Trimethylpyrrole 350 ppm(N) at 52 °C



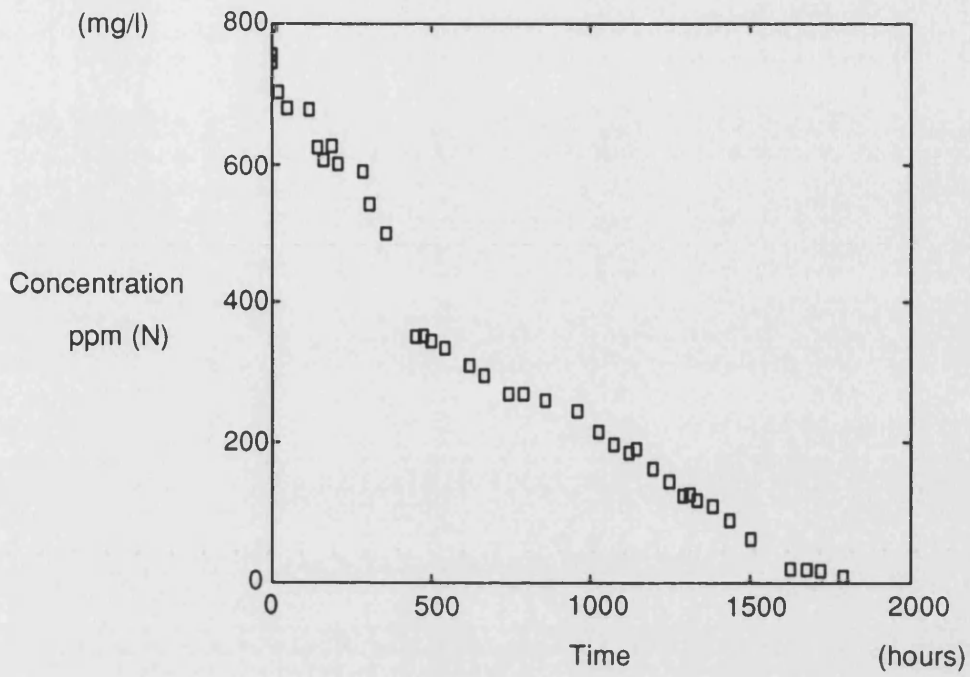
Degradation of 1,2,5-Trimethylpyrrole 1650 ppm(N) at 65 °C



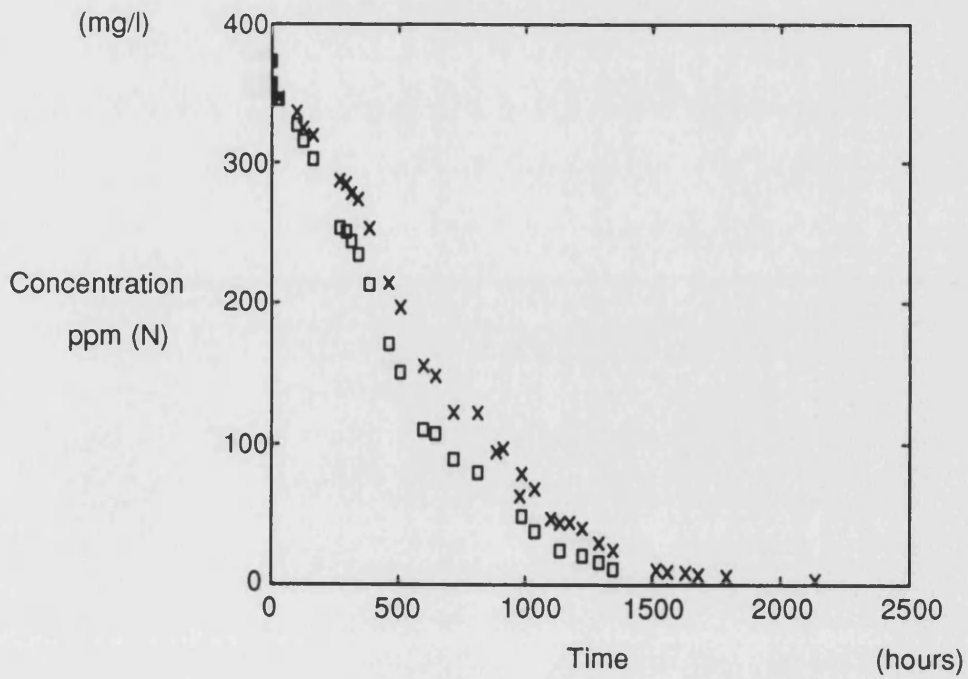
Degradation of 1,2,5-Trimethylpyrrole 1290 ppm(N) at 65 °C



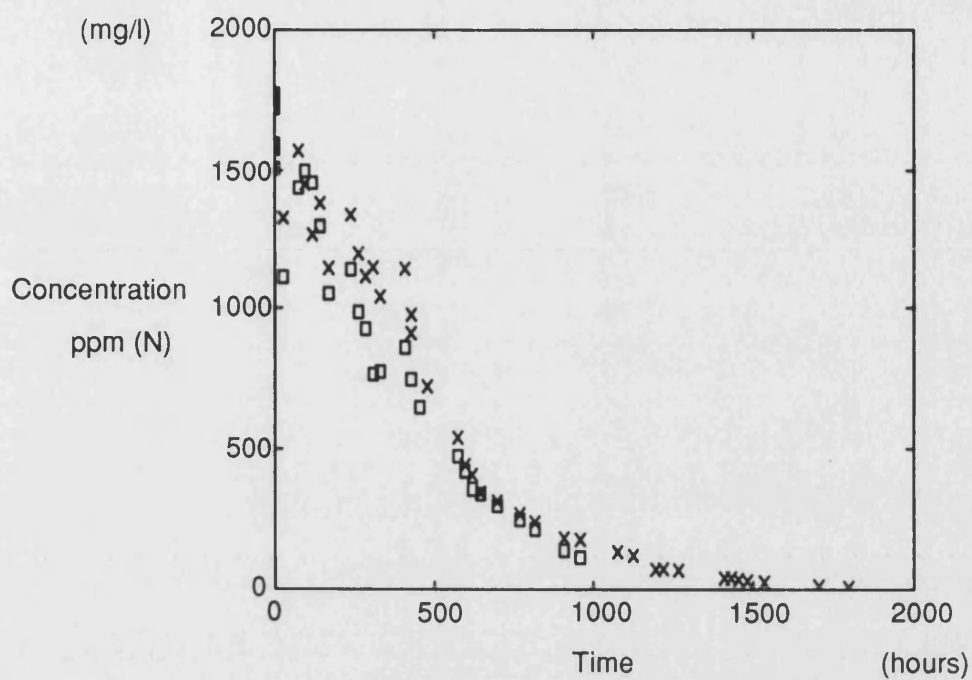
Degradation of 1,2,5-Trimethylpyrrole 750 ppm(N) at 65 °C



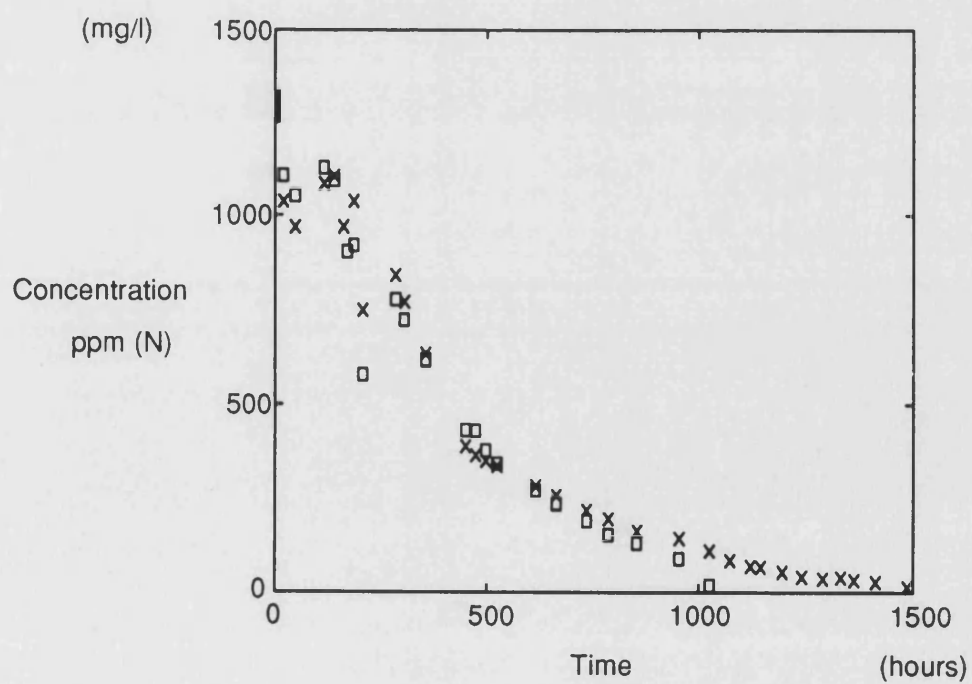
Degradation of 1,2,5-Trimethylpyrrole 350 ppm(N) at 65 °C



Degradation of 1,2,5-Trimethylpyrrole 1650 ppm(N) at 70 °C

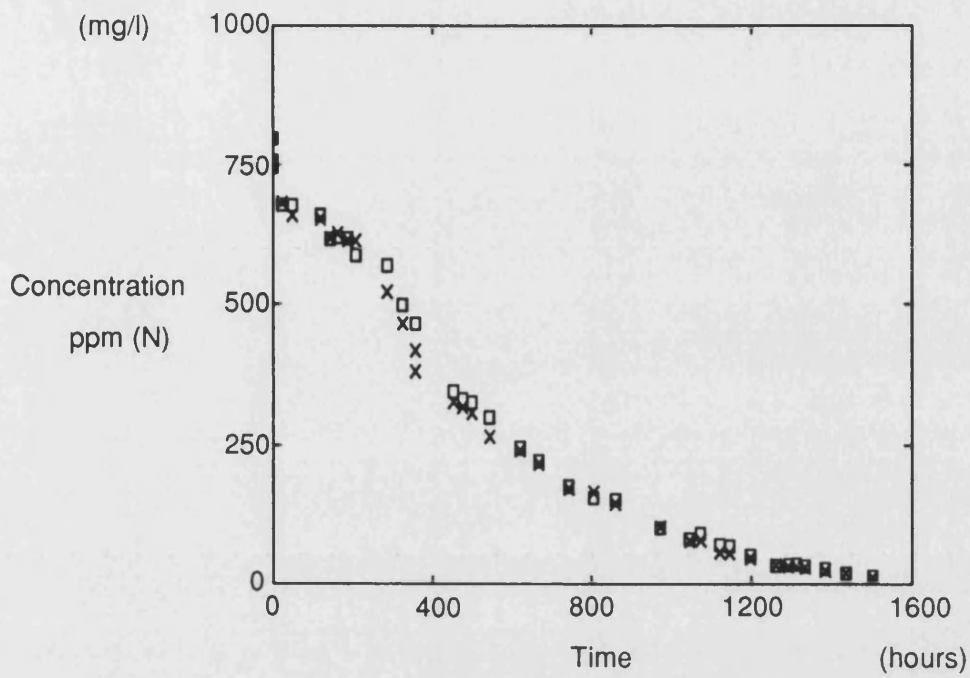


Degradation of 1,2,5-Trimethylpyrrole 1290 ppm(N) at 70 °C

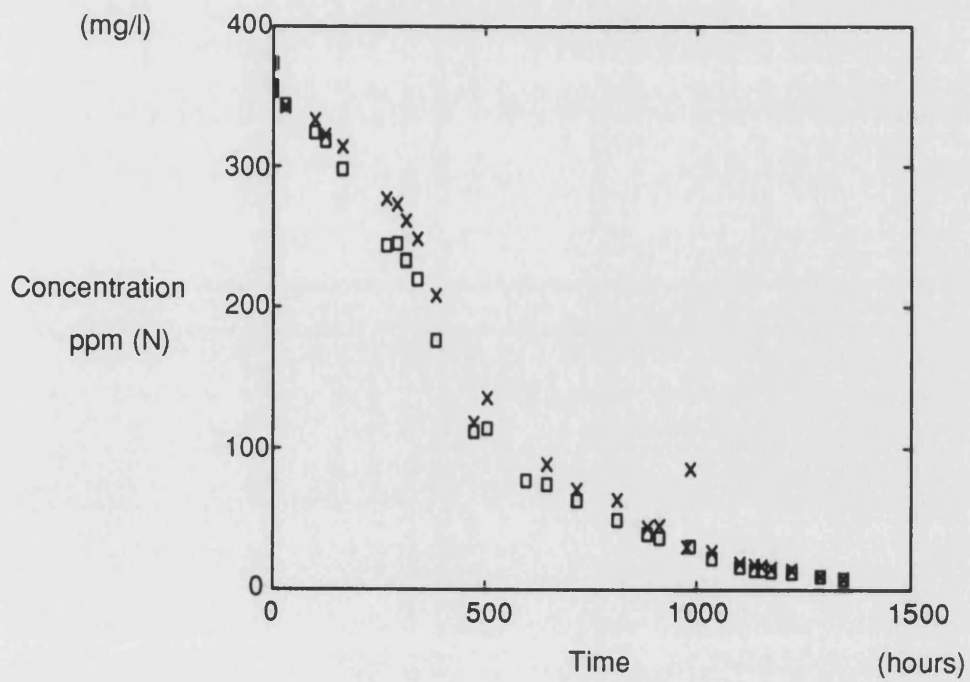




Degradation of 1,2,5-Trimethylpyrrole 750 ppm(N) at 70 °C

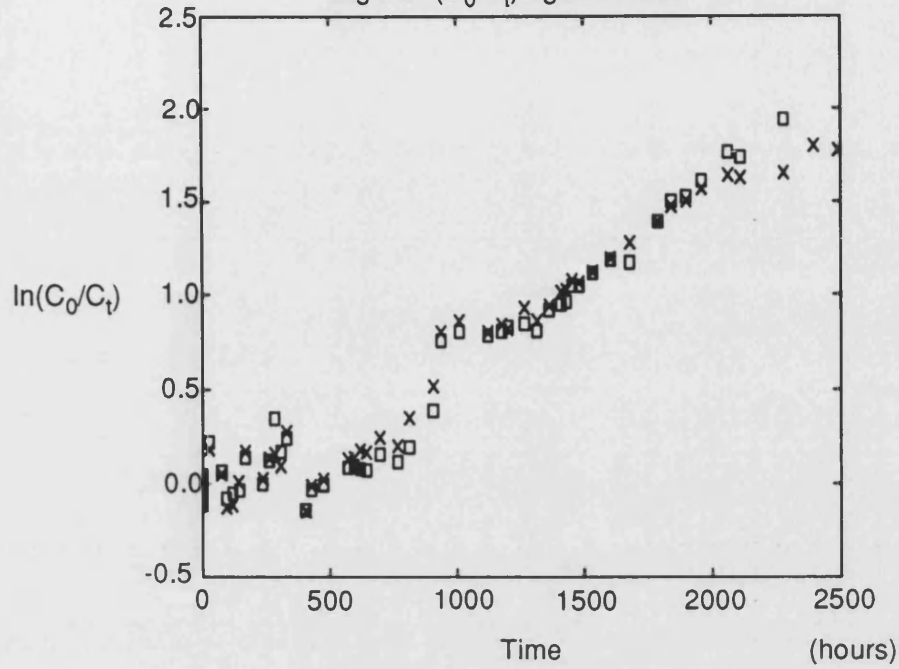


Degradation of 1,2,5-Trimethylpyrrole 350 ppm(N) at 70 °C



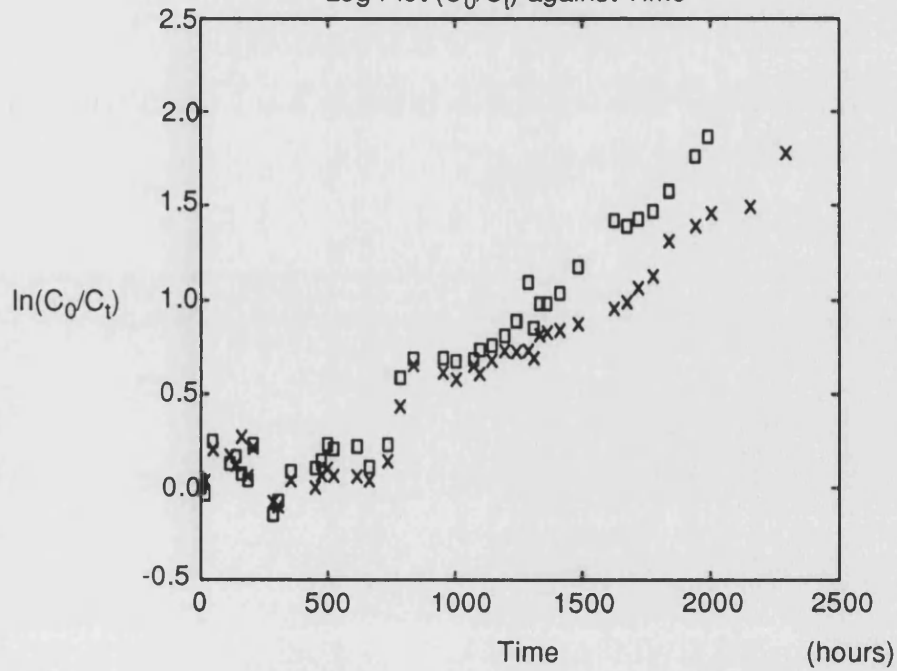
Degradation of 1,2,5-Trimethylpyrrole 1650 ppm(N) at 40 °C

Log Plot ( $C_0/C_t$ ) against Time

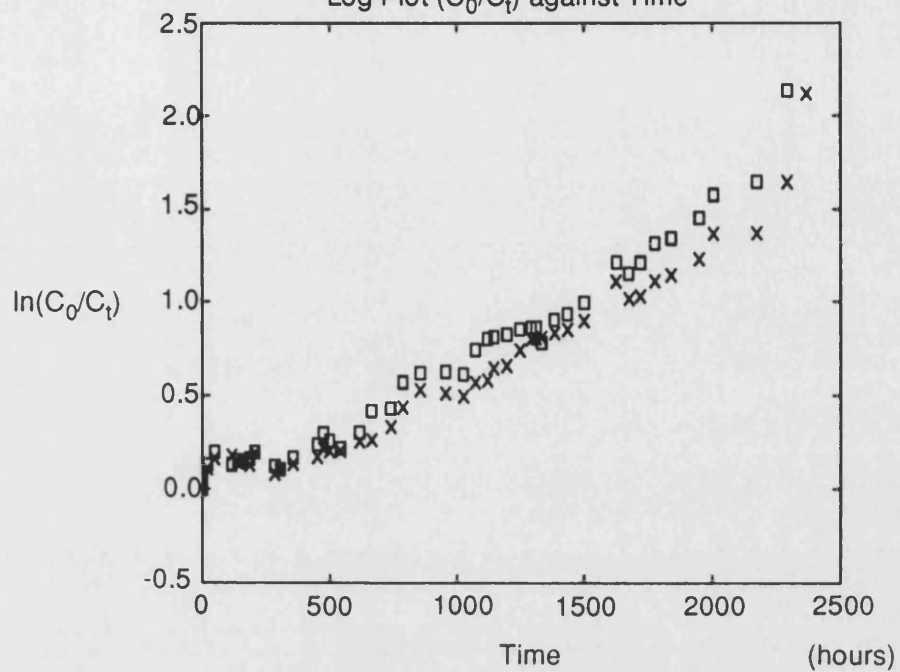


Degradation of 1,2,5-Trimethylpyrrole 1290 ppm(N) at 40 °C

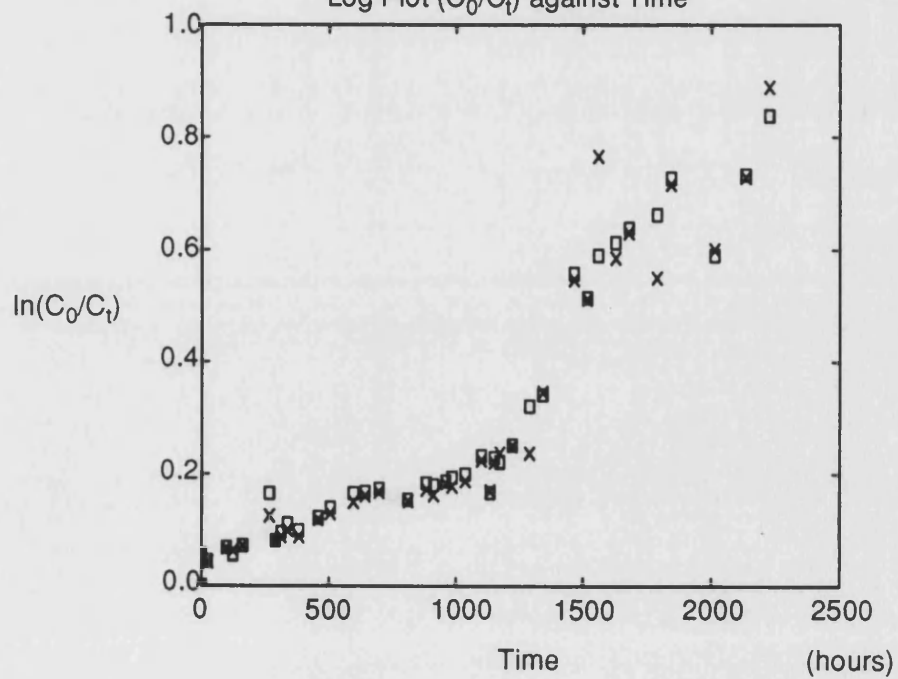
Log Plot ( $C_0/C_t$ ) against Time



## Degradation of 1,2,5-Trimethylpyrrole 750 ppm(N) at 40 °C

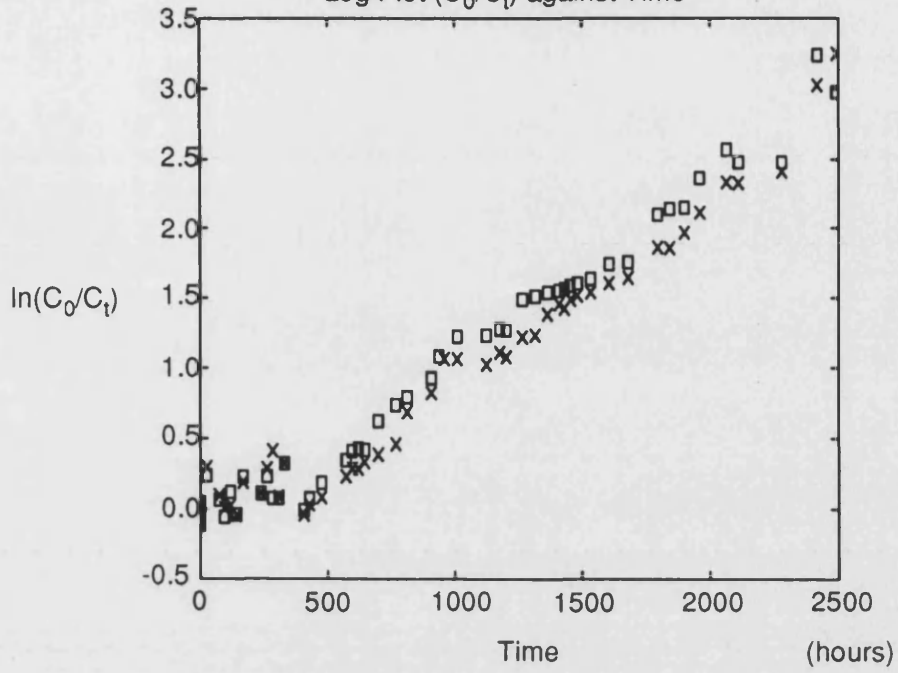
Log Plot ( $C_0/C_t$ ) against Time

## Degradation of 1,2,5-Trimethylpyrrole 350 ppm(N) at 40 °C

Log Plot ( $C_0/C_t$ ) against Time

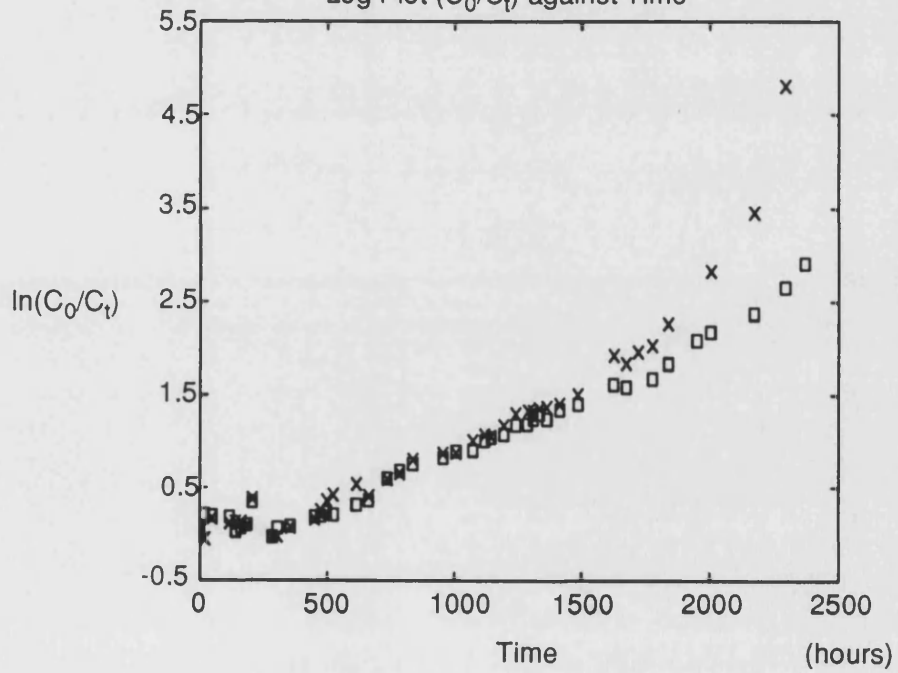
Degradation of 1,2,5-Trimethylpyrrole 1650 ppm(N) at 52 °C

Log Plot ( $C_0/C_t$ ) against Time

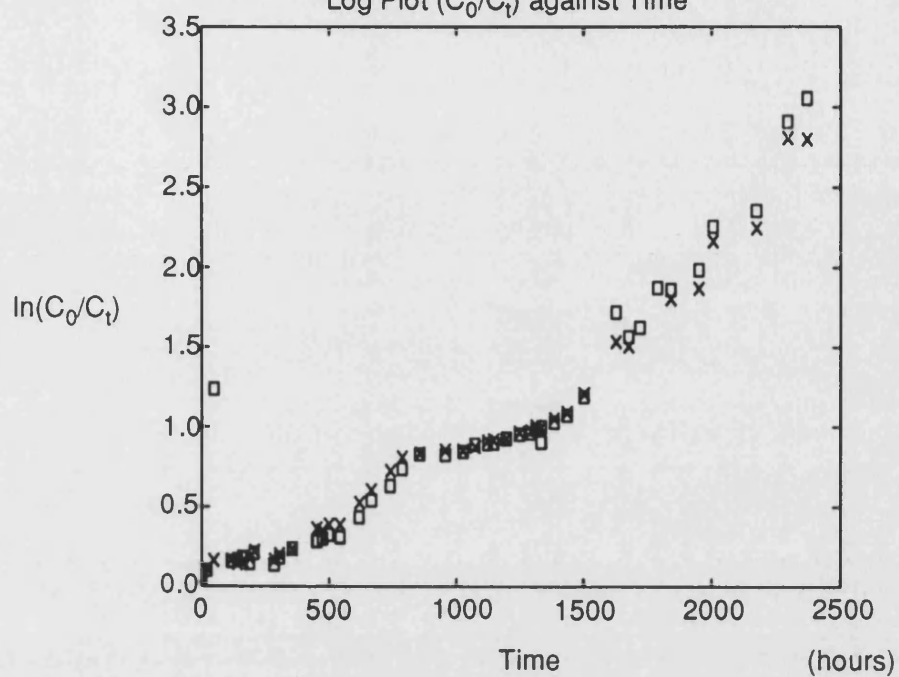


Degradation of 1,2,5-Trimethylpyrrole 1290 ppm(N) at 52 °C

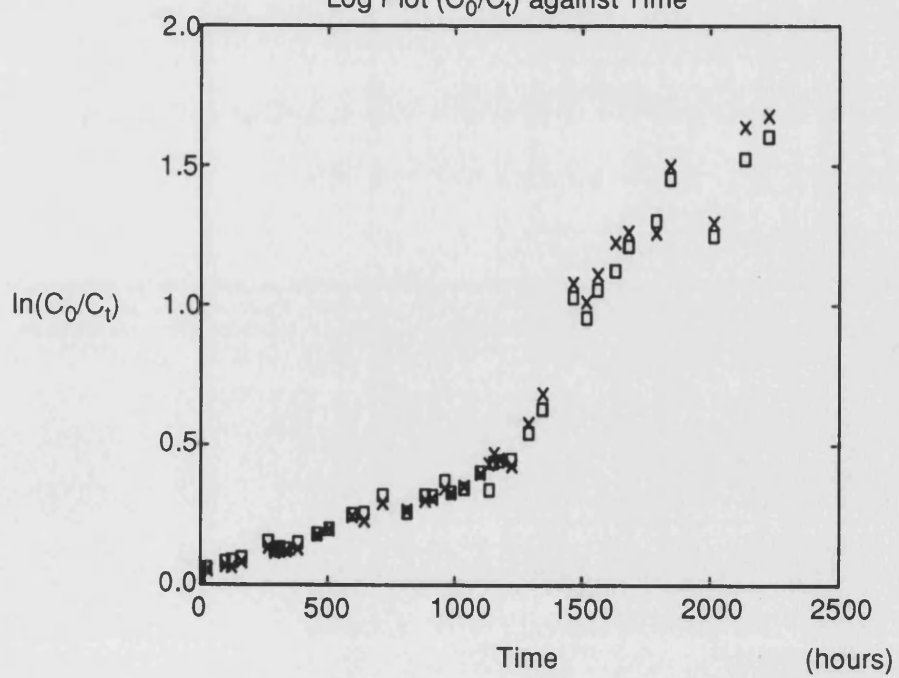
Log Plot ( $C_0/C_t$ ) against Time



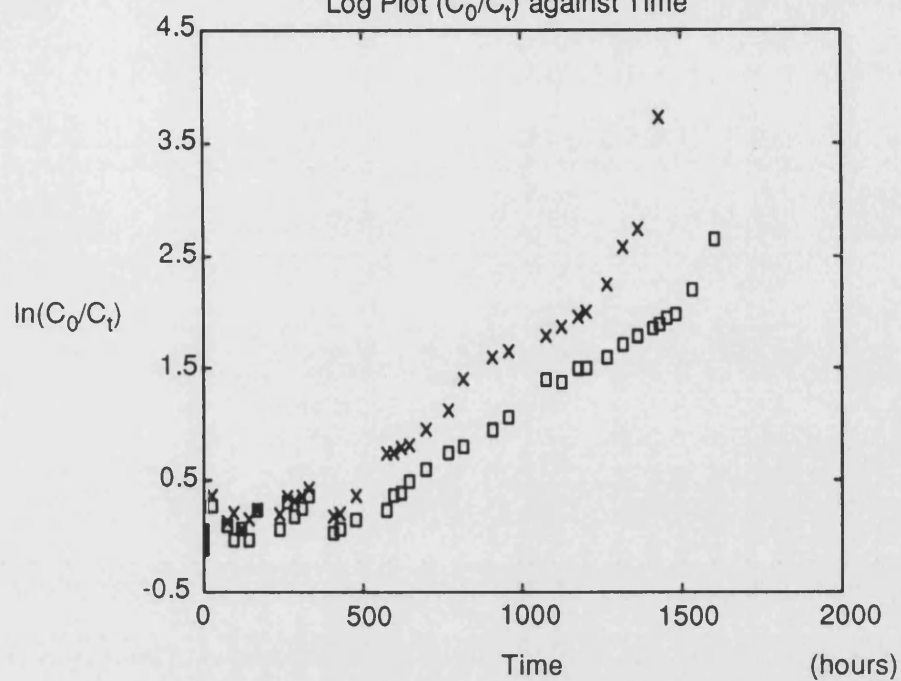
Degradation of 1,2,5-Trimethylpyrrole 750 ppm(N) at 52 °C

Log Plot ( $C_0/C_t$ ) against Time

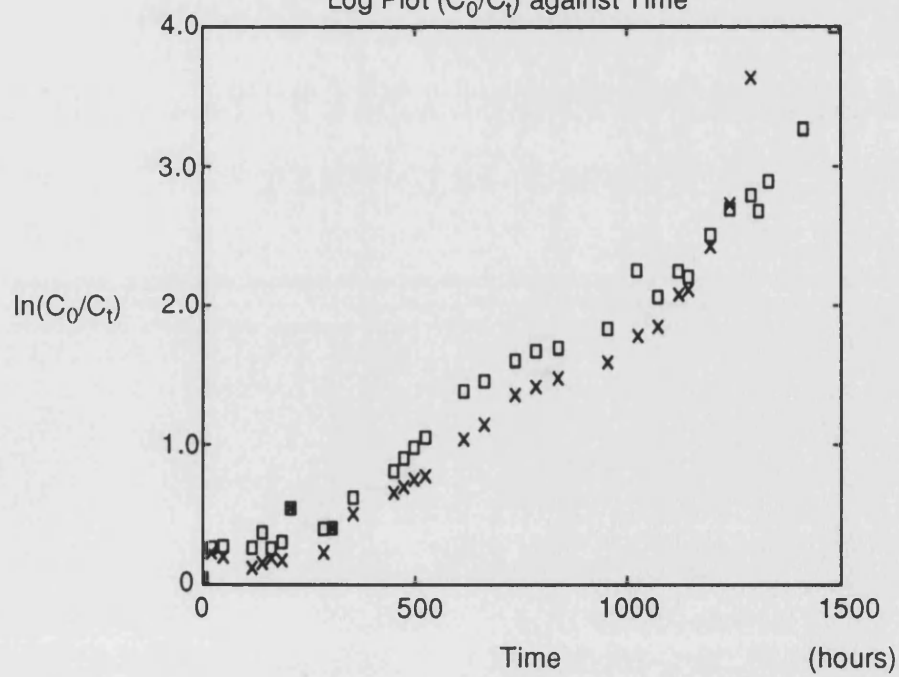
Degradation of 1,2,5-Trimethylpyrrole 350 ppm(N) at 52 °C

Log Plot ( $C_0/C_t$ ) against Time

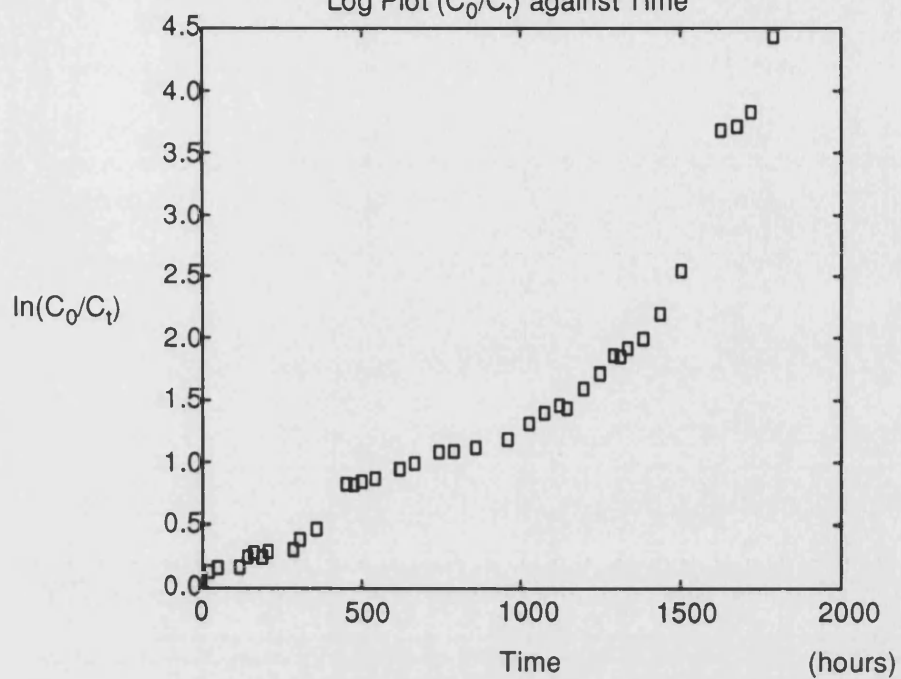
Degradation of 1,2,5-Trimethylpyrrole 1650 ppm(N) at 65 °C

Log Plot ( $C_0/C_t$ ) against Time

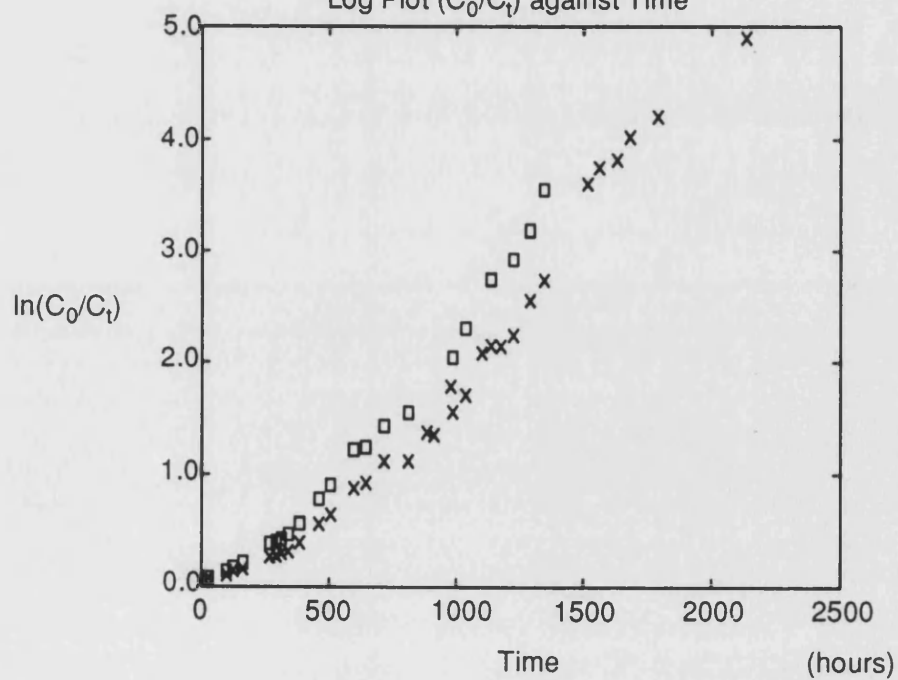
Degradation of 1,2,5-Trimethylpyrrole 1290 ppm(N) at 65 °C

Log Plot ( $C_0/C_t$ ) against Time

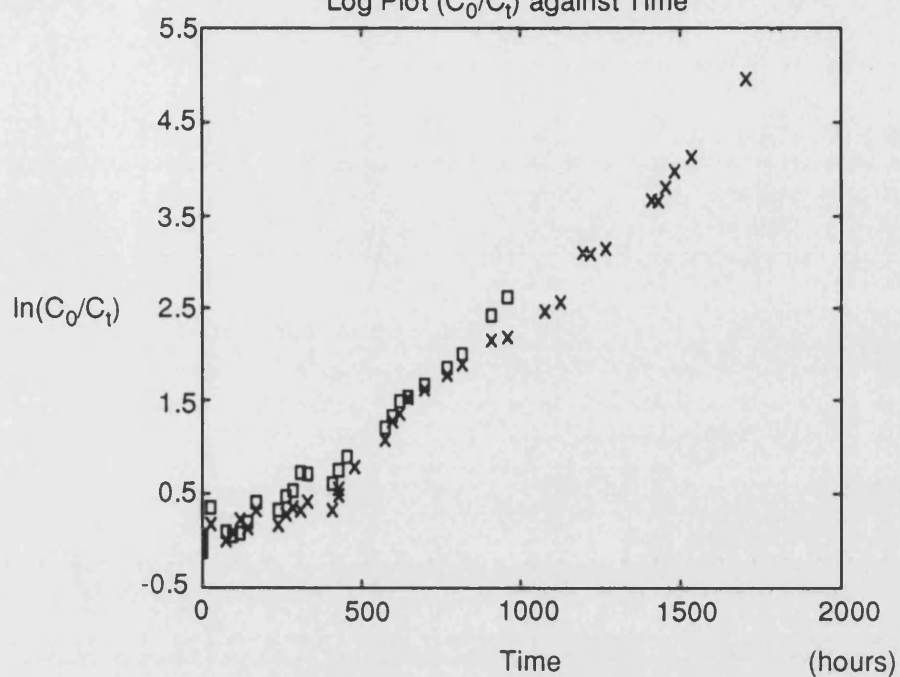
Degradation of 1,2,5-Trimethylpyrrole 750 ppm(N) at 65 °C

Log Plot ( $C_0/C_t$ ) against Time

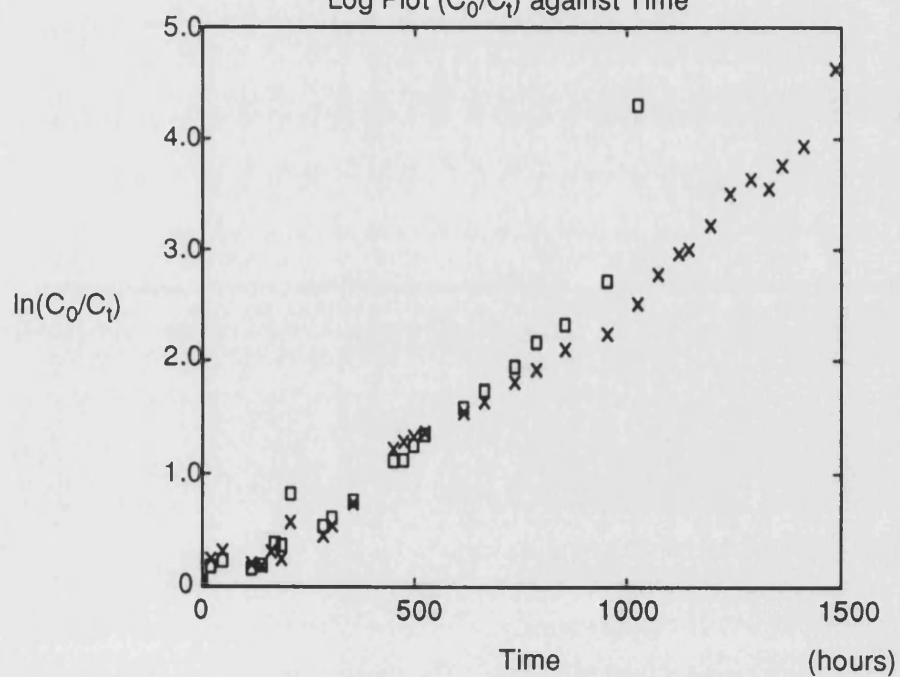
Degradation of 1,2,5-Trimethylpyrrole 350 ppm(N) at 65 °C

Log Plot ( $C_0/C_t$ ) against Time

## Degradation of 1,2,5-Trimethylpyrrole 1650 ppm(N) at 70 °C

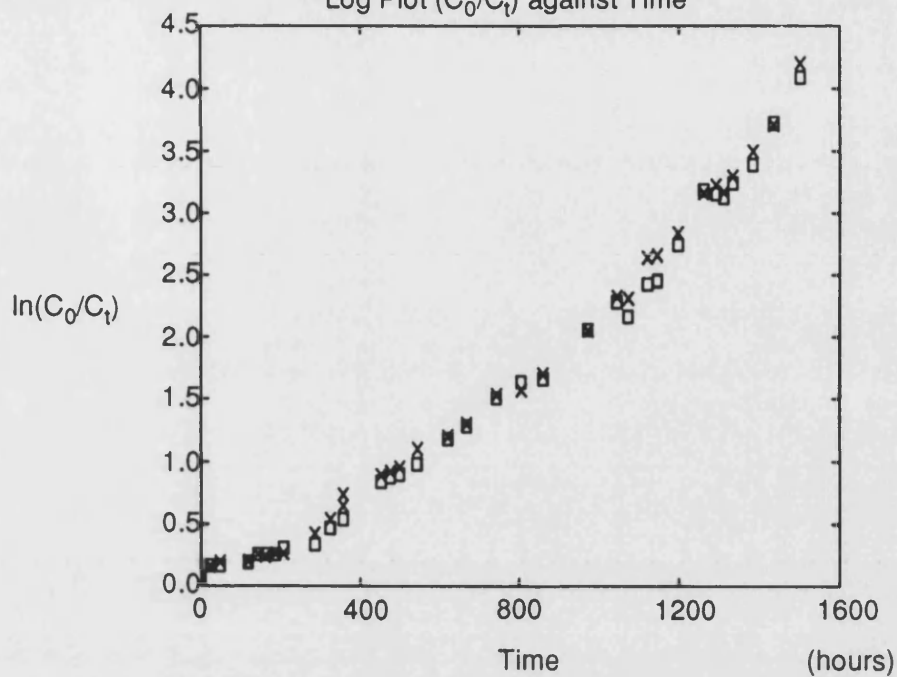
Log Plot ( $C_0/C_t$ ) against Time

## Degradation of 1,2,5-Trimethylpyrrole 1290 ppm(N) at 70 °C

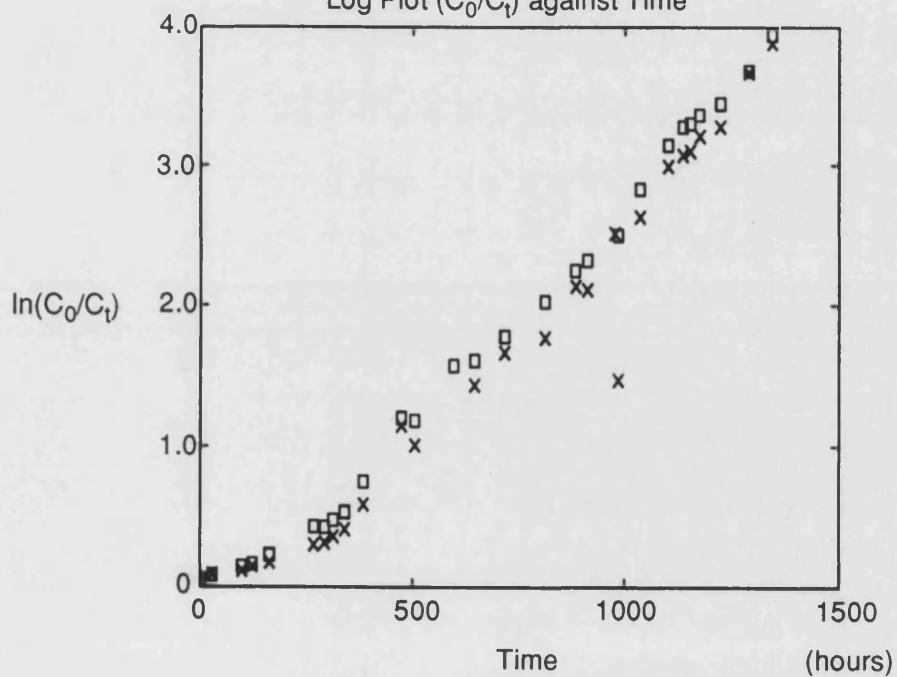
Log Plot ( $C_0/C_t$ ) against Time



## Degradation of 1,2,5-Trimethylpyrrole 750 ppm(N) at 70 °C

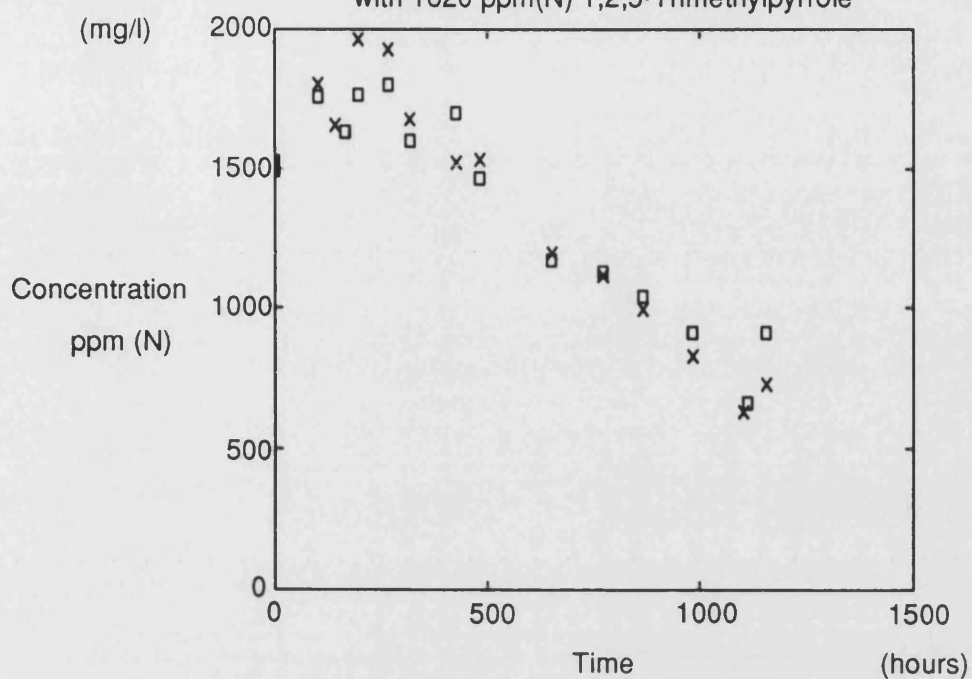
Log Plot ( $C_0/C_t$ ) against Time

## Degradation of 1,2,5-Trimethylpyrrole 350 ppm(N) at 70 °C

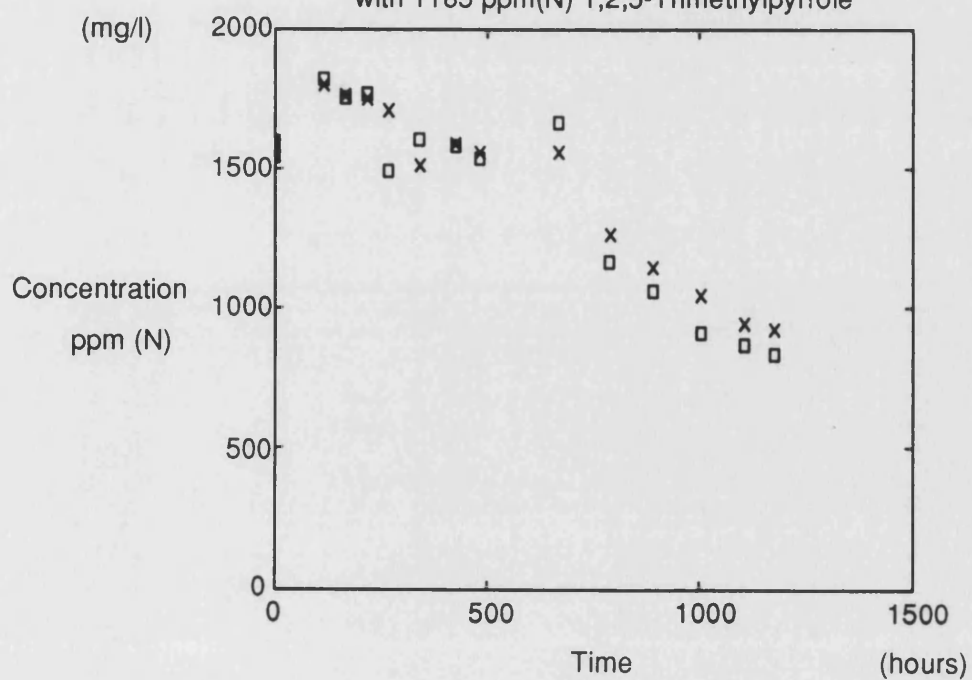
Log Plot ( $C_0/C_t$ ) against Time

## Data from the Combined Dopant System

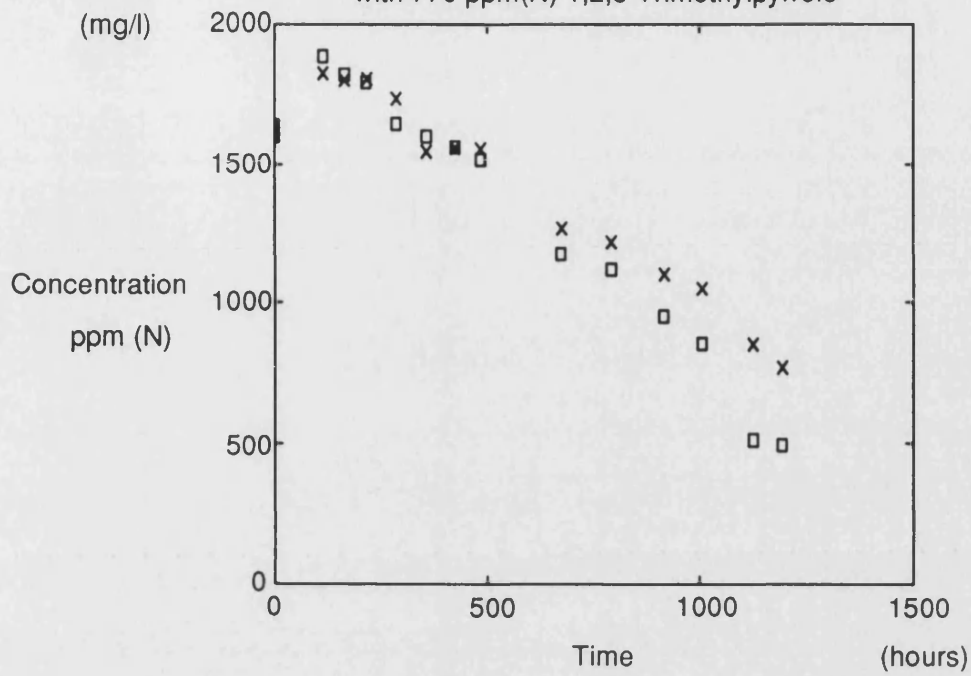
Degradation of 2,5-Dimethylpyrrole 1690 ppm(N) mg/l at 40 °C  
with 1620 ppm(N) 1,2,5-Trimethylpyrrole



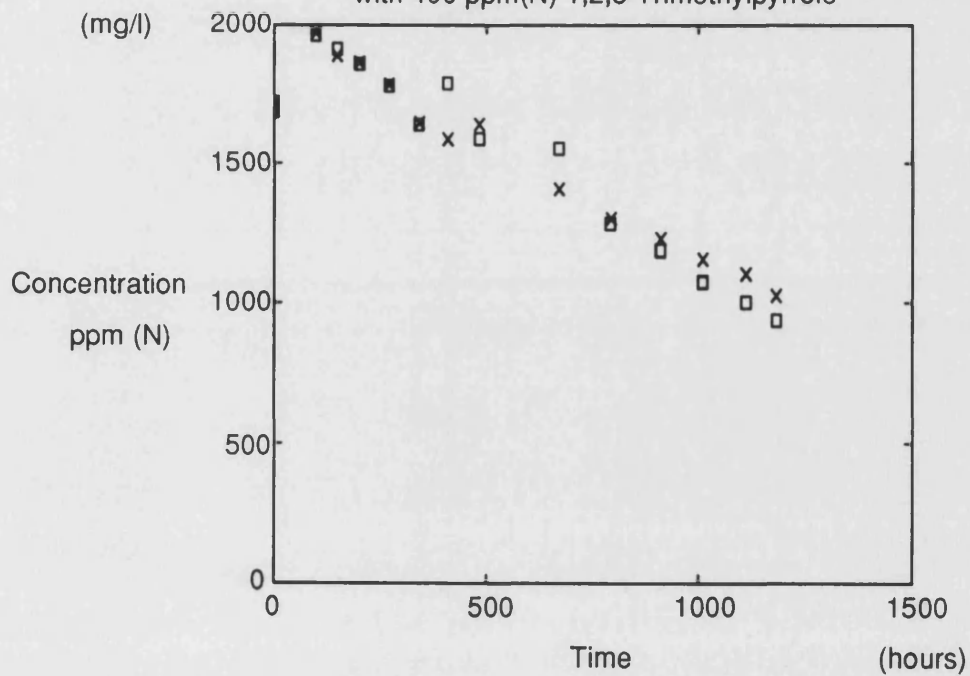
Degradation of 2,5-Dimethylpyrrole 1680 ppm(N) mg/l at 40 °C  
with 1185 ppm(N) 1,2,5-Trimethylpyrrole



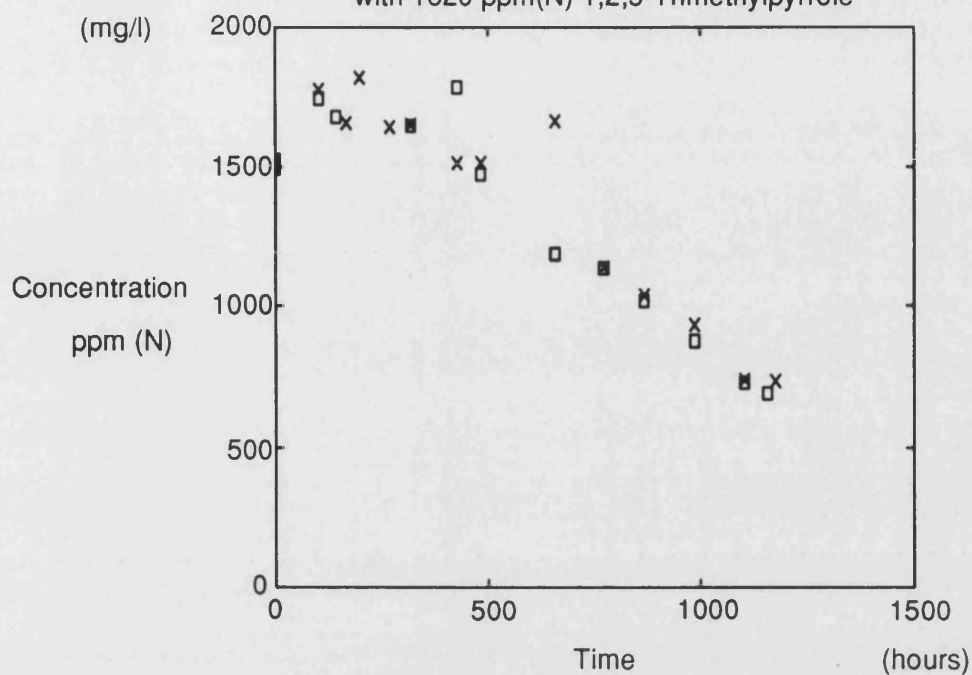
Degradation of 2,5-Dimethylpyrrole 1620 ppm(N) mg/l at 40 °C  
with 770 ppm(N) 1,2,5-Trimethylpyrrole



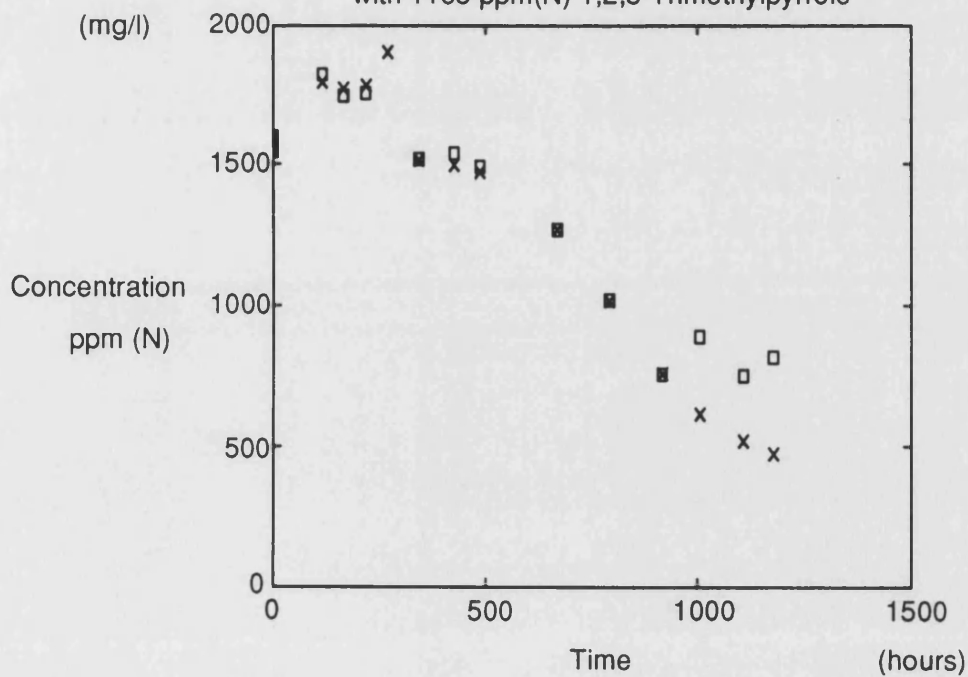
Degradation of 2,5-Dimethylpyrrole 1660 ppm(N) mg/l at 40 °C  
with 400 ppm(N) 1,2,5-Trimethylpyrrole



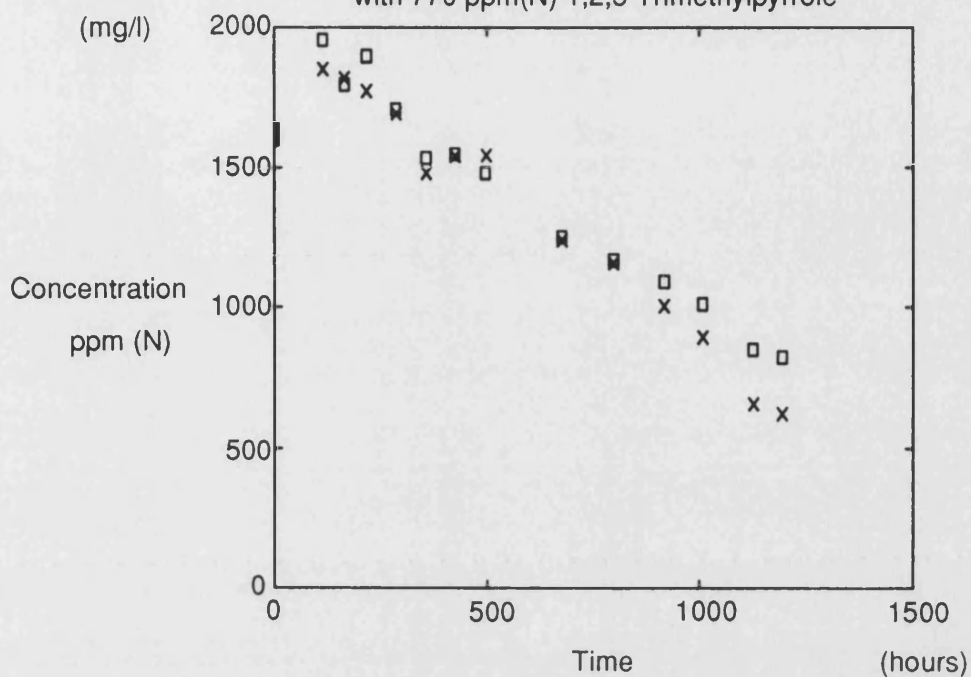
Degradation of 2,5-Dimethylpyrrole 1690 ppm(N) mg/l at 52 °C  
with 1620 ppm(N) 1,2,5-Trimethylpyrrole



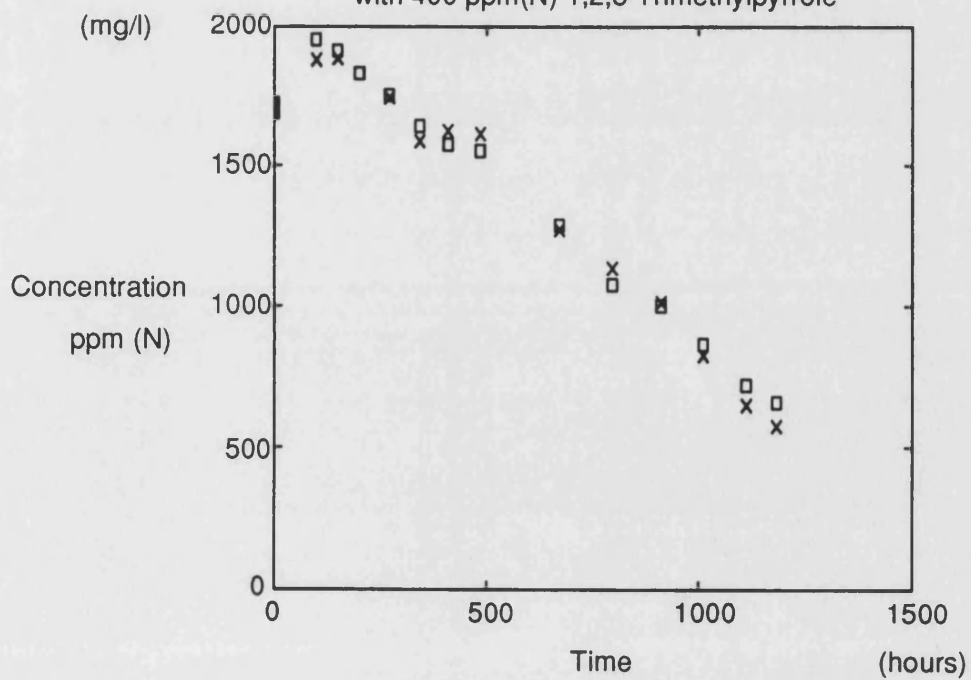
Degradation of 2,5-Dimethylpyrrole 1680 ppm(N) mg/l at 52 °C  
with 1185 ppm(N) 1,2,5-Trimethylpyrrole



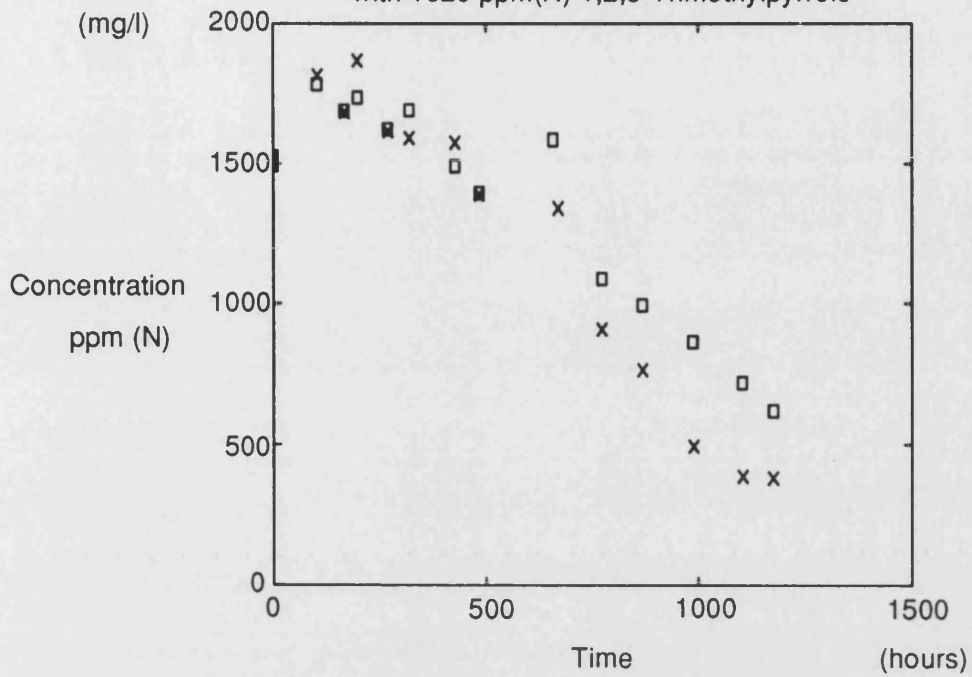
Degradation of 2,5-Dimethylpyrrole 1620 ppm(N) mg/l at 52 °C  
with 770 ppm(N) 1,2,5-Trimethylpyrrole



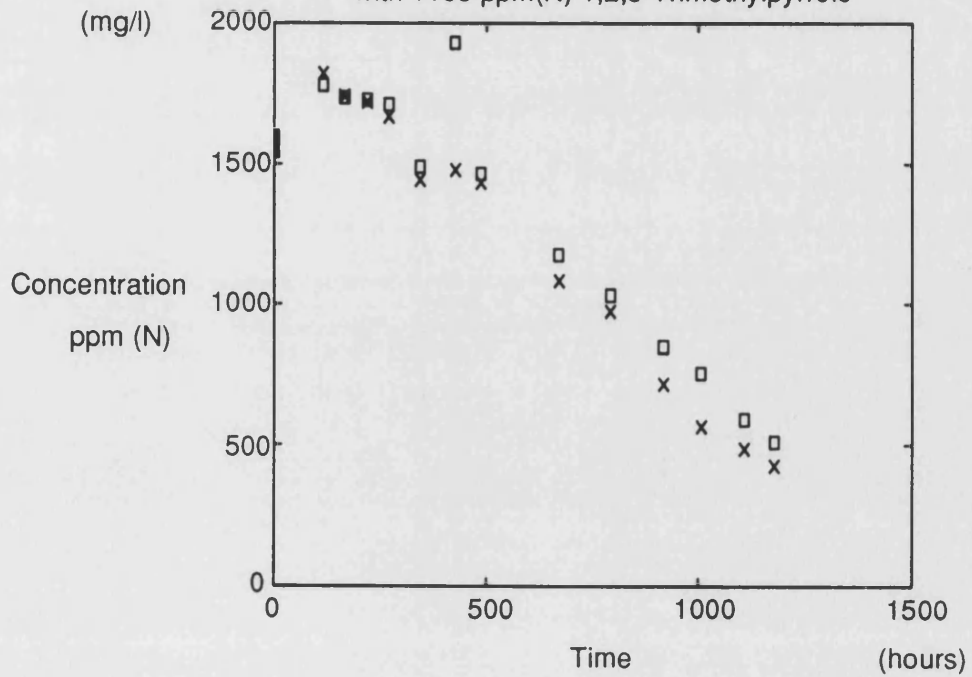
Degradation of 2,5-Dimethylpyrrole 1660 ppm(N) mg/l at 52 °C  
with 400 ppm(N) 1,2,5-Trimethylpyrrole



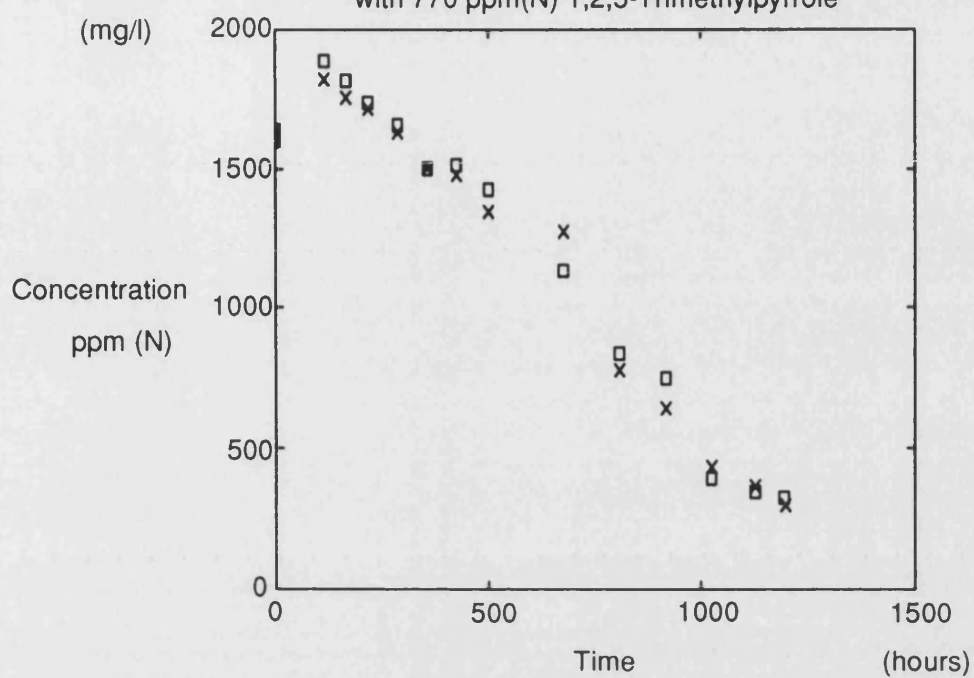
Degradation of 2,5-Dimethylpyrrole 1690 ppm(N) mg/l at 65 °C  
with 1620 ppm(N) 1,2,5-Trimethylpyrrole



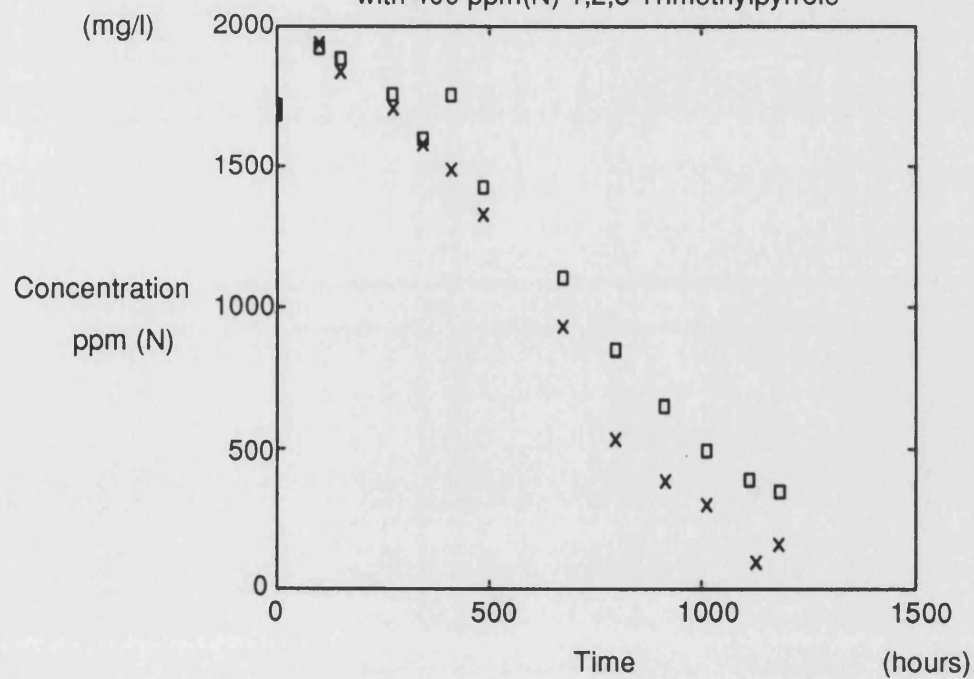
Degradation of 2,5-Dimethylpyrrole 1680 ppm(N) mg/l at 65 °C  
with 1185 ppm(N) 1,2,5-Trimethylpyrrole



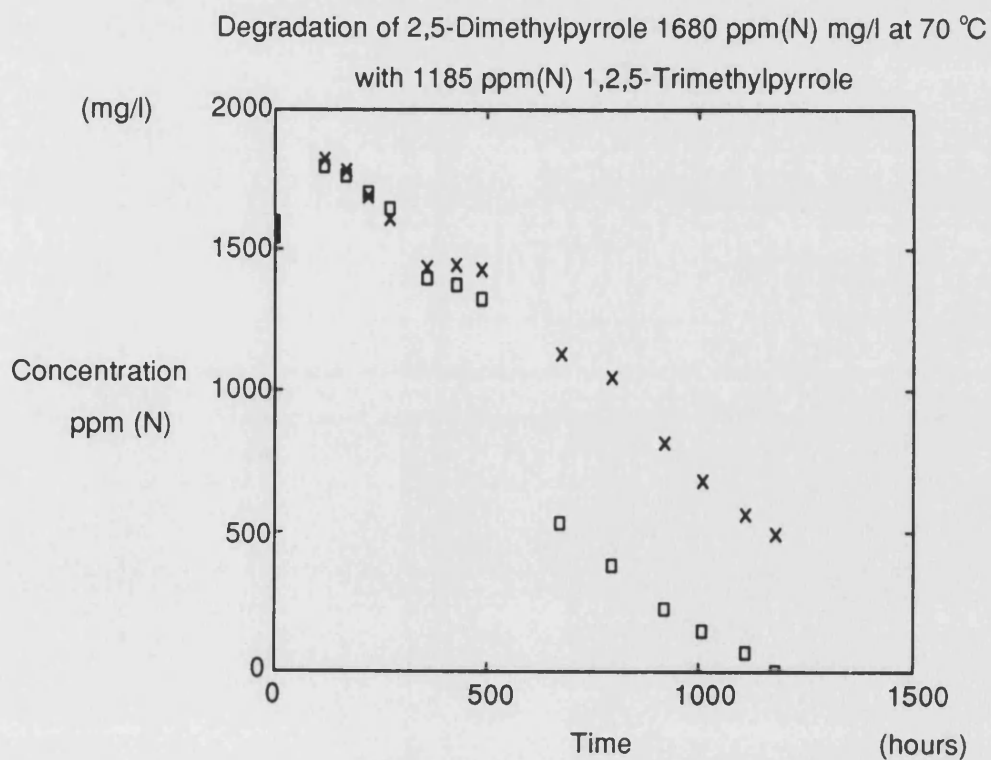
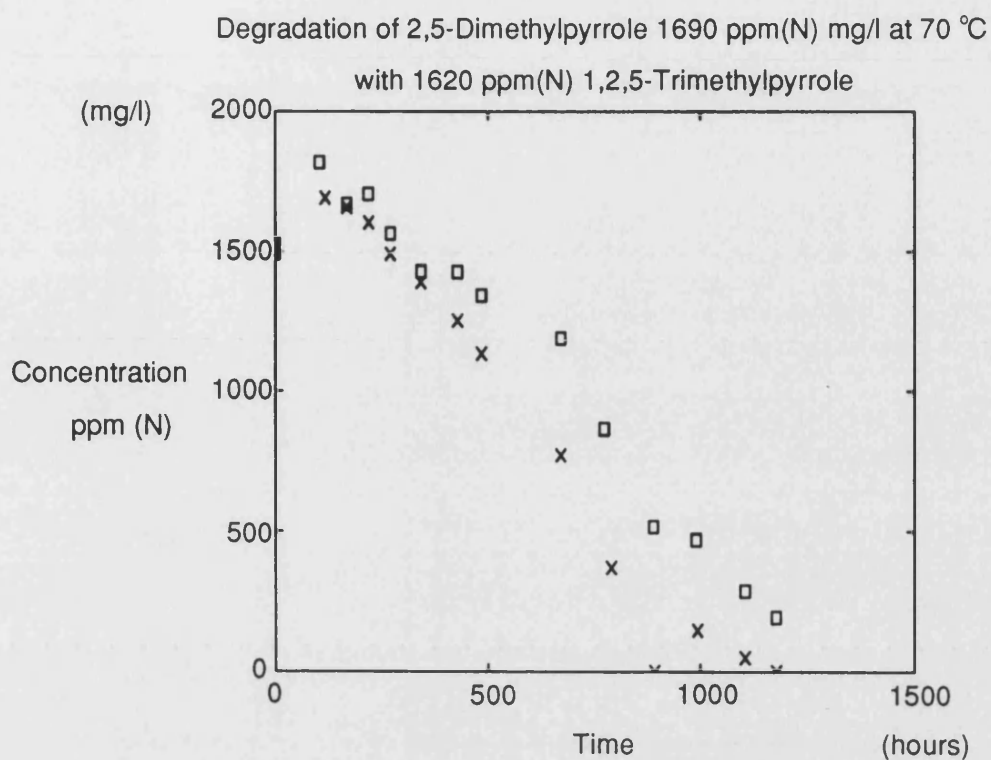
Degradation of 2,5-Dimethylpyrrole 1620 ppm(N) mg/l at 65 °C  
with 770 ppm(N) 1,2,5-Trimethylpyrrole



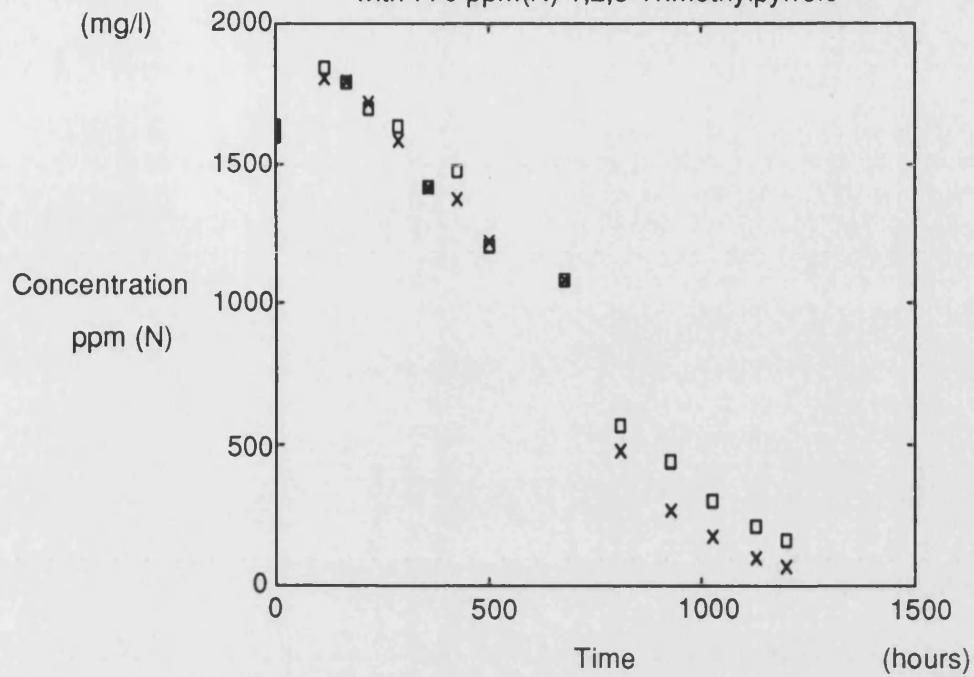
Degradation of 2,5-Dimethylpyrrole 1660 ppm(N) mg/l at 65 °C  
with 400 ppm(N) 1,2,5-Trimethylpyrrole



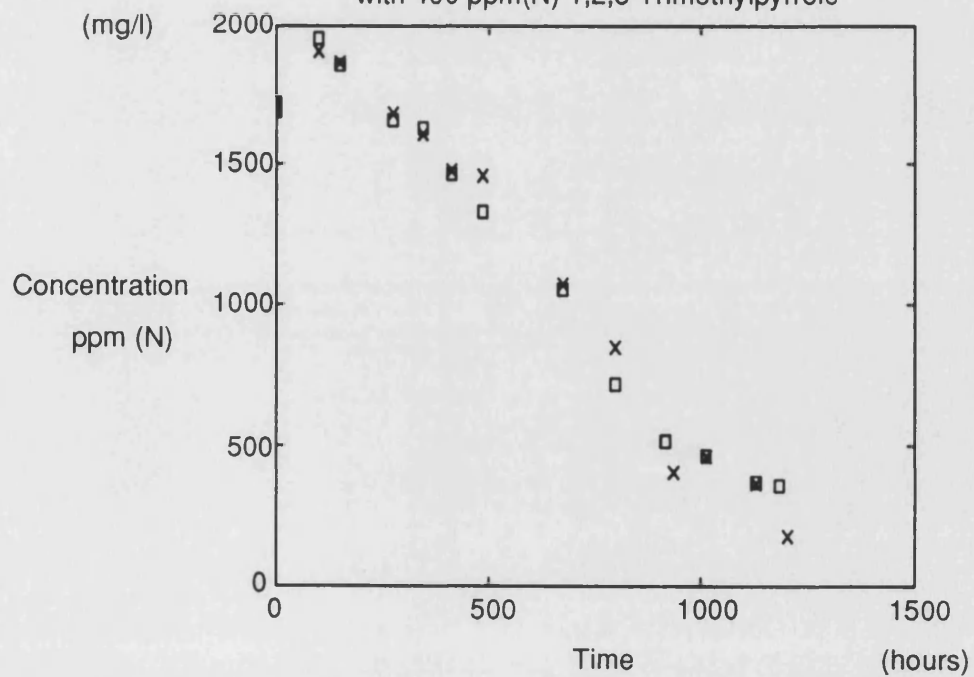




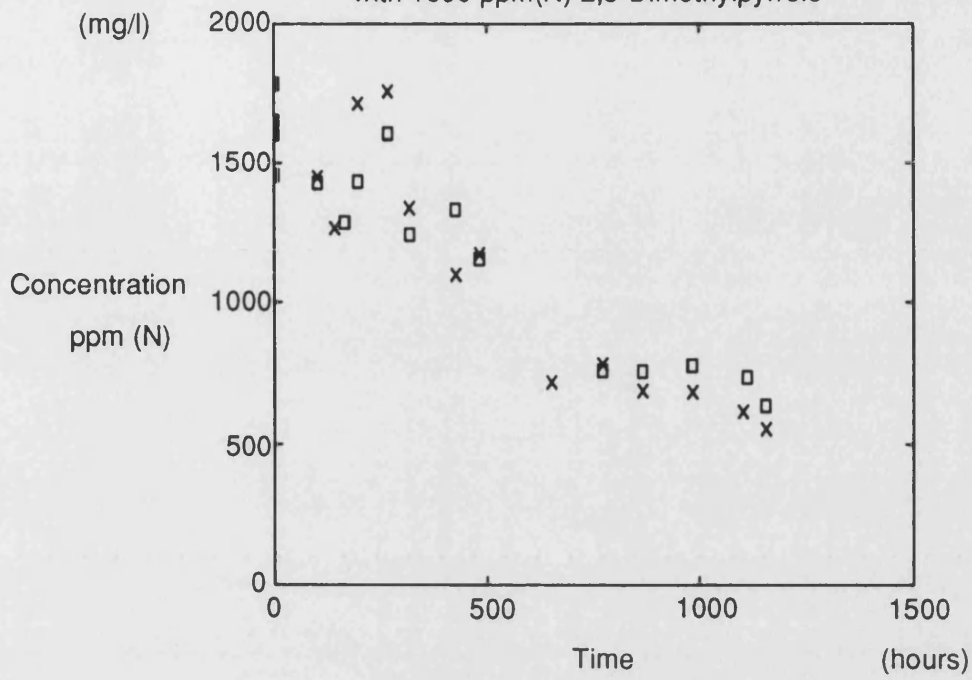
Degradation of 2,5-Dimethylpyrrole 1620 ppm(N) mg/l at 70 °C  
with 770 ppm(N) 1,2,5-Trimethylpyrrole



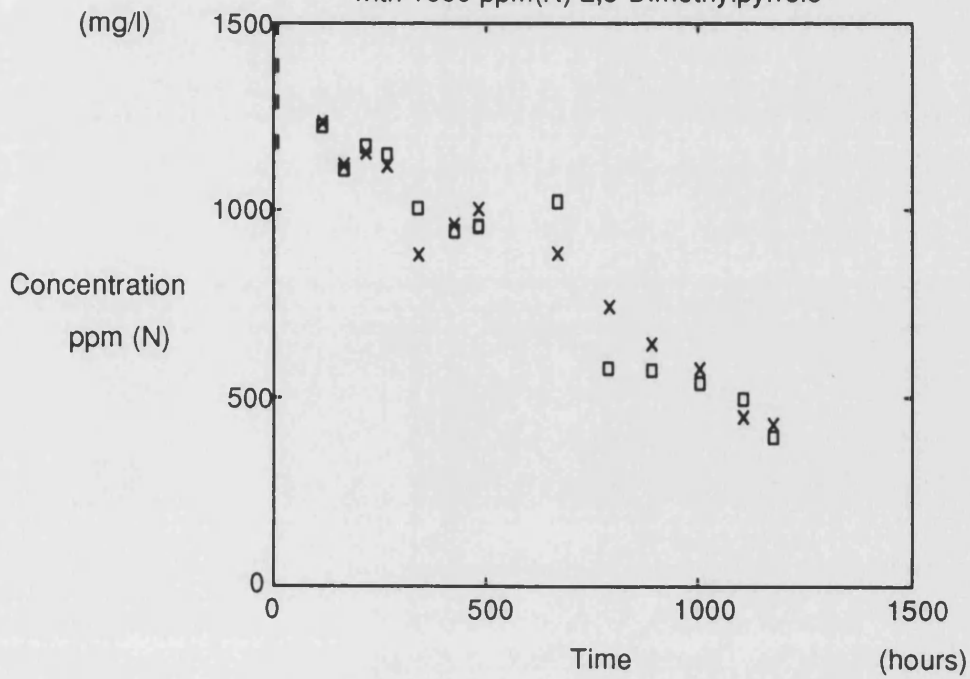
Degradation of 2,5-Dimethylpyrrole 1660 ppm(N) mg/l at 70 °C  
with 400 ppm(N) 1,2,5-Trimethylpyrrole



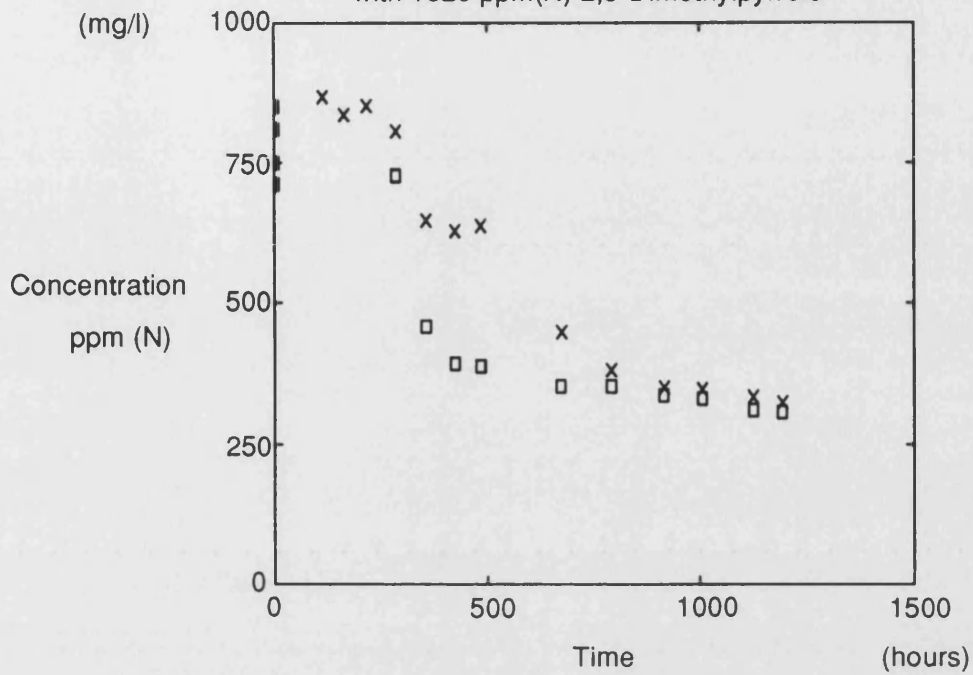
Degradation of 1,2,5-Trimethylpyrrole 1620 ppm(N) mg/l at 40 °C  
with 1690 ppm(N) 2,5-Dimethylpyrrole



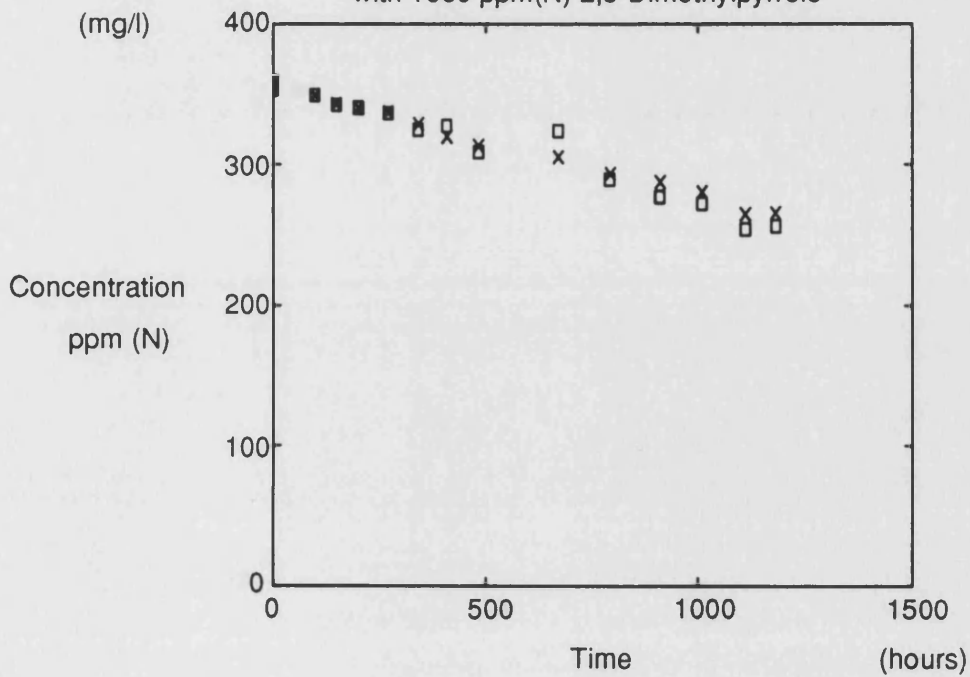
Degradation of 1,2,5-Trimethylpyrrole 1185 ppm(N) mg/l at 40 °C  
with 1680 ppm(N) 2,5-Dimethylpyrrole



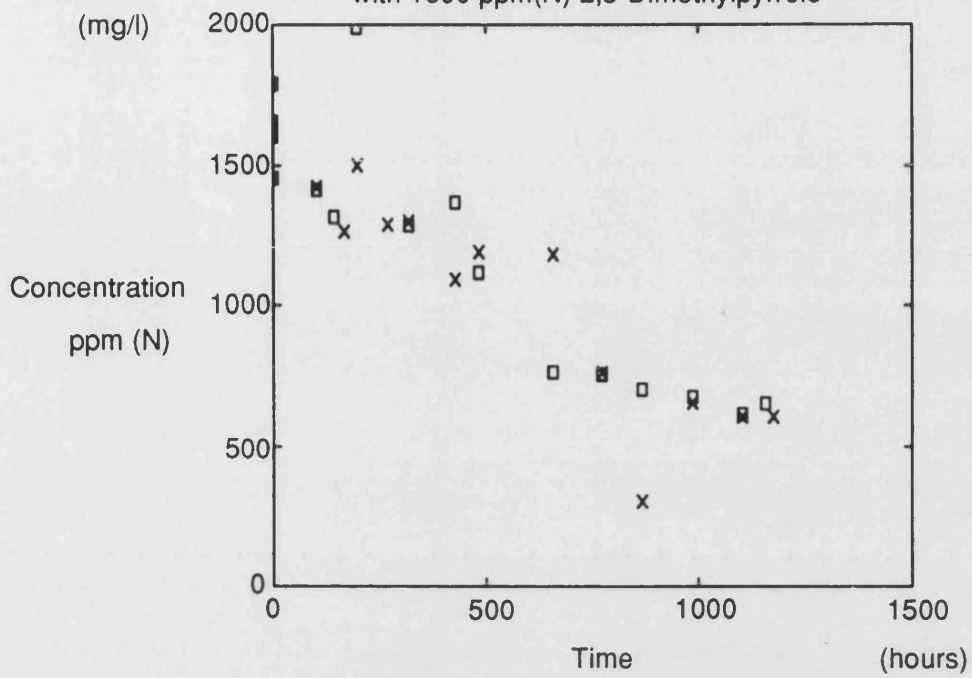
Degradation of 1,2,5-Trimethylpyrrole 770 ppm(N) mg/l at 40 °C  
with 1620 ppm(N) 2,5-Dimethylpyrrole



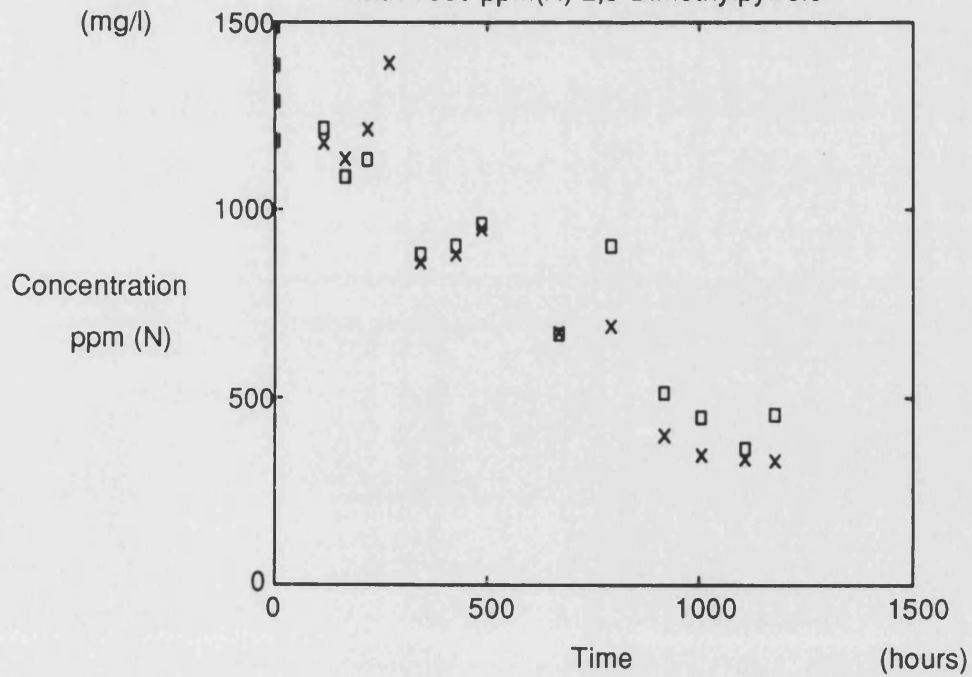
Degradation of 1,2,5-Trimethylpyrrole 400 ppm(N) mg/l at 40 °C  
with 1660 ppm(N) 2,5-Dimethylpyrrole



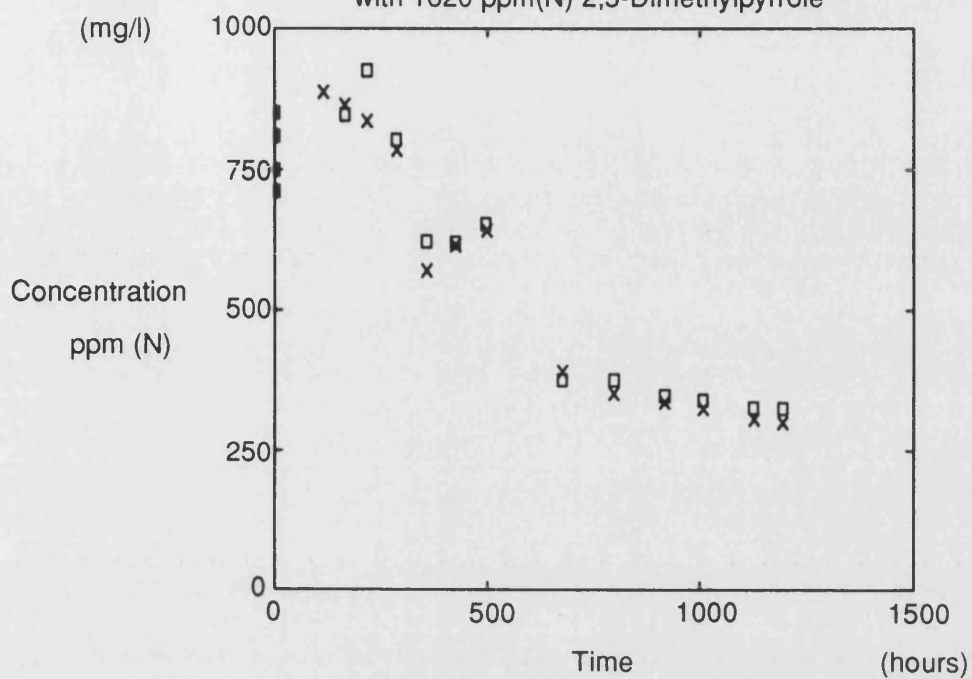
Degradation of 1,2,5-Trimethylpyrrole 1620 ppm(N) mg/l at 52 °C  
with 1690 ppm(N) 2,5-Dimethylpyrrole



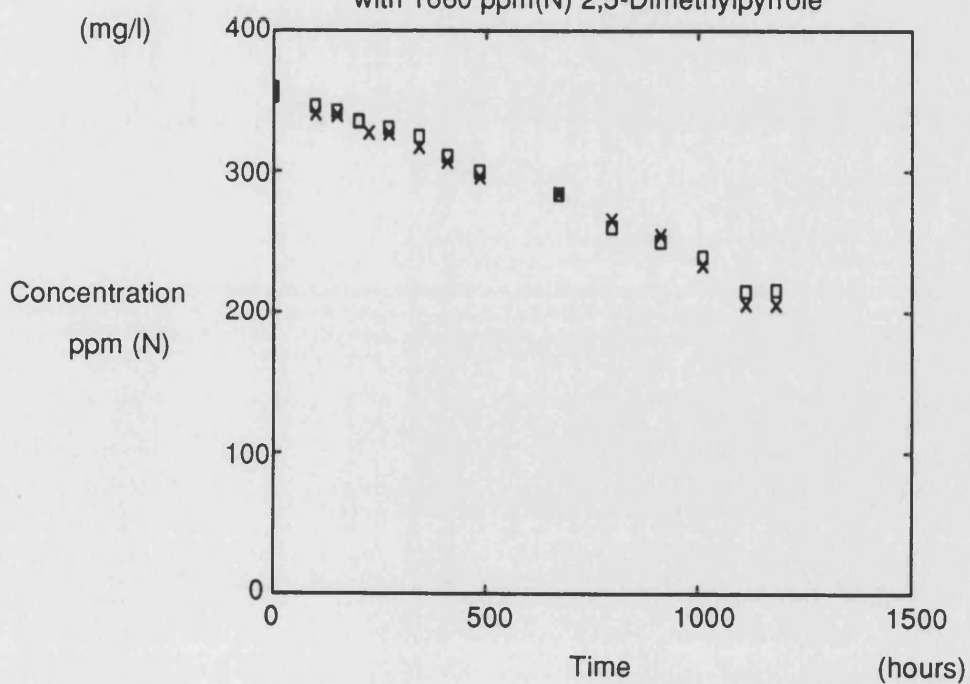
Degradation of 1,2,5-Trimethylpyrrole 1185 ppm(N) mg/l at 52 °C  
with 1680 ppm(N) 2,5-Dimethylpyrrole



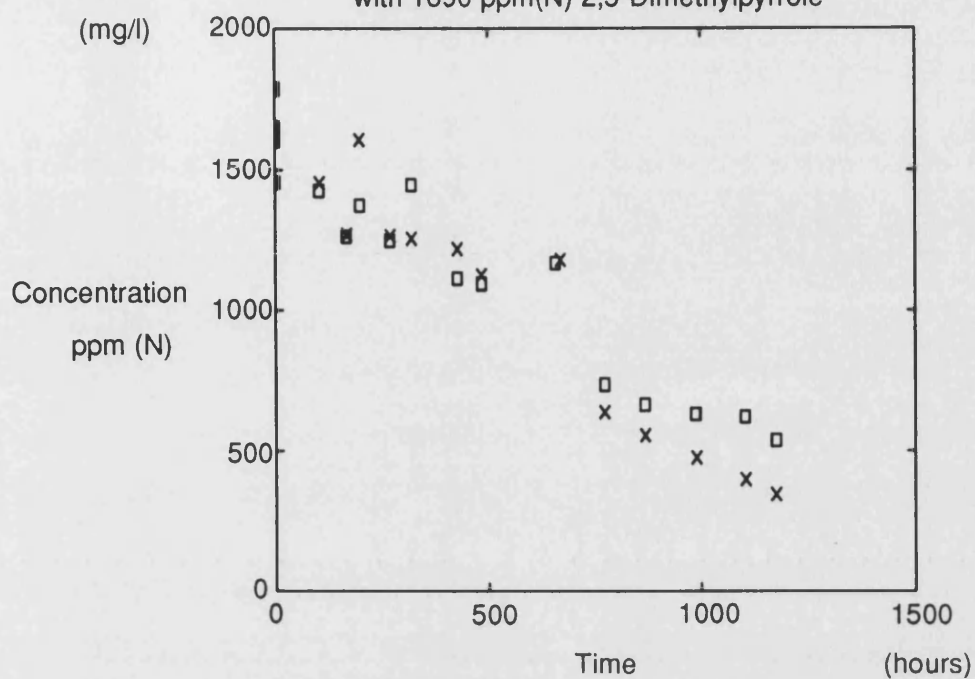
Degradation of 1,2,5-Trimethylpyrrole 770 ppm(N) mg/l at 52 °C  
with 1620 ppm(N) 2,5-Dimethylpyrrole



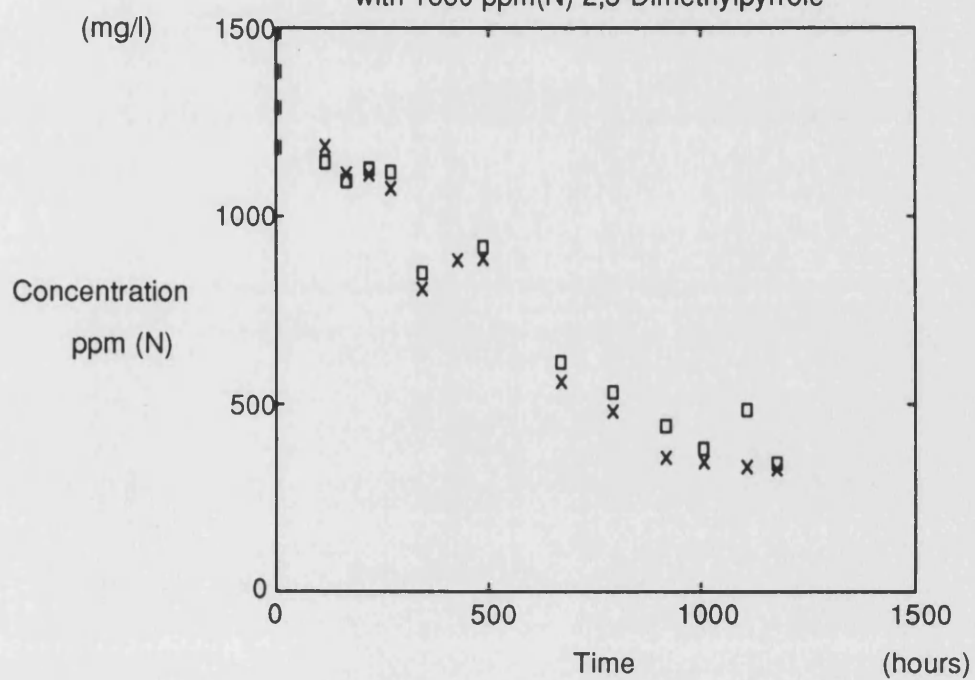
Degradation of 1,2,5-Trimethylpyrrole 400 ppm(N) mg/l at 52 °C  
with 1660 ppm(N) 2,5-Dimethylpyrrole



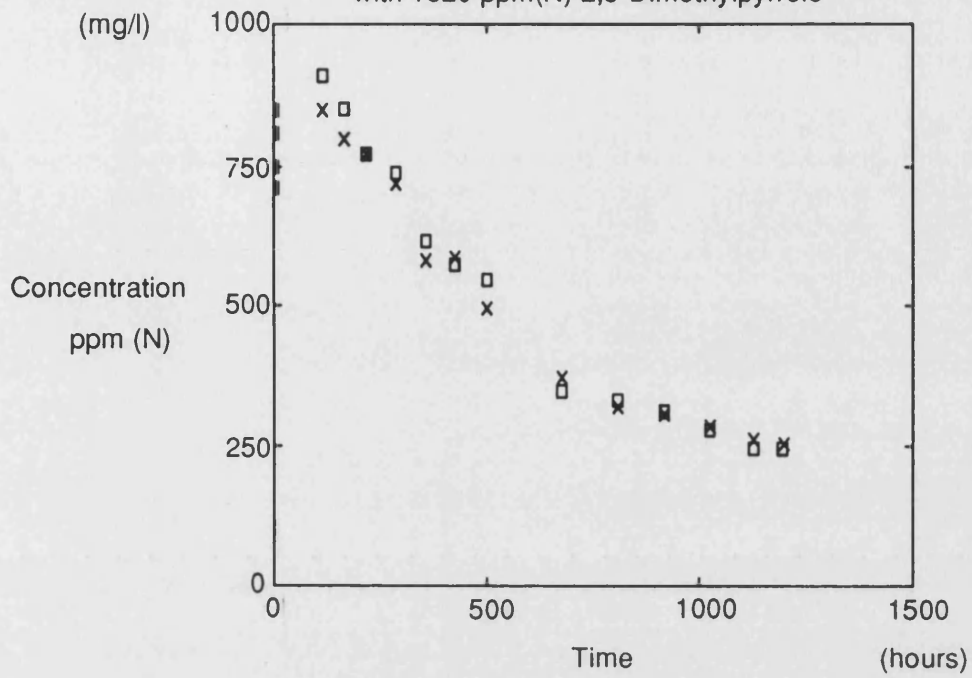
Degradation of 1,2,5-Trimethylpyrrole 1620 ppm(N) mg/l at 65 °C  
with 1690 ppm(N) 2,5-Dimethylpyrrole



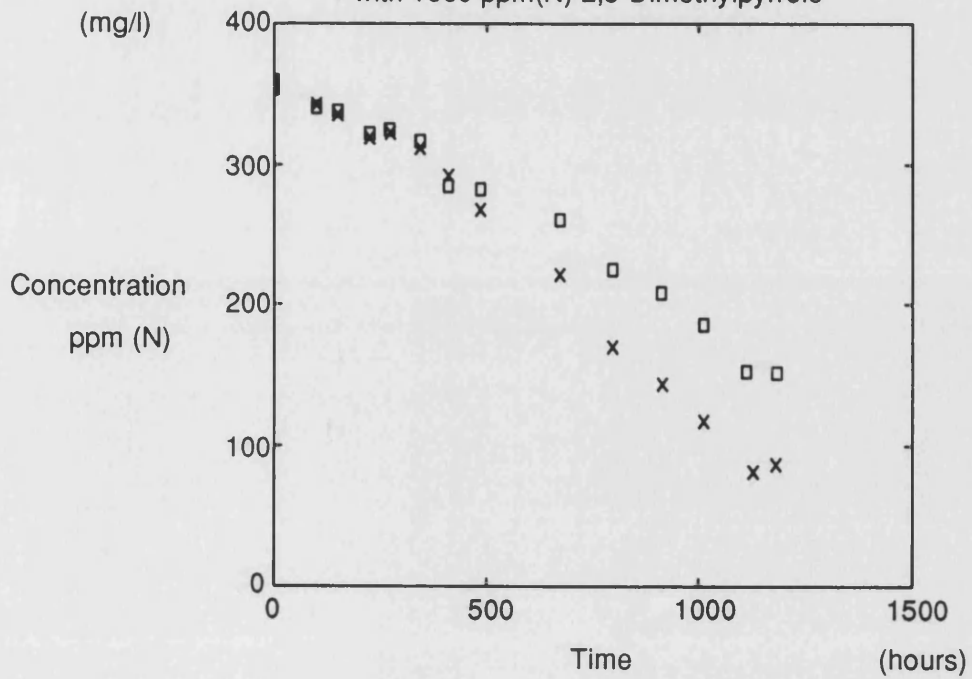
Degradation of 1,2,5-Trimethylpyrrole 1185 ppm(N) mg/l at 65 °C  
with 1680 ppm(N) 2,5-Dimethylpyrrole



Degradation of 1,2,5-Trimethylpyrrole 770 ppm(N) mg/l at 65 °C  
with 1620 ppm(N) 2,5-Dimethylpyrrole

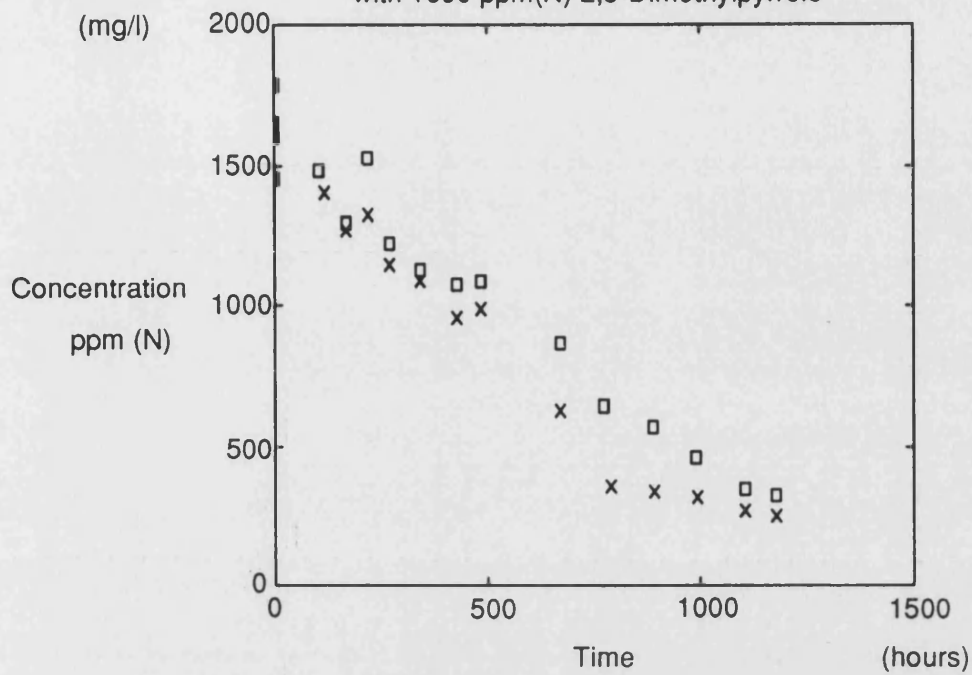


Degradation of 1,2,5-Trimethylpyrrole 400 ppm(N) mg/l at 65 °C  
with 1660 ppm(N) 2,5-Dimethylpyrrole

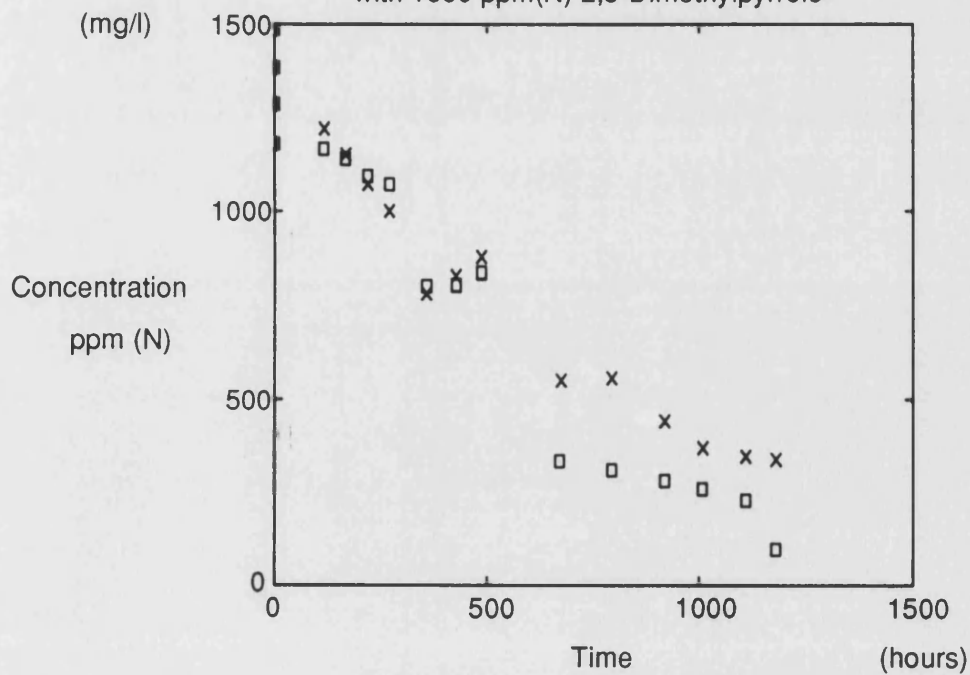




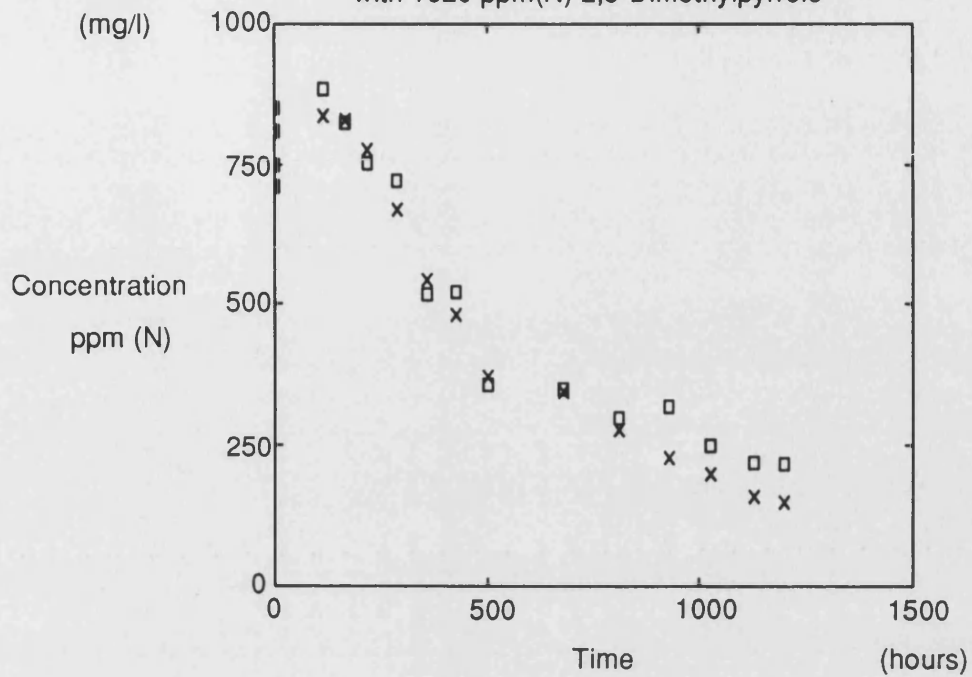
Degradation of 1,2,5-Trimethylpyrrole 1620 ppm(N) mg/l at 70 °C  
with 1690 ppm(N) 2,5-Dimethylpyrrole



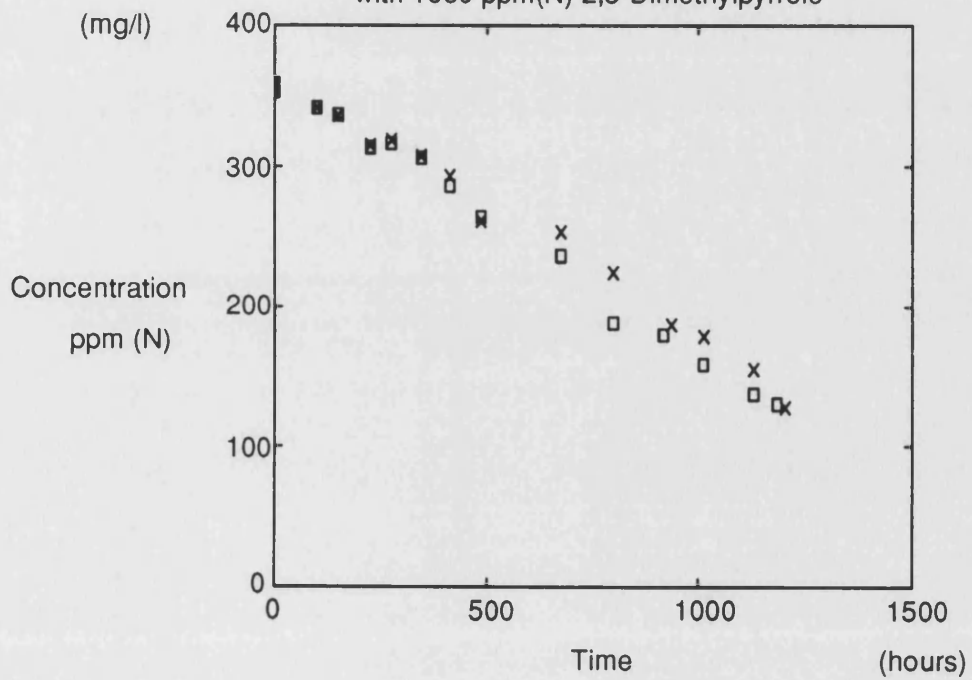
Degradation of 1,2,5-Trimethylpyrrole 1185 ppm(N) mg/l at 70 °C  
with 1680 ppm(N) 2,5-Dimethylpyrrole



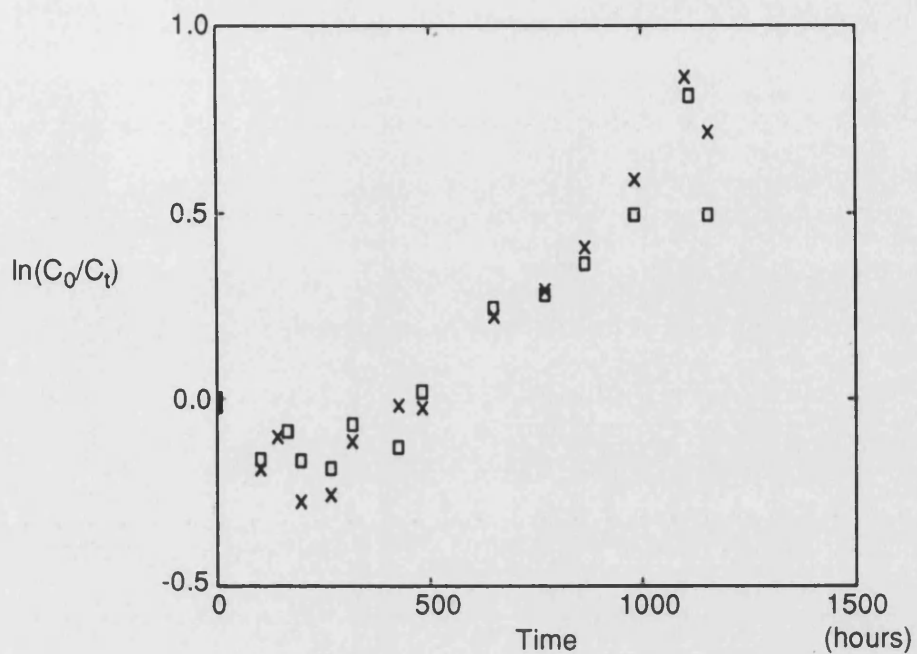
Degradation of 1,2,5-Trimethylpyrrole 770 ppm(N) mg/l at 70 °C  
with 1620 ppm(N) 2,5-Dimethylpyrrole



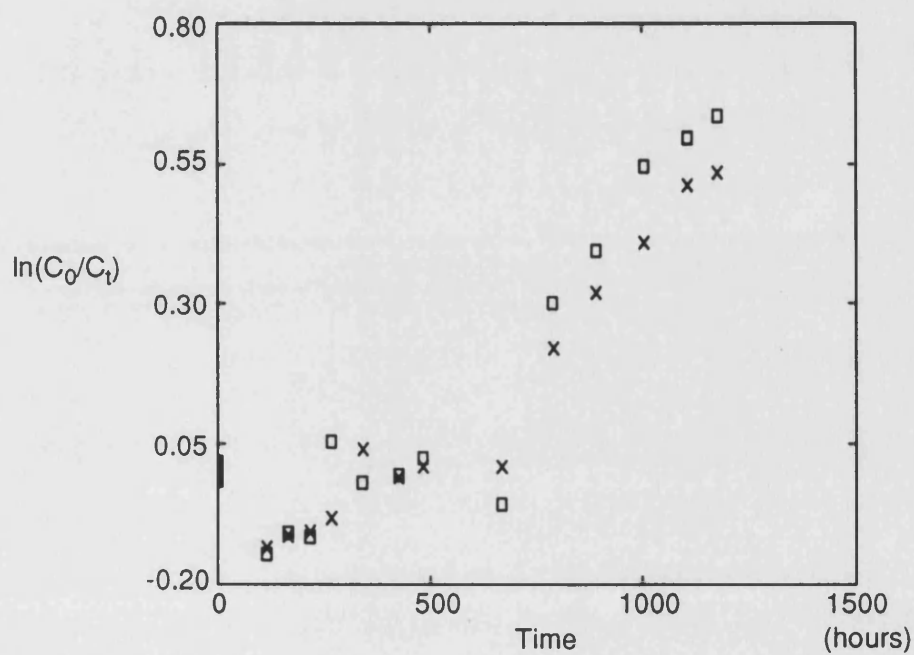
Degradation of 1,2,5-Trimethylpyrrole 400 ppm(N) mg/l at 70 °C  
with 1660 ppm(N) 2,5-Dimethylpyrrole



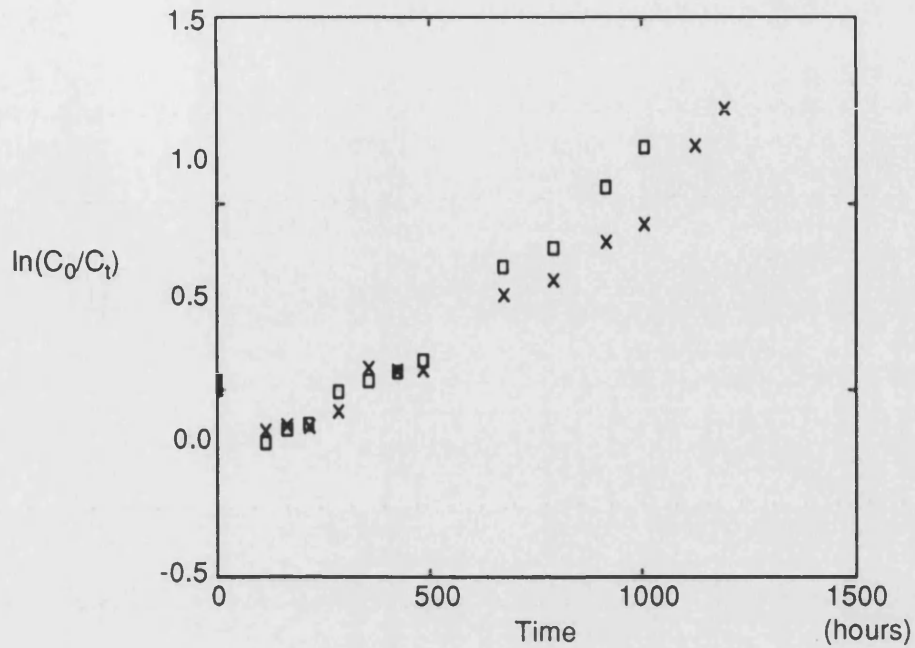
Degradation of 2,5-Dimethylpyrrole 1680 ppm(N) mg/l at 40 °C  
with 1620 ppm(N) 1,2,5-Trimethylpyrrole ( $\ln(C_0/C_t)$  against Time)



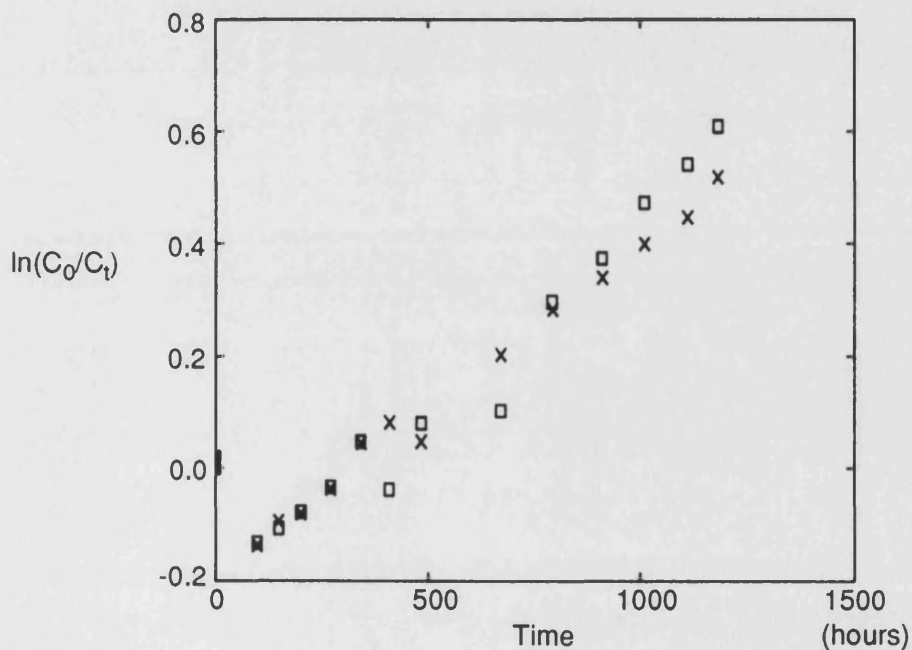
Degradation of 2,5-Dimethylpyrrole 1680 ppm(N) mg/l at 40 °C  
with 1190 ppm(N) 1,2,5-Trimethylpyrrole ( $\ln(C_0/C_t)$  against Time)



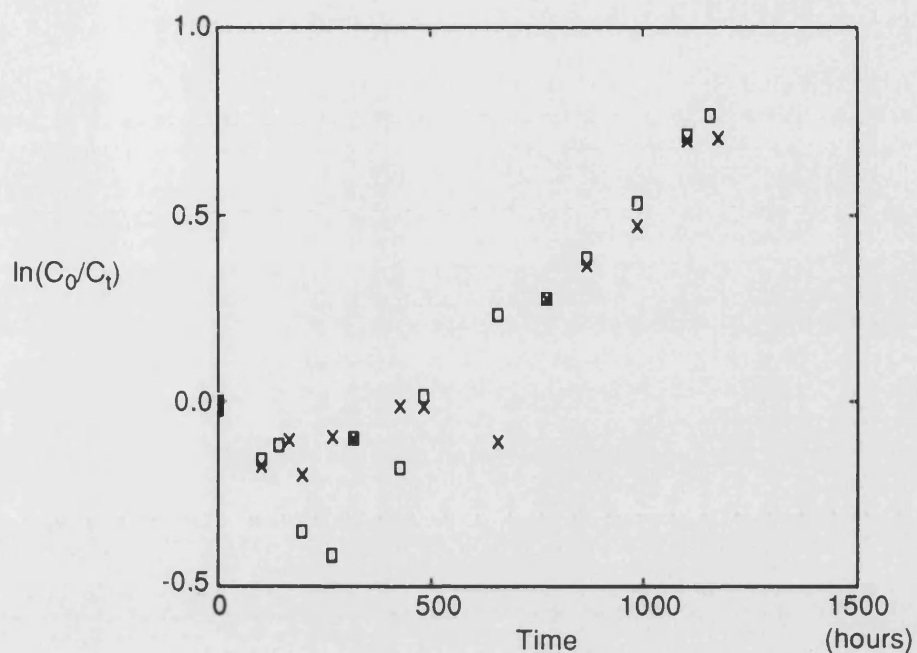
Degradation of 2,5-Dimethylpyrrole 1620 ppm(N) mg/l at 40 °C  
with 770 ppm(N) 1,2,5-Trimethylpyrrole ( $\ln(C_0/C_t)$  against Time)



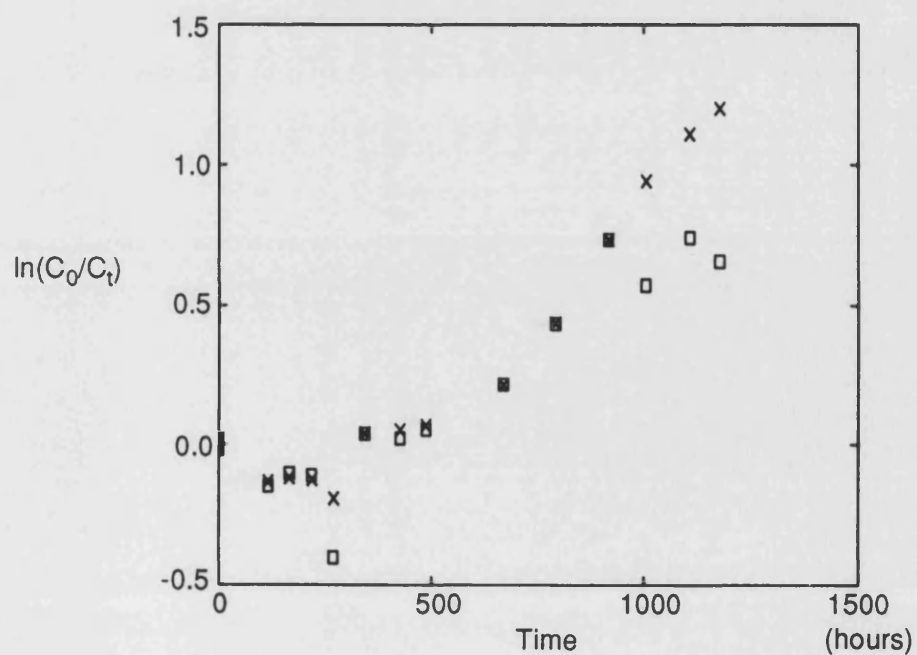
Degradation of 2,5-Dimethylpyrrole 1660 ppm(N) mg/l at 40 °C  
with 400 ppm(N) 1,2,5-Trimethylpyrrole ( $\ln(C_0/C_t)$  against Time)



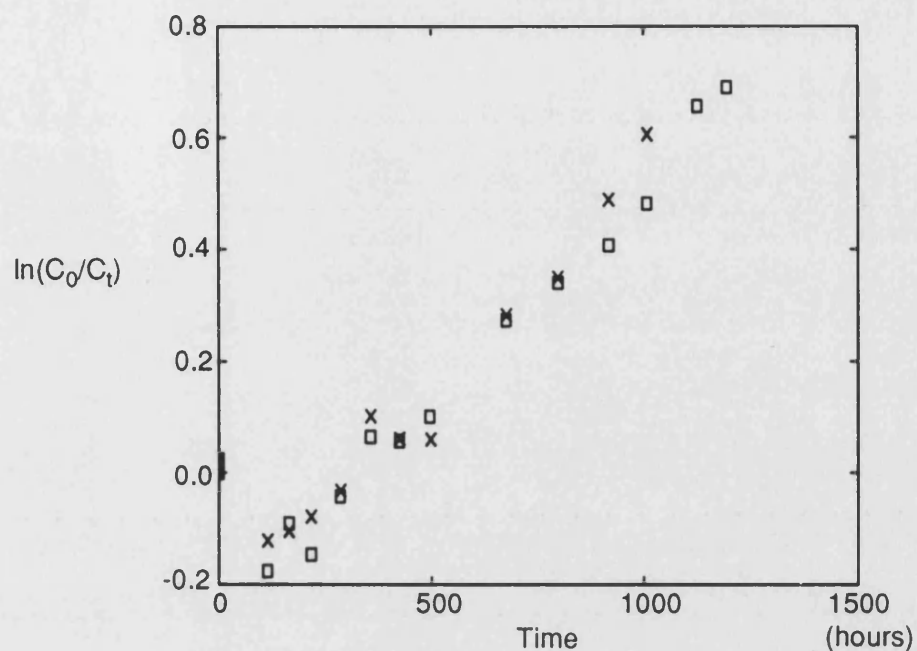
Degradation of 2,5-Dimethylpyrrole 1680 ppm(N) mg/l at 52 °C  
with 1620 ppm(N) 1,2,5-Trimethylpyrrole ( $\ln(C_0/C_t)$  against Time)



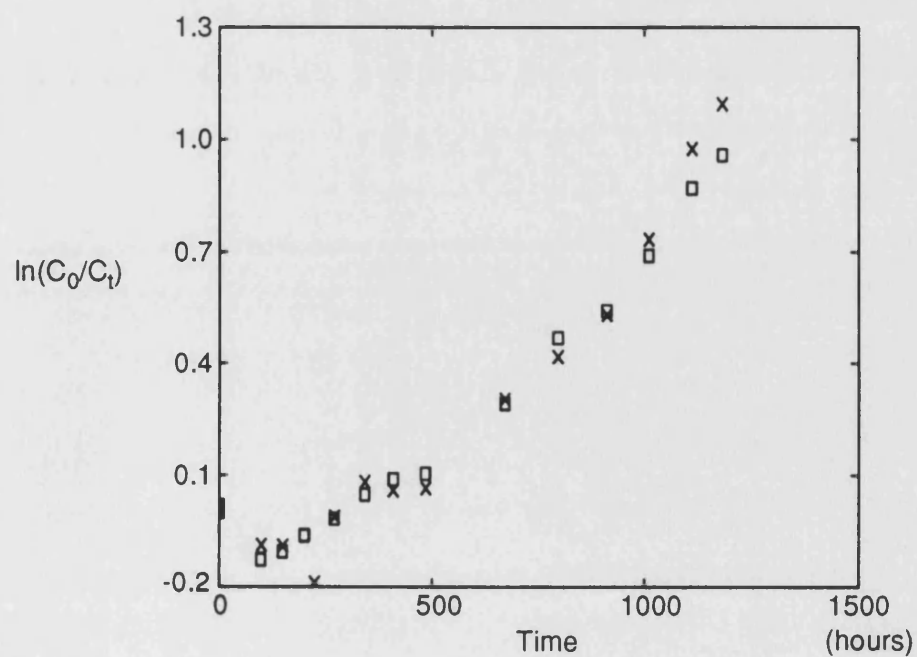
Degradation of 2,5-Dimethylpyrrole 1680 ppm(N) mg/l at 52 °C  
with 1190 ppm(N) 1,2,5-Trimethylpyrrole ( $\ln(C_0/C_t)$  against Time)



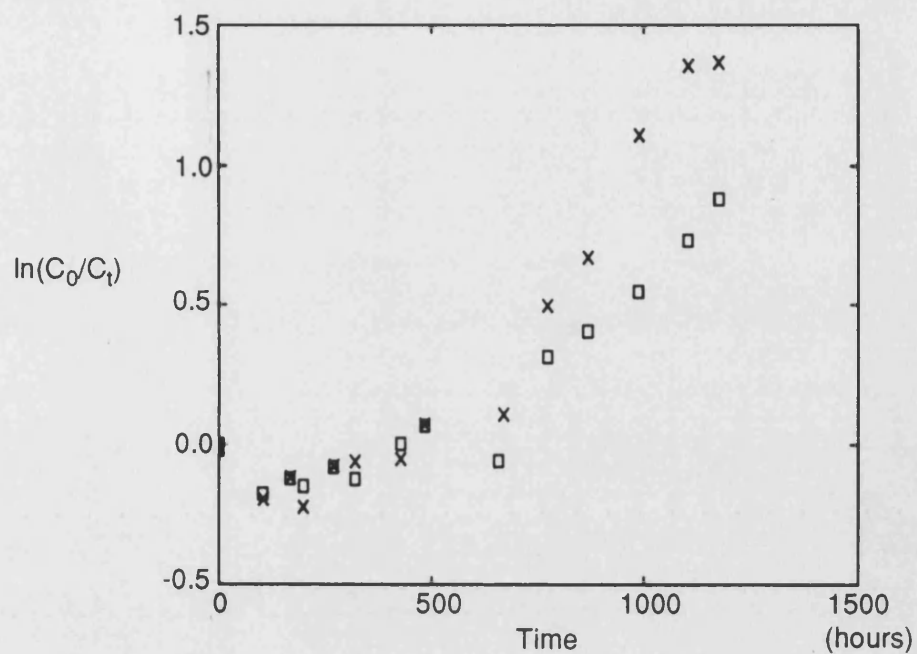
Degradation of 2,5-Dimethylpyrrole 1620 ppm(N) mg/l at 52 °C  
with 770 ppm(N) 1,2,5-Trimethylpyrrole ( $\ln(C_0/C_t)$  against Time)



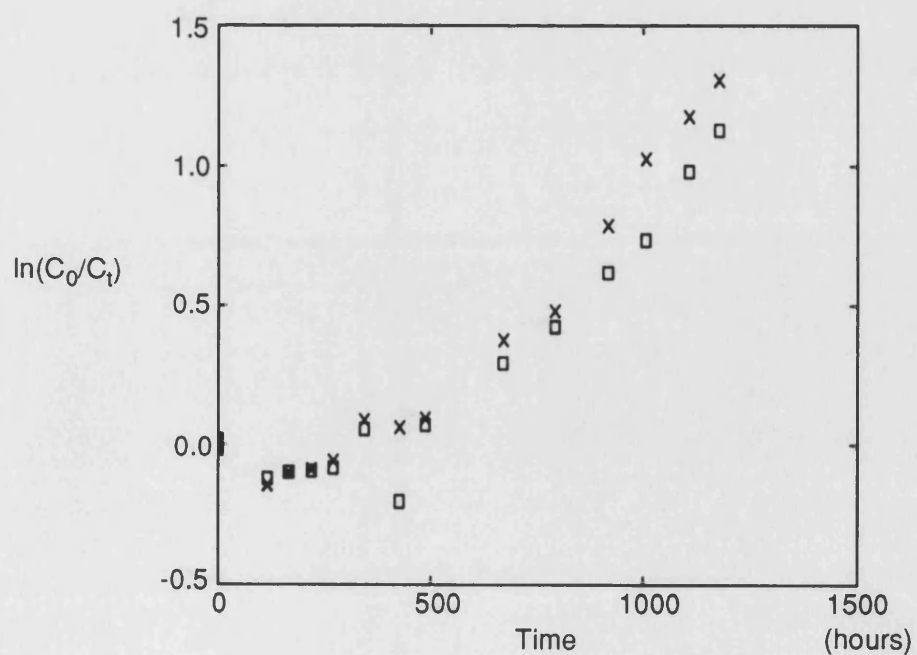
Degradation of 2,5-Dimethylpyrrole 1660 ppm(N) mg/l at 52 °C  
with 400 ppm(N) 1,2,5-Trimethylpyrrole ( $\ln(C_0/C_t)$  against Time)



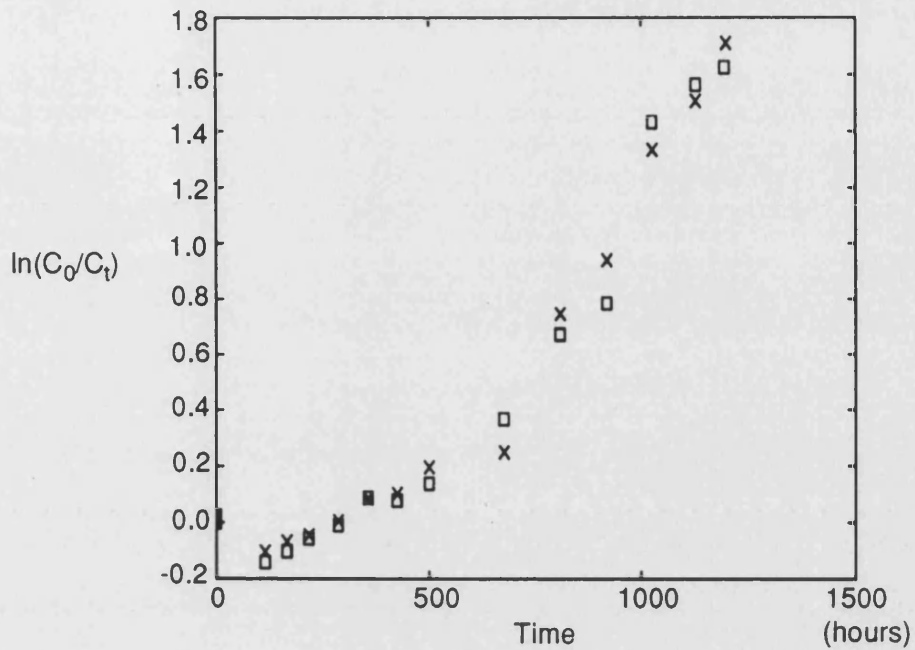
Degradation of 2,5-Dimethylpyrrole 1680 ppm(N) mg/l at 65 °C  
with 1620 ppm(N) 1,2,5-Trimethylpyrrole ( $\ln(C_0/C_t)$  against Time)



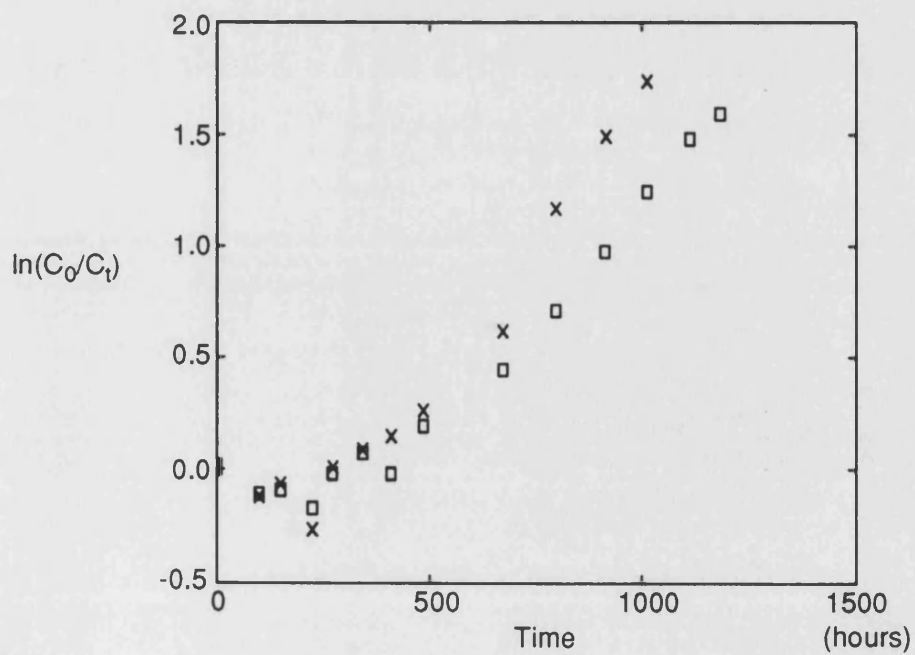
Degradation of 2,5-Dimethylpyrrole 1680 ppm(N) mg/l at 65 °C  
with 1190 ppm(N) 1,2,5-Trimethylpyrrole ( $\ln(C_0/C_t)$  against Time)



Degradation of 2,5-Dimethylpyrrole 1620 ppm(N) mg/l at 65 °C  
with 770 ppm(N) 1,2,5-Trimethylpyrrole ( $\ln(C_0/C_t)$  against Time)

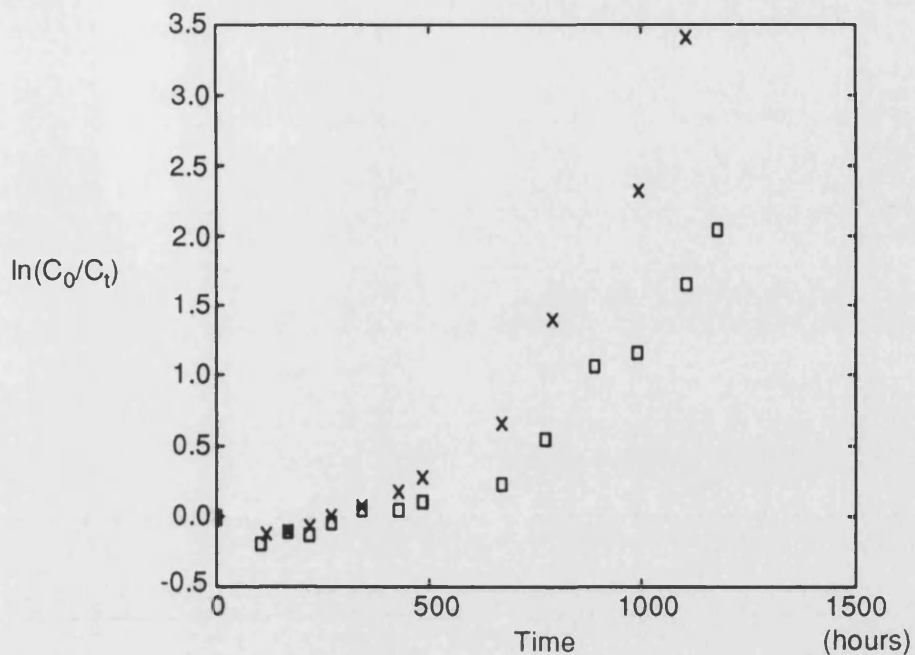


Degradation of 2,5-Dimethylpyrrole 1660 ppm(N) mg/l at 65 °C  
with 400 ppm(N) 1,2,5-Trimethylpyrrole ( $\ln(C_0/C_t)$  against Time)

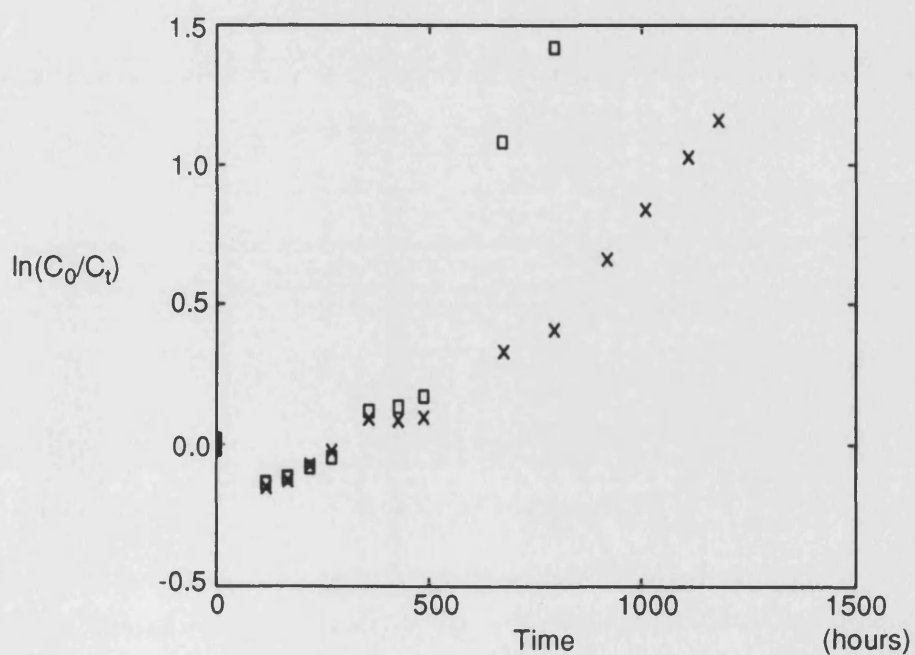




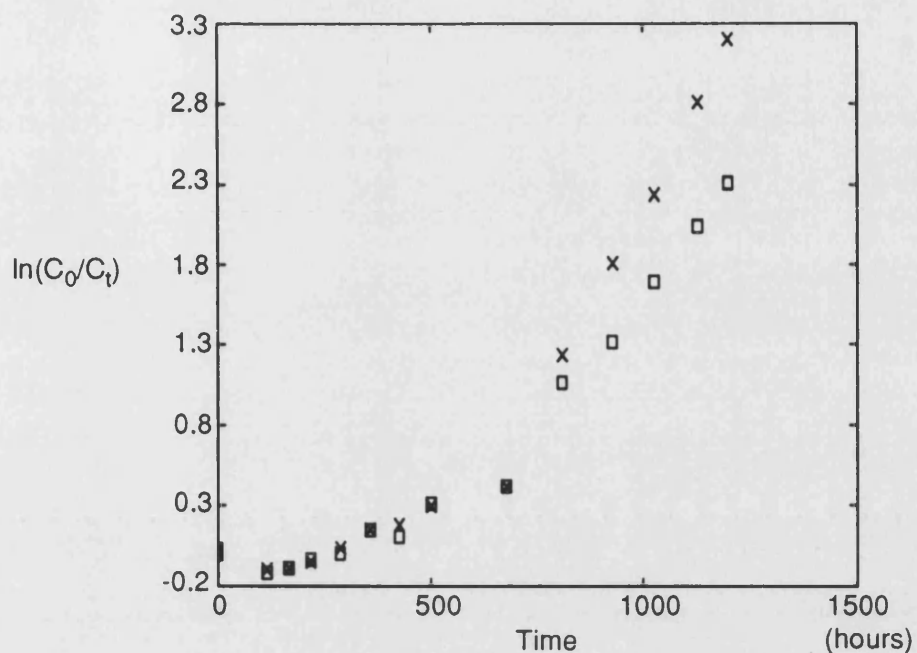
Degradation of 2,5-Dimethylpyrrole 1680 ppm(N) mg/l at 70 °C  
with 1620 ppm(N) 1,2,5-Trimethylpyrrole ( $\ln(C_0/C_t)$  against Time)



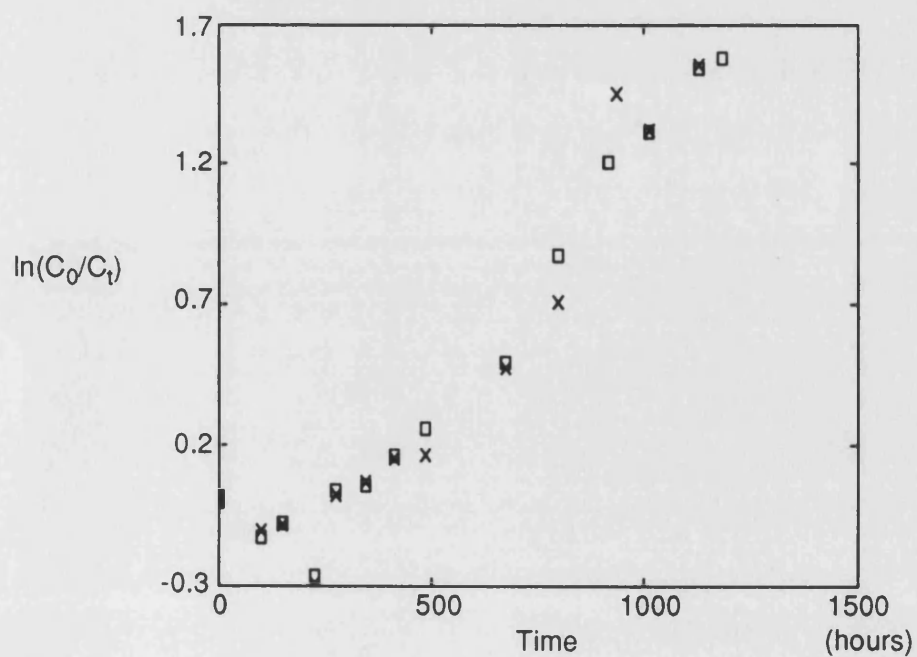
Degradation of 2,5-Dimethylpyrrole 1680 ppm(N) mg/l at 70 °C  
with 1190 ppm(N) 1,2,5-Trimethylpyrrole ( $\ln(C_0/C_t)$  against Time)



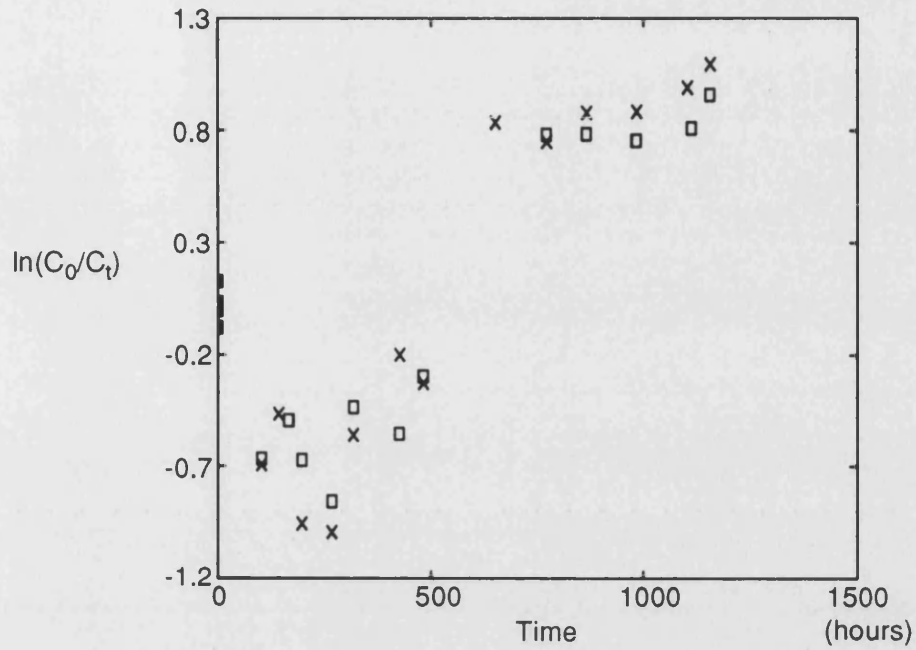
Degradation of 2,5-Dimethylpyrrole 1620 ppm(N) mg/l at 70 °C  
with 770 ppm(N) 1,2,5-Trimethylpyrrole ( $\ln(C_0/C_t)$  against Time)



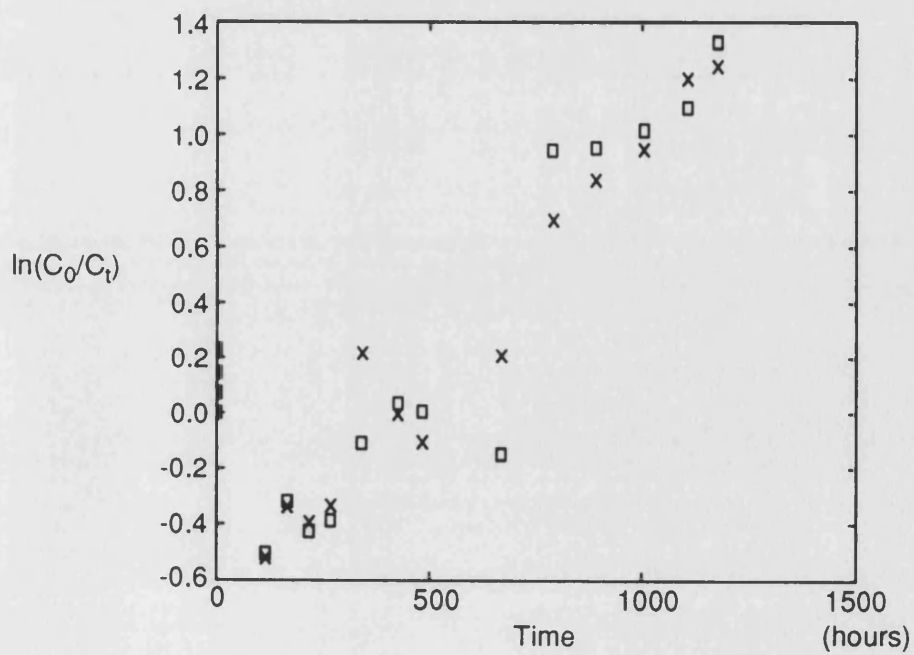
Degradation of 2,5-Dimethylpyrrole 1660 ppm(N) mg/l at 70 °C  
with 400 ppm(N) 1,2,5-Trimethylpyrrole ( $\ln(C_0/C_t)$  against Time)



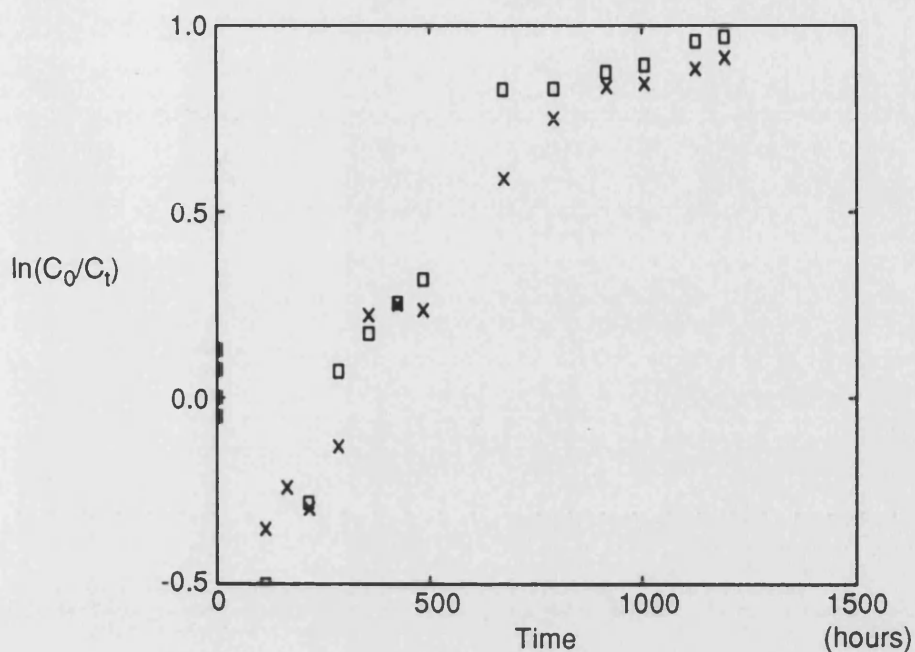
Degradation of 1,2,5-Trimethylpyrrole 1620 ppm(N) mg/l at 40 °C  
with 1680 ppm(N) 2,5-Dimethylpyrrole ( $\ln(C_0/C_t)$  against Time)



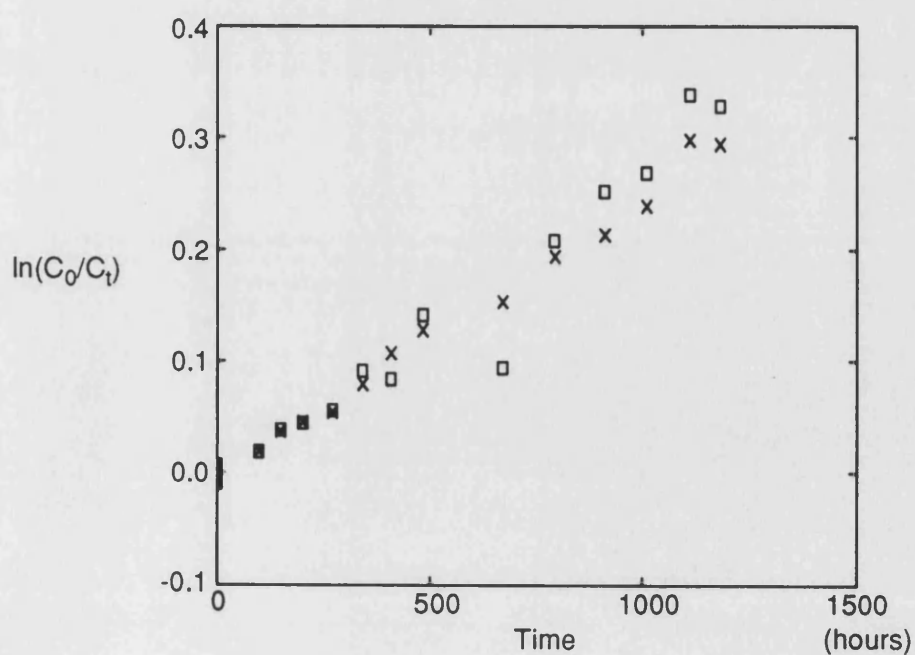
Degradation of 1,2,5-Trimethylpyrrole 1190 ppm(N) mg/l at 40 °C  
with 1680 ppm(N) 2,5-Dimethylpyrrole ( $\ln(C_0/C_t)$  against Time)



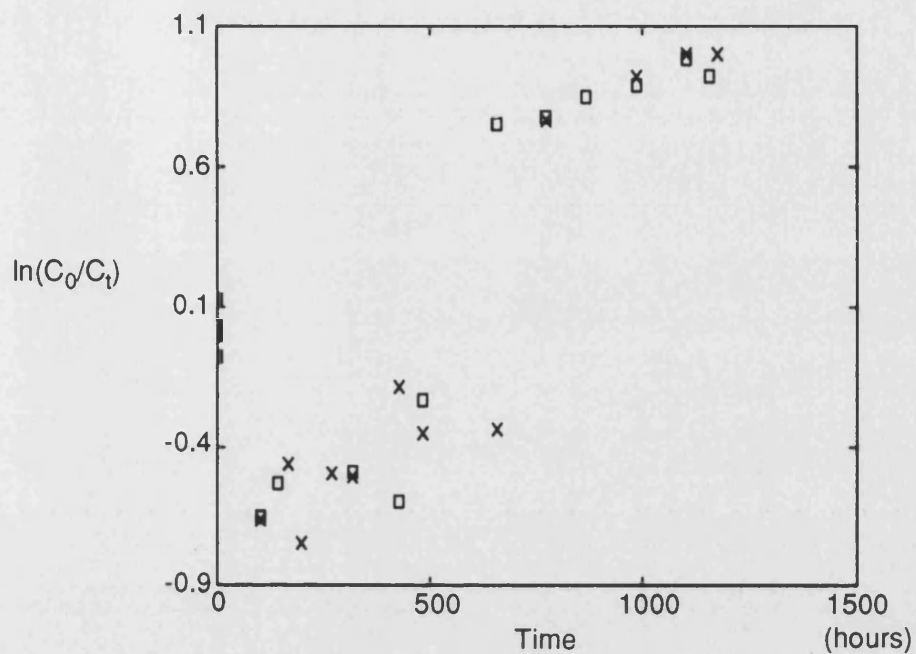
Degradation of 1,2,5-Trimethylpyrrole 770 ppm(N) mg/l at 40 °C  
with 1620 ppm(N) 2,5-Dimethylpyrrole ( $\ln(C_0/C_t)$  against Time)



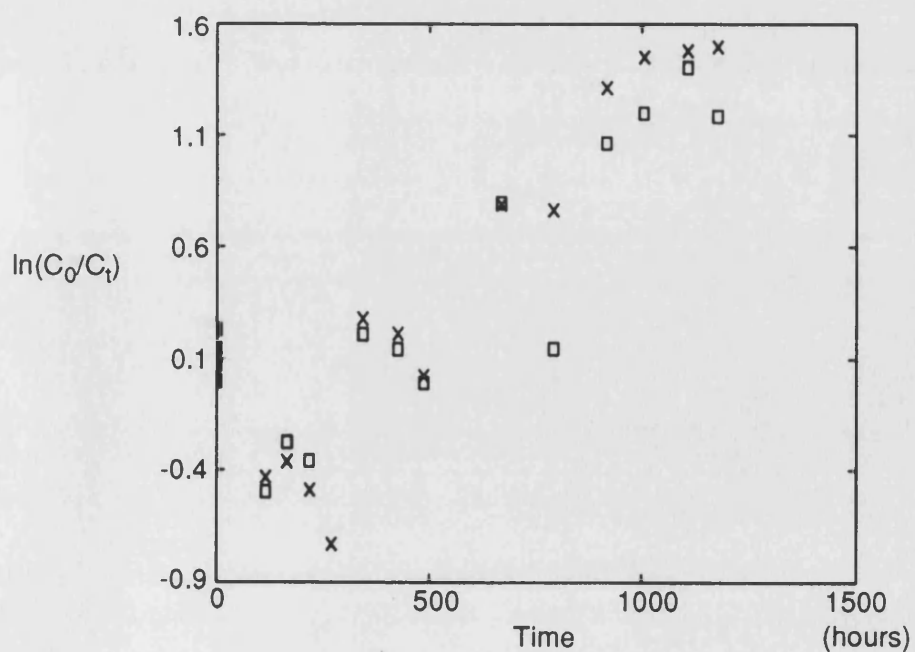
Degradation of 1,2,5-Trimethylpyrrole 400 ppm(N) mg/l at 40 °C  
with 1660 ppm(N) 2,5-Dimethylpyrrole ( $\ln(C_0/C_t)$  against Time)



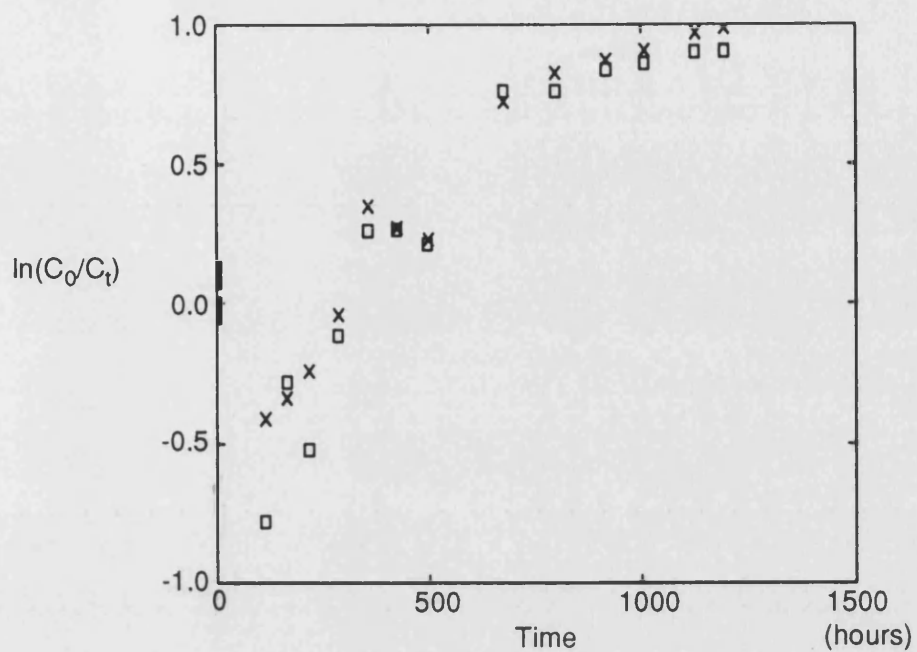
Degradation of 1,2,5-Trimethylpyrrole 1620 ppm(N) mg/l at 52 °C  
with 1680 ppm(N) 2,5-Dimethylpyrrole ( $\ln(C_0/C_t)$  against Time)



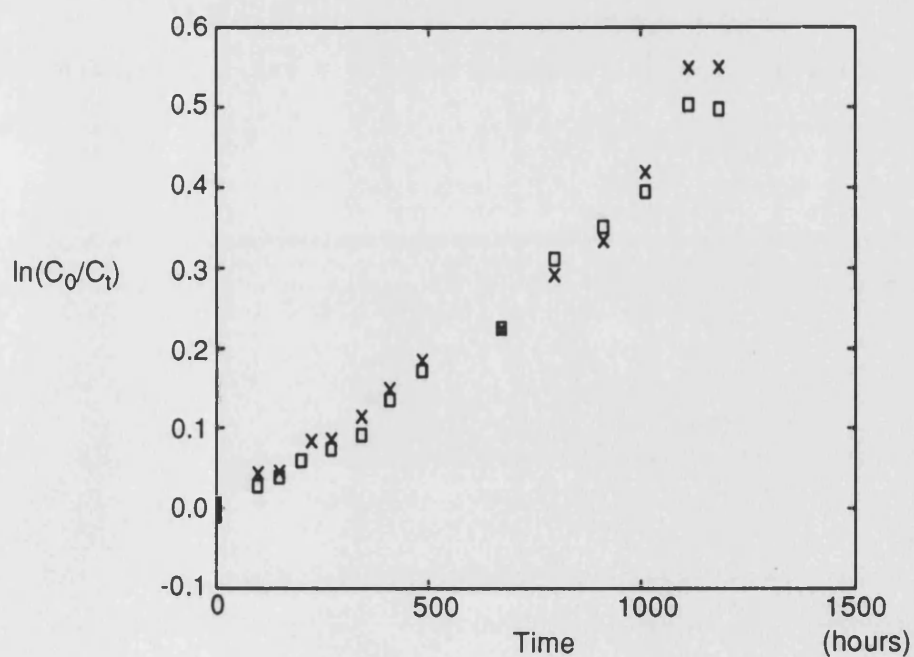
Degradation of 1,2,5-Trimethylpyrrole 1190 ppm(N) mg/l at 52 °C  
with 1680 ppm(N) 2,5-Dimethylpyrrole ( $\ln(C_0/C_t)$  against Time)



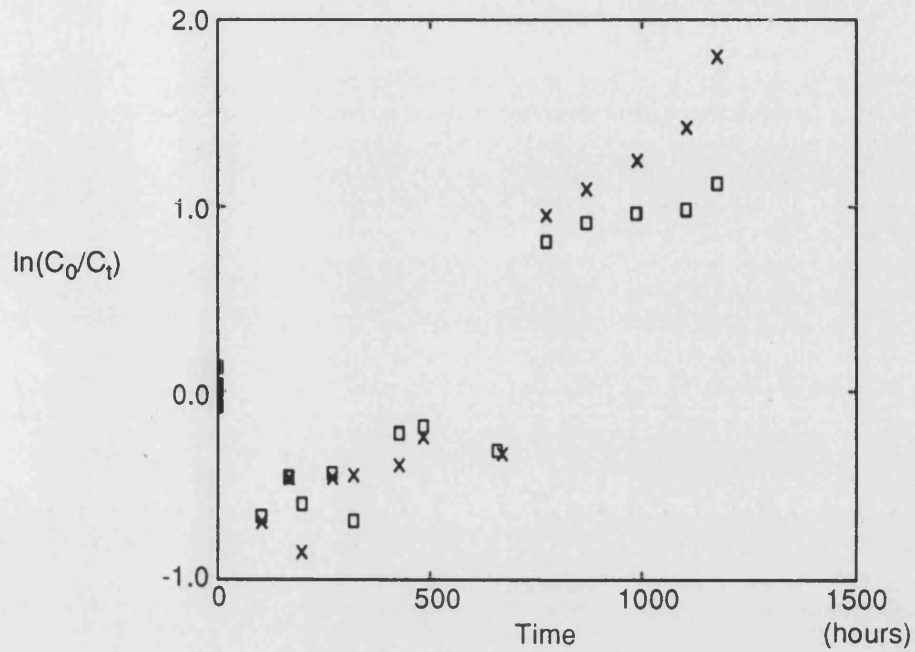
Degradation of 1,2,5-Trimethylpyrrole 770 ppm(N) mg/l at 52 °C  
with 1620 ppm(N) 2,5-Dimethylpyrrole ( $\ln(C_0/C_t)$  against Time)



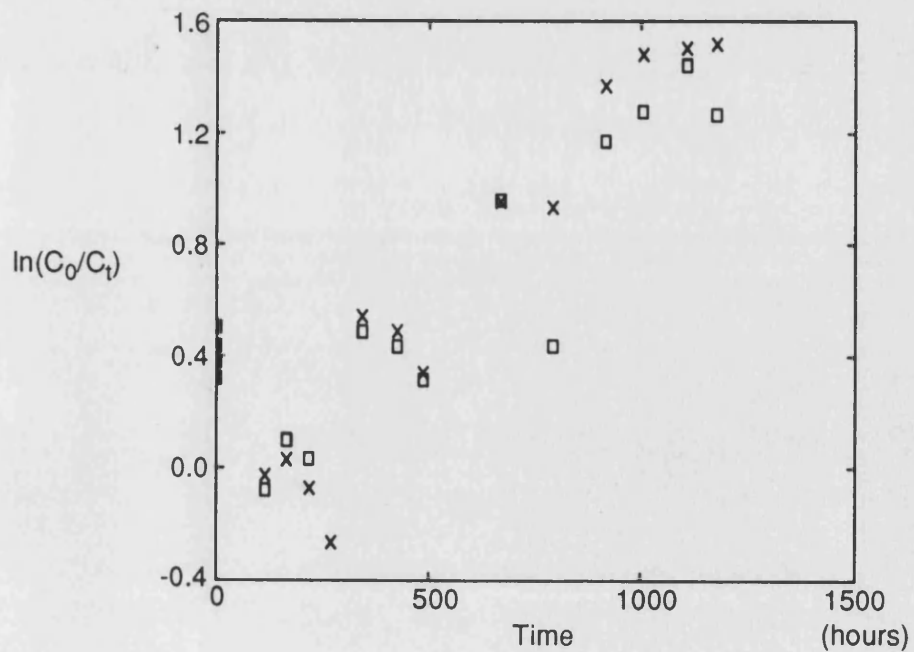
Degradation of 1,2,5-Trimethylpyrrole 400 ppm(N) mg/l at 52 °C  
with 1660 ppm(N) 2,5-Dimethylpyrrole ( $\ln(C_0/C_t)$  against Time)



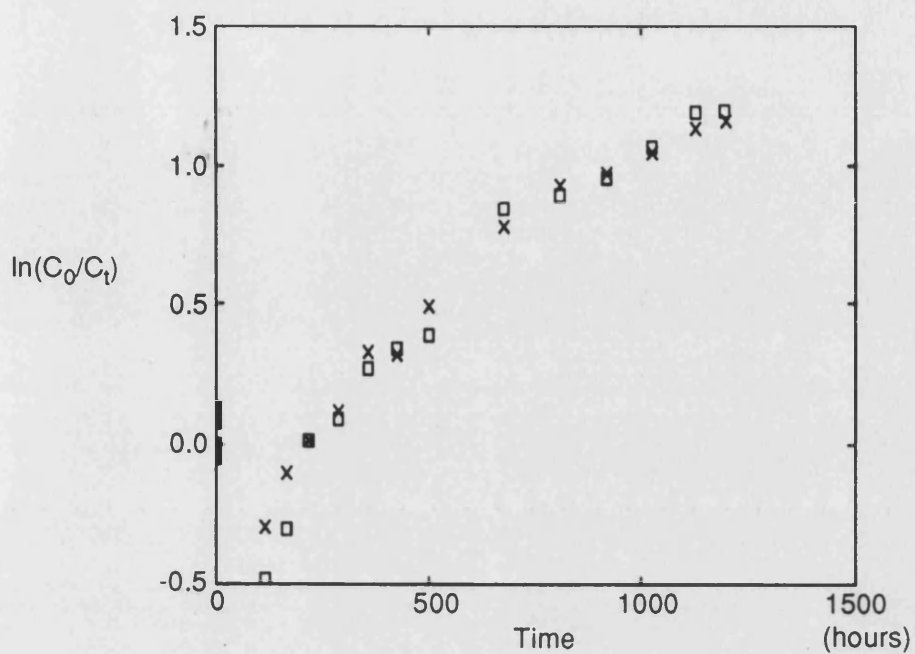
Degradation of 1,2,5-Trimethylpyrrole 1620 ppm(N) mg/l at 65 °C  
with 1680 ppm(N) 2,5-Dimethylpyrrole ( $\ln(C_0/C_t)$  against Time)



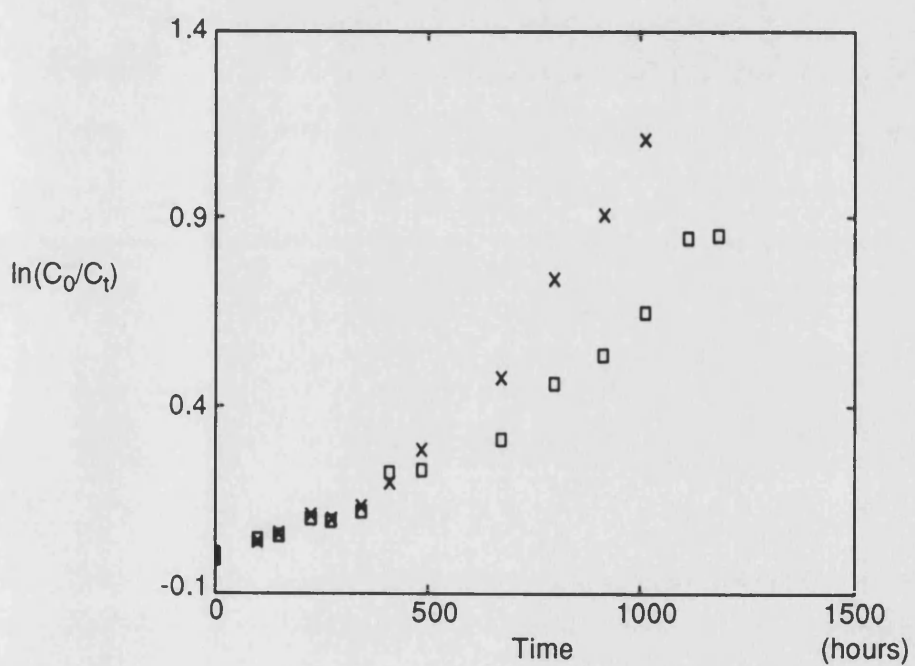
Degradation of 1,2,5-Trimethylpyrrole 1190 ppm(N) mg/l at 65 °C  
with 1680 ppm(N) 2,5-Dimethylpyrrole ( $\ln(C_0/C_t)$  against Time)



Degradation of 1,2,5-Trimethylpyrrole 770 ppm(N) mg/l at 65 °C  
with 1620 ppm(N) 2,5-Dimethylpyrrole ( $\ln(C_0/C_t)$  against Time)

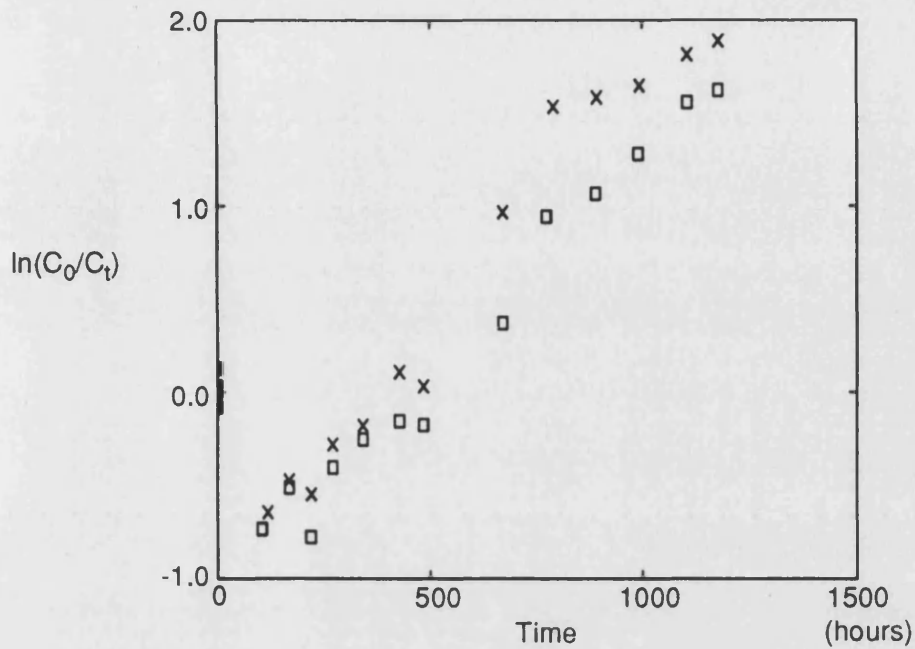


Degradation of 1,2,5-Trimethylpyrrole 400 ppm(N) mg/l at 65 °C  
with 1660 ppm(N) 2,5-Dimethylpyrrole ( $\ln(C_0/C_t)$  against Time)

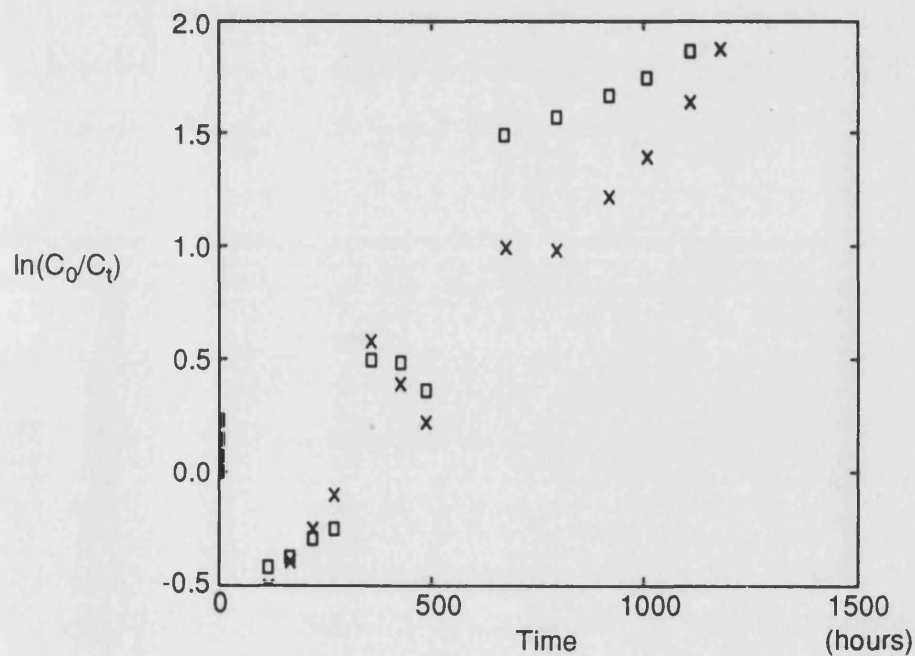




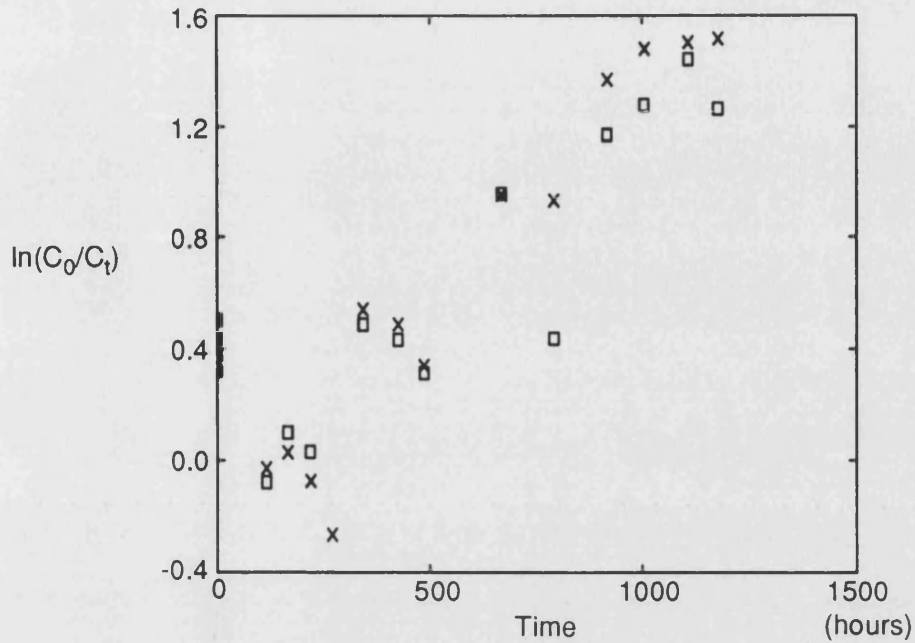
Degradation of 1,2,5-Trimethylpyrrole 1620 ppm(N) mg/l at 70 °C  
with 1680 ppm(N) 2,5-Dimethylpyrrole ( $\ln(C_0/C_t)$  against Time)



Degradation of 1,2,5-Trimethylpyrrole 1190 ppm(N) mg/l at 70 °C  
with 1680 ppm(N) 2,5-Dimethylpyrrole ( $\ln(C_0/C_t)$  against Time)



Degradation of 1,2,5-Trimethylpyrrole 770 ppm(N) mg/l at 70 °C  
with 1620 ppm(N) 2,5-Dimethylpyrrole ( $\ln(C_0/C_t)$  against Time)



Degradation of 1,2,5-Trimethylpyrrole 400 ppm(N) mg/l at 70 °C  
with 1660 ppm(N) 2,5-Dimethylpyrrole ( $\ln(C_0/C_t)$  against Time)

